

University of New Hampshire

University of New Hampshire Scholars' Repository

Doctoral Dissertations

Student Scholarship

Fall 1988

The chemical and structural properties of sea ice in the southern Beaufort Sea

Debra A. Meese

University of New Hampshire, Durham

Follow this and additional works at: <https://scholars.unh.edu/dissertation>

Recommended Citation

Meese, Debra A., "The chemical and structural properties of sea ice in the southern Beaufort Sea" (1988). *Doctoral Dissertations*. 1553.

<https://scholars.unh.edu/dissertation/1553>

This Dissertation is brought to you for free and open access by the Student Scholarship at University of New Hampshire Scholars' Repository. It has been accepted for inclusion in Doctoral Dissertations by an authorized administrator of University of New Hampshire Scholars' Repository. For more information, please contact Scholarly.Communication@unh.edu.

INFORMATION TO USERS

The most advanced technology has been used to photograph and reproduce this manuscript from the microfilm master. UMI films the original text directly from the copy submitted. Thus, some dissertation copies are in typewriter face, while others may be from a computer printer.

In the unlikely event that the author did not send UMI a complete manuscript and there are missing pages, these will be noted. Also, if unauthorized copyrighted material had to be removed, a note will indicate the deletion.

Oversize materials (e.g., maps, drawings, charts) are reproduced by sectioning the original, beginning at the upper left-hand corner and continuing from left to right in equal sections with small overlaps. Each oversize page is available as one exposure on a standard 35 mm slide or as a 17" x 23" black and white photographic print for an additional charge.

Photographs included in the original manuscript have been reproduced xerographically in this copy. 35 mm slides or 6" x 9" black and white photographic prints are available for any photographs or illustrations appearing in this copy for an additional charge. Contact UMI directly to order.



300 North Zeeb Road, Ann Arbor, MI 48106-1346 USA

Order Number 8827313

**The chemical and structural properties of sea ice in the southern
Beaufort Sea**

Meese, Debra A., Ph.D.

University of New Hampshire, 1988

U·M·I
300 N. Zeeb Rd.
Ann Arbor, MI 48106

PLEASE NOTE:

In all cases this material has been filmed in the best possible way from the available copy. Problems encountered with this document have been identified here with a check mark .

1. Glossy photographs or pages _____
2. Colored illustrations, paper or print _____
3. Photographs with dark background _____
4. Illustrations are poor copy _____
5. Pages with black marks, not original copy
6. Print shows through as there is text on both sides of page _____
7. Indistinct, broken or small print on several pages
8. Print exceeds margin requirements _____
9. Tightly bound copy with print lost in spine _____
10. Computer printout pages with indistinct print _____
11. Page(s) _____ lacking when material received, and not available from school or author.
12. Page(s) _____ seem to be missing in numbering only as text follows.
13. Two pages numbered _____. Text follows.
14. Curling and wrinkled pages
15. Dissertation contains pages with print at a slant, filmed as received _____
16. Other _____

U·M·I

THE CHEMICAL AND STRUCTURAL PROPERTIES OF SEA ICE IN THE SOUTHERN
BEAUFORT SEA

BY

DEBRA A. MEESE
B.A., Gustavus Adolphus College, 1978
M.S., University of New Hampshire, 1985

DISSERTATION

Submitted to the University of New Hampshire
in Partial Fulfillment of
the Requirements for the Degree of

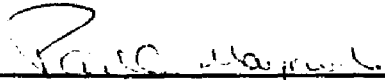
Doctor of Philosophy

in

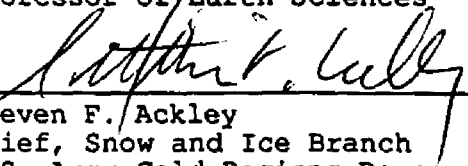
Earth Science

September, 1988

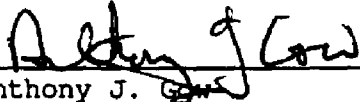
This dissertation has been examined and approved.



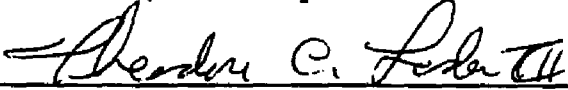
Dissertation director, Paul A. Mayewski
Professor of Earth Sciences



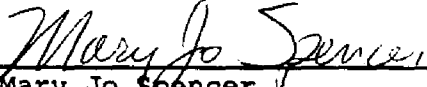
Steven F. Ackley
Chief, Snow and Ice Branch
U.S. Army Cold Regions Research and
Engineering Laboratory
Hanover, New Hampshire



Anthony J. Gow
Geologist
U.S. Army Cold Regions Research and
Engineering Laboratory
Hanover, New Hampshire



Theodore C. Loder, III
Associate Professor of Earth Sciences



Mary Jo Spencer
Research Assistant Professor



Walter B. Tucker, III
Geologist
U.S. Army Cold Regions Research and
Engineering Laboratory
Hanover, New Hampshire

18 July 1988
Date

ACKNOWLEDGEMENTS

There are many people who contributed significantly to this work and without their help and encouragement I would not have been able to complete this project. I was supported through a cooperative program with the Cold Regions Research and Engineering Laboratory (CRREL) and the University of New Hampshire (UNH). Without the financial support and field support (not to mention emotional support) from the people at CRREL, in particular my advisors Tony Gow, Terry Tucker and Steve Ackley, I would not have been able to pursue this degree.

In addition to the financial support from CRREL additional support for field work was provided by the Office of Naval Research (ONR) and the Naval Oceanographic Research and Development Activity (NORDA).

Each of my advisors has played a special role in my education and I would like to thank them for participating in this effort. I would like to thank Paul Mayewski for introducing me to the subject of sea ice and accepting me a graduate student. I would like to thank Tony Gow for taking me under his wing and teaching me just about everything I know about sea ice. Without his help in particular I would not have been able to complete this project. I would like to thank Terry Tucker for including me in the field program and all the discussions about statistics and sea ice in general. I would also like to thank him for the use of his office and computer when he was away (and when he wasn't). Steve Ackley introduced me to the cooperative program

and without his suggestion I would not have been able to continue in graduate school. I would also like to thank him for the many discussions about nutrients and biological activity in sea ice. Mary Jo Spencer had the task of trying to teach me some chemistry. I have learned alot from her not only chemical principles but also techniques. Ted Loder first introduced me to nutrients and I am thankful to him for that and his interesting discussions.

There are several other people who assisted in sampling and the chemical analyses and I am indebted to them. Tony Gow and Terry Tucker included me in their field program to Prudhoe Bay both years. Not only am I grateful to them for that but also for the wealth of knowledge they were and are always willing to share. In addition, John Govoni participated in the field program both years and I am grateful to him for his assistance. Many members of the Glacier Research Group at UNH help in anion analyses. Sue Welch performed the nutrient analyses for the 1986 samples at UNH and Kathy Kroglund from the University of Washington performed the nutrient analyses in Prudhoe Bay in 1987. The cation analyses were performed at CRREL and I would like to thank Alan Hewitt for helping get set up in the lab and showing me how to use the AA.

Several people at CRREL also assisted in the preparation of my defense and this dissertation. I would like to thank Rob Wills for writing the macro to make the depth plots and for getting me started on the Mac. I would also like to thank Bob Demars and Tom Vaughan in photo for the photos and slides and Ed

Perkins for the drafting of some figures. In addition, Sandy Smith and Joi Cattabriga for help with word processing problems and use of their printer. Thanks also go to Nancy Perron for having the ability and willingness to cut circles. I would also like to thank Jim Cragin and Dan Leggett for some interesting discussions on ice chemistry and chemistry in general.

Last, but not least, I would like to thank my parents for all of their love and encouragement.

TABLE OF CONTENTS

ACKNOWLEDGEMENTS.....	iii
LIST OF FIGURES.....	ix
LIST OF TABLES.....	xii
ABSTRACT.....	xvi
INTRODUCTION.....	1
I. BACKGROUND.....	2
Formation, Growth and Structure of Sea Ice.....	5
Oceanic Frazil Production.....	9
Multiyear Ice.....	11
Equilibrium Growth.....	14
Summer Ice Decay.....	14
Annual Layering.....	15
Salinity Distribution in Sea Ice.....	16
Chemistry of Sea Ice.....	23
Study Area Description.....	28
II. Objectives.....	30
III. METHODOLOGY.....	33
Sample Collection.....	33
Blanks.....	37
Chemical Analyses.....	41
Thin Sections.....	45
Data Reduction.....	45
IV. RESULTS AND DISCUSSION.....	49
First-year Ice.....	49
Core Profiles.....	49
Core FY186.....	49
Core FY286.....	54
CORE SI86.....	58
CORE A87.....	62
CORE C87.....	66
CORE D87.....	70
CORE H87.....	74

CORE O87	78
CORE SI87	82
CORE WD87	86
Structure vs. Chemistry	90
Major Elements	93
Nutrients	95
All Chemical Species Normalized to Cl	96
Major Elements Normalized to Cl	97
Nutrients Normalized to Cl	99
Summary of Statistical Analysis Based on Ice Type	100
Bulk Salinity	101
Dilution Curves	103
Cations/Anions	113
Linear Regressions	113
Statistical Analysis for All Chemical Species	116
Statistical Analysis for Major Elements	121
Statistical Analysis of Nutrients	123
Statistical Analysis for All Chemical Species Normalized to Cl	125
Statistical Analysis for Major Elements Normalized to Cl	126
Statistical Analysis for Nutrients Normalized to Cl	127
MULTIYEAR ICE	129
Core Profiles	129
CORE F1SA86	129
CORE F1SB86	134
Core F1SC86	138
CORE F1SD86	142
CORE F2SA86	146
CORE F3SA86	150
CORE F4SA86	154
CORE F1SA87	158
CORE F1SB87	162

CORE F2SA87	166
Bulk Salinity.....	170
Dilution Curves.....	171
Linear Regression	180
Cations/Anions	181
Statistical Analysis	181
Statistical Analysis for all Chemical Species	182
Statistical Analysis for Major Elements	186
Statistical Analysis for Nutrients	188
Statistical Analysis for All Chemical Species Normalized to Cl	189
Statistical Analysis for Major Elements Normalized to Cl	191
Statistical Analysis for Nutrients Normalized to Cl	192
Comparison of First-year and Multiyear Ice.....	193
Statistical Analysis for all Chemical Species	194
Statistical Analysis for Major Elements	196
Statistical Analysis for Nutrients	197
Statistical Analysis for All Chemical Species Normalized to Cl	198
Statistical Analysis for Major Species Normalized to Cl.....	200
Statistical Analysis for Nutrients Normalized to Cl	201
V. SUMMARY	202
VI. CONCLUSIONS.....	207
VII. FUTURE WORK.....	210
REFERENCES CITED.....	212

LIST OF FIGURES

Fig. 1. Sea ice extent in the Northern Hemisphere 3

Fig. 2. Effect of salinity on the temperature of maximum density (dashed curve) and the freezing point temperature (solid curve)6

Fig. 3. Growth rates in multiyear and thick first-year ice as a function of season in the Central Arctic 13

Fig. 4. Average salinity of sea ice as a function of ice thickness for cold ice samples during the growth season20

Fig. 5. Average salinity of sea ice as a function of ice thickness for warm sea ice sampled during or at the end of the melt season21

Fig. 6. Bulk salinity values of ice cores as a function of floe thickness 22

Fig. 7. Phase diagram for "standard sea" ice25

Fig. 8. Ion concentration profiles for sea ice from Churchill, Manitoba26

Fig. 9. Location map showing major rivers in the Prudhoe Bay area. 29

Fig. 11. Comparison between MBS calcium standards, seawater standards and both sets with a lanthanum-cesium matrix modifier added.....43

Fig. 12. Calcium standards additions for 3 samples 44

Fig. 13. Salinity-structure profiles of core FY18651

Fig. 14. Chemistry profiles for core FY186.....52

Fig. 14. (cont.) 53

Fig. 15. Salinity-structure profile of core FY286. 55

Fig. 16. Chemistry profiles for core FY286.....56

Fig. 16. (cont.) 57

Fig. 17. Salinity-structure profile of core SI86.59

Fig. 18. Chemistry profiles for core SI86.....60

Fig. 18. (cont). 61

Fig. 19. Salinity-structure profiles for core A87. 63

Fig. 20. Chemistry profiles for core A87.....64

Fig. 20. (cont.) 65

Fig. 21.	Salinity-structure profile for core C87.	67
Fig. 22.	Chemistry profiles for core C87.	68
Fig. 22.	(cont.).	69
Fig. 23.	Salinity-structure profiles for core D87.	71
Fig. 24.	Chemistry profiles for core D87.	72
Fig. 22.	(cont.).	73
Fig. 25.	Salinity-structure profiles for core H87.	75
Fig. 26.	Chemistry profiles for core H87.	76
Fig. 26.	(cont.).	77
Fig. 27.	Salinity-structure profiles for core O87.	79
Fig. 28.	Chemistry profiles for core O87.	80
Fig. 28.	(cont.).	81
Fig. 29.	Salinity-structure profiles for Core SI87.	83
Fig. 30.	Chemistry profiles for core SI87.	84
Fig. 30	(cont.).....	85
Fig. 31.	Salinity-structure profiles for core WD87.	87
Fig. 32.	Chemistry profiles for core WD87.	88
Fig. 32.	(cont.).	89
Fig. 33	Bulk salinity values of ice cores as a function of floe thickness.	103
Fig. 34.	Dilution curves for Br, SO ₄ , Ca and Mg	108
Fig. 35.	Dilution curves for Na	109
Fig. 36.	Dilution curves for K	110
Fig. 37.	Dilution curves for all samples for PO ₄ , SiO ₄ and NH ₄	111
Fig. 38.	Dilution curves for NO ₃ +NO ₂	112
Fig. 39.	Structure-salinity profiles from core F1SA86.	131
Fig. 40.	Chemistry profiles for core F1SA86.	132
Fig. 40.	(cont.).	133
Fig. 41.	Salinity-structure profiles for core F1SB86.	135
Fig. 42.	Chemistry profiles for core F1SB86.	136
Fig. 43.	Salinity-structure profiles for core F1SC86.	139
Fig. 44.	Chemistry profiles for core F1SC86.	140
Fig. 44.	(cont.).	141
Fig. 45.	Salinity-structure profiles for core F1SD86.	143
Fig. 46.	Chemistry profiles for core F1SD86.	144
Fig. 46.	(cont.).	145

Fig. 47.	Salinity-structure profiles for core F2SA86.	147
Fig. 48.	Chemistry profiles for core F2SA86.	148
Fig. 48.	(cont.).	149
Fig. 49.	Salinity-structure profiles of core F3SA86.	151
Fig. 50.	Chemistry profiles for core F3SA86.	152
Fig. 50.	(cont.).	153
Fig. 51.	Salinity-structure profiles for core F4SA86.	155
Fig. 52.	Chemistry profiles for core F4SA86.	156
Fig. 52.	(cont.).	157
Fig. 53.	Salinity-structure profile of core F1SA87.	159
Fig. 54.	Chemistry profiles for core F1SA87.	160
Fig. 54.	(cont.).	161
Fig. 55.	Salinity-structure profile of core F1SB87.	163
Fig. 56.	Chemistry profiles for core F1SB87.	164
Fig. 56.	(cont.).	165
Fig. 57.	Salinity-structure profiles for core F2SA87. F2SA87.	168
Fig. 58.	(cont.).	169
Fig. 59.	Bulk salinity versus thickness for multiyear ice. ...	171
Fig. 60.	Dilution curves for multiyear ice for Br, SO ₄ , Na and Mg	174
Fig. 61.	Dilution curves for multiyear ice for Ca	175
Fig. 62.	Dilution curves for multiyear ice for K	176
Fig. 63.	Dilution curves for multiyear ice for PO ₄	177
Fig. 64.	Dilution curves for multiyear ice for NO ₃ +NO ₂	178
Fig. 65.	Dilution curves for multiyear ice for SiO ₄ and NH ₄ ...	179

LIST OF TABLES

Table 1. Results of blank analyses.	39
Table 1. (cont.)	40
Table 2. List of analyses, methodology and detection limits. ..	41
Table 3. Comparison of absorbances for Ca standards made with seawater, seawater with LaCs and AA standards and AA standards with LaCs.	43
Table 4. Results of Ca standard addition test.	44
Table 5. Summary for correlation coefficient matrices for core SI86 based on ice type.	93
Table 6. Summary of factor analysis based on ice type for core SI86.	93
Table 7. Summary table for correlation coefficient matrices for core SI86 based on ice type for major elements.	94
Table 8. Summary table of factor analysis results based on ice type for core SI86.	95
Table 9. Summary table of correlation coefficient matrices based on ice type for core SI86 for nutrients.	95
Table 10. Summary table for factor analysis based on ice type for core SI86 for nutrients.	96
Table 11. Summary table of correlation coefficient matrices based on ice type for core SI86 for all chemical species normalized to Cl.	97
Table 12. Summary table for factor analysis results based on ice type for core SI86 for all chemical species normalized to Cl.	97
Table 13. Summary table of correlation coefficient matrices based on ice type for core SI86 for major elements normalized to Cl.	98
Table 14. Summary table for factor analysis results based on ice type for core SI86 for major elements normalized to Cl.	98
Table 15. Summary table of correlation coefficient matrices based on ice type for core SI86 for nutrients normalized to Cl.	100

Table 16.	Summary table for factor analysis results based on ice type for core SI86 for nutrients normalized to Cl.	100
Table 17.	Summary table for correlation coefficient matrices for first-year ice for all elements.	119
Table 17.	(cont.).	120
Table 18.	Summary table for factor analysis results for first-year ice for all chemical species.....	121
Table 19.	Summary table for correlation coefficient matrices for first-year ice for major elements.	122
Table 21.	Summary table of correlation coefficient matrices in first-year ice for nutrients.....	124
Table 22.	Summary table for factor analysis results for first-year ice for nutrients.	124
Table 23.	Summary table for correlation coefficient matrices for first-year ice for all chemical species normalized to Cl.	125
Table 24.	Summary table for factor analysis results for first-year ice for all chemical species normalized to Cl.	126
Table 25.	Summary table of correlation coefficient matrices for first-year ice for major elements normalized to Cl.	126
Table 26.	Summary table for factor analysis results for first-year ice for major elements normalized to Cl.....	127
Table 27.	Summary table for correlation coefficient matrices for first-year ice for nutrients normalized to Cl.	128
Table 28.	Summary table for factor analysis results for first-year ice for nutrients normalized to Cl.	128
Table 29.	Summary table of correlation coefficient matrices for multiyear ice based on all chemical species.....	184
Table 29.	(cont.).	185
Table 30.	Summary table of factor analysis for multiyear ice for all samples.....	186
Table 31.	Summary table for correlation coefficient matrices for multiyear ice for major elements.	187
Table 32.	Summary table of factor analysis for multiyear ice for major elements.	188

Table 33. Summary table for correlation coefficient matrices for multiyear ice for nutrients.....	189
Table 34. Summary table of factor analysis for multiyear ice for nutrients.....	189
Table 35. Summary table for correlation coefficient matrices for multiyear ice for all elements normalized to Cl.	190
Table 36. Summary table of factor analysis for multiyear ice for all elements normalized to Cl.....	191
Table 37. Summary table of correlation coefficient matrices for multiyear ice for major elements normalized to Cl.	192
Table 38. Summary table for factor analysis for multiyear ice for major elements normalized to Cl.	192
Table 39. Summary table for correlation coefficient matrices for multiyear ice for nutrients normalized to Cl.	193
Table 40. Summary table of factor analysis for multiyear ice for nutrients normalized to Cl.....	193
Table 41. Summary for correlation coefficient matrices for first-year and multiyear ice for all chemical species.	195
Table 41. (cont).	195
Table 42. Summary of factor analysis for first-year and multiyear ice for all chemical species.....	195
Table 43. Summary for correlation coefficient matrices for first-year and multiyear ice for major elements.....	196
Table 44. Summary of factor analysis for first-year and multiyear ice for major elements.....	197
Table 45. Summary for correlation coefficient matrices for first-year and multiyear ice for nutrients.	198
Table 46. Summary of factor analysis for first-year and multiyear ice for nutrients.	198
Table 47. Summary for correlation coefficient matrices for first-year and multiyear ice for all chemical species normalized to Cl.	199
Table 48. Summary of factor analysis for first-year and multiyear ice for all chemical species normalized to Cl.	199

Table 49. Summary for correlation coefficient matrices for first-year and multiyear ice for major species normalized to Cl.	200
Table 50. Summary of factor analysis for first-year and multiyear ice for the major species normalized to Cl.....	200
Table 51. Summary for correlation coefficient matrices for first-year and multiyear ice for nutrients normalized to Cl.	201
Table 52. Summary of factor analysis for first-year and multiyear ice for nutrients normalized to Cl.	201

ABSTRACT

The purpose of this study is to provide a detailed chemical and structural profile of first-year and multiyear Arctic sea ice. Ice cores were collected during April-May 1986 and 1987 near Prudhoe Bay, Alaska. Concentrations of Cl, Br, SO₄, Na, Ca, K, Mg, PO₄, SiO₄, NO₃, NO₂ and NH₄ were determined for samples chosen on the basis of structural ice type.

Chemical and statistical analyses indicate that finer-grained structures incorporate more impurities and that major ion chemistry is controlled almost entirely by salinity. Mg is enriched in the ice indicating precipitation is occurring at temperatures higher than previously reported. K is depleted in the ice suggesting preferential drainage. Ratios of the major ions are the same for first-year and multiyear ice and are similar to that of seawater indicating that as the ice ages no significant changes occur in ice chemistry. Nutrient concentrations in the ice are enriched with respect to the underlying water indicating that biological activity occurs in the ice and processes other than the overall salinity effect and brine drainage are affecting nutrient concentrations within the ice.

INTRODUCTION

To date chemical analysis of sea ice cores has been very limited. Sampling and subsectioning of cores has been inconsistent and results from different studies vary greatly. The aims of this study are to provide a comprehensive chemical profile of first-year and multiyear Arctic sea ice, assess extent of ice structure control on brine chemistry and to determine what if any consistent trends exist within the ice pack, and what physio/chemical processes determine the chemical profile.

During April-May 1986 and 1987, ten first-year and 10 multiyear cores were collected near Prudhoe Bay, Alaska. Concentrations of Cl, Br, SO₄, Na, Ca, K, Mg, PO₄, SiO₄, NO₃, NO₂ and NH₄ were determined for samples chosen on the basis of structural ice type. Statistical correlations for each core were determined and comparisons were made for all samples. In addition, correlations for each ice type were determined and comparisons made.

I. BACKGROUND

The World Meteorological Organization (WMO) has developed a taxonomy for the classification of sea ice based on its stage of development (WMO, 1956) where multiyear ice is defined as ice that has survived at least two summers. Distinguishing visually between second-year and multiyear ice is often difficult since one melt season gives the ice the surface relief typical of multiyear ice with alternating hummocks and melt ponds (Gow et al., 1987). Therefore, the only distinction that will be made here is between first-year and multiyear ice (ice that has survived at least one summer season). The Arctic seasonal sea ice zone (SSIZ) covers approximately 14×10^6 km² at maximum extent. Seasonal ice forms in the peripheral seas surrounding the Arctic Basin (Fig. 1). The area covered by the SSIZ in the Arctic is about the same as that of the multiyear ice (Maykut, 1985). Undeformed first-year ice in the SSIZ is generally less than 2 m thick. Ice-ocean-atmosphere interactions in the shelf regions of the SSIZ have an important effect on the large-scale structure and circulation of the world ocean. Salt fractionation during freezing leads to the formation of cold, dense water on the shelves which is critical in maintaining the thermocline structure of the Arctic and other oceans (McPhee, 1980).

Shorefast ice occurs along most coasts in the Arctic. It forms early in the winter in shallow water. The extent of fast ice is determined by bottom and shoreline topography and,

therefore, tends to be highly variable. Near Point Barrow the zone is approximately 15 km wide while at Harrison Bay it extends 60 km offshore (Maykut, 1985).

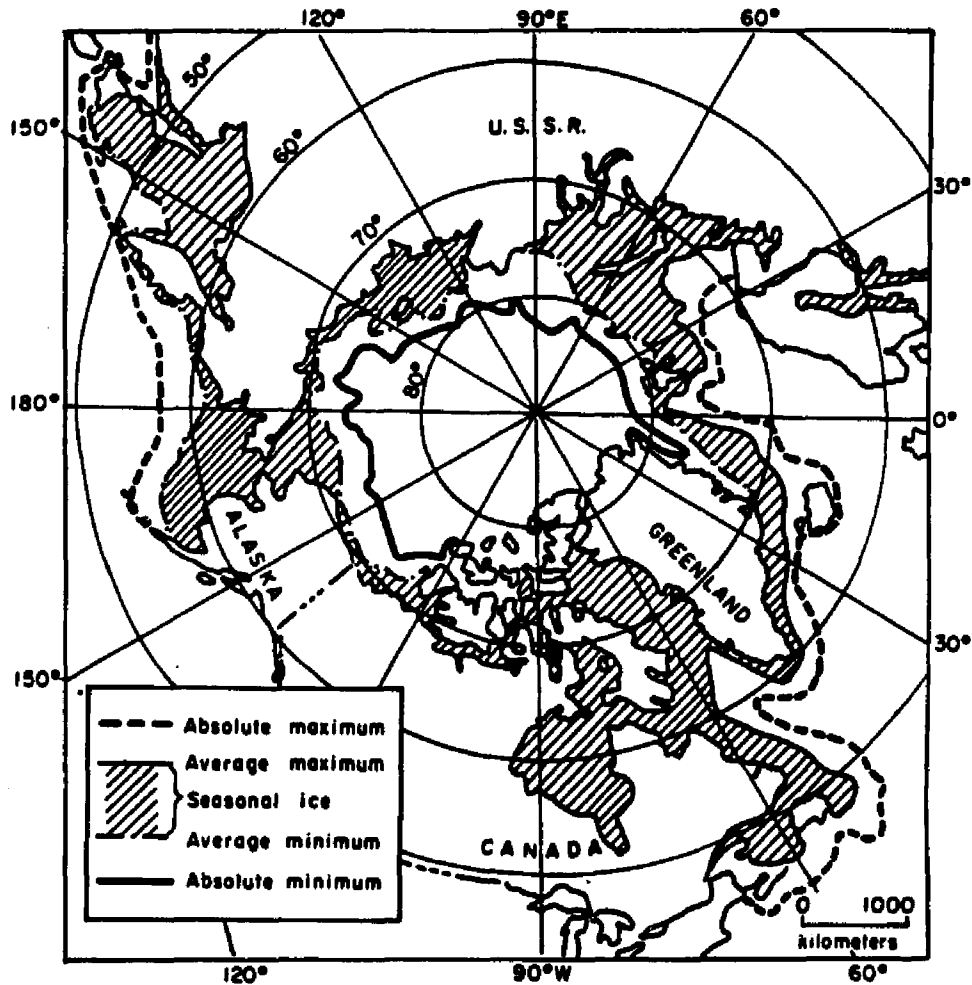


Fig. 1. Sea ice extent in the Northern Hemisphere (From Maykut, 1985).

A zone of highly deformed first-year ice (the shear zone) exists in coastal regions along the Alaskan North Slope and Canadian Archipelago. In late summer and early fall multiyear floes remain in shallow coastal areas. Where floes are grounded they provide strength and stability to newly forming ice. Ice

growth continues seaward until grounding is no longer possible. Without the stability from the grounded features, deformational stresses will produce significant ridging which continues until areas of higher concentrations of thick multiyear ice are reached in which the stresses are not large enough to deform the thicker ice.

The marginal ice zone (MIZ) is located near the boundary between the ice and open ocean and is ice which is affected by the presence of the open ocean. The MIZ is approximately 150-200 km in width (Maykut, 1985). Oceanic surface waves penetrating into the pack break the ice into smaller floes whose average size increases rapidly with distance in from the edge (Maykut, 1985). The outer portion of the MIZ is characterized by large horizontal gradients in the properties of the ice, ocean and atmosphere. Advection of air across the ice edge can produce large changes in turbulent heat transfer, surface stress, cloudiness and radiative fluxes (Maykut, 1985). Changes also occur in the mechanical properties of the ice, surface roughness and solar input to the ocean (Maykut, 1985). Horizontal density structure and surface stress may give rise to a variety of mesoscale phenomena in the ocean (eddies, jets and upwelling) which impact biological productivity and acoustical properties across the MIZ (Maykut, 1985). During the summer, floe breakup and increasing oceanic stratification beneath the ice due to the melting ice affect the response of the ice to winds and currents and the rate at which heat is transferred from the water to the ice (Maykut, 1985).

Formation, Growth and Structure of Sea Ice

The addition of salt to water depresses the freezing point of the solution (Fig. 2). Since seawater with a salinity greater than 24.7 o/oo has a freezing point higher than its temperature of maximum density (Fig. 2), surface cooling of this solution yields an unstable vertical density distribution causing convective mixing which continues until the water reaches the freezing point (Weeks and Ackley, 1982). Density gradients in the upper ocean usually limit the depth to which water must be cooled before freezing can begin. Therefore, the density structure of the ocean is a major factor in determining the onset of freezing (Maykut, 1985). Once the mixed layer in the upper ocean reaches the freezing point, additional heat loss produces slight supercooling of the water and ice formation begins. The amount of supercooling necessary to initiate ice growth is small although observations near Greenland have shown a supercooling of as much as 0.2-0.4° C down to depths of tens of meters (Maykut, 1985).

Initial ice formation occurs at or near the surface of the water in the form of small platelets and needles called frazil. Frazil crystals usually do not exceed 3-4 mm in diameter. Continued freezing results in the production of grease ice, a soupy mixture of unconsolidated frazil crystals. Under quiescent conditions the frazil crystals freeze together to form a solid, continuous ice cover with thicknesses between 1 and 10 cm. More often, however, wind induced turbulence in the water causes abrasion between the crystals inhibiting development of a solid

cover. Wind and wave action advect frazil crystals downwind where accumulations up to 1 m thick may form. In the presence of a wave field pancakes usually form. These circular masses of semiconsolidated slush range from 0.3-3.0 m in diameter. Pancakes often display irregular raised rims around their perimeters due to constant bumping. Eventually, the pancakes consolidate by freezing together to form a continuous sheet of ice (Weeks and Ackley, 1982).

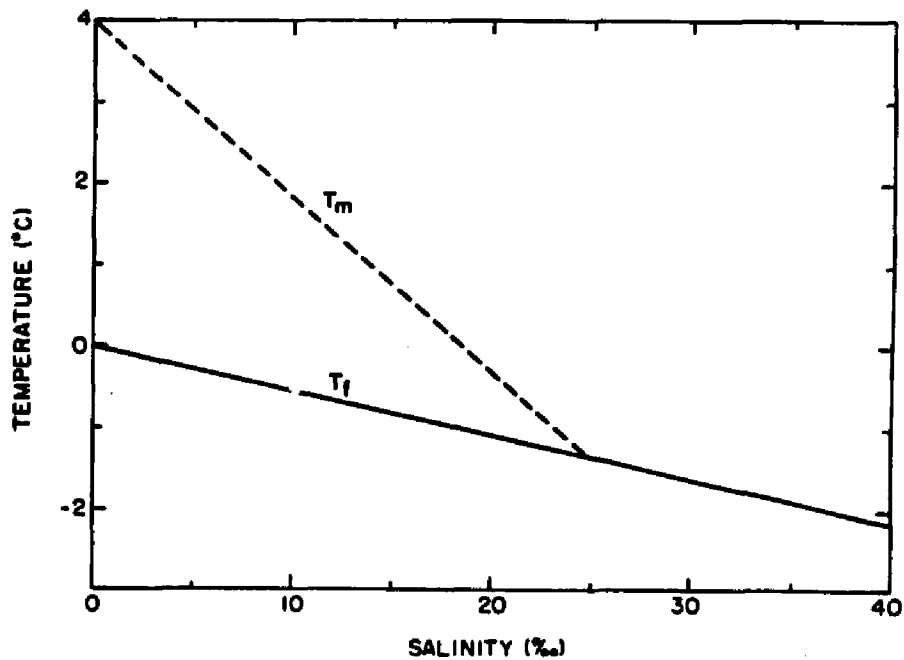


Fig. 2. Effect of salinity on the temperature of maximum density (dashed curve) and the freezing point temperature (solid curve) (From Maykut, 1985).

Once a continuous ice sheet has formed the underlying ocean is separated from the cold air, therefore, latent heat is extracted through the ice sheet, and the growth rate is determined by the temperature gradient in the ice and its

effective conductivity (Weeks and Ackley, 1982). Also, once a continuous sheet has formed ice crystals lose a degree of growth freedom and crystal growth can proceed without one grain interfering with the growth of another only if the grain boundaries are perpendicular to the freezing interface (congelation growth) (Weeks and Ackley, 1982). In this transition zone between frazil and congelation growth geometric selection occurs with crystals in the favored growth direction eliminating crystals in the unfavored orientation ultimately producing a characteristic growth fabric. This layer is usually 5-10 cm thick (Weeks and Ackley, 1982). Below the transition a zone of columnar ice is found in which there exists a strong crystal elongation parallel to the direction of heat flow, a pronounced crystal orientation with the c-axes all oriented within a few degrees of the horizontal plane and an increase in crystal size with depth (Weeks and Ackley, 1982). Once congelation growth begins, crystals whose c-axes are parallel to the ice-water interface quickly begin to dominate the structure of the ice sheet. Crystals whose c-axes are closer to the horizontal grow downward into the water faster than those with a more vertical orientation, edging out the slower growing crystals. This process proceeds rapidly until only those crystals with c-axes parallel to the freezing interface remain (Weeks and Ackley, 1982).

Within crystals in the columnar zone a substructure of long, vertical plates with parallel layers of brine inclusions is developed, a direct result of constitutional supercooling or the

process by which seawater incorporates residual brine at the ice/water interface as freezing progresses (Weeks and Ackley, 1982). The residual brine is that brine that cannot be rejected away from the interface and since it cannot be incorporated within the ice crystal lattice, it is segregated instead as inclusions between the plates. The plates are pure ice dendrites with tips protruding down into the seawater. The brine is then entrapped in the grooves between the dendrites. Plate width may vary from a few tenths of a millimeter to 1 mm and is dependent on the rate of growth, more rapid growth resulting in narrower plate spacing and a higher salinity (Weeks and Ackley, 1982 and Gow et al., 1987).

Weeks and Gow (1978 and 1980) found that strong crystallographic c-axis alignments exist over large areas of the Arctic. Near shore observations using current meters indicate that the c-axes are closely oriented in the direction of the average current. These observations have been further substantiated with laboratory work by Langhorne (1983), Langhorne and Robinson (1986) and others (A.J. Gow, personal communication, 1988).

Maximum ice thickness attained during a freezing season will vary due to climatic conditions and location. During the 1984 Marginal Ice Zone Experiment (MIZEX-84) in Fram Strait it was found that first-year ice thicknesses ranged from 38 cm in a newly frozen lead to 236 cm in a floe several km in diameter (Gow and Tucker, 1987). In Hebron Fiord, Labrador Gow (1987) found ice thicknesses of 150 cm with frazil generally confined to the

top 20-30 cm of the ice. Occurrences of thicker frazil are believed to be related to sustained turbulence in the water column (Gow, 1987).

Oceanic Frazil Production

In the coastal regions of the Arctic divers have observed accumulations of slush on the underside of congelation ice (Maykut, 1985). This slush may reach thicknesses of at least 2.5 m, however 50% or more of the layer appears to consist of unfrozen water. Frazil crystals form the bulk of the slush and large numbers of silt particles are often located in interstices between the frazil crystals. These particles are usually scavenged from the water column but direct entrainment by ice crystals forming on the sea floor can also occur. Upward loss of heat through the overlying congelation ice will eventually cause the interstitial water in the slush to freeze, producing a solid layer. Congelation ice then forms below the frozen slush (Weeks and Ackley, 1982). Biological activity is severely reduced by the presence of silt-laden ice. Below this ice light transmission and photosynthesis are negligible. Advection and melting of this ice after spring breakup could be important sediment transport mechanisms in the Arctic (Maykut, 1985). Most underice diving has taken place within a few kilometers of the coast and, therefore, it is not known whether such intense frazil generation also occurs in deeper water where little if any sediment would be entrained. In the Central Arctic frazil

production occurs in leads and in water below the ice, but there is little evidence from field data to suggest a significant effect on ice thickness (Maykut, 1985).

Several mechanisms dependent on supercooling and water column turbulence have been proposed to explain the occurrence of frazil ice in the oceans. Wind induced mixing is one mechanism. However, its effects are only felt near the surface and are rapidly damped out. With the uprise of water through the column toward the surface the pressure decreases and raises the freezing point producing supercooling and the potential for frazil formation. This mechanism is believed to be responsible for frazil production near ice shelves, icebergs and pressure ridge keels (Maykut, 1985). In addition, contact between water masses of different salinity which are each at their freezing point can cause ice to form at the interface through the process of double diffusion. This is a process in which descending brine gains heat but diffuses salt at a lower rate, cooling adjacent waters to a temperature below their freezing points. Ice crystals nucleate then rise and the remaining water descends at a new equilibrium freezing temperature and salinity (Weeks and Ackley, 1982). Along the Beaufort Sea coast permafrost extends beneath the sea floor promoting downward conduction of heat and the formation of anchor ice. Periodic release of anchor ice could contribute to sediment loading and ice accumulation at the bottom of the ice cover (Weeks and Ackley, 1982). While most of these mechanisms are location specific, frazil ice can also form as a result of thermohaline convection, a process associated with sea

ice throughout the polar regions (Maykut, 1985). Drainage of cold dense brine from within the ice sheet occurs during most of the year and produces descending plumes of brine that cause supercooling of adjacent water. This process results in the formation of hollow stalactites around the brine where it drains from the ice.

Multiyear Ice

The Arctic Basin is a closed system in which ice floes can drift for several years before they exit through Fram Strait or melt in place. As a result the multiyear ice zone in the Arctic (poleward of 75-80° N) contains approximately two-thirds of all multiyear sea ice found in the World Ocean (Maykut, 1985). Ice thickness averages 3-4 m in the central part of the basin and increases significantly north of Greenland and Ellesmere Island due to ice ridging. The age of the ice is uncertain but some may be as old as tens of years in the Beaufort Sea (Maykut, 1985).

During MIZEX-84 it was found that up to 85% of the ice exiting the Arctic Basin through Fram Strait was multiyear ice (Gow and Tucker, 1987; Tucker et al., 1987). The low percentage of first-year ice is either a result of deformation and crushing before the first-year ice enters Fram Strait or due to the fact that first-year ice does not exist in large quantities in the source regions (Gow and Tucker, 1987).

Arctic multiyear ice can be distinguished from first-year ice by several characteristics including its hummocky surface

caused by differential melt, its depressed salinity profile, annual layering (Weeks and Ackley, 1982), its greater thickness and its thick snow cover in some areas (Tucker et al., 1987).

Structurally, Arctic multiyear sea ice consists primarily of columnar ice. In Fram Strait, granular ice (mainly frazil) represents less than 25% of the total ice examined and less than 15% in undeformed floes (Tucker et al., 1987).

Differences in thermal mass strongly affect how the ice responds to conditions at the upper surface such that growth of thicker ice depends more on its thermal history than on the immediate heat balance at the surface (Maykut, 1987). Maykut and Untersteiner (1971) developed a model for multiyear ice which predicted growth rate as a function of ice thickness and season (Fig. 3). It can be seen that in November ice thicker than 3 m continues to ablate because fall cooling has not yet affected the bottom of the ice. By January cooling has penetrated all but the thickest ice. A 5°C air temperature in April is reflected by decreased growth rates in ice less than 3 m thick. Growth rates in thicker ice are unaffected by this warming and increase due to continued cooling at the bottom. A 10-15°C warming trend in May causes a sharp drop in the growth rate for thinner ice while the growth rate for ice thicknesses greater than 5 m is slightly larger than that for April. The magnitude of this spring warming effect decreases with increasing thickness and thus explains the predicted increase in the growth rate between 1-3 m (Maykut, 1987). Therefore, it can be seen that a linear temperature profile for thick ice is invalid. This nonlinearity is due to

the presence of brine pockets which act as thermal buffers that retard temperature changes (Maykut, 1985). As the ice cools, some of the entrapped brine begins to freeze, releasing latent heat and slowing the rate of cooling. Increasing the temperatures causes melting of the ice around the brine pockets and a decrease in the rate of warming (Maykut, 1987).

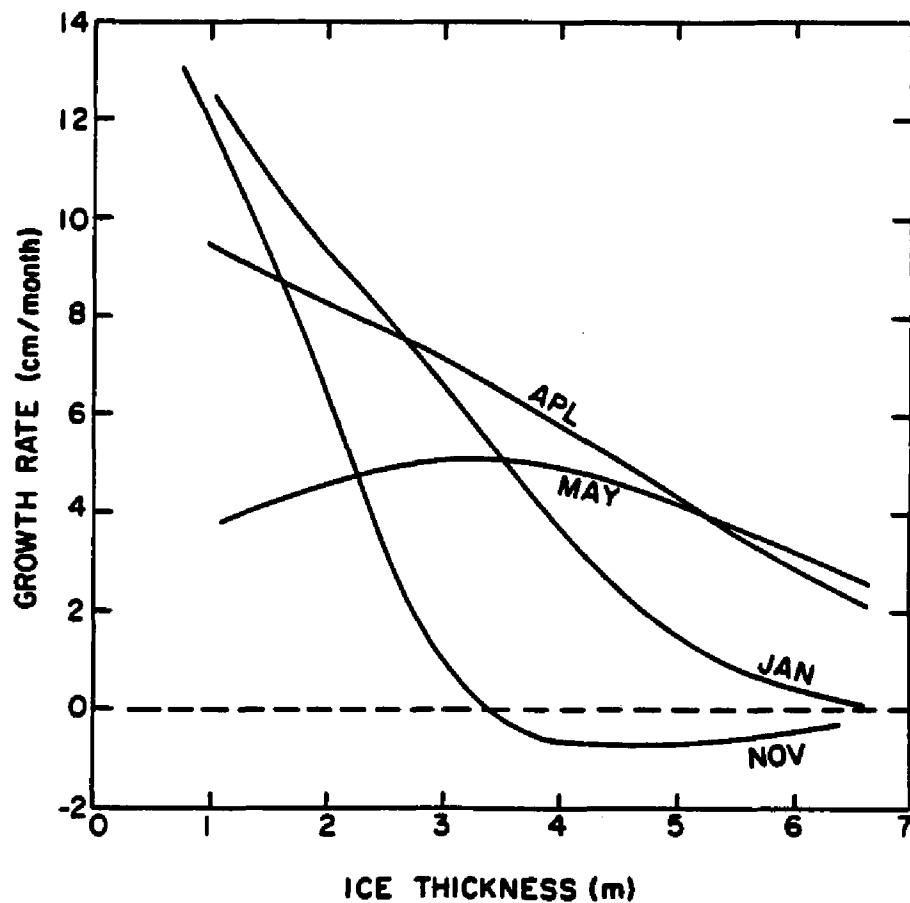


Fig. 3. Growth rates in multiyear and thick first-year ice as a function of season in the Central Arctic (From Maykut, 1987).

Equilibrium Growth

If interannual variations in atmospheric and oceanic forcing are small, the ice will attain an equilibrium thickness where summer ablation essentially balances net annual accretion (Maykut, 1985). The ice is then in thermodynamic equilibrium with the environment. Model simulations indicate that the equilibrium thickness is sensitive to factors that affect the amount of surface melting including: air temperature, ice albedo, incoming radiation and turbulent heat exchange (Maykut, 1985). Field observations show that undeformed older ice in the Arctic Basin ranges in thickness between 2-3 m (Gow et al., 1987 and Tucker et al., 1987), which is less than the theoretical equilibrium thickness (3 m) in the region (Maykut and Untersteiner, 1971). Although equilibrium ice in the Arctic may exist for any period of time, observations of floes discharging into Fram Strait show they do not exceed 4-5 years (Tucker et al., 1987). Ice which has reached its equilibrium thickness over an annual cycle will lose 40-50 cm of ice from the surface and will be replaced by an equal amount of new ice at the bottom (Maykut, 1985).

Summer Ice Decay

Significant differences exist in the summer melt cycle between regions of perennial ice, seasonal ice and coastal ice (Maykut, 1985). Summer ice decay in the Arctic begins with loss

of the snow cover as the surface air temperature rises above the melting point. Due to the lack of surface topography initial melting of seasonal ice produces melt pond coverage of 60% or more of the surface. The presence of melt ponds lowers the albedo and dust blown onto the ice in coastal regions further reduces it. Deepening of melt ponds cause a decrease in areal extent of ponds throughout the summer with values as low as 10% by the end of August (Maykut, 1985) with some ponds melting through the ice and connecting with the ocean. In coastal areas air temperatures are warmer than the ice and turbulent fluxes contribute substantially to melting. Lower albedos and thinner ice also allow greater input of solar energy to the underlying ocean in areas of seasonal ice. Therefore, even when incoming radiation fluxes are similar, ice decay proceeds more rapidly in coastal regions and areas of first-year ice than in the interior pack (Maykut, 1985).

Annual Layering

Horizontal layers believed to develop during the annual thaw cycles have been observed in multiyear Arctic sea ice (Cherepanov, 1957 and Schwarzacher, 1959). Two types of layering have been identified. The most commonly observed is a 2-5 mm thick layer, milky white in color with a sharp upper boundary and an irregular lower boundary. The origin of this layer is uncertain but it appears to form during the summer after the ice has stopped growing (Weeks and Ackley, 1982). The milkiness may

be associated with biological activity at the ice/water interface (Cherepanov, 1957 as cited in Weeks and Ackley, 1982). The formation of the milky layer does not appear to be associated with recrystallization or nucleation of new grains since new growth proceeds on existing crystals with no apparent change in crystallographic orientation (Schwarzacher, 1959). The second type usually consists of a 1-10 cm thick layer that shows a sharp decrease in grain size (Weeks and Ackley, 1982). The ice in these layers does not have the platy substructure of sea ice and the salinity is usually much less (1-1.5 o/oo) than in the surrounding layers of congelation ice (Weeks and Ackley, 1982). The formation of this layer is the result of surface meltwater that penetrates beneath the ice and freezes onto the bottom of the floe. The freshwater may originate via flow through natural drain holes or by runoff into nearby leads that subsequently close (Weeks and Ackley, 1982).

Salinity Distribution in Sea Ice

A delicate layer of long vertical ice platelets with parallel layers of brine inclusions exists on the underside of growing sea ice. When seawater freezes most impurities are rejected from the ice lattice resulting in plates of pure ice. The plates originate as dendrites with tips protruding downward into the seawater. It is between these dendrites that brine is systematically trapped. The plate width can vary from a few tenths of a millimeter to 1 mm and is dependent on the rate of

growth. The faster freezing occurs, the narrower the plate spacing and the greater the salinity.

Changes in this substructure occur in response to changes in the thermal regime of the ice, therefore, day-to-day variation in surface air temperature can cause significant changes in the geometry of the inclusions and the concentration of the entrapped brine. With increased warming disconnected brine inclusions coalesce into vertical channels which can lead to redistribution of the brine, drainage and desalination of the ice. Untersteiner (1968) described four mechanisms by which brine is drained from the ice: 1) migration of fluid inclusions through ice crystals, 2) brine expulsion, 3) brine drainage and 4) flushing. Brine pocket migration is stimulated by maintaining phase equilibrium thus the temperature gradient in the ice establishes a concentration gradient in brine pockets. This causes diffusion of solute from the cold, saline upper end of the brine pocket to the warmer, less saline lower end of the pocket. The ice at the warm end of the pocket dissolves while freezing occurs at the cold end, resulting in the migration of the brine pocket toward the warm side of the ice (Weeks and Ackley, 1982).

Brine expulsion occurs when a pressure buildup occurs in the brine pockets to the point where the liquid portion of the inclusion separates from the vapor bubble. This pressure may become sufficient to cause the surrounding ice to fail along the basal planes allowing brine to escape and migrate toward the warm side of the ice sheet. It has been found that brine expulsion

accounts for only a minor amount of the desalination of first-year ice (Cox and Weeks, 1974).

Gravity drainage is the process whereby brine under the influence of gravity drains out of the ice sheet into the underlying seawater. As the ice thickens its surface gradually rises above sea level to maintain isostatic equilibrium producing a pressure head in the interconnected brine channels which drives the underlying brine out of the ice. Because the density of the brine in equilibrium with the ice is determined by the temperature distribution during the time when the temperature within the ice increases downward an unstable vertical density distribution exists within the brine channels in the ice. This produces convective overturning of the brine within the ice as well as an exchange between the denser brine within the sea ice and underlying seawater (Weeks and Ackley, 1982). Cox and Weeks (1975) determined that this may be one of the dominant desalination mechanisms in sea ice.

Flushing is a type of gravity drainage that occurs in spring and summer due to the hydrostatic head produced by surface meltwater. It is believed that flushing is the most effective mechanism for desalination because the time when flushing starts corresponds to the time during the spring and early summer when major changes occur in the salinity of the ice (Weeks and Ackley, 1982).

Cox and Weeks (1974) produced plots of average salinity versus ice thickness in the Arctic for cold ice (Fig. 4) and warm ice (Fig.5). For cold ice a linear decrease in salinity

associated with an increase in thickness to approximately 0.4 m occurs, where the slope abruptly changes (Fig. 4) indicating a possible shift in the dominant desalination mechanism from brine expulsion to gravity drainage. The relationship between salinity (S_i) in o/oo and thickness (h) in meters can be represented by two best fit regression lines based on thickness:

$$S_i = 14.24 - 19.39h \quad h < 0.4m$$

$$S_i = 7.88 - 1.59h \quad h > 0.4m$$

A plot of S_i versus h values for warm ice (Fig. 5) shows that the average salinity of warm ice is lower than that observed for cold ice of similar thickness. A linear regression line for this data gives:

$$S_i = 1.57 + 0.18h$$

Although a wide range of growth conditions is represented, salinity as a function of thickness displays little scatter.

Tucker et al. (1987) and Gow et al. (1987) found a sharp distinction between bulk salinities of first-year and multiyear ice from Fram Strait (Fig. 6). For warm multiyear ice the best fit regression is:

$$S_i = 1.58 + 0.18h$$

The best fit regression for warm first-year ice is:

$$S_i = 3.75 + 0.22h$$

It can be seen that the least squares fit for multiyear ice is in excellent agreement with Cox and Weeks (1974). Overgaard et al. (1983) on the YMER-80 cruise in the Greenland and Barents Seas found a linear regression for first-year ice of:

$$S_i = 2.15 + 0.19h$$

and a best fit regression for multiyear ice:

$$S_i = 1.59 + 0.37h$$

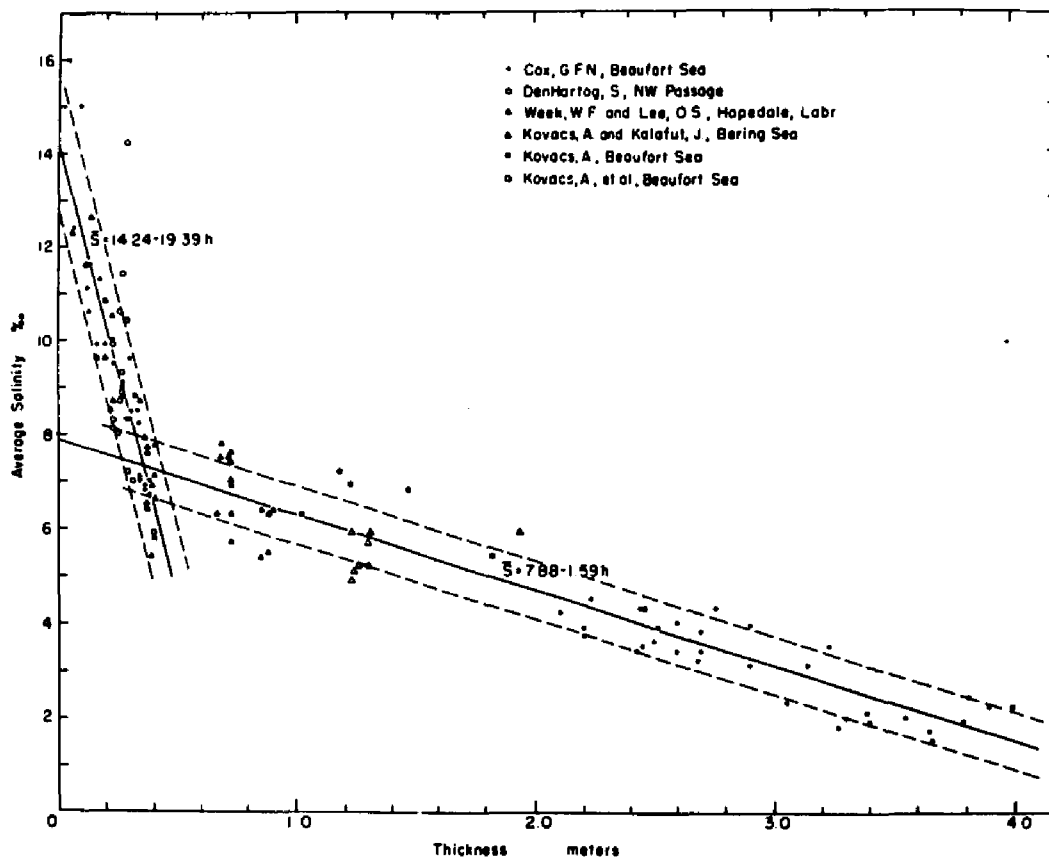


Fig. 4. Average salinity of sea ice as a function of ice thickness for cold ice samples during the growth season (From Cox and Weeks, 1974).

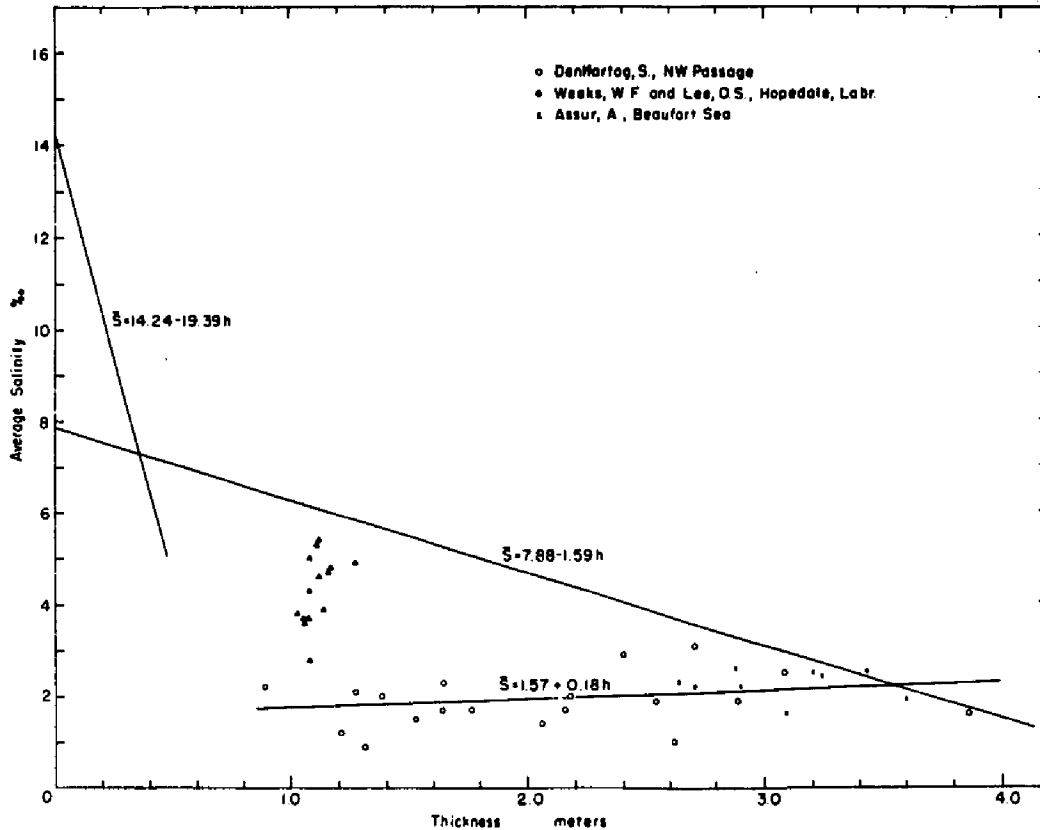


Fig. 5. Average salinity of sea ice as a function of ice thickness for warm sea ice sampled during or at the end of the melt season (From Cox and Weeks, 1974).

The YMER-80 first-year ice data indicate lower salinities than those found by Cox and Weeks (1974) and Tucker et al. (1987). The YMER-80 samples were collected later in the summer than the other reported data and the results are consistent with the trend of decreasing ice salinities during summer warming (Tucker et al., 1987 and Gow et al., 1987). The slope for the multiyear YMER-80 data has a slope that is twice that found by either Cox and Weeks (1974) or Tucker et al. (1987) and Gow et al. (1987). This indicates that thicker ice sampled during YMER-80 was more saline (0.8 o/oo for 3.0 m thick ice) but the differences may not

be significant due to the large scatter in bulk salinities in thicker ice (Tucker et al., 1987).

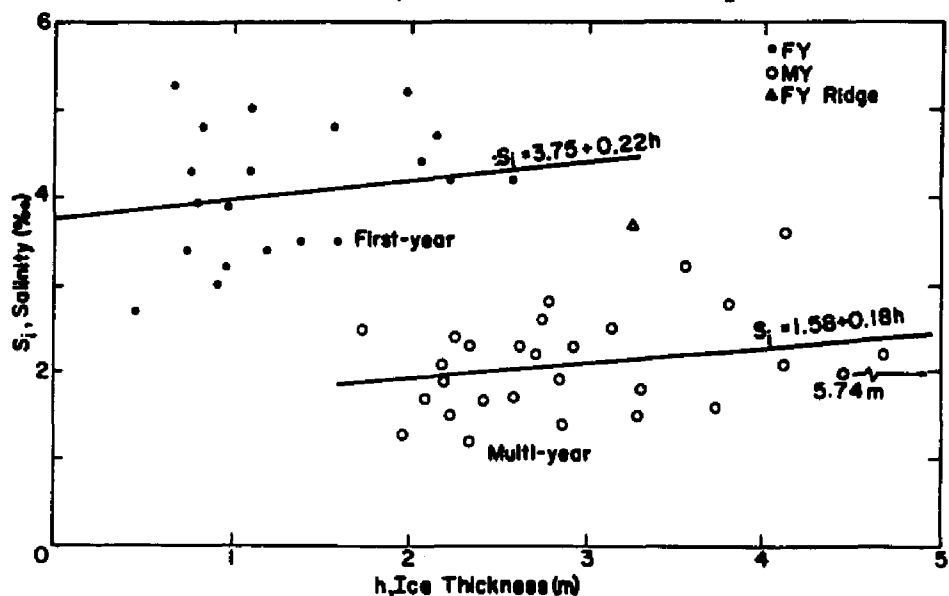


Fig. 6. Bulk salinity values of ice cores as a function of floe thickness (From Gow et al., 1987).

Salinity profiles of melt hummocks differed significantly from those of depressions in the Arctic. Hummocks showed an increase in salinity with depth from 0 ‰ at the surface to approximately 4 ‰ at the bottom whereas depressions showed large, irregular salinity fluctuations, and the upper layers showed salinity values up to 6.3 ‰. In general Cox and Weeks (1974) found that salt content is lower in the upper portion of the hummock than in the adjacent depressions. The salinity of the ice beneath the depressions is both greater and more variable. The salinity in the center of the ice is distributed irregularly with isolated high and low salinity pockets. The lower more uniform portion of the ice represents growth from the

previous winter. The low salinity of the upper portions of the hummocks is due primarily to brine drainage by flushing. A strong inverse correlation was found between the average salinity of the ice and the ice thickness such that as the ice thickness increases, the average salinity decreases.

Tucker et al. (1984) studied small-scale horizontal variations of salinity profiles in a first-year ice sheet and found that substantial horizontal variations occur in closely spaced ice cores. For cores spaced from 38 to 76 cm apart, the bulk deviations range from 0.2 to 0.78 o/oo; an average deviation of 0.39 o/oo was found between salinities from the same depth levels. The maximum salinity difference at a given level was 2.0 o/oo. These results confirmed observations made earlier by Untersteiner (1968). General trends of higher salinities at top and bottom and in the granular ice occurred in all profiles, but the peak salinities of these features were substantially different. It is believed that these variations result from the irregular distribution of brine drainage channels in the ice.

Chemistry of Sea Ice

A phase diagram for standard sea ice (sea ice of a composition such that its meltwater will have the same relative concentration of ions to each other as normal seawater) has been developed by Assur (1960) (see Fig. 7). The diagram assumes that the ratios of the ions relative to each other remain constant. If they vary, the crystallization temperatures of the solid salts change. With cooling, ice forms and the remaining

brine becomes more saline. As cooling continues, different solid salts precipitate from the brine. However, they precipitate over a temperature range rather than at a fixed eutectic temperature. From temperatures as low as -70°C small amounts of brine are believed to be present in the ice and at least five solid salts have precipitated in the order listed: calcium carbonate, sodium sulfate, sodium chloride, potassium chloride and magnesium chloride (Weeks and Ackley, 1982). Therefore, temperature gradients in sea ice provide a means of selectively mobilizing specific cryohydrates which leads to fractionation and variation in major element ratios.

Additional and more detailed chemical studies have been performed in which the major ion concentrations and fractionation trends were determined. Reeburgh and Springer-Young (1983) determined that $\text{SO}_4\text{-Cl}$ ratios in ice are different from the ratios in seawater. On aging, SO_4 in the ice is mobilized and removed in a constant ratio to Cl , indicating conservative behavior. A comparison of first-year and multiyear ice chemistry suggests that fractionation occurs during ice formation, but that further fractionation within the ice does not occur. It was also found that CaCO_3 is the only sea water cryohydrate with a high enough eutectic temperature to survive a summer thermal cycle and thus alkalinity may be useful as a means of determining the age of sea ice in addition to being a meltwater tracer.

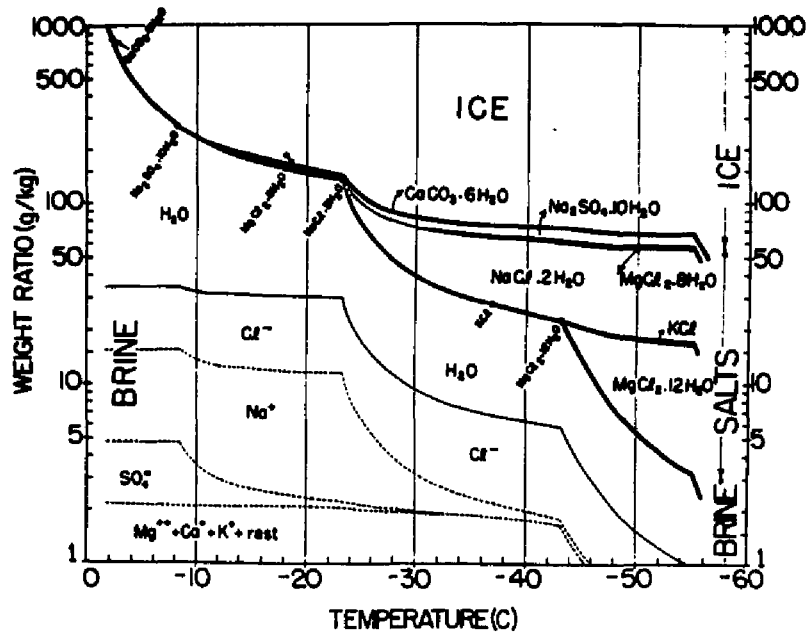


Fig. 7. Phase diagram for "standard sea" ice. Circles on the brine-salt line indicate temperatures at which the different salts precipitate (From Assur, 1960).

Addison (1977) studied ion concentrations in sea ice from Churchill, Manitoba and found that in a 30 cm sample concentrations of chemical species varied with depth (Fig. 8). The top 7 cm had a high salinity. At approximately 7 cm (which corresponded to the structural transition zone between frazil and congelation) peaks are seen in the Na, Cl and SO₄ curves. Below this, the salinity and other major element concentrations fell off as the structure became more regular. At greater depth, the salinity again increased, possibly as a result of faster freezing resulting in an increase of brine entrapment. The SO₄ profile is different from the others. A zone of lower salinity occurs between 7-15 cm, and the difference in the sulfate curve arises, at least in part, from downward brine transport. The high values of SO₄/Na ratio at the transition layer, suggest that solid

Na_2SO_4 was left behind in an area that had suffered a depletion of brine through drainage and migration. In general, however, it was found that the impurity ratios in sea ice remain similar to those in seawater.

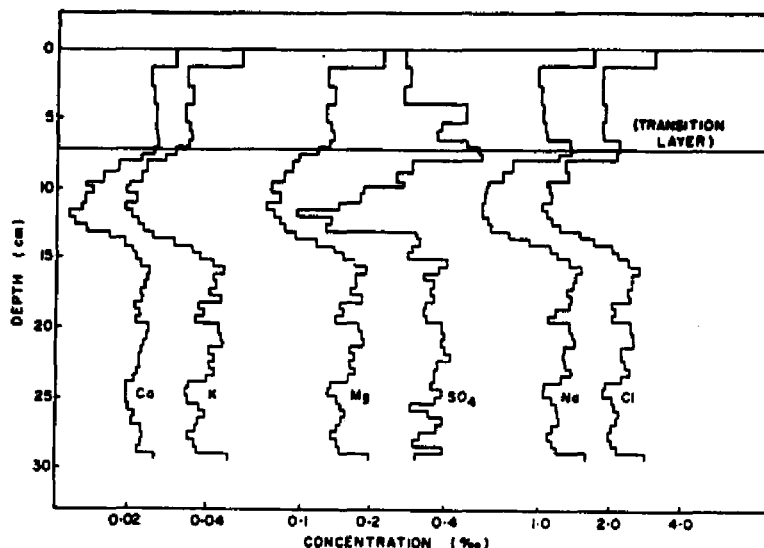


Fig. 8. Ion concentration profiles for sea ice from Churchill, Manitoba (From Addison, 1977).

Anderson and Jones (1985) studying several Arctic sea ice samples of varying types demonstrated the occurrence of enrichment and depletion in the SO_4/Cl ratios. Ca and alkalinity concentrations were also determined. It was found that the CaCO_3 which precipitates in sea ice as it forms and ages does not totally redissolve when the ice melts. They also concluded that a typical composition for sea ice does not exist nor is there one that corresponds closely to that of sea ice produced in the laboratory. These and other studies in which chemical concentrations of various species were determined are summarized in Appendix A. It can be seen that there is a wide variation in the chemical species analyzed between studies and most data

represents analyses from one or two ice samples. Also, there is little consistency in sample location and sample sectioning.

Clarke and Ackley (1984) found that rapid ice growth is important in determining the distribution and structure of the biological and chemical components in the ice. They hypothesize that frazil ice can incorporate cells by two mechanisms, either by cells stimulating nucleation of frazil ice crystals or by incidental incorporation (scavenging) of cells as frazil crystals float through the water column. This results in higher initial chlorophyll-a in the ice than in the water (Clarke and Ackley, 1984). However, in congelation ice growth algal cells may be rejected by processes similar to brine rejection. For frazil ice correlations were shown between chlorophyll-a and depth, phaeopigment and ice type and chlorophyll-a and phaeopigment, indicating that surface samples are lower in chlorophyll-a than samples at depth, however, the relationship is not continuous with depth (Clarke and Ackley, 1984). In congelation ice it is believed that the biological community may be enhanced by passive water exchange in the lower ice. This process allows nutrients to be cycled continually. Water exchange replenishes the nutrients, thereby not limiting biological growth (Clarke and Ackley, 1984). It was also found that salinity and nutrient concentrations are higher in the surface waters and reduced in the ice. When nutrient values were plotted against the salinities of the ice cores along with curves based on values from surface water diluted to the salinity of the ice samples

(dilution curves), the following conclusions were made (Clarke and Ackley, 1984): 1) PO_4 values are of similar magnitude to the dilution curve, 2) SiO_4 and NO_3 are depleted in the ice relative to the surface waters due to diatom growth and 3) NO_2 values in the ice exceed those in the surface waters due to nitrification of NH_4 by bacteria.

Study Area Description

In 1968 oil was discovered at Prudhoe Bay, Alaska. Since then industrial activity has increased as a result of offshore lease sales and drilling for oil from natural and artificial islands. Because of this activity, large programs of biological and physical studies of the marine ecosystem were funded to provide background information for environmental impact statements (Barnes et al., 1984).

The continental shelf of the southern Beaufort Sea is less than 150 km wide in most places and is shallow. The shelf break occurs over most areas at approximately 65 m in depth. Between Barrow and Barter Island, the slope has the classical features of a steep upper slope and a more gentle lower slope descending to floor of the deeper basin (Hufford, 1974).

Annual runoff into the Beaufort Sea is approximately 813 km^3 per year (Antonov, 1958). Approximately 50% of the runoff is from the Colville, Kuparuk, Sagavanirktok and Canning rivers (Fig. 9). Approximately 80% of the total discharge occurs in June (Hufford, 1974). Runoff from the Kuparuk and Sagavanirktok

rivers may have an impact on many of the first-year ice samples collected in 1987 for this study.

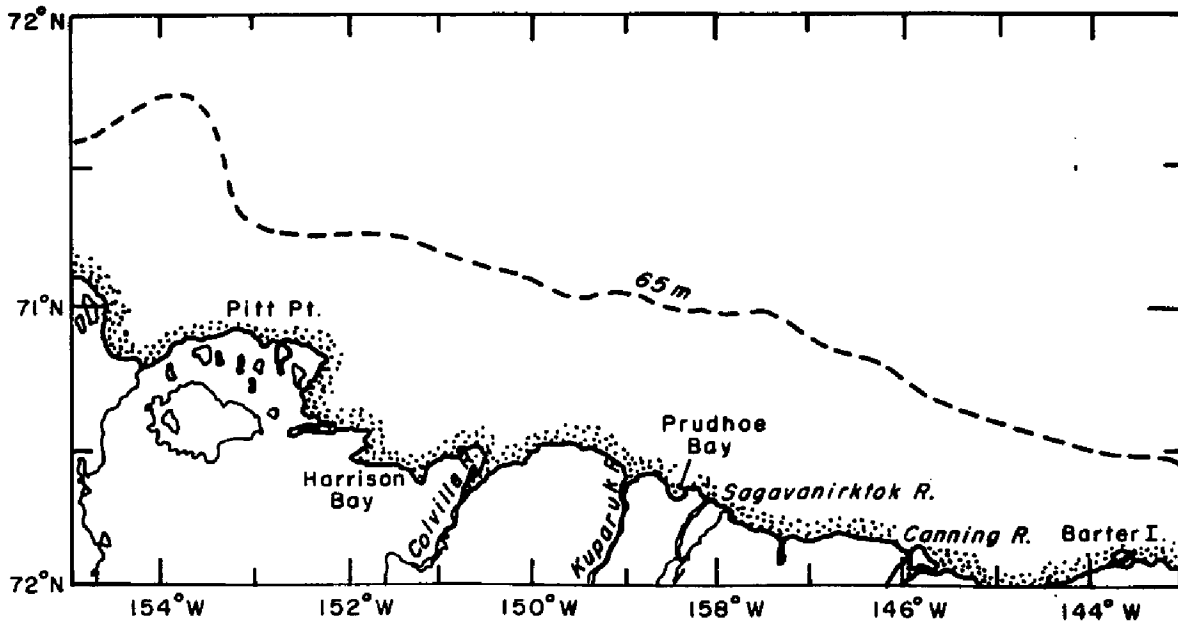


Fig. 9. Location map showing major rivers in the Prudhoe Bay area. Dashed line represents shelf break (From Hufford, 1974).

In the southern Beaufort Sea landfast ice forms in the fall and by late winter may extend as much as 50 km offshore. The ice pack shears against the landfast ice creating an extensive pressure ridge system that is usually grounded (shear zone) in shallow areas. The presence of this ice and the force that it exerts against offshore structures has been a major concern for the oil industry.

The Southern Beaufort Sea is composed of three major water masses of the Arctic Ocean: 1) Arctic Surface water comprises the top 250 m. This water comes from the Bering Sea through the Bering Strait and Chukchi Sea. Below this (250-900 m) is Atlantic Water below which is Arctic Bottom Water (Hufford,

1974). Bering Sea-Chukchi Sea water is present in the arctic surface water mass in the Southern Beaufort Sea in three layers: near surface, with temperatures above 0°C; at 75 m where the water is characterized by a subsurface temperature maximum (when overlain by cold, less saline local surface water); and at 125 m (identified by a temperature minimum that represents Bering Sea-Chukchi Sea winter water). Oceanographic processes on the Beaufort Sea shelf are influenced by the southern edge of the anticyclonic Beaufort Gyre which creates a region of westward water and ice motion (Aagaard, 1984). However, at the 50 m isobath (the outer edge of the continental shelf) the average subsurface motion is a strong flow in a mean easterly direction known as the Beaufort Undercurrent (Aagaard, 1984) originating in the Bering Sea. Current measurements indicate that the flow of the 3 major water masses is similar (Hufford, 1974) with current speeds averaging between 0-8 cm/sec. Coastal currents depend on wind conditions and velocities vary between 0-60 cm/sec (Hufford, 1974).

The distribution of biota along the Beaufort coast is a reflection of the effects of water and ice movements, water mass and bottom characteristics and the availability of food. Many species congregate at the MIZ and move with the ice. In the coastal environment along the barrier islands, simple food webs reach summer peaks of secondary biological productivity greater than those in the open Arctic seas (Craig, 1984).

II. OBJECTIVES

- The primary objective of this study is to determine what, if any, chemical trends exist in sea ice in the Southern Beaufort Sea, and to what extent those trends can be related to physical and structural properties of the ice.

The Southern Beaufort Sea was chosen for this study because sea ice floes from other parts of the Arctic Ocean are brought into the area by the Beaufort Gyre and are frozen in during the winter thereby providing an opportunity to study ice from a variety of source locations in the Arctic. In addition, this project was part of a much larger study in which the inclusion of chemical properties measurements was considered an important adjunct to ice thickness and physical property studies of Beaufort sea ice.

To date, detailed chemical analyses (including major ions and nutrients) have not been conducted on sea ice to the extent that it has on sea water. Previous studies on sea ice have included analyses of some of the major species or nutrients but a comprehensive study had not yet been performed. Therefore, through this study, it will be determined what, if any, relationships exist between the major ions and nutrients.

- The second objective is to determine the extent of chemical fractionation in the ice.

Ratios of the various chemical species compared to those of the underlying seawater or standard seawater will allow for

determination of fractionation patterns in the ice. To date, too few systematic measurements have been made to determine if definitive trends exist.

- The third objective is to determine if variations in the concentrations of chemical species with depth can be correlated with changes of ice type (snow ice, frazil and congelation).

Thus far the only report of any correlation between chemical species variation and ice structure is that of Addison (1977) working in the transition between frazil and congelation ice in the upper layers of Arctic sea ice.

III. METHODOLOGY

Sample Collection

Sea ice and surface water samples were collected during April-May of 1986 and 1987 in the Beaufort Sea, north of Prudhoe Bay (Fig. 10). In 1986 a total of 7 multiyear and 3 first-year ice cores were collected and during the 1987 field season 3 multiyear cores and 7 first-year cores were collected (see Fig. 10 and individual core descriptions for core locations). This study was part of a much larger project, therefore, cores were taken whenever possible. In 1986 it was necessary to travel as far as 60 miles north of Prudhoe Bay to locate multiyear ice floes and, therefore, the majority of the time was spent at these locations. However, in 1987, multiyear ice was found closer inland which allowed more time to collect first-year ice samples.

Ice samples were collected using a power driven 4" diameter coring auger. The core was removed from the barrel immediately and holes were drilled into the ice every 10 cm along the length of the core in order to measure ice temperatures using an Omega 866 thermometer that is accurate to $\pm 0.2^{\circ}$ C. In order to prevent brine loss the bottom 20 cm of each core was immediately cut into two 10 cm long pieces in the field and placed in precleaned containers. The remainder of the core was wrapped in plastic tubing, placed in core tubes and flown to the laboratory at Prudhoe Bay for further sectioning. All containers were precleaned by rinsing 3 times with double-distilled deionized

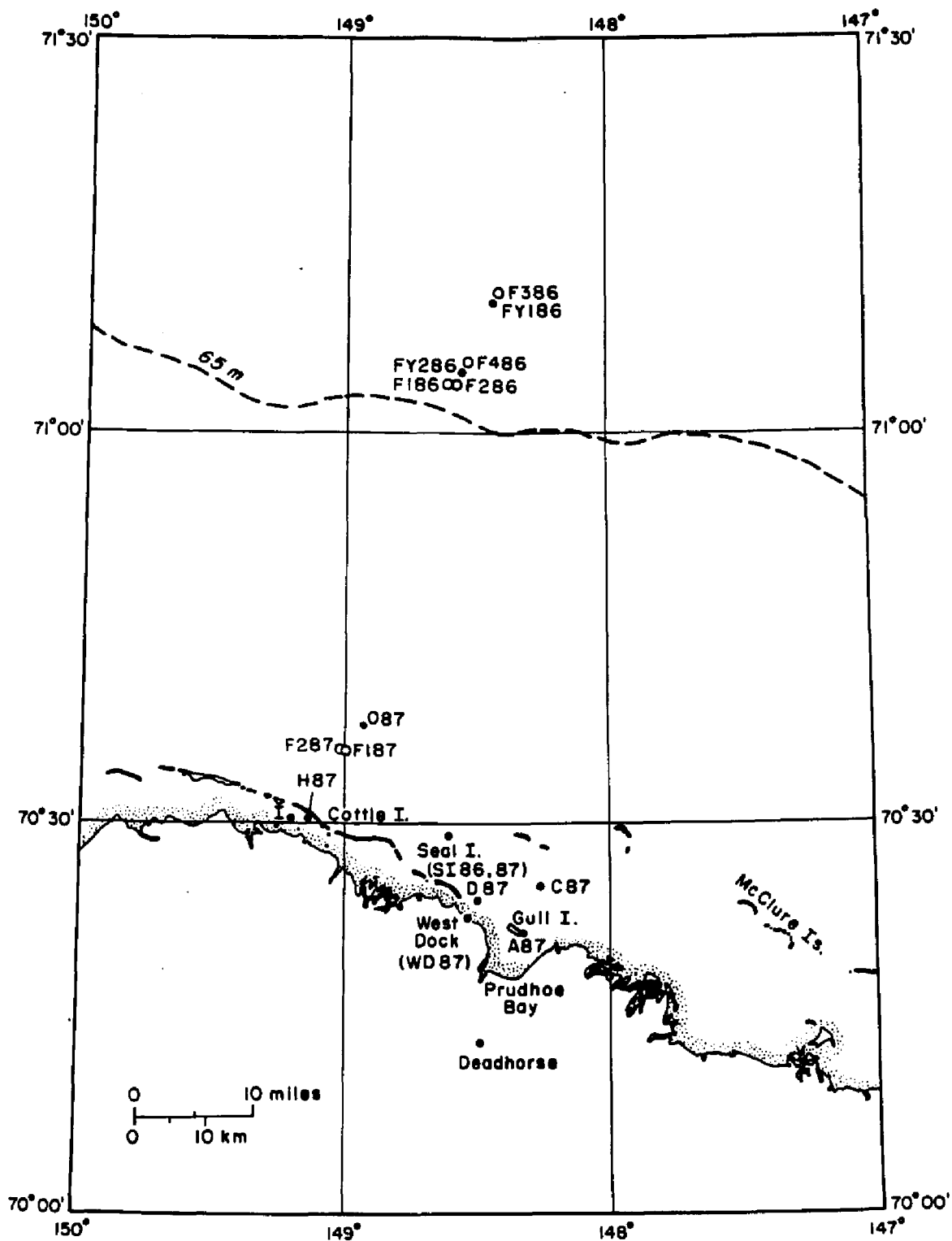


Fig. 10. Location map of sampling area. • represent first-year sites and o represent multiyear sites. The dashed line is the 65 m depth contour.

water (Milli-Q water), filling, allowing them to soak overnight and then rinsing 3 times before they were shipped.

Whenever possible, a water sample from the ice/water interface was collected. After a core had been drilled the hole was cleaned of remaining ice chips. Water samples were then collected in polyethylene scintillation vials for major element and nutrient analyses and a 1 liter polyethylene bottle of seawater was collected for chlorophyll-a analysis.

As soon as possible after the cores were collected, a vertical slice approximately 0.5 cm thick was taken from the cores and examined between crossed polarized sheets to determine the nature and structure of the ice crystals, ice type and the location of structural breaks. Horizontal and vertical thick sections of major structural features and discontinuities were taken at the same time and set aside for shipment back to CRREL. Cores were then sectioned every 10 cm (or at major stratigraphic breaks) for chemical analyses.

During the 1986 field season the outer 2 cm of each sample was cut off with a band saw following which the samples were rinsed with Milli-Q water that had been shipped from UNH and placed in precleaned freezer containers. The samples were rinsed in this manner to eliminate any contaminants introduced during sampling and preliminary handling. To examine the effects of potential contamination, a separate study was conducted in which a core was cut in half vertically. One half was prepared using clean techniques (handling with plastic gloves, discarding the outer 2 cm and rinsing each sample) and the other half was

prepared by simply cutting sections with the band saw and placing them directly in containers. Because of small scale horizontal salinity variations known to occur in sea ice (Tucker et al., 1984) it is difficult to determine the variation that may occur naturally due to irregular locations of brine channels, chemical fractionation or contamination. It was determined, however, that in samples with the same salinity occurring at the same depth the chloride difference between the two samples was less than 2% which is less than analytical error. Therefore, since it was determined that the elaborate procedures of removing the outer portions of the core and rinsing were not necessary no such prior processing of samples was performed on 1987 samples.

The 1986 samples were shipped frozen to CRREL and stored at -20° C until they were analyzed for nutrients. They were thawed at room temperature and meltwater salinities measured with a Beckman Type RB-5 Solu-Bridge (accurate to 0.2 o/oo). An aliquot of each sample was taken for each constituent to be analyzed and the samples were then refrozen until analysis except for the nutrient samples which were analyzed immediately. In 1987 access to an AutoAnalyzer II at Prudhoe Bay provided an opportunity for immediate nutrient analysis. Therefore, after sectioning, samples were thawed at room temperature, their salinities measured and 3 aliquots of each sample poured into 30 ml polyethylene scintillation vials. One sample was used for nutrient analysis and the remaining vials were taped shut, stored in the dark and shipped to CRREL.

Water samples were collected through the core holes in the ice and brought back to Prudhoe Bay, where salinity and nutrient concentrations were measured before storing them with the ice samples. Additional water samples were collected for chlorophyll-a determination. These samples were filtered as soon as possible after collection and the filters frozen and stored in the dark until analysis.

Blanks

Several sets of blanks were prepared to determine levels of contamination from sample handling, storage, containers and sample transport. As sample containers were cleaned 10 were refilled with Milli-Q water after the final rinse, taped shut, placed in polyethylene bags and shipped with the empty containers (wet blanks). Another set was left empty after the final rinse, taped shut, placed in polyethylene bags and shipped (dry blanks). Half of the containers were returned to CRREL empty and filled with Milli-Q water for a minimum of 48 hours before beginning detailed chemical analyses. The remaining containers were filled with Milli-Q water at Prudhoe Bay. The latter were analyzed for nutrient contamination. These containers were then shipped back to CRREL with the remaining water for further analyses (see Table 1 for blank results).

The scintillation vials for the 1987 samples were shipped to Prudhoe Bay after it was determined that we had access to a Technicon AutoAnalyzer for nutrient analyses. They had not been

precleaned so each vial was rinsed 3 times with sample before it was filled to eliminate any surface contaminants. Blanks for unrinsed scintillation vials appear in Table 1 as scintillation vial blanks 3A-6B and represent the maximum contamination possible.

The 1986 blanks analyzed for major elements were all below the detection limit for each species. Some of the nutrient blanks had slightly elevated concentrations (Table 1) that may indicate some contamination during shipping, however, the levels were low enough that they were considered to be insignificant.

The 1987 blanks analyzed for major elements showed a wider range of concentration. Wet blanks (those filled with Milli-Q water at CRREL: Blanks 1-3) had Cl concentrations that ranged from 18.8-52.6 ug/l. All of these containers leaked during shipping and it is believed that this is the source of contamination. Previous studies performed by the Glacier Research Group at UNH have shown contamination in blank containers stored in polyethylene bags that have leaked substantiating the above (M.J. Spencer, personal communication). Dry blanks (those shipped with samples and filled approximately 48 hours before analyses: Dry blanks 2-5) showed detectable levels of Cl and SO₄ (6.91-11.8 and ND-3.47 ug/l, respectively). Although slight contamination is indicated, these levels are insignificant when compared to the high concentrations of the sea ice samples. Dry Blanks 6A and 6B and the scintillation vial blanks were filled with Milli-Q water in Prudhoe Bay that had been shipped from CRREL. Cl and SO₄ concentrations in these

blanks are high (20.2-off scale and 31.8-186 ug/l, respectively). As these blanks are the only blanks that had significant levels of Cl and SO₄ it is believed that the Milli-Q water shipped to Prudhoe Bay was contaminated and these levels are not an indication of container or sample contamination. Since this water was used only for making blanks it did not pose any problems with respect to sample contamination.

Table 1. Results of blank analyses. Blanks that were below the detection level are indicated by ND.

	Cl (ug/l)	Br (ug/l)	SO ₄ (ug/l)	Na (mg/l)	Ca (mg/l)	K (mg/l)	Mg (mg/l)
<u>1986 Blanks</u>							
Blank 1						ND	ND
Blank 2						ND	ND
Blank 3						ND	
Blank 4							ND
Blank 5							ND
Dry Blank 1					ND		ND
Dry Blank 2				ND		ND	ND
Dry Blank 3	ND	ND	ND		ND		ND
Dry Blank 4	ND	ND	ND		ND		ND
Dry Blank 5	ND	ND	ND		ND		ND
<u>1987 Blanks</u>							
Blank 1	18.8	ND	1.11	ND	ND	ND	ND
Blank 2	23.2	ND	27.4	ND	ND	ND	ND
Blank 3	52.6	ND	11.2	ND	ND	ND	ND
Blank 4						ND	
Dry Blank 1	6.91	ND	3.47	ND		ND	
Dry Blank 2	8.09	ND	ND		ND		ND
Dry Blank 3	11.8	ND	ND		ND		ND
Dry Blank 4	8.23	ND	ND		ND		ND
Dry Blank 5						ND	
Dry Blank 6A	Off Scale	ND		ND		ND	
Dry Blank 6B	Off Scale	ND	186	0.1		ND	
<u>Scintillation</u>							
Vial Blank 3A	20.5	ND	32.3		ND		ND
3B	20.2	ND	31.8		ND		ND
6A	70.8	ND	85.4		ND		ND
6B	144	ND	ND		ND		ND

Table 1. (cont.)

1986 Blanks

	PO4 (uM)	SiO4 (uM)	NO3 (uM)	NO2 (uM)	NH4 (uM)
Blank 1	0.05		0.25		
Blank 2	0.07		0.16		
Blank 3	ND	ND			0.17
Blank 4		ND			0.15
Blank 5		ND	0.07		0.24
Dry Blank 1	ND	ND	0.09		0.13
Dry Blank 2		ND	0.09		0.4
Dry Blank 3		ND	ND		0.06
Dry Blank 4		ND	0.04		0.11
Dry Blank 5		ND	ND		0.07

1987 Blanks

Blank 1	ND	ND	ND	ND	ND
Blank 2	ND	ND	ND		ND
Blank 3	LOST	ND	ND		ND
Blank 4	LOST	ND	ND	ND	ND
Dry Blank 1	ND		ND		
Dry Blank 2		ND		ND	
Dry Blank 3		ND		ND	
Dry Blank 4		ND		ND	
Dry Blank 5	ND	ND	ND		ND

Scintillation

Vial Blank 3A	ND		ND		
3B	ND		ND		
6A	ND	0.15			
6B		ND	0.2		

Scintillation

Vial Dry Blank 6A			ND	0.3	
-------------------	--	--	----	-----	--

6B ND 0.3

Chemical Analyses

Two types of chemical species were analyzed. The first type are the conservative or major elements in seawater and include Cl, Br, SO₄, Na, Ca, K and Mg. Throughout this report they will be referred to simply as major elements. The second type of species are nutrients (PO₄, SiO₄, NO₃, NO₂ and NH₄). A list of the analyses performed and methods used is shown in Table 2. All analyses were conducted using standard techniques. Nutrients for the 1986 samples were analyzed using the techniques of Glibert and Loder (1977) and 1987 samples were analyzed using the techniques of Whitley et al. (1981). The ion chromatograph analyses were conducted using an eluent of 1.125 mM sodium bicarbonate and 3.5 mM sodium carbonate. Chlorophyll-a and phaeopigment concentrations were determined on selected samples using the techniques of Strickland and Parsons (1972).

Table 2. List of analyses, methodology and detection limits.

Chemical Species	Instrument	Detection Limit	Accuracy	Reference	
Cl	Ion Chromatograph	32.1 ug/l	+/-3%	Dionex Corp. (1987)	
Br		3.65 ug/l	+/-5%		
SO ₄		4.6 ug/l	+/-3%		
Na	Atomic Absorption	0.01 mg/l	+/-3%	Perkin Elmer Corp (1976)	
Ca		0.2 mg/l	+/-5%		
K		0.1 mg/l	+/-5%		
Mg		0.05 mg/l	+/-5%		
PO ₄	AutoAnalyzer II	0.02 uM	0.02 uM	1986 Samples-Glibert and Loder (1977)	
SiO ₄		0.1 uM	0.05 uM		
NO ₃		0.04 uM	0.05 uM		1987 Samples-Whitley et al (1981)
NO ₂		0.01 uM	0.05 uM		
NH ₄		0.03 uM	0.05 uM		

Atomic absorption spectrophotometric analyses (AA) were conducted using standard techniques (Perkin Elmer, 1976). It was

not known whether there would be a matrix or chemical interference problem with the Ca, K and Mg analyses, therefore, several experiments were conducted to determine if a matrix modifier was necessary for any of these analyses. In each case, standards were prepared using diluted AA standards and another set prepared using Copenhagen seawater. Because the sea ice samples are frozen seawater it is believed that the matrix effect may be eliminated using standard seawater for standards and diluting both standards and samples in the same manner (Kaltenback, 1976). To determine whether this is valid for low salinity ice samples the two types of standards were compared for each element. In addition, a mixture of lanthanum and cesium, following the method of Smith et al. (1983), was added and compared to the above standards. It was determined that the difference between dilute AA standards (Baker) and dilute Copenhagen seawater was less than 1% (Table 3). Standards with the lanthanum-cesium mixture compared to standards without the mixture were consistently higher and had variations of less than 10% within the linear range for each constituent (Fig. 11). Standard additions (Perkin Elmer, 1976) were performed for 3 samples. A comparison of expected concentration versus actual concentration in the standard addition test showed a variation of less than 10% for each constituent (Table 4 and Fig. 12). In addition, Copenhagen seawater was diluted, analyzed and compared to regular standards and seawater standards. In all cases, the seawater was within 2% of the expected concentration and, therefore, standard seawater was used to make all standards.

Based on these results it was determined that although absorbances were enhanced with the lanthanum-cesium mixture, the remaining results were sufficiently accurate not to require a matrix modifier. Indeed rediluting and adding the mixture may result in an even greater significant error.

Table 3. Comparison of absorbances for Ca standards made with seawater, seawater with LaCs and AA standards and AA standards with LaCs. See Fig. 11 for plot.

Standard Concentration	Seawater	Seawater with LaCs	Standard	Standard with LaCs
.2	.012	-	.011	-
.6	.033	.046	.032	-
1.0	.059	.068	.062	.08
2.0	.105	.126	.111	.135
3.0	.149	.181	.154	.194
4.0	.193	.242	.194	.246
5.0	.228	.291	.227	

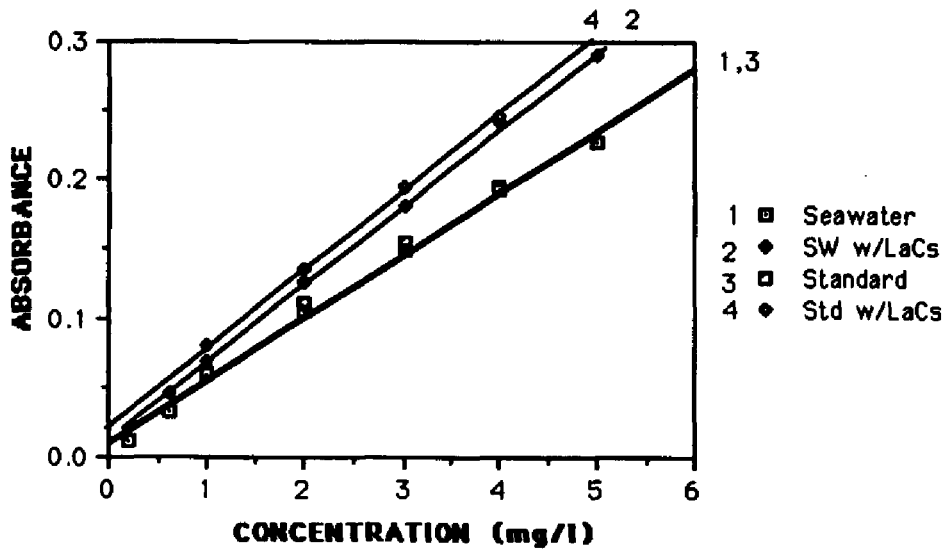


Fig. 11. Comparison between MBS calcium standards, seawater standards and both sets with a lanthanum-cesium matrix modifier added.

Table 4. Results of Ca standard addition test. See Fig. 12 for plot.

Sample	Seawater Standard Concentration	Standard Addition Concentration
D water	0.433	0.458
A-1	0.307	0.308
F1SB25	0.379	0.401

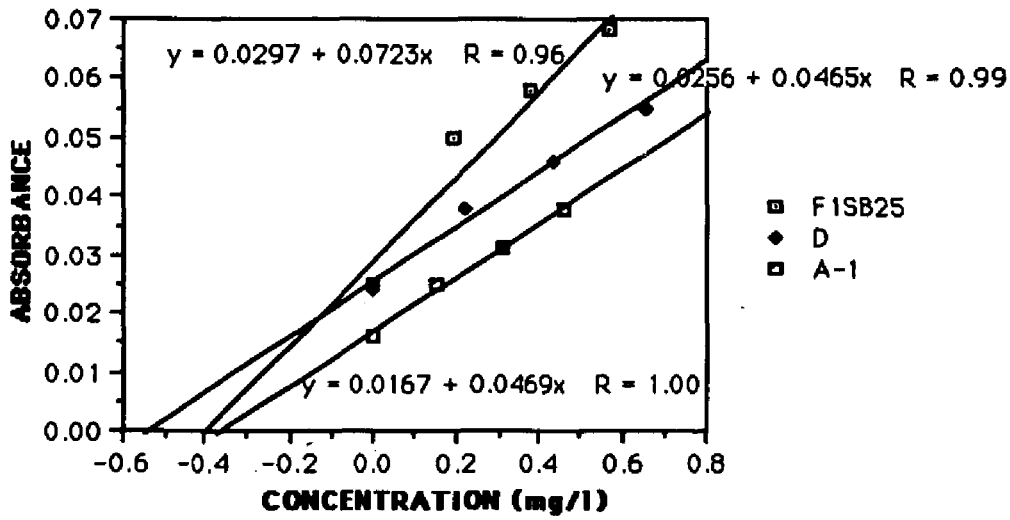


Fig. 12. Calcium standards additions for 3 samples. The intersection with the x-axis is the expected concentration.

Thin Sections

As mentioned previously, thick sections for determining structural changes were prepared in the field. Sections approximately 0.5 cm thick were cut and shipped to CRREL frozen where vertical and horizontal thin sections were prepared using the techniques of Weeks and Gow (1978 and 1980). Thick sections were frozen to glass plates and thinned to approximately 1 mm on a bandsaw then thinned to 0.5 mm using a microtome. Thin sections were examined and photographed in both reflected light and between crossed polarizers in order to determine ice type, sizes, shapes and c-axis orientations of crystals. The techniques involved are essentially the same as those used in petrographic studies of conventional rock thin sections.

Data Reduction

Relationships between concentrations of the various chemical species and ice type were determined by visual comparisons of concentration versus depth plots, cation to anion ratios, linear regressions between chemical species and by statistical analyses.

Ionic balances (difference between the sum of the cations and anions) were calculated for each sample in order to examine the accuracy of the analyses since all of the major cations and anions were analyzed with the exception of bicarbonate. Also

ratios of each species to chloride were calculated for each sample to determine if fractionation had occurred in the ice.

Linear regressions were obtained for all cores with each element plotted versus Cl in order to determine linearity with salinity. This was done in order to determine variations between cores and to determine any significant trends.

Statistical analysis (including correlation coefficients and factor analysis) was performed on the entire data set for each core. In addition the data for each core were divided into subsets based on chemical species (major elements and nutrients) and the statistics reanalyzed. The data for each core were then normalized relative to chloride and these data sets were then statistically analyzed. In seawater primary concentration variations are related to salinity or Cl variations where salinity (S_i) is defined as:

$$S_i \text{ o/oo} = 1.80655 \times \text{Cl o/oo}$$

Therefore, the total mass in grams of the major constituents is related to Cl and when normalized to Cl, the salinity effect or the primary variation is removed and secondary variations or specific fractionation can be determined.

Correlation coefficient matrices and factor analysis tables were produced for each data set using the Statview 512+ program (Feldman et al., 1986). Factor analysis is used to identify relationships among sets of interrelated variables (Norusis, 1985). The first step in such an analysis is the generation of the correlation coefficient matrix which is the calculation of appropriate measures of association for a set of variables (Kim,

1975). Choosing the variables that will be used is the most important step because they will change the factor results and, therefore, interpretations of relationships. As a result, chemical analyses were separated into various groups to determine primary relationships (those due to salinity) and secondary relationships or processes (those independent of salinity).

The second step in factor analysis is the extraction of initial factors based on interrelations in the data. These factors are independent from each other or orthogonal. The first factor or principal component is the best summary of linear relationships in the data. The second factor is the second best linear combination of variables which is orthogonal to the first. Additional components are characterized similarly until all variance in the data is explained.

The third step is rotation. One purpose of rotation is to simplify the factor structure. Also, the loadings in the unrotated solution depend on the number of variables. If one variable is deleted (i.e. a dimension is deleted) the loadings on the unrotated factors may change drastically, therefore, rotated factors are more stable.

In all factor analysis solutions in this report orthogonal varimax rotation was employed. This is a means of simplifying the columns of a factor matrix which is equivalent to maximizing the variance of the squared loadings in each column (Kim, 1975) or minimizing the number of variables that have high loadings on a factor (Norusis, 1985). High loadings are indicative of the importance of a particular parameter within each factor.

Therefore, if several parameters have approximately equal high positive or negative loadings on a factor they are related or are affected by the processes in some way.

IV. RESULTS AND DISCUSSION

In this chapter the results of the structural, chemical and statistical analyses are discussed. The chapter is divided into two main sections: 1) first-year ice and 2) multi-year ice. These sections are further divided into subsections which will include results of core profile measurements, structural and chemical comparisons, bulk salinity, dilution curves, linear regressions, cation to anion ratios and statistical analyses.

First-year Ice

Core Profiles

For each first-year core a salinity-depth profile and an ice structure profile is provided that includes photographs of thin sections taken at various locations throughout each core. In addition, a brief description of each core is included with depth profiles for all chemical constituents analyzed. Data for all chemical analyses for each core are given in Appendix B.

Core FY186

This 160-cm long core was taken from first-year pack ice adjacent to a multiyear floe that was also sampled (F386) (Fig. 10). The core consisted entirely of congelation (columnar) ice (Fig. 13) with crystal size increasing with depth. Throughout the core a strong alignment of the crystallographic c-axis was present (indicated by the arrows in the photomicrographs of thin sections) (Fig. 13). This alignment, consistent with the

observations of Weeks and Gow (1978 and 1980), indicates the influence of current direction on growth of congelation ice while tightly held in the winter pack.

Although the bulk salinity of the core is typical of first-year sea ice the depth profile does not have the C-shaped profile normally associated with cold first-year sea ice (Weeks and Lee, 1958). However, the depth profiles of the major elements do have a C-shaped profile with the exception of Na (Fig. 14) which in the top two samples has values approximately 50% lower than expected. It is believed that these low Na values are due to fractionation in the upper layers. The nutrient depth plots (Fig. 14) exhibit a variety of results. PO_4 and NO_3+NO_2 have more uniform concentrations down core with increases in the bottom 10 cm especially with PO_4 . SiO_4 and NH_4 have wider variation in concentration with no definitive trends. None of the chemical variations correlate with changes in crystal size.

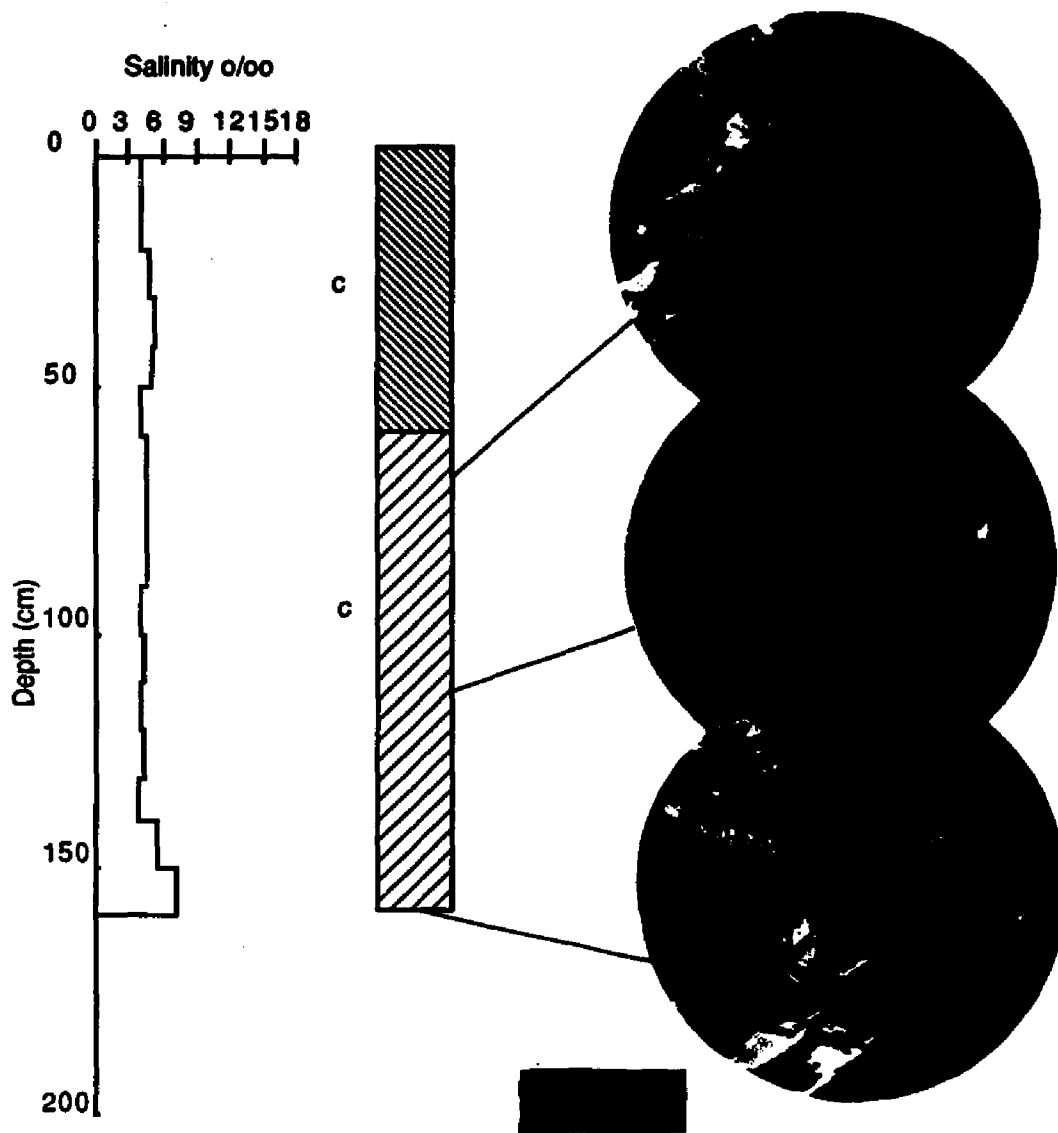


Fig. 13. Salinity-structure profiles of core FY186. Scale subdivisions beside bottom thin section measure 1 mm. In the structure diagram, the symbol c designates columnar sea ice. Increasing distance between hatches represents increasing crystal size.

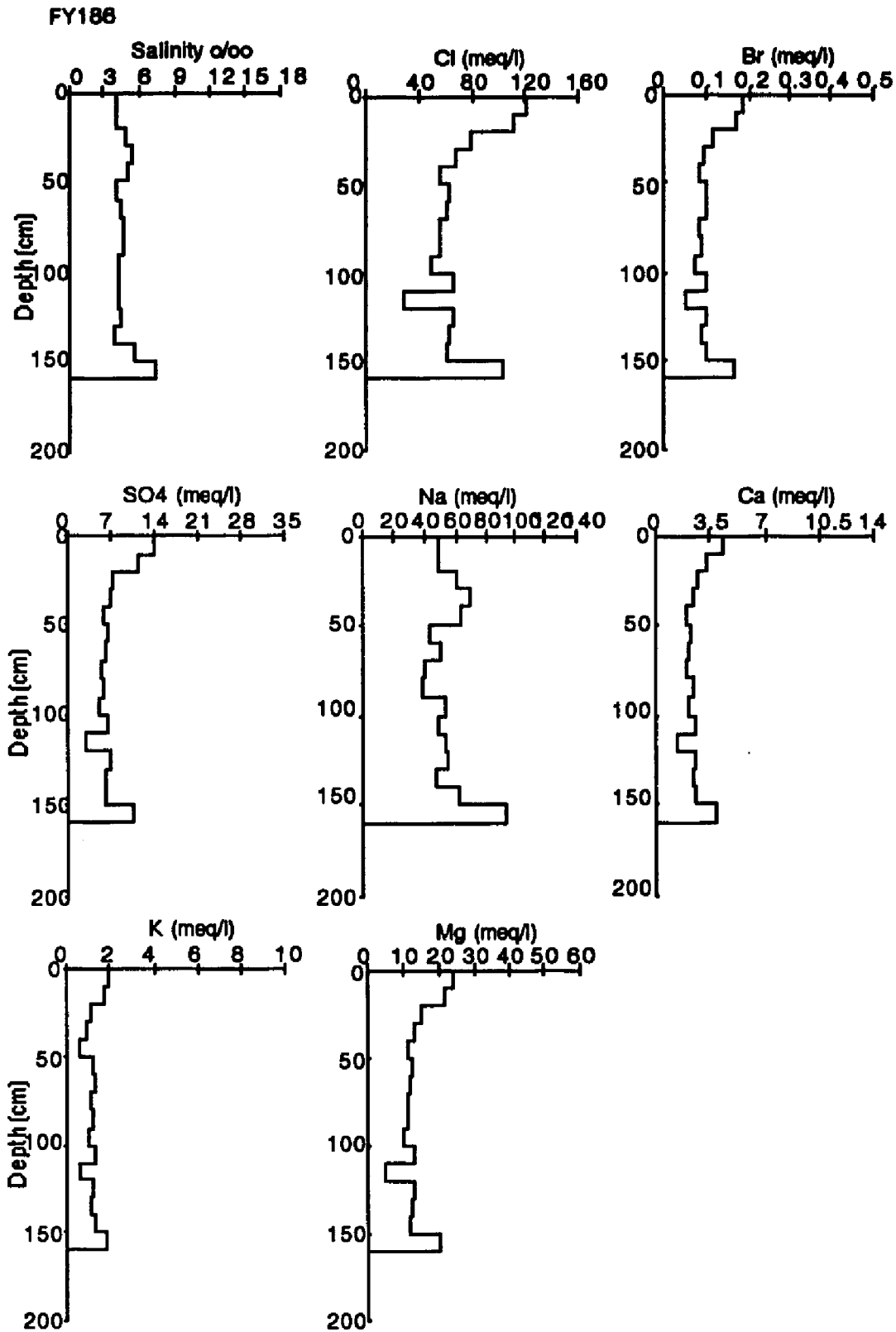


Fig. 14. Chemistry profiles for core FY186.

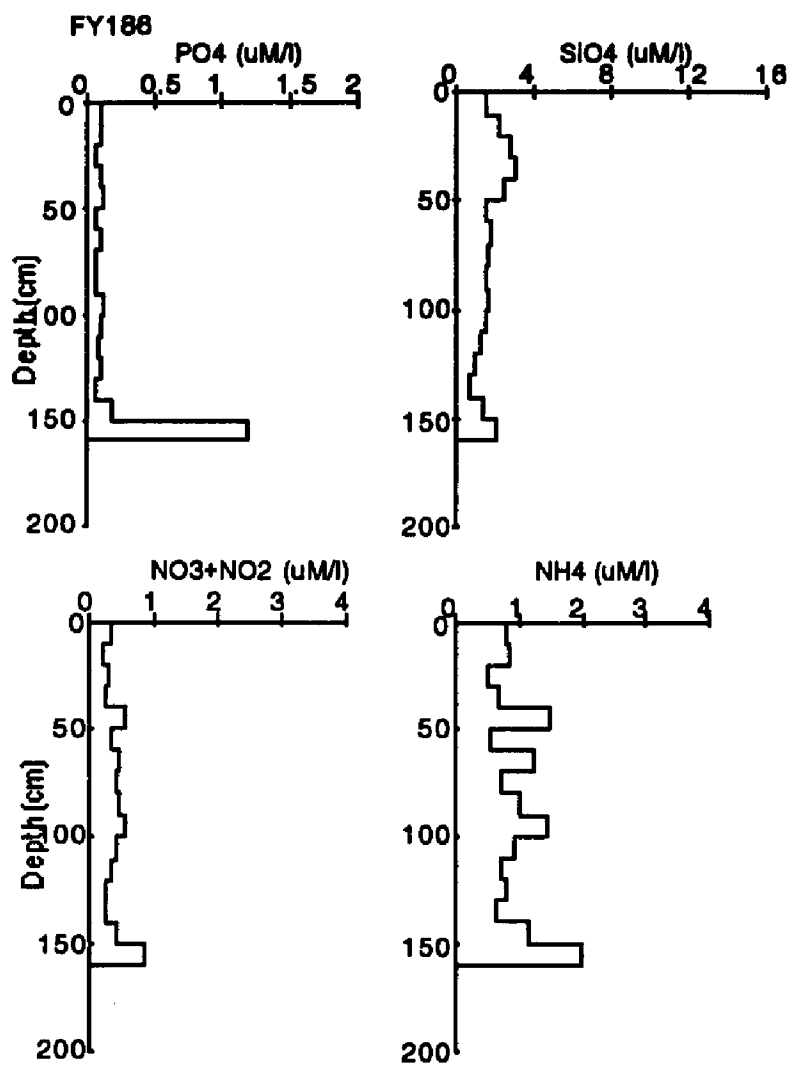


Fig. 14. (cont.).

Core FY286

This core was 142 cm long and was also taken in pack ice adjacent to multiyear floes that were sampled (F186, F286 and F486) (Fig. 10). The vertical thick section showed the top 3 cm to be composed of snow ice followed by 53 cm of medium to coarse grained columnar ice. Below this was 17 cm of fine-grained columnar ice. The remaining core consisted of columnar ice whose crystal size increased with depth. Below 70 cm a crystallographic c-axis alignment is apparent as shown by the arrows on the photomicrographs (Fig. 15).

The salinity profile reveals the typical C-shaped profile of first-year ice (Fig. 15). All of the conservative elements show similar trends down core (Fig. 16). The nutrient-depth profiles are almost identical to those in FY186 (Fig. 16) where PO_4 and NO_3+NO_2 have lower values through most of the core with peaks in concentration in the bottom 10 cm while concentrations of SiO_4 and NH_4 have greater variations within the ice. NH_4 also has a maximum value at the bottom of this core. As with FY186 none of the chemical trends correlate with variations in crystal size or structure.

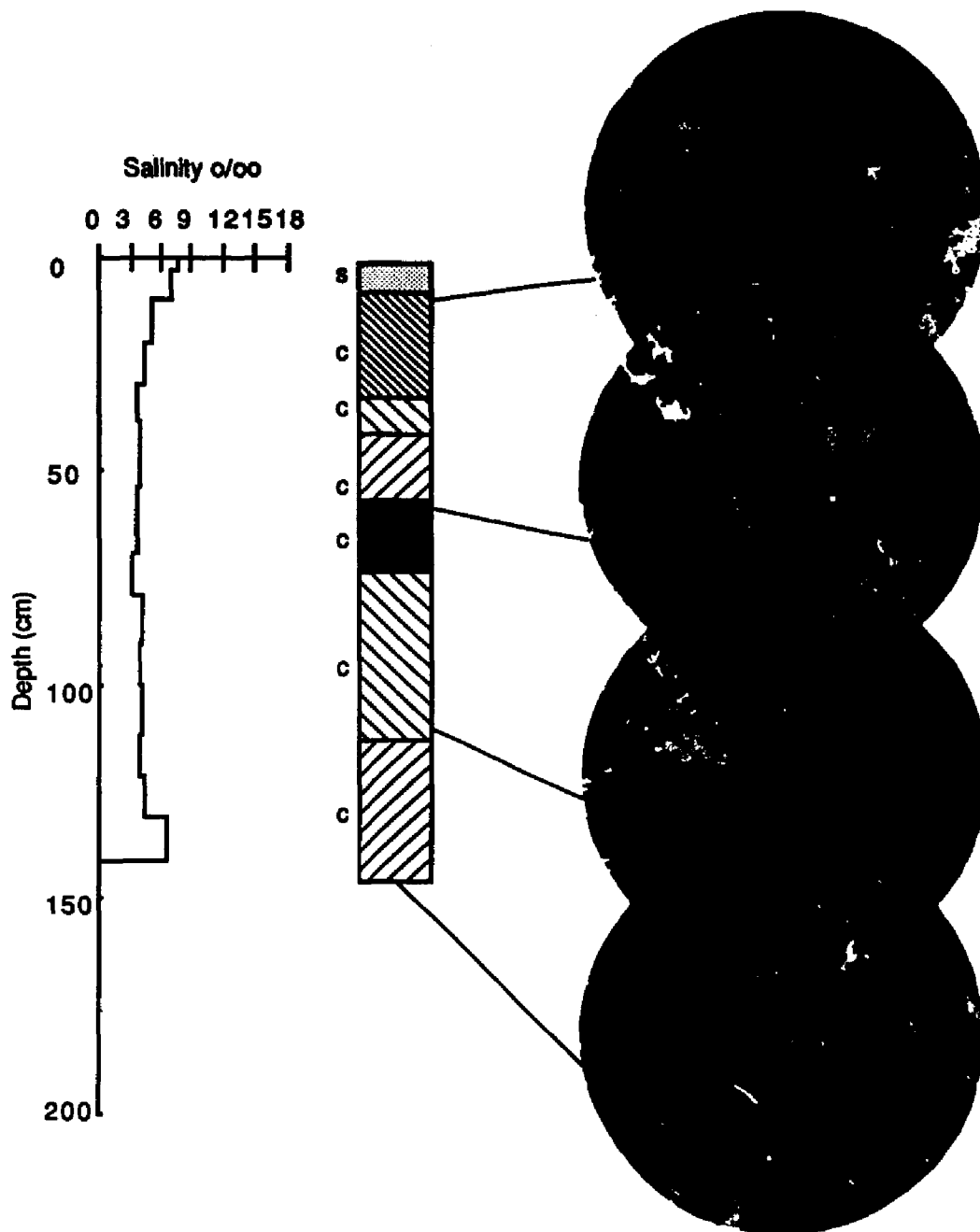


Fig. 15. Salinity-structure profile of core FY286. In the structure diagram the symbols s and c designate snow ice and congelation respectively. Increasing distance between hatches indicates increasing crystal size.

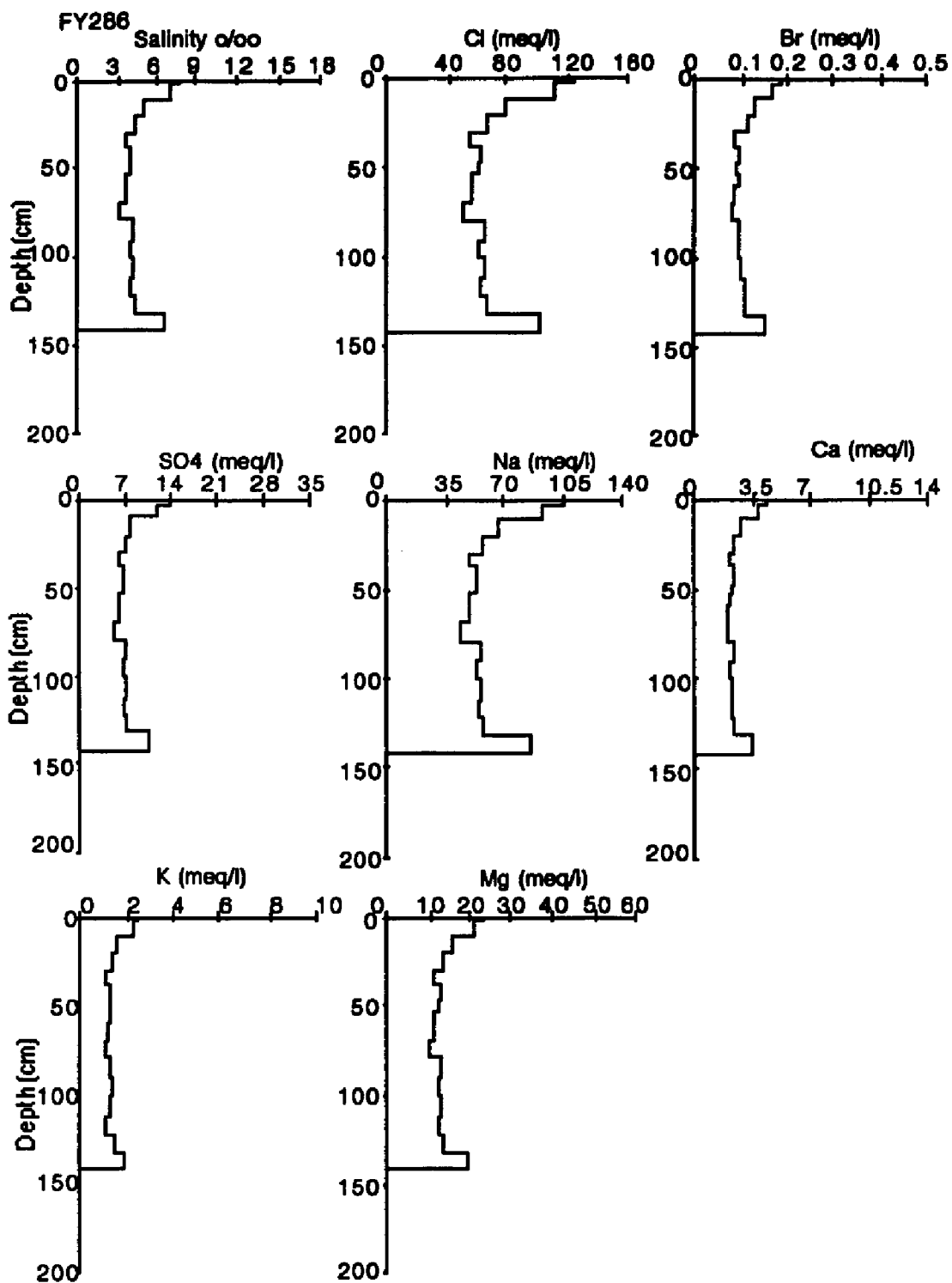


Fig. 16. Chemistry profiles for core FY286.

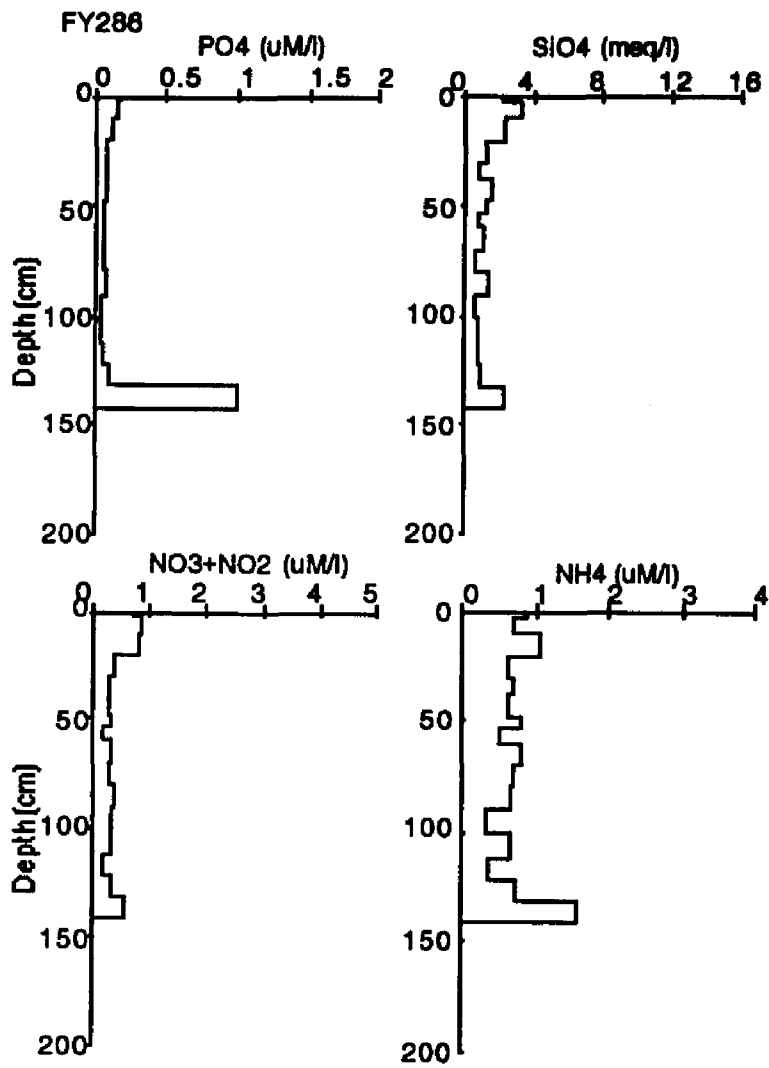


Fig. 16. (cont.).

CORE SI86

This core was taken in first-year ice adjacent to Seal Island (Fig. 10). The vertical thick section on this 204-cm long core revealed that it contained a considerable amount of frazil ice which is attributed to turbulent water conditions during early ice formation. The top 110 cm was composed of fine-grained granular with 2 debris bands located at 22-26 and 95-96 cm respectively. The transition between frazil and columnar ice was found between 110-114 cm. Columnar ice with crystal size increasing with depth persisted to the bottom of the core (Fig. 17).

Salinity (Fig. 17) and all of the conservative elements except Ca and K (Fig. 18) show the C-shaped profiles typical of first-year sea ice. Ca is depressed in the top 10 cm. The K profile is depressed throughout the length of the core but still retains a slight C-shape. The lowest SO_4 value in the core occurs between 20-30 cm. This section also contains a debris band. It is believed that SO_4 reduction is occurring in the debris resulting in the minimal concentration. The nutrient profiles all show considerable scatter with no consistent trend.

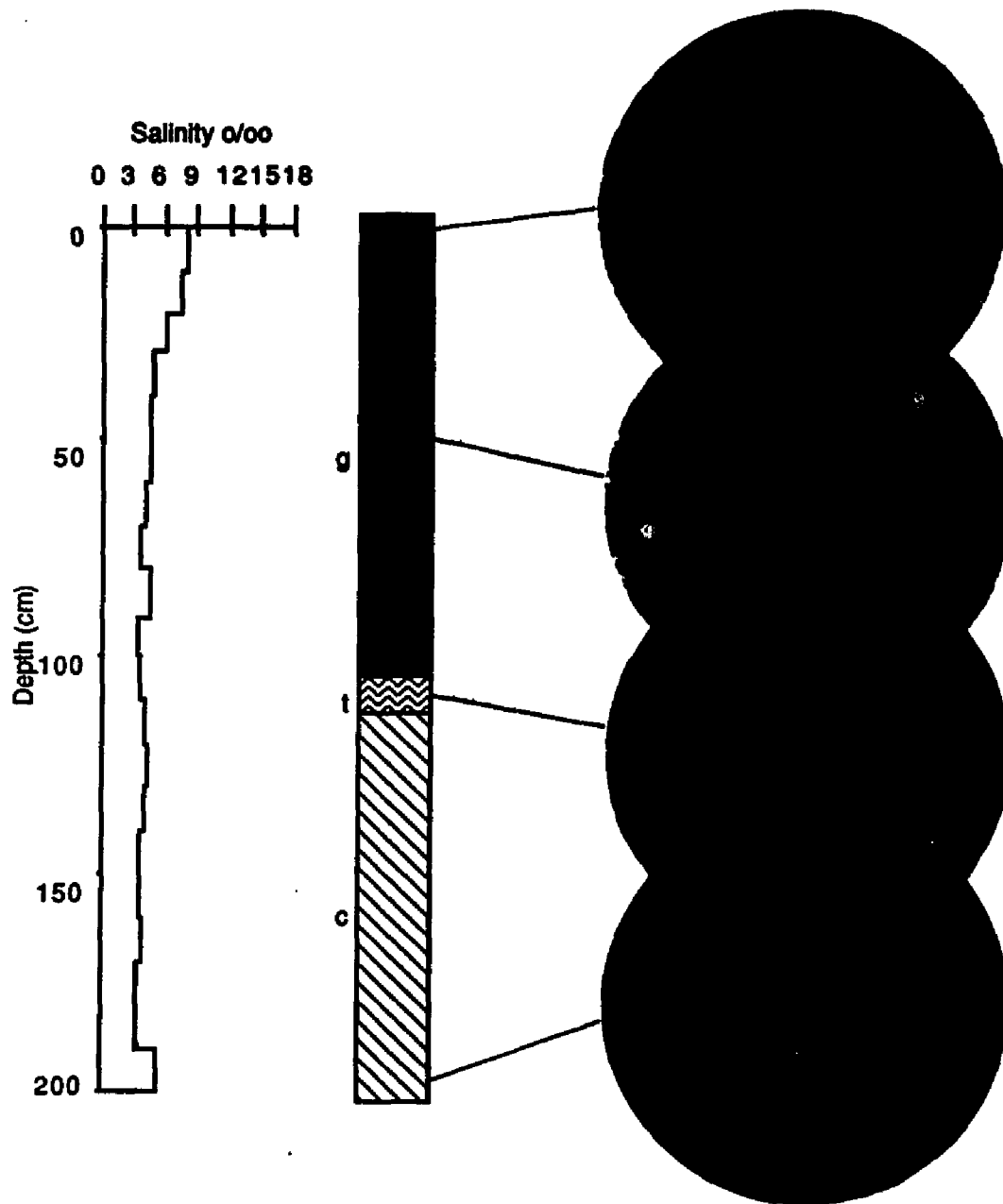


Fig. 17. Salinity-structure profile of core SI86. In the structure diagram g, t and c designate granular, transitional and columnar ice, respectively.

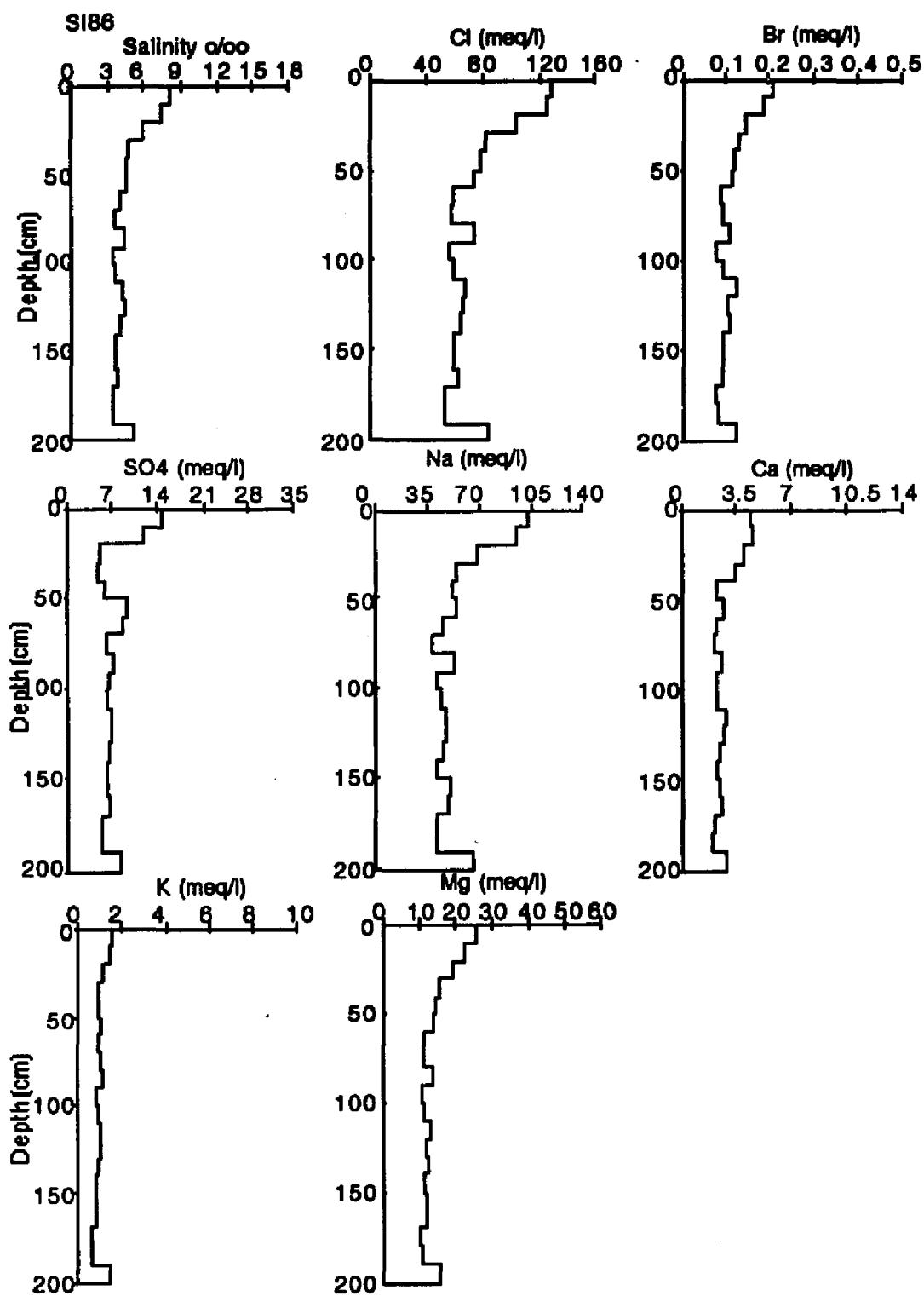


Fig. 18. Chemistry profiles for core SI86.

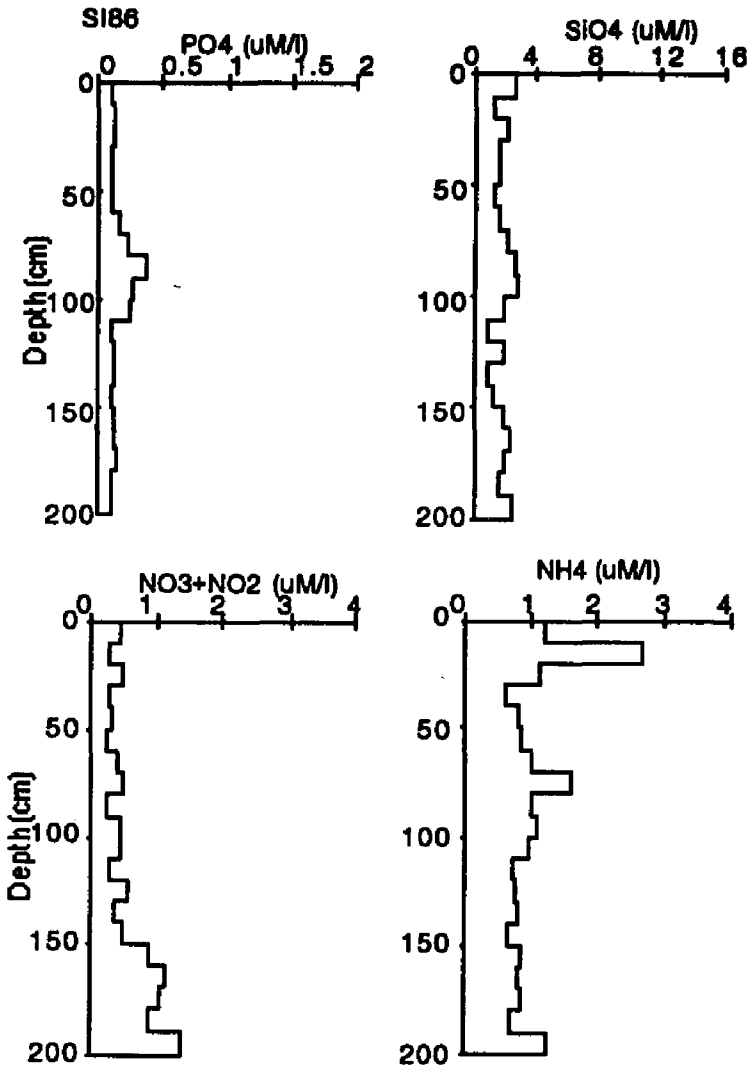


Fig. 18. (cont).

CORE A87

This core was taken in first-year ice adjacent to Gull Island (Fig. 10) in a closed lagoon in which the seawater salinity was 56 o/oo. Water depth at this location was 230 cm. The core was 170 cm long and consisted of 160 cm of congelation overlain by 10 cm of snow ice. Photomicrographs of thin sections taken at 100 and 160 cm show coarse-grained columnar ice with c-axes strongly aligned as shown by the arrows (Fig. 19).

Salinity (Fig. 19) and major element (Fig. 20) profiles show a C-shaped profile, with concentrations being extremely high in the bottom 10 cm (18 o/oo salinity) resulting from the high seawater salinity. The nutrient profiles (Fig. 20) scatter but in all cases there is an increase in concentration in the bottom 10 cm, especially in NH_4 where the concentration is 4 $\mu\text{M}/\text{l}$. The increased nutrient concentration in the bottom 10 cm is probably the result of nutrient buildup that is known to occur in the surface water throughout the winter (Alexander, 1974).

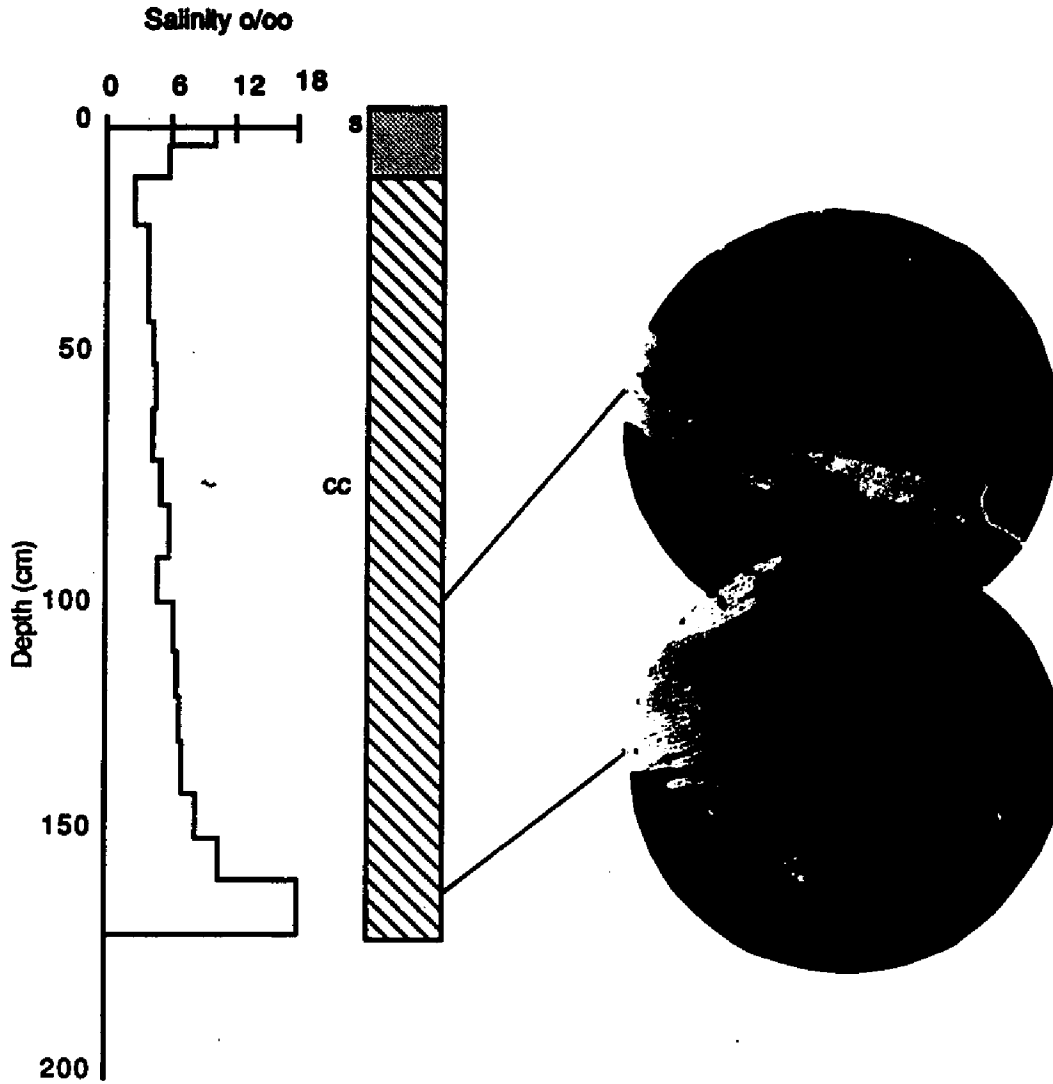


Fig. 19. Salinity-structure profiles for core A87. In the structure profile s and c designate snow ice and congelation ice, respectively.

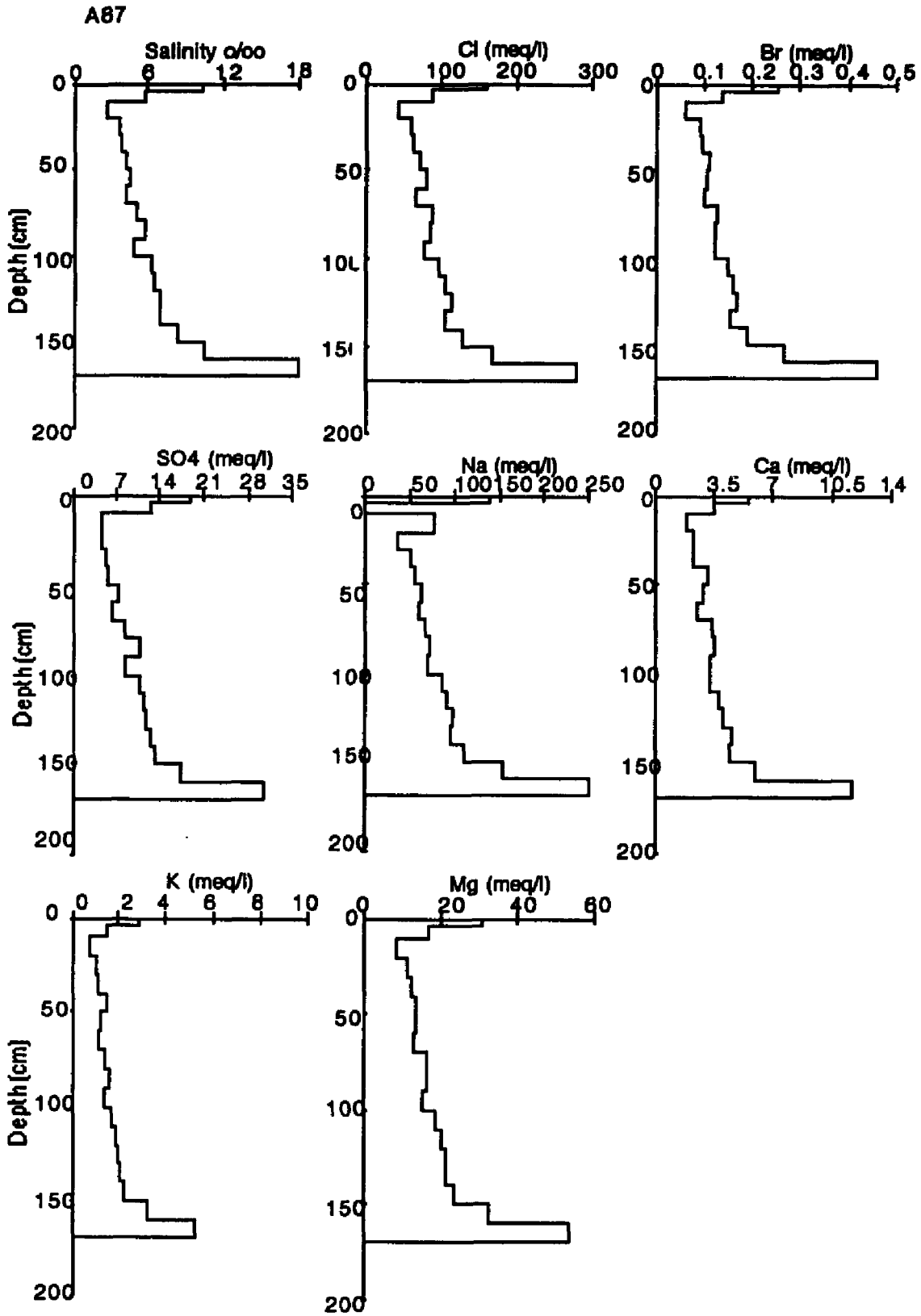


Fig. 20. Chemistry profiles for core A87.

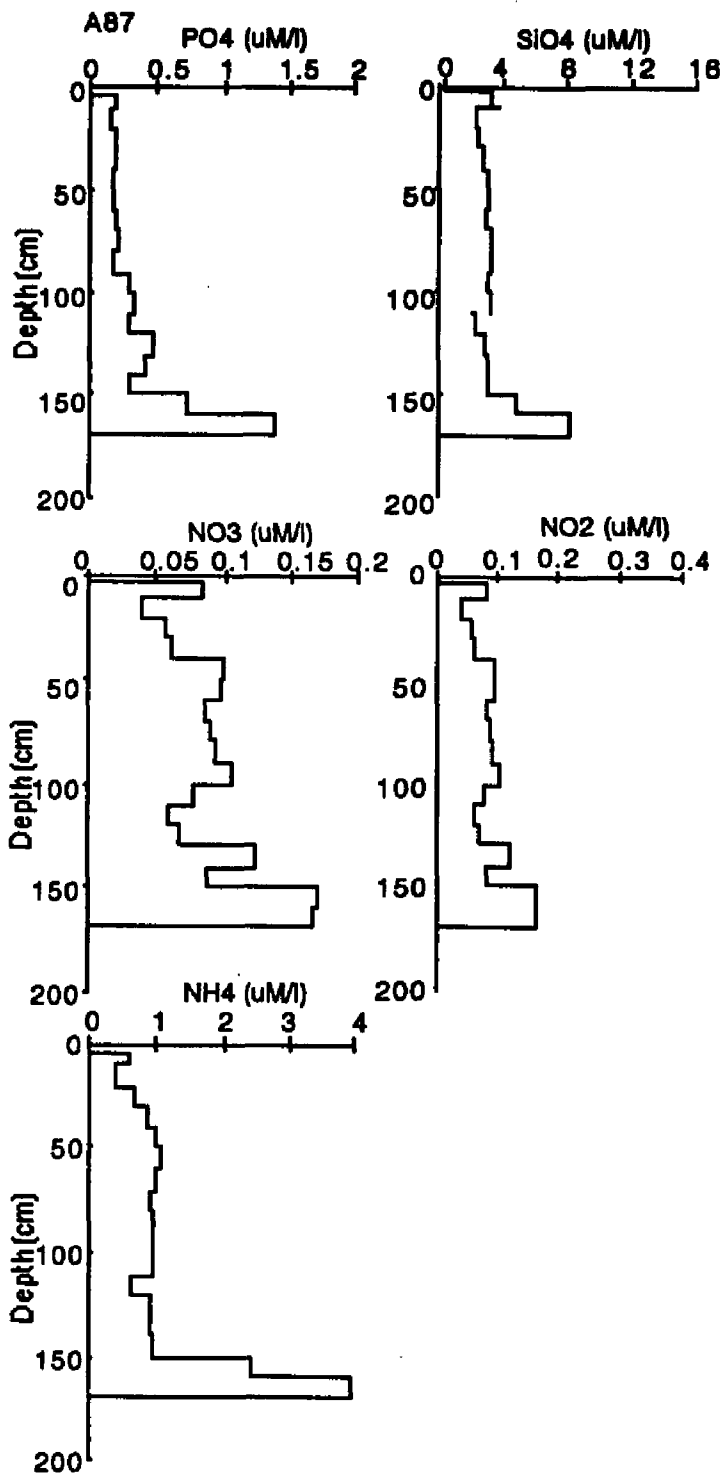


Fig. 20. (cont.).

CORE C87

Core C87 was taken in first-year ice approximately 5 miles northeast of core A87 (Fig. 10). This core was 190-cm long and consisted entirely of oriented columnar ice. Four growth bands of alternating opaque and clear ice were visible in the top 10 cm (Fig. 21). Each band was cut for chemical analysis to ascertain whether significant differences existed.

Salinity and major element depth profiles again show the typical C-shaped profile (Fig. 21). The depth profiles (Fig. 22) reveal that the top 4 samples of alternating opaque and clear ice do have concentration trends where opaque layers have higher concentrations than the clear ice. Depth profiles for PO_4 and NO_3 (Fig. 22) show similar trends. SiO_4 has a maximum concentration between 90-100 cm. NO_2 also has an increase in concentration at this depth but its maximum concentration is in the top 2 cm. NH_4 concentrations vary greatly with depth with the maximum concentration being in the top 2 cm while the minimum lies between 90-100 cm where SiO_4 and NO_2 were also very high.

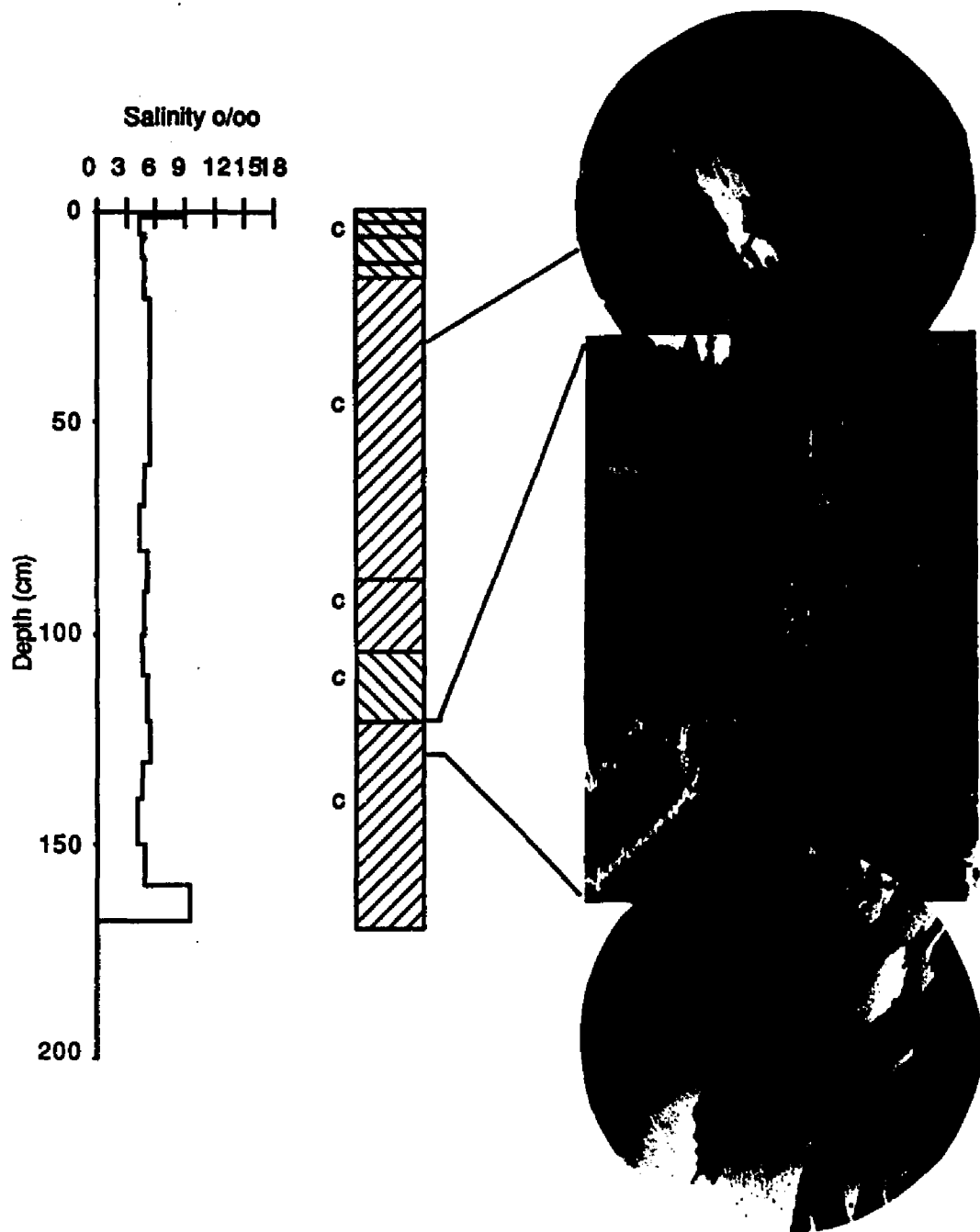


Fig. 21. Salinity-structure profile for core C87. In the structure diagram, c represents columnar ice.

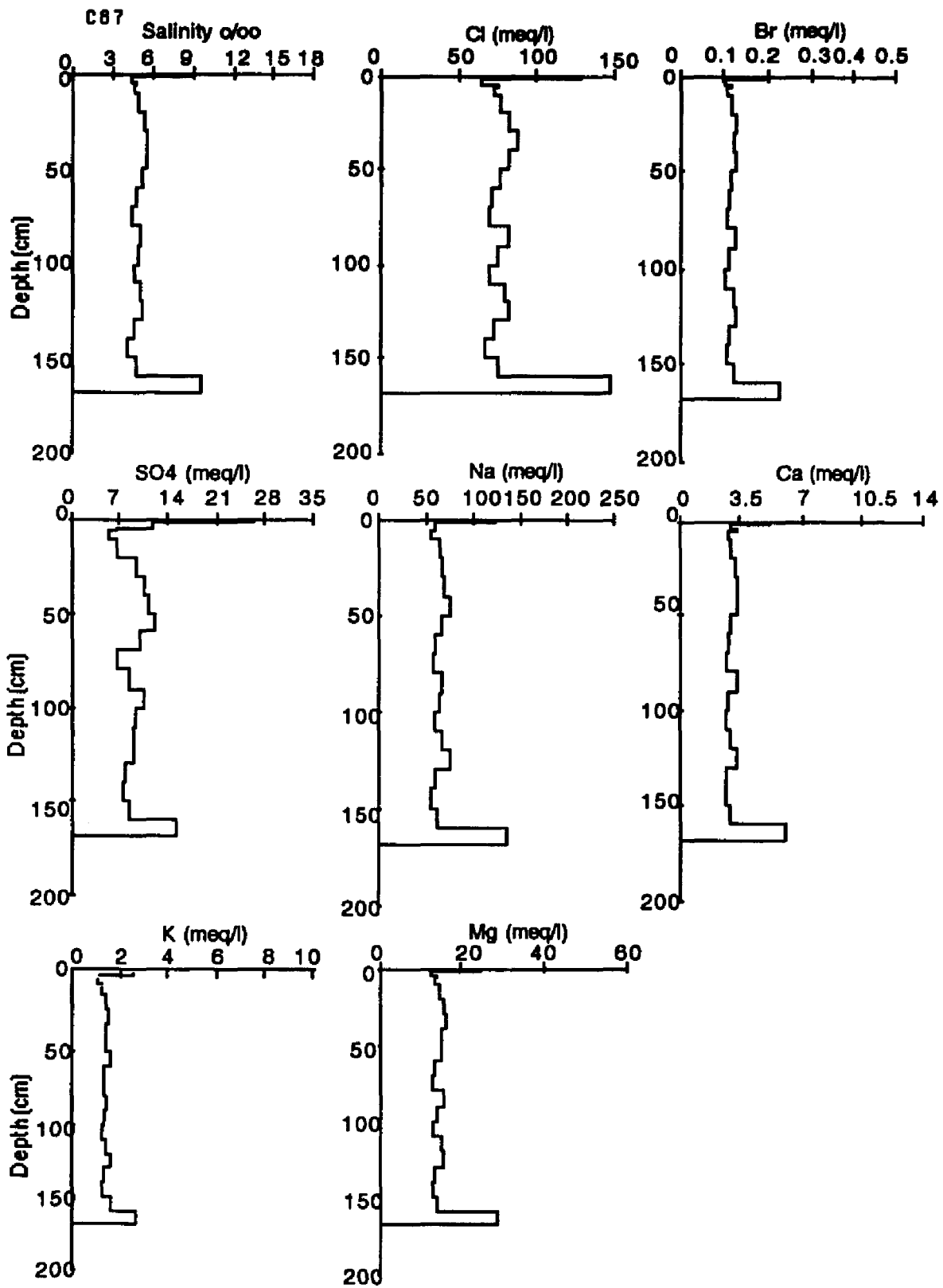


Fig. 22. Chemistry profiles for core C87.

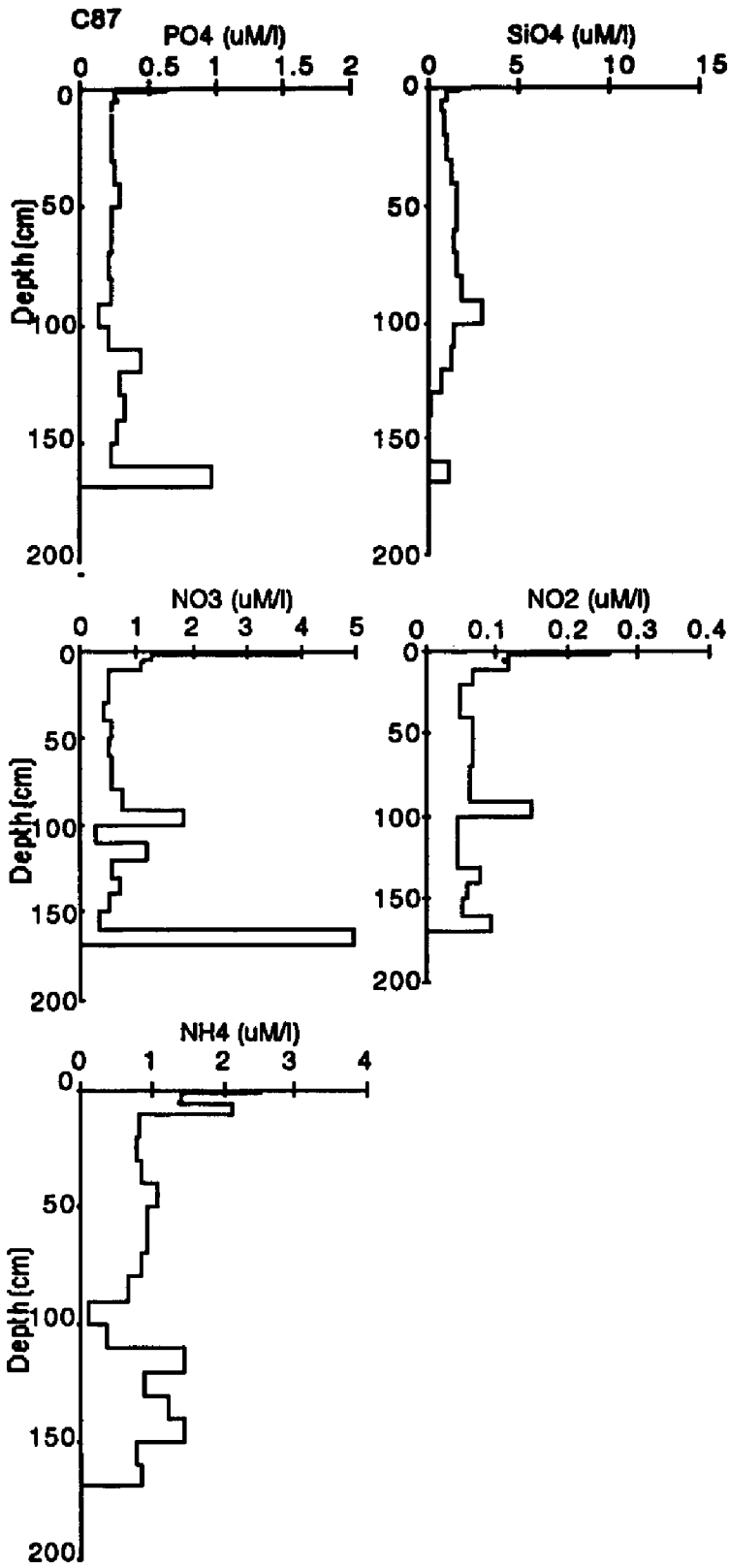


Fig. 22. (cont.).

CORE D87

This core was taken approximately 2 miles northeast of West Dock in shorefast ice (Fig. 10). The core was 177 cm long, consisting entirely of columnar ice, including a transitional zone in the top 25 cm composed of alternating layers of clear and opaque columnar ice (Fig. 23). Concentrations of the clear and opaque layers alternate with the clear layers having higher concentrations than the opaque which is the opposite of that found in core C87. The salinity (Fig. 23) and major element (Fig. 24) depth plots show modified C-shaped profiles. The nutrient concentrations vary with no apparent relation to crystal structure or major element profiles.

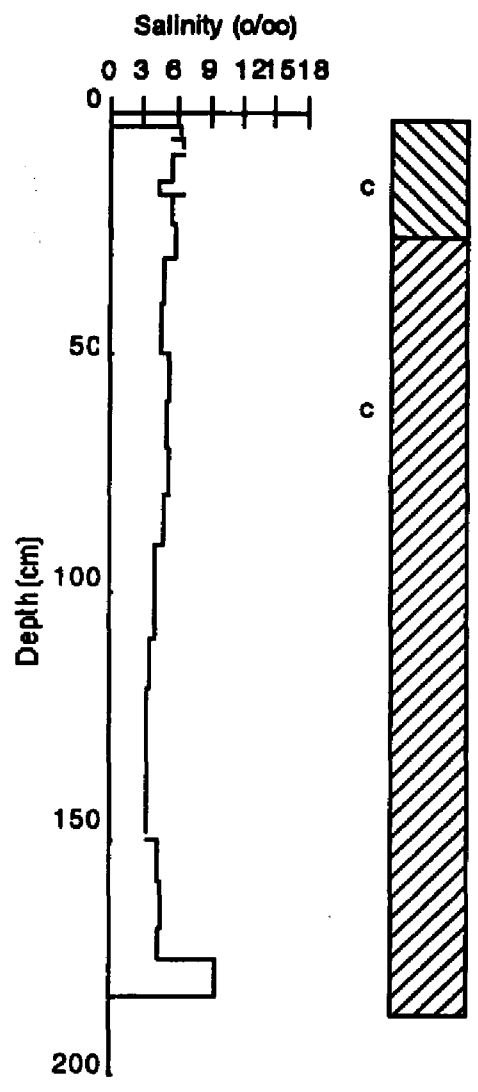


Fig. 23. Salinity-structure profiles for core D87. Symbols in the structure profile are as indicated previously.

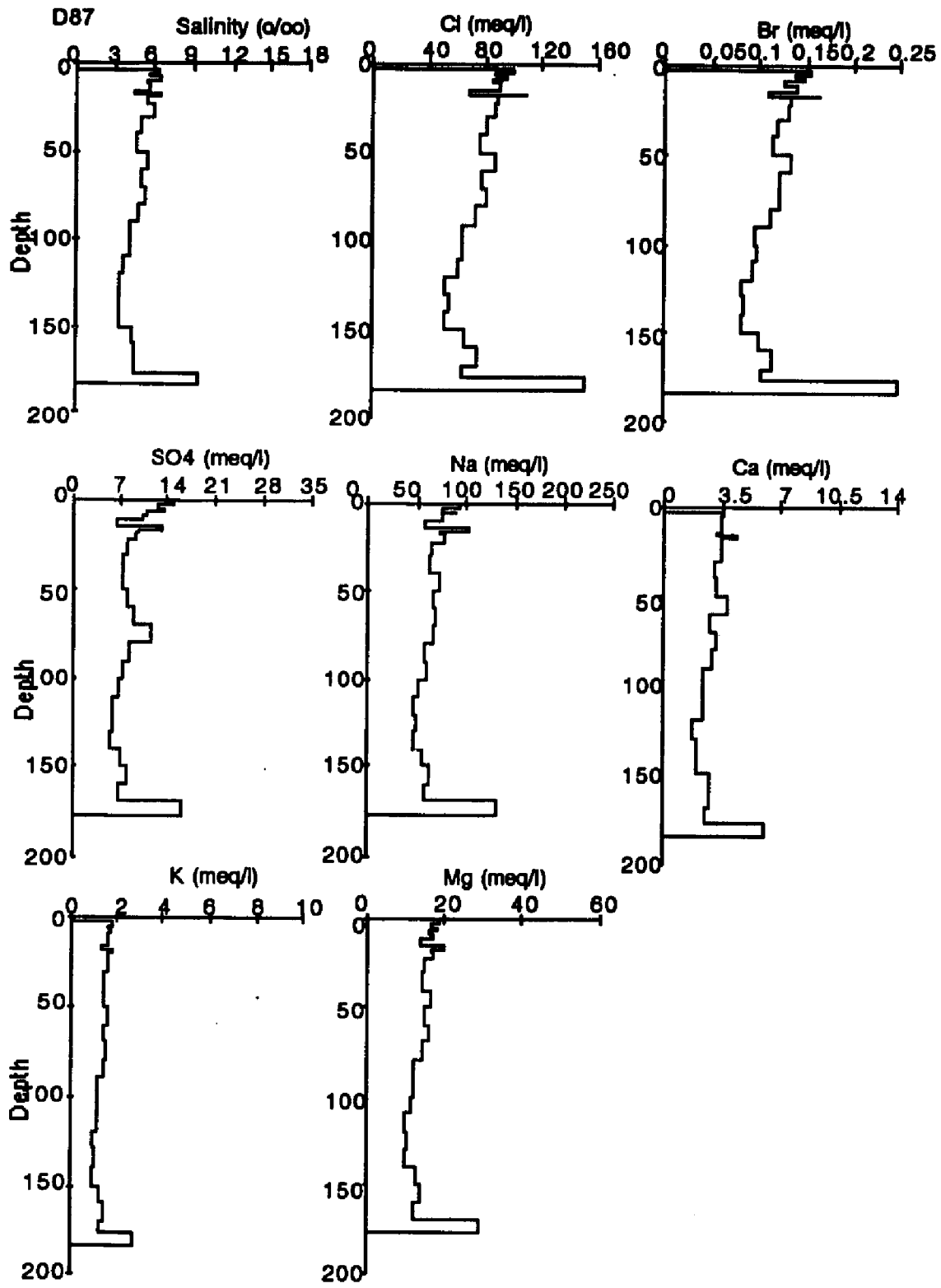


Fig. 24. Chemistry profiles for core D87.

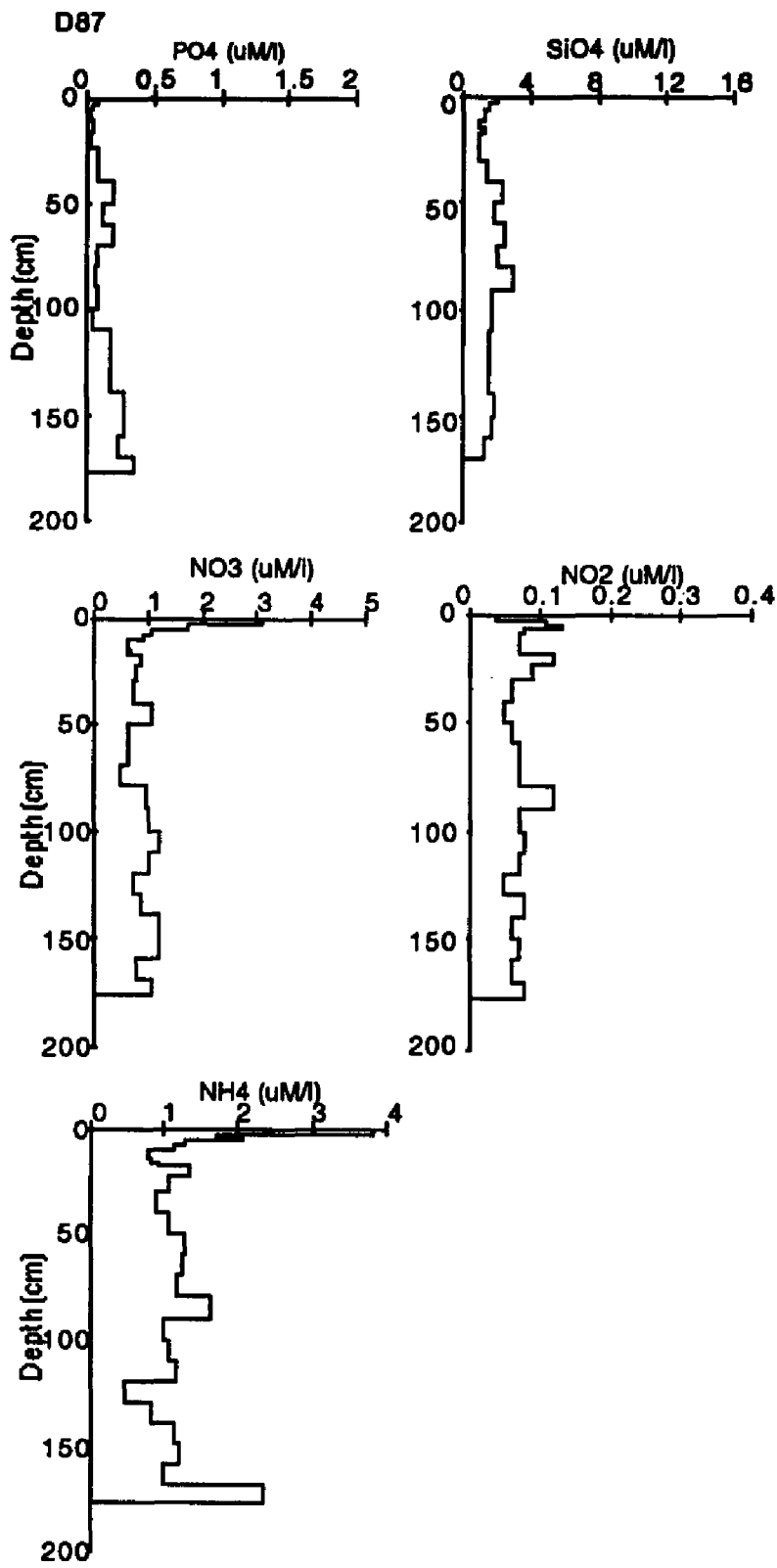


Fig. 22. (cont.).

CORE H87

Core H87 was taken on the seaward side of Cottle Island (Fig. 10). The core was 180 cm long and consisted of 170 cm of columnar ice (Fig. 25) overlain by 4 cm of transitional ice and 6 cm of snow ice. Between 100 and 140 cm a layer of fine-grained congelation existed. From the salinity profile (Fig. 25) and the major element profiles (Fig. 26) it can be seen that a slight increase in chemical concentration occurs in this zone which is attributed to greater brine entrapment in the finer-grained structure. Below 130 cm there were 5 bands of alternating vertical tubular and rounded bubbles indicated changes in the rate of ice growth. A photomicrograph of a thin section taken at 170 cm shows the c-axes to be highly oriented as indicated by the arrows (Fig. 25).

Salinity (Fig. 25) and conservative element (Fig. 26) depth-profiles are strongly C-shaped. As with the previous cores the nutrient-depth profiles vary. SiO_4 and NO_3 profiles show similar trends of increasing concentration between 50 and 120 cm. Concentrations of NH_4 are high in this core and range from 1.44-4.02 $\mu\text{M}/\text{l}$ with the highest concentration being in the top 10 cm.

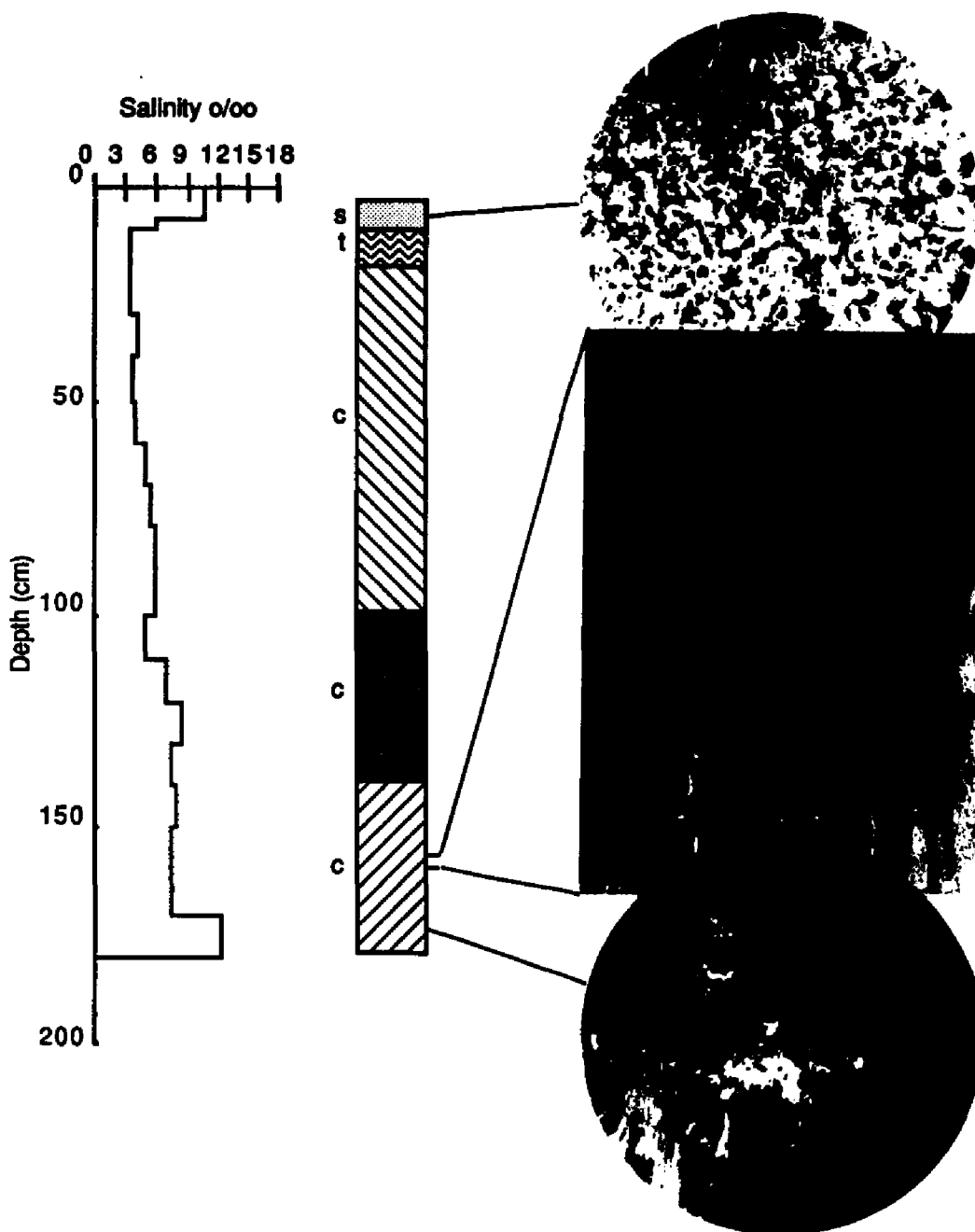


Fig. 25. Salinity-structure profiles for core H87. Symbols in the structure diagram are as indicated previously.

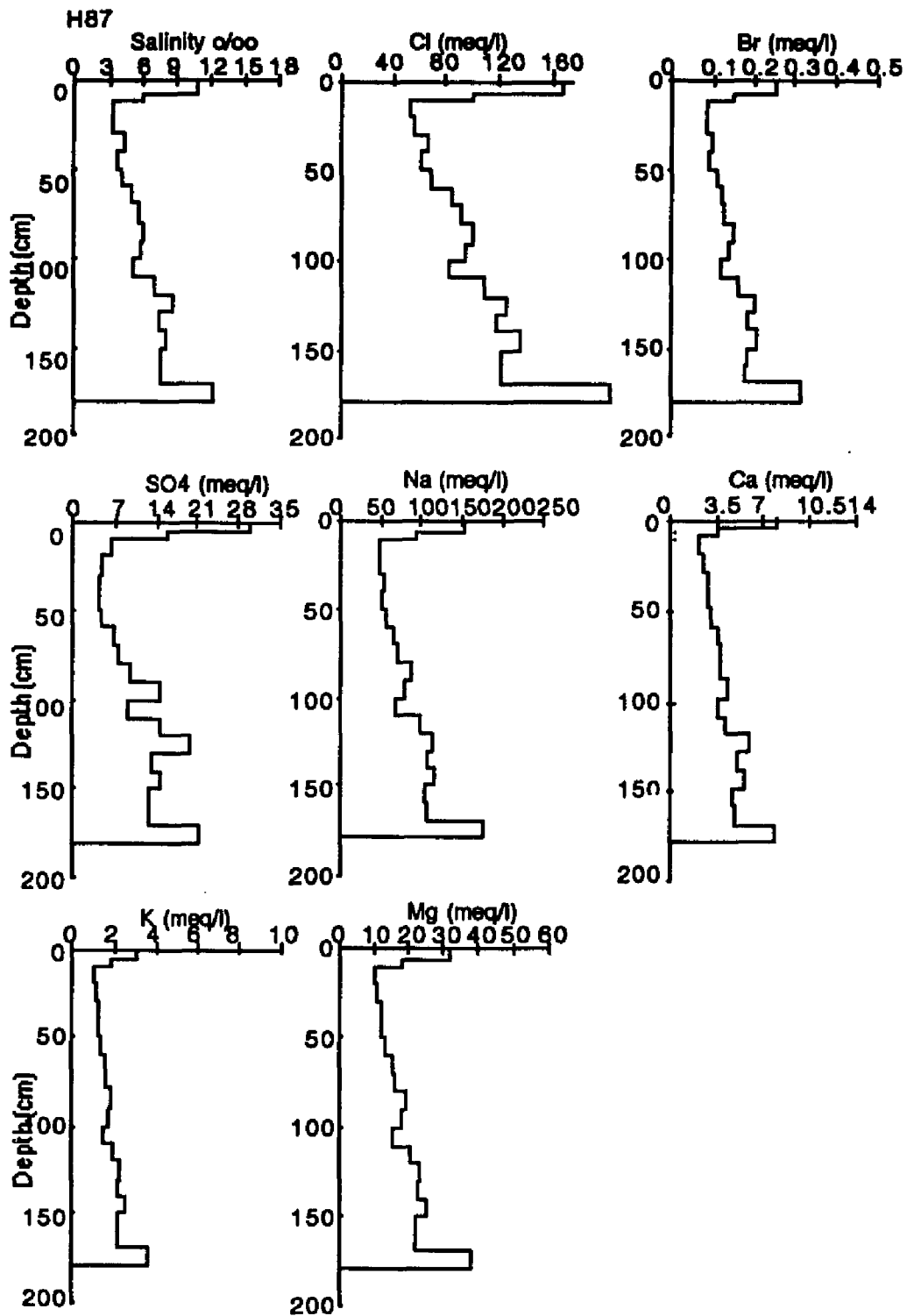


Fig. 26. Chemistry profiles for core H87.

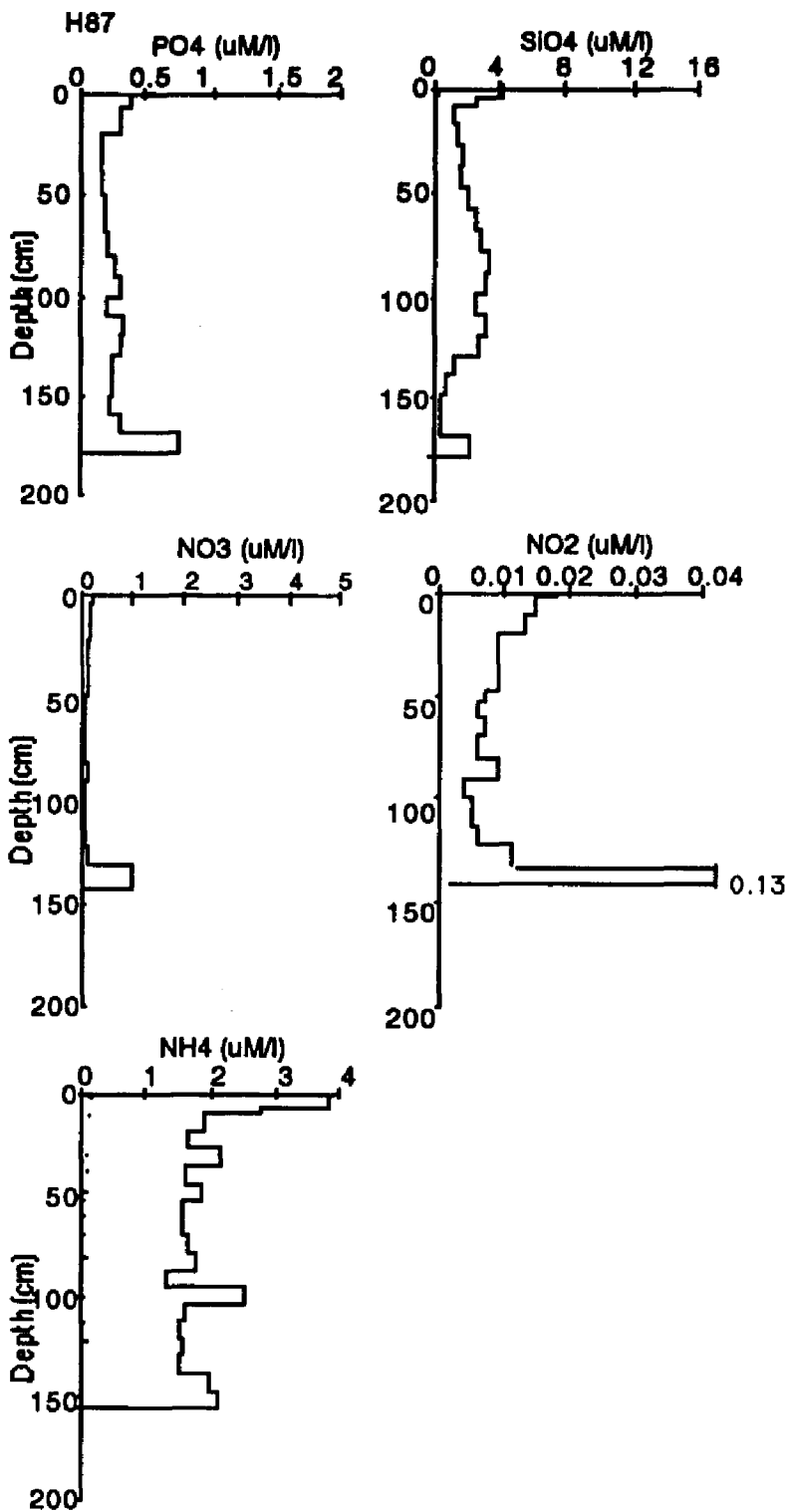


Fig. 26. (cont.).

CORE 087

This core was taken approximately 10 miles northeast of Cottle Island, adjacent to the two multiyear floes that were also sampled (Fig. 10). The core was 89 cm long and consisted of 4 cm of snow ice followed by 6 cm of transitional ice. The remaining 70 cm was columnar ice. Photomicrographs of horizontal thin sections taken at 60 and 85 cm show a strong alignment of the c-axes as indicated by the arrows (Fig. 27).

Salinity (Fig. 27) and all other species analyzed (Fig. 28) show C-shaped profiles. The NH_4 profile is less distinct due to the peak centering around 50 cm. Concentrations tend to decrease at the break in structure between the fine-grained and normal columnar ice.

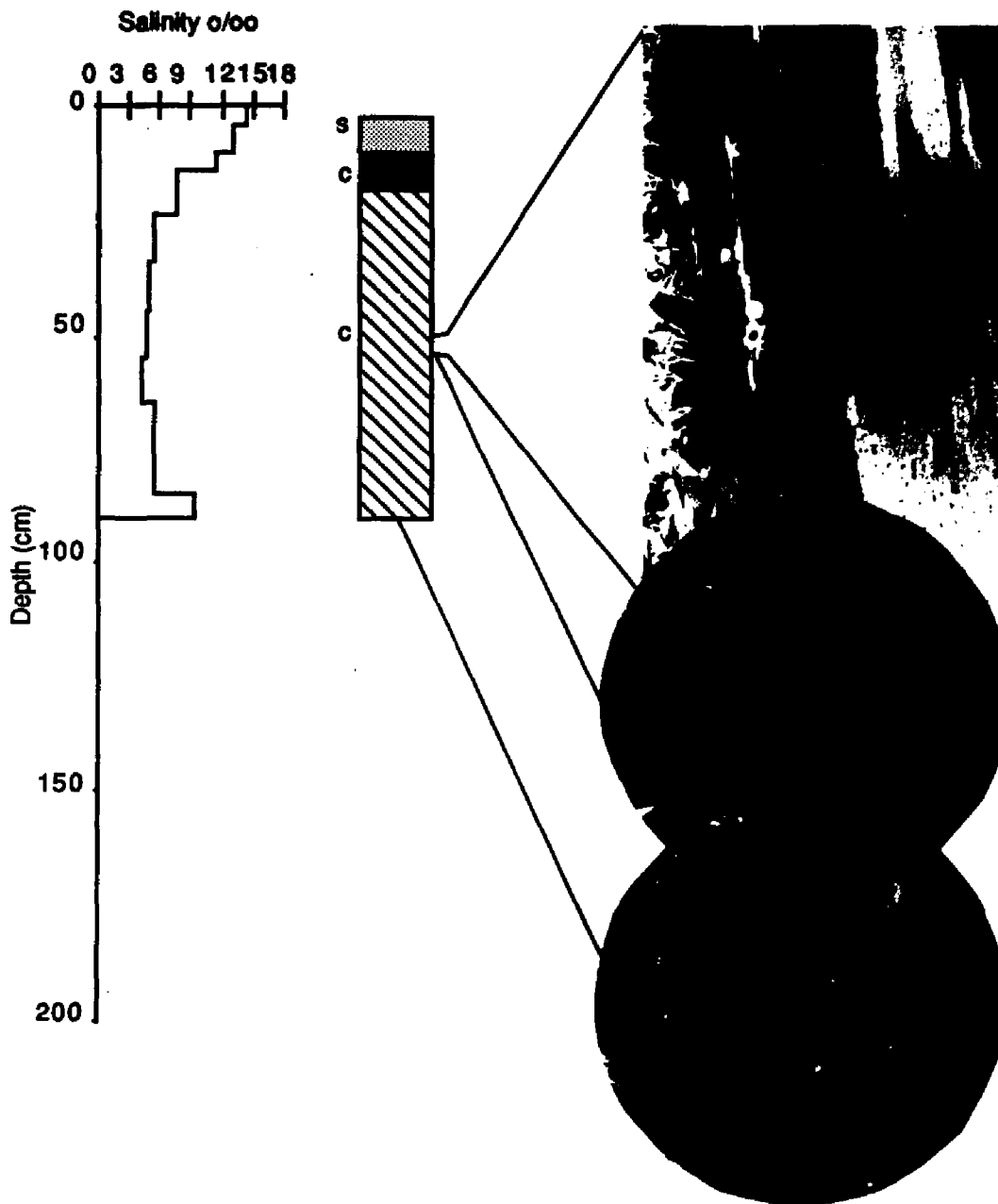


Fig. 27. Salinity-structure profiles for core O87. Symbols on the structure profile are as designated previously.

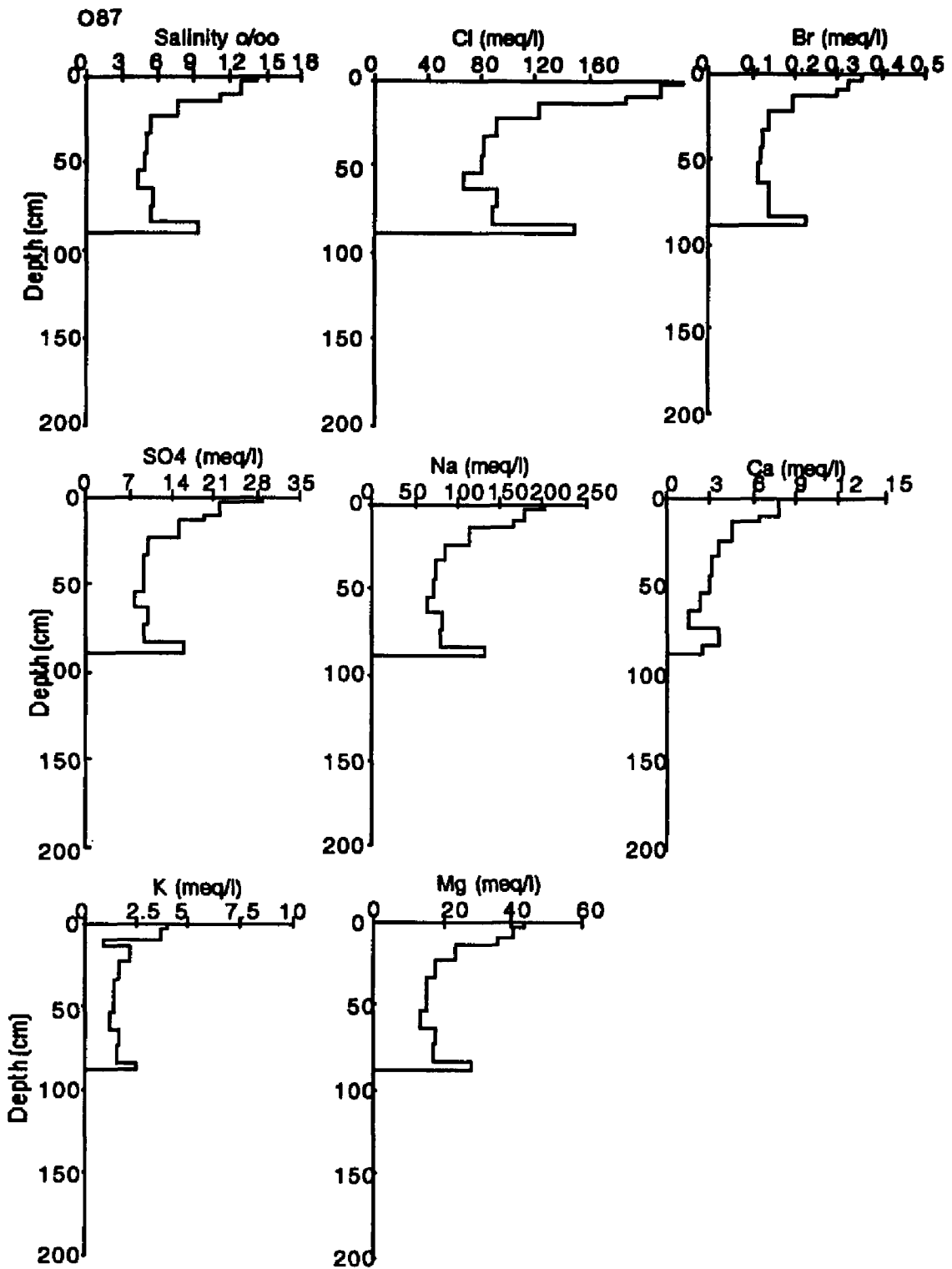


Fig. 28. Chemistry profiles for core O87.

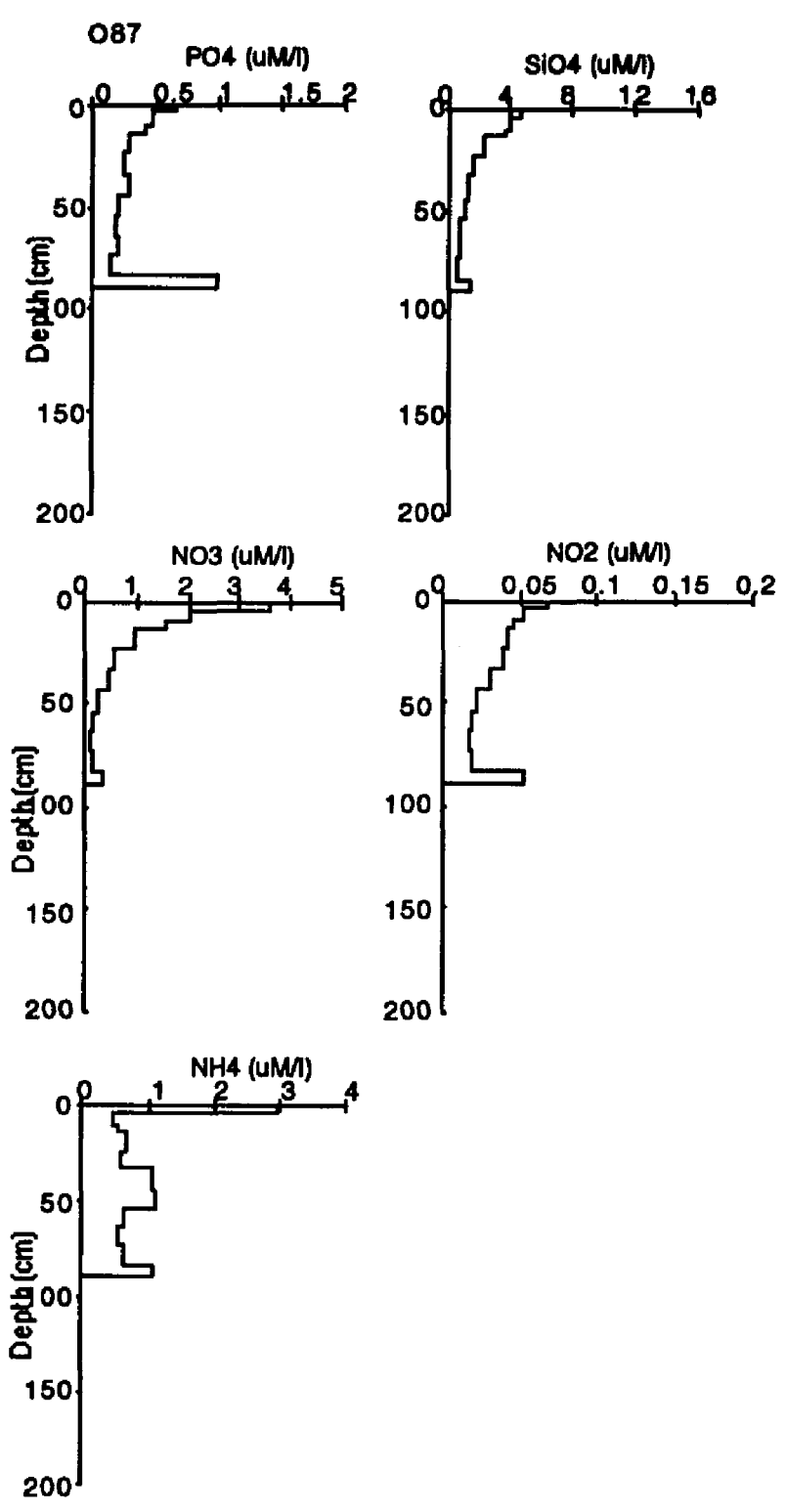


Fig. 28. (cont.).

CORE SI87

This 182 cm long core was taken within 50 m of Core SI86 on the fast ice adjacent to Seal Island (Fig. 10). In contrast to the 1986 ice sample this core consisted entirely of columnar ice. Photomicrographs of a vertical thin section taken between 30-40 cm and of horizontal thin sections at 100 and 170 cm all show columnar ice with c-axes aligned as indicated by the arrows (Fig. 29).

Salinity (Fig. 29) and major element (Fig. 30) depth profiles all reveal typical C-shaped profiles. Nutrient profiles (Fig. 30) vary and show no correlation with structure.

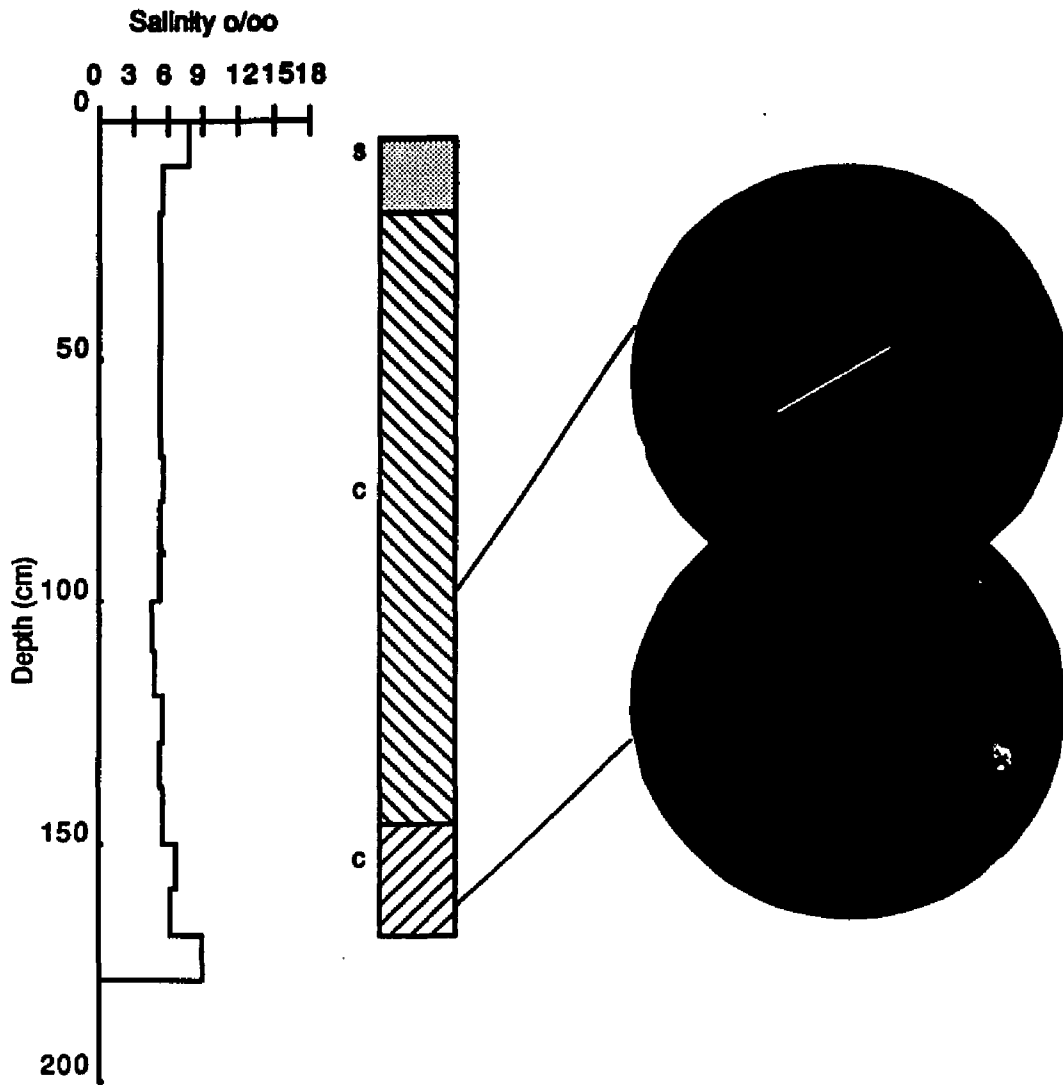


Fig. 29. Salinity-structure profiles for core SI87. Symbols in the structure profile are as designated previously.

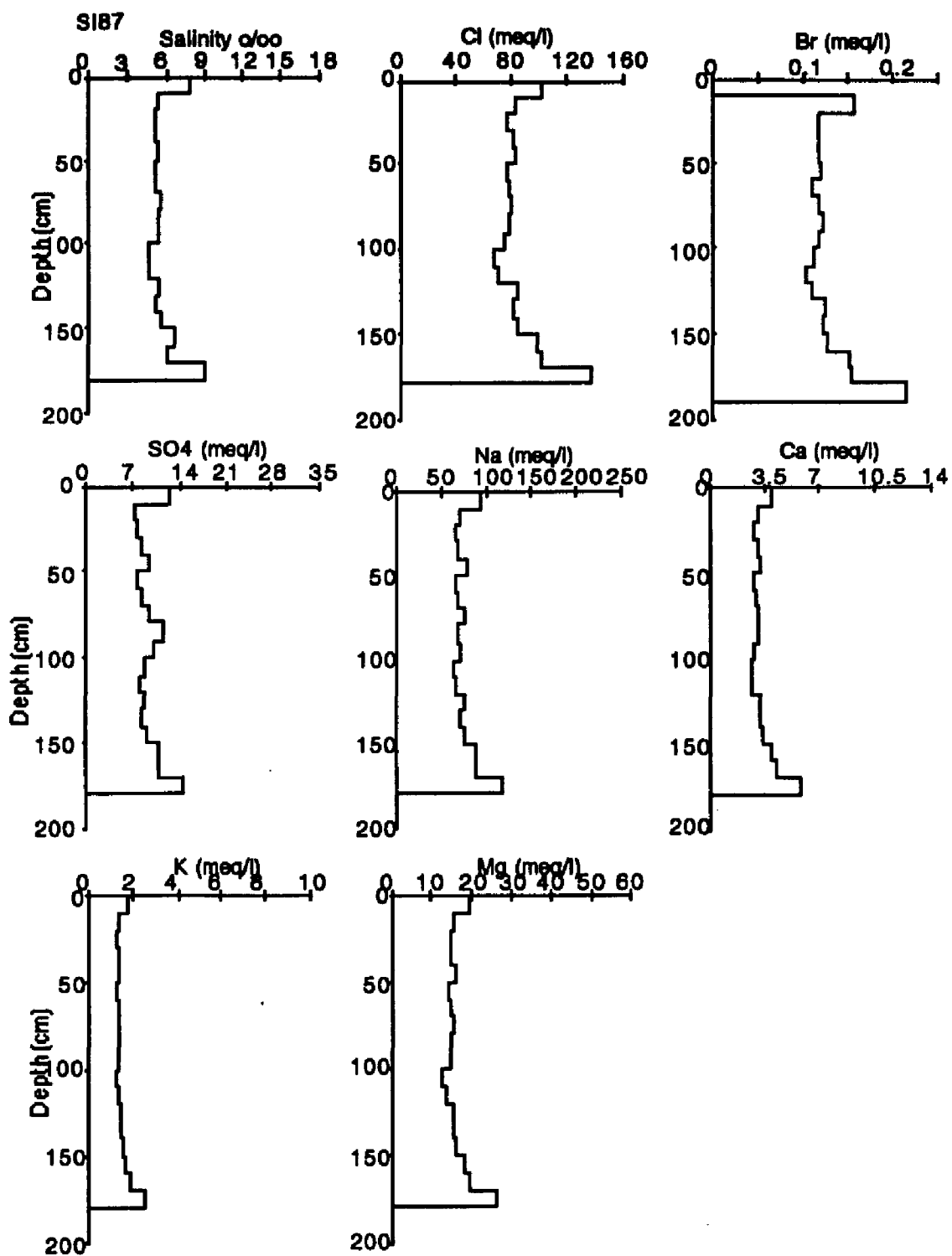


Fig. 30. Chemistry profiles for core SI87.

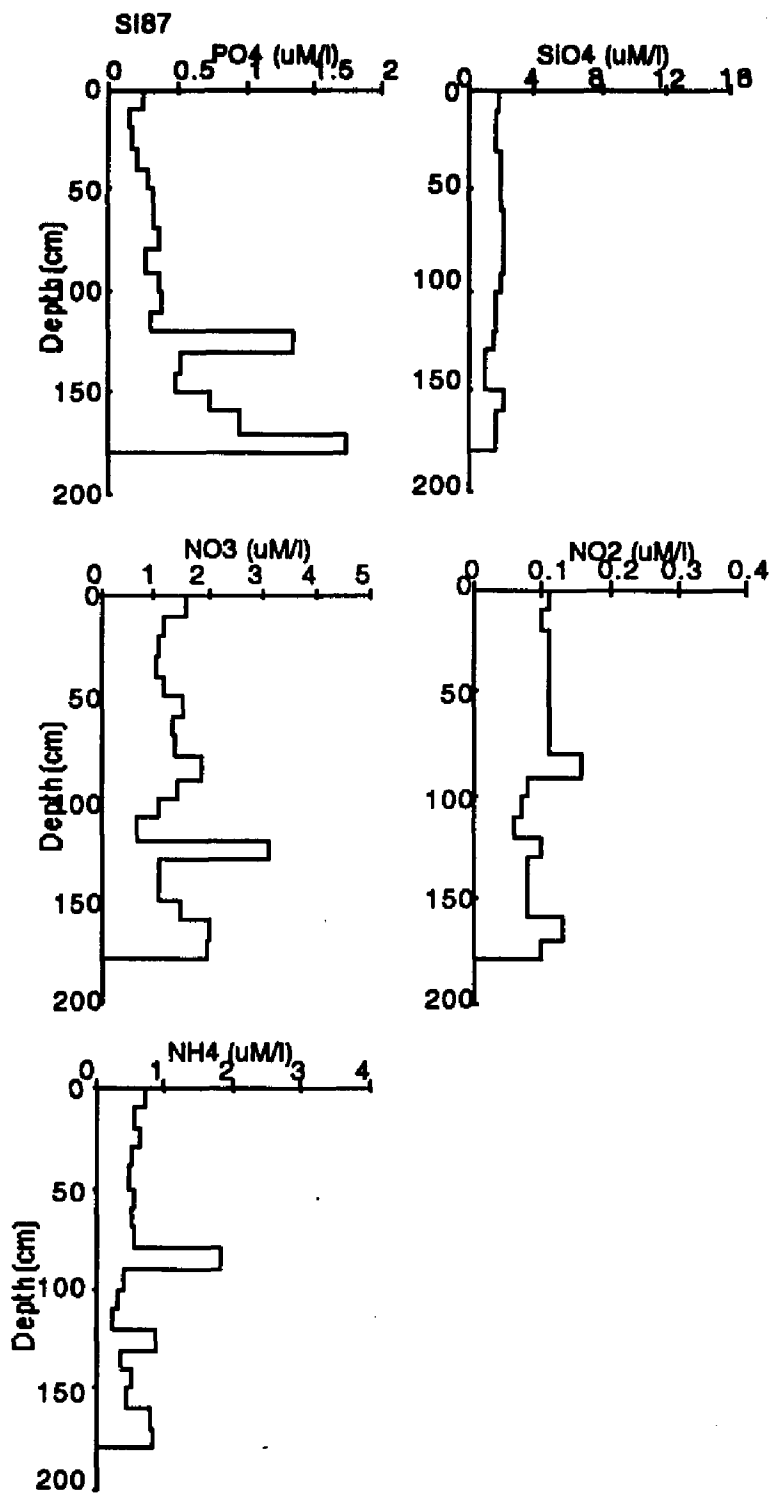


Fig. 30 (cont.).

CORE WD87

This 165 cm long core was taken at West Dock (Fig. 10). The top 2 cm was snow ice followed by 163 cm of columnar ice. The top 30 cm of columnar ice consisted of alternating layers of clear and opaque ice. Photomicrographs of horizontal thin sections taken at 15 cm (clear layer) and 25 cm (opaque layer) show that the ice is fine-grained columnar ice and that there is little apparent crystallographic difference between the layers. The photomicrograph of a horizontal thin section taken at 135 cm shows large-grained columnar ice with aligned c-axes (Fig. 31).

Salinity (Fig. 31) and major element (Fig. 32) depth-profiles are all C-shaped. The K-profile (Fig. 32), however, is slightly depressed when compared to the others. Nutrient concentrations show considerable scatter (Fig. 32). The NO_3 profile is very similar to those of the major elements which may indicate that NO_3 concentrations are related to salinity in this core. The highest NH_4 concentrations were found in the alternating layers of clear and opaque ice. Species concentration profiles compared to alternating layers of clear and opaque ice do not show significant correlations as was seen in other cores.

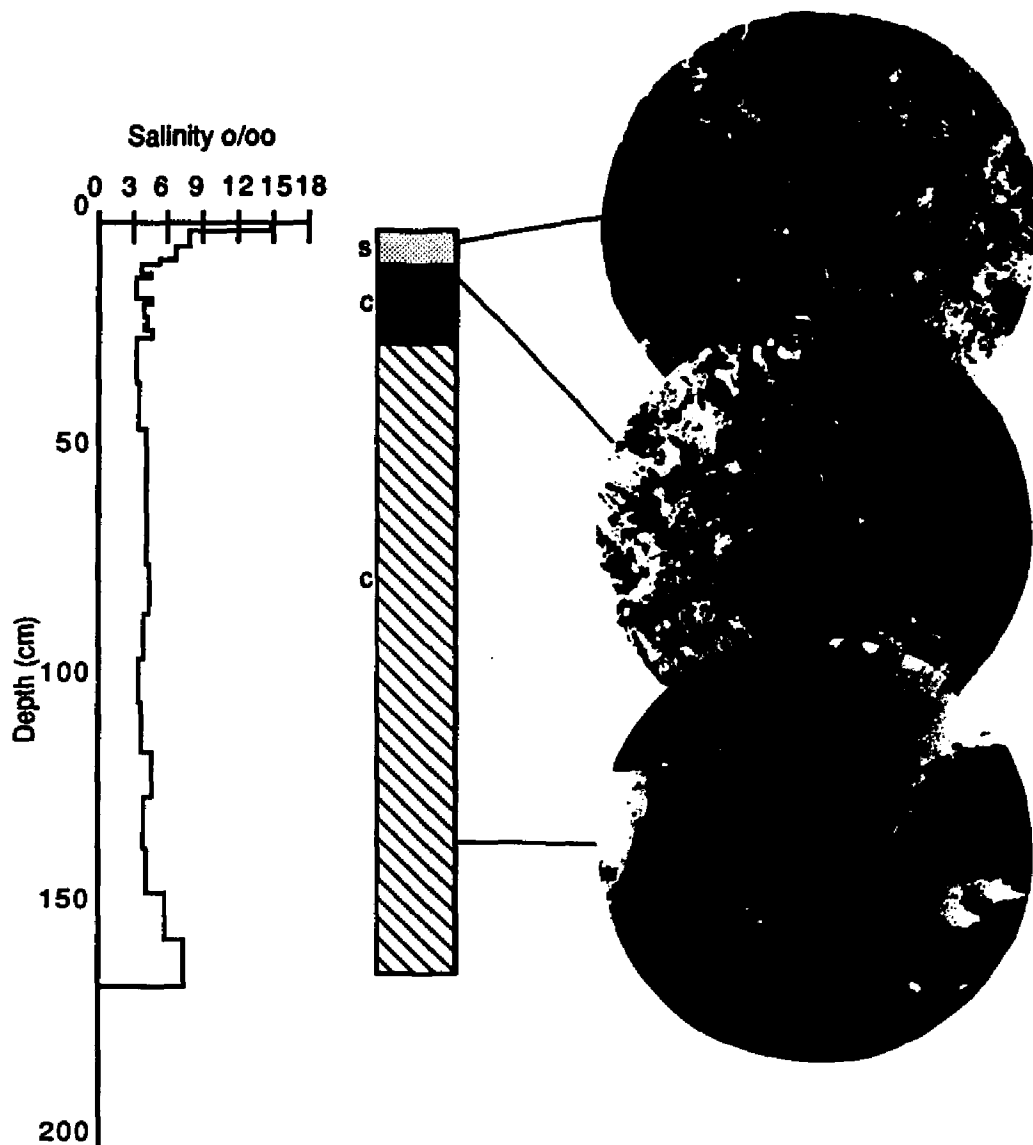


Fig. 31. Salinity-structure profiles for core WD87. Symbols in the structure profile are as designated previously.

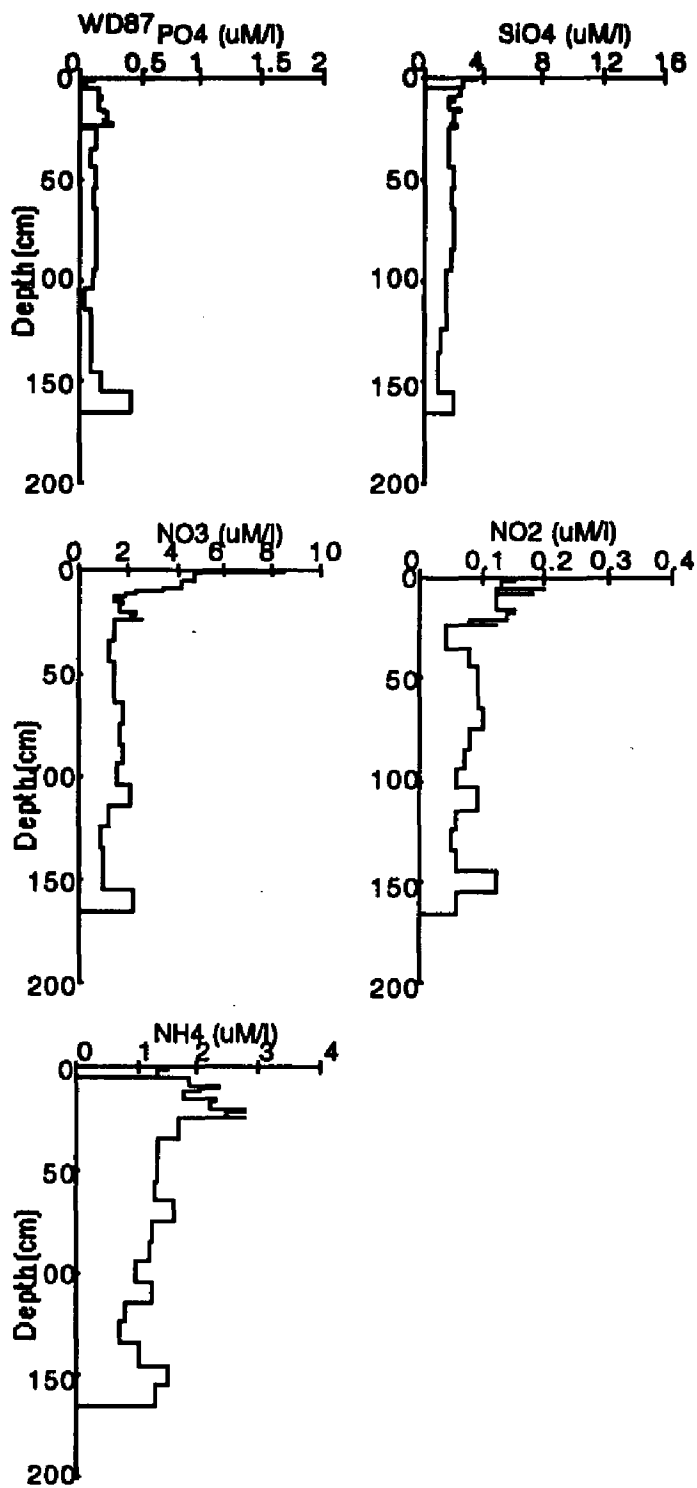


Fig. 32. (cont.).

Structure vs. Chemistry

As described earlier, vertical thick sections of each core were examined in the field to determine ice type and the locations of major stratigraphic breaks. Examination of these sections revealed that more than 90% of the first-year ice collected was columnar (congelation) ice. Plots were produced and statistical analyses were performed on the data from all ice samples and on the columnar ice data to determine if chemical relationships were related to ice type. It was found that with the notable exception of just one core there was no significant difference between the data sets at the 99% confidence interval, therefore, all of the first-year samples were kept in one data set for statistical analyses.

The exception to the above situation is core SI86 where the top 50% of the core was composed of granular or frazil ice. Since frazil ice is a product of turbulent conditions it is believed that the waters near Seal Island during the 1986 freezing season were much more turbulent than in 1987 when the ice sheet consisted entirely of columnar ice. Samples of core SI86 were separated on the basis of ice type and statistical analyses performed on each group. Correlation coefficient matrices and factor analysis tables were produced for all the SI86 data, columnar ice data and frazil or granular ice data to determine what, if any correlations exist between chemical species. Table 5 is a summary of the results of the correlation coefficient matrices produced for columnar ice (C), granular or frazil ice (F) and all samples combined (A) for SI86. All listed

correlations are significant at the 99% confidence interval for each group represented. The minimum value for correlation coefficients at the 99% confidence interval for these samples is 0.735. A negative coefficient indicates a negative correlation for those samples. From Table 5 it can be seen that for the major elements most correlate significantly with each other at the 99% confidence interval regardless of ice type. In addition, NH_4 correlates with all of the major elements for all ice samples indicating that it is salinity dependent. Table 6 is a summary of results of factor analysis produced for columnar ice (C), granular or frazil ice (F) and all ice samples combined (A). All listings in the table represent high positive loadings for that particular factor in the individual factor analysis solutions (i.e. in Factor 1, columnar ice, frazil ice and all ice samples have high positive loadings in the original factor analysis solutions for salinity, Cl, Br, SO_4 , Ca and Mg). From the table it can be seen that with the exceptions of Na in columnar ice and K for all ice samples all ice types have high positive loadings in factor 1 for all species between salinity and Mg. These results indicate that the major elements are strongly salinity dependent and are not affected by ice type or changes in crystal structure. High positive loadings for the nutrients occur in factors 2 and 3 and do not have a definitive trend between ice types. This indicates that in this case processes affecting the nutrients are independent of salinity and that PO_4 and the nitrogen species are affected by ice type.

It is important to note the combinations of ice types that have significant correlations or high loadings in the tables. In some cases frazil and congelation correlate while in others congelation and all ice samples or frazil and all ice samples correlate. The fact that samples of only one ice type and all ice samples combined can correlate significantly indicates that a particular ice type can have a major influence on statistical analyses and must be taken into account for data reduction on ice that is composed of more than one ice type.

Statistics were then run on data sets with divisions based on chemical species (i.e. major elements, nutrients, major elements normalized to Cl and nutrients normalized to Cl) and summary tables produced (Tables 7-16). This was done in order to determine if correlations exist between major groups of chemical species (major elements and nutrients) and to determine if any correlations exist in these same groups of species after the salinity effect has been removed (normalization to Cl).

Table 5. Summary for correlation coefficient matrices for core SI86 based on ice type. All correlations listed are significant at the 99% confidence interval. C, F and A designate columnar, granular and all ice, respectively.

	Depth	Sal	Cl	Br	SO4	Na	Ca	K	MG	PO4
Depth										
Salinity	-F, -A									
Cl	-F, -A	C, F, A								
Br	-F, -A	C, F, A	C, F, A							
SO4		C, A	C, F, A	C, A						
Na	-F, -A	C, F, A	C, F, A	F, A	C, F, A					
Ca	-F, -A	C, F, A	C, F, A	C, F, A	C, A	F, A				
K		C, F, A								
Mg	-F, -A	C, F, A								
PO4	F									
SiO4									A	
NO3+NO2	C, -A									C
NH4		A	A	A		C, A	A	A	A	

Table 6. Summary of factor analysis based on ice type for core SI86. C, F and A designate columnar, granular and all ice, respectively.

	Factor 1	Factor 2	Factor 3
Depth			
Salinity	C, F, A		
Cl	C, F, A		
Br	C, F, A		
SO4	C, F, A		
Na	F, A		
Ca	C, F, A		
K	C, F		
Mg	C, F, A		
PO4		A	F
SiO4		C, F, A	
NO3+NO2		C, F	A
NH4			

Major Elements

Statistical analyses were run on the major elements to determine if there are factors other than salinity variations which may affect species concentrations and/or ratios. Most of the major elements in core SI86 have significant correlations at

the 99% confidence interval between each other for all ice types (Table 7). The exceptions to this are SO₄ to Cl, Br, Ca and Mg in frazil ice and Na to Br and Ca in congelation ice. The latter results are also borne out in the factor analysis results (Table 8) where SO₄ has a high positive loading for frazil ice in factor 2 and Na has a high negative loading for congelation ice. Since these species are separated out and appear in factor 2 this may be an indication that fractionation of SO₄ and Na in these ice types is occurring. From the phase diagram it follows that SO₄ and Na are the first elements affected since Na₂SO₄ precipitates at -8.2°C (Assur, 1958). However, it is unclear as to why SO₄ is the element most affected in frazil ice and all ice samples and Na in congelation ice.

Table 7. Summary table for correlation coefficient matrices for core SI86 based on ice type for major elements. All correlations listed are significant at the 99% confidence interval. C, F and A designate columnar ice, granular ice and all samples, respectively.

	Cl	Br	SO ₄	Na	Ca	K	Mg
Cl							
Br	C, F, A						
SO ₄	C, A	C, A					
Na	C, F, A	F, A	C, F, A				
Ca	C, F, A	C, F, A	C, A	F, A			
K	C, F, A	C, F, A	C, F, A	C, F, A	C, F, A		
Mg	C, F, A	C, F, A	C, A	C, F, A	C, F, A	C, F, A	

Table 8. Summary table of factor analysis results based on ice type for core SI86. C, F and A designate columnar ice, frazil ice and all ice samples.

	Factor 1	Factor 2	Factor 3
Cl	C, F, A		
Br	C, F, A	C	
SO4	C, F, A	F, A	
Na	C, F, A	-C	
Ca	C, F, A		
K	C, F		
Mg	C, F, A		

Nutrients

Statistical analysis on nutrients were performed in order to determine relationships that exist between nutrients. The summary table for nutrients (Table 9) shows that one significant correlation at the 99% confidence interval exists for the different ice types which is for NO_3+NO_2 and PO_4 for congelation ice. Factor analysis (Table 10) reveals that high positive loadings exist for NO_3+NO_2 , NH_4 and SiO_4 in factor 1 for congelation ice. This may indicate that in congelation ice the nitrogen species and silicate values are affected by the same process. It is believed that this relationship is due to winter nutrient buildup and recycling (Alexander, 1974) that occurs more readily between the crystal platelets in congelation ice.

Table 9. Summary table of correlation coefficient matrices based on ice type for core SI86 for nutrients. All correlations listed are significant at the 99% confidence interval. C, F and A designate columnar ice, frazil ice and all ice samples, respectively.

	PO4	SiO4	NO3+NO2	NH4
PO4				
SiO4				
NO3+NO2	C			
NH4				

Table 10. Summary table for factor analysis based on ice type for core SI86 for nutrients. C, F and A designate columnar ice, frazil ice and all ice samples respectively.

	Factor 1	Factor2
PO ₄	A	C
SiO ₄	C, F, A	
NO ₃ +NO ₂	C	A
NH ₄	C	F

All Chemical Species Normalized to Cl

All chemical species were normalized to Cl to determine if there are secondary processes that are affecting species concentration or if concentration is entirely dependent on salinity. The summary table for all chemical species (Table 11) reveals one significant correlation between the major elements, that for SO₄ to Na in frazil ice, suggesting that Na₂SO₄ precipitates in frazil ice. Although a number of correlations were observed between major elements and nutrients they show no definitive trend between ice types indicating that there are additional processes affecting nutrient concentration and may be dependent on ice type.

Factor analysis results for all chemical species normalized to Cl (Table 12) are highly variable and difficult to interpret. High loadings exist for species for one ice type or another, however, specific processes causing these relationships cannot be defined. Based on the above, it is clear that samples should always be subsectioned on the basis of ice type rather than a predetermined depth interval.

Table 11. Summary table of correlation coefficient matrices based on ice type for core SI86 for all chemical species normalized to Cl. All correlations listed are significant at the 99% confidence interval. C, F and A designate columnar ice, frazil ice and all ice samples respectively.

	Br	SO4	Na	Ca	K	Mg	PO4	SiO4	NO3+NO2	NH4
Br										
SO4			F							
Na										
Ca										
K										
Mg										
PO4					F					
SiO4	-C, -A			C		F		F, A		
NO3+NO2	C		C					C, F		
NH4										

Table 12. Summary table for factor analysis results based on ice type for core SI86 for all chemical species normalized to Cl. C, F and A designate columnar ice, frazil ice and all ice samples respectively.

	Factor 1	Factor 2	Factor 3	Factor 4
Br	-C		A	-F
SO4		C, F		
Na		F, A		
Ca				F, A
K	F		C	
Mg			F	
PO4	F, A			
SiO4	C, F			
NO3+NO2	C, F	A		
NH4				

Major Elements Normalized to Cl

Major elements were normalized to Cl in order to remove the salinity effect and determine if significant correlations exist between species which would be an indication of a secondary process such as fractionation. As stated earlier, there is one

significant correlation for the major elements normalized to Cl (Table 13) which is for SO₄ to Na for frazil ice. Factor analysis of these data (Table 14) reveals that in factor 1 there are high positive loadings on Br in congelation ice, SO₄ and Na in frazil ice and all ice samples and a high negative loading on Na in congelation ice. As explained earlier, high loadings on SO₄ and Na are to be expected because Na₂SO₄ precipitates at -8.2°C and, therefore, such a relationship between the two elements should occur. Reasons for other high loadings such as occurs for Br for congelation ice in factor 1 are unclear.

Table 13. Summary table of correlation coefficient matrices based on ice type for core SI86 for major elements normalized to Cl. All correlations listed are significant at the 99% confidence interval. C, F and A designate columnar ice, frazil ice and all ice samples respectively.

	Br	SO ₄	Na	Ca	K	Mg
Br						
SO ₄			F			
Na						
Ca						
K						
Mg						

Table 14. Summary table for factor analysis results based on ice type for core SI86 for major elements normalized to Cl. C, F and A designate columnar ice, frazil ice and all ice samples respectively.

	Factor 1	Factor 2	Factor 3
Br	C	F, A	
SO ₄	F, A	C	
Na	-C, F, A		
Ca		C, -F	A
K			F
Mg			C, F

Nutrients Normalized to Cl

Nutrients were normalized to Cl in order to determine relationships that exist between the nutrients after the salinity effect has been removed. The summary table for the correlation coefficient matrices for nutrients normalized to Cl (Table 15) reveals that significant correlations exist for SiO_4 to PO_4 for frazil and all samples combined and for NO_3+NO_2 to SiO_4 for frazil and congelation. Factor analysis (Table 16) reveals that high positive loadings exist for PO_4 for frazil ice and all ice samples, SiO_4 for frazil ice and congelation ice and NO_3+NO_2 for congelation ice in factor 1. The high positive loadings for PO_4 and SiO_4 in frazil ice may indicate that sediment particles have been incorporated in the frazil or have acted as nucleation sites. The relationship could be due to dissolution and desorption of these nutrients in the ice over the winter. High positive loadings for SiO_4 and NO_3+NO_2 in congelation ice in factor 1 is probably the result of seasonal increases and recycling of nutrients, whereas the high positive loading on PO_4 in factor 2 indicates that PO_4 concentration is dependent on some other process, possibly biological utilization.

Table 15. Summary table of correlation coefficient matrices based on ice type for core SI86 for nutrients normalized to Cl. C, F and A designate columnar ice, frazil ice and all ice samples respectively.

	PO4	SiO4	NO3+NO2	NH4
PO4				
SiO4	F,A			
NO3+NO2	F,C			
NH4				

Table 16. Summary table for factor analysis results based on ice type for core SI86 for nutrients normalized to Cl. C, F and A designate columnar ice, frazil ice and all ice samples respectively.

	Factor 1	Factor 2
PO4	F,A	C
SiO4	F,C	
NO3+NO2	C	A
NH4		F

Summary of Statistical Analysis Based on Ice Type

Based on these analyses of core SI86 it has been clearly determined that subsectioning of ice samples must be based on ice type. It was also determined that the primary factor affecting the major chemistry of sea ice in all ice types is salinity where the ratio of major ions remains constant throughout the ice. Statistics on the major elements normalized to Cl indicate that fractionation has occurred for those ions (Ca, Na and SO4) that precipitate at the higher temperatures (>-10° C). While nutrient concentrations may be salinity dependent, based on ice type, they may be controlled by other processes (such as nitrogen reduction or oxidation or biological utilization) as seen when nutrients were normalized to Cl. Processes affecting correlations are sometimes evident (winter nutrient buildup and recycling,

biological utilization and desorption and dissolution due to incorporation of sediment particles) but in many cases reasons for the correlations remain unclear.

Bulk Salinity

First-year ice was collected from three different environments in the Southern Beaufort Sea: pack-ice, near-shore ice seaward of the barrier islands and near-shore ice inside the barrier islands (Fig. 10). Bulk salinities of cores from the various areas increased shorewards with the exception of core O87 which had a bulk salinity 2.2 ‰ higher than any other core. It is not known why the salinity in this core is so much higher than the others but is probably due to local flooding, therefore, it was excluded from the regressions due to the skewness it caused in the relationship.

The average salinity for first-year ice collected inside the barrier islands is 6.0 ‰ and that of samples collected seaward of the barrier islands is 5.2 ‰. The average salinity obtained for the two first-year pack ice cores collected in 1986 is 4.6 ‰. The first-year pack ice collected for this study is assumed to be the most comparable to that collected in other Arctic areas such as Fram Strait and the Barents Sea because it formed in deep water outside the influence of near-shore conditions. In addition, the average bulk salinity of the pack ice cores is comparable to that found by Tucker and Gow (1987) in Fram Strait (4 ‰).

A best-fit linear regression obtained for near-shore ice seaward of the barrier islands is:

$$S_i = 3.94 + 0.6 h$$

where S_i is bulk salinity in o/oo and h is thickness in m. The regression obtained for all first-year ice except core O87 is:

$$S_i = 3.39 + 1.13h$$

The low R-values for these regressions which are not significant at the 95% confidence interval is attributable to the lack of samples over the entire thickness range. Compared to regressions obtained from previous studies, the salinities of ice in the Prudhoe Bay area are higher. For 1.5 m of ice the salinity obtained from Tucker et al. (1987), Gow et al. (1987), Gow and Tucker (1987) and Cox and Weeks (1974) is 4.1 o/oo. The above regressions yield salinities of 5.7 and 6.8 o/oo for 1.5 m thick ice seaward of the barrier islands and for all 1.5 m thick first-year ice, respectively. The higher salinity of ice found in the Southern Beaufort Sea is probably related to time of sampling. Cores were collected in April and May as opposed to June and July in Fram Strait indicating that the ice was colder (-12.8° C at the surface) and less brine drainage had occurred in the Beaufort Sea cores, resulting in higher salinities.

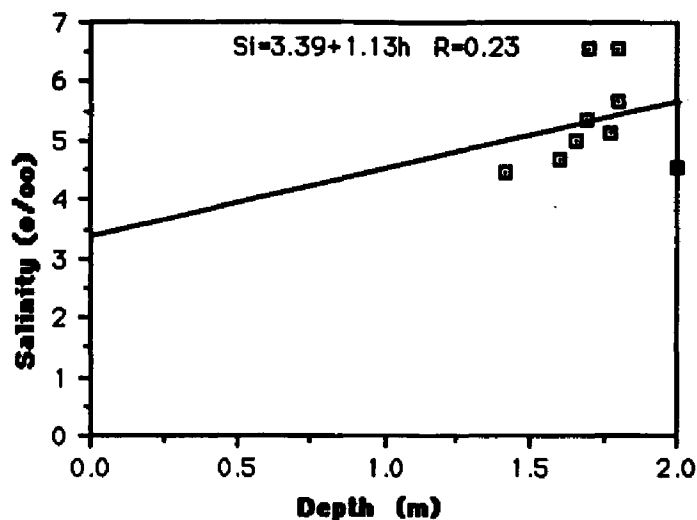


Fig. 33 Bulk salinity values of ice cores as a function of floe thickness.

Reasons for higher salinities for cores from the seaward side of the barrier islands are unknown. All of these cores were collected in relatively shallow water (<50 m) but it is unknown as to why this may have resulted in higher bulk salinities.

Only two cores were collected inside the barrier islands and, therefore, may not be very representative. However, this area is affected by closed lagoonal systems where water salinities are very high (56 o/oo at site A). These high water salinities normally result in higher bulk ice salinities as noted in these cores (core A=6.56 o/oo and core H=6.55 o/oo). Therefore, it can be seen that the water salinity and the local environment in which ice is formed can greatly affect core bulk salinity.

Dilution Curves

In order to determine if the conservative or major element and nutrient concentrations were enriched or depleted with respect to seawater values dilution curves were produced. This is a method in which concentrations of individual species in the ice are compared to the salinity of the ice where the dilution curve is based on expected values from surface seawater diluted to the salinity of the ice sample (Clarke and Ackley, 1984). All of the conservative elements are linear with some degree of scatter. Br, Ca, Mg, and SO_4 show the same trends for both years and are summarized in figures 34 (a-d). Ca and SO_4 show the most scatter around the dilution curve. This is not surprising as CaCO_3 and Na_2SO_4 are the first salts to precipitate during freezing. As brine drains the ratio of these species with respect to Cl occur resulting in variations in relation to the dilution curve.

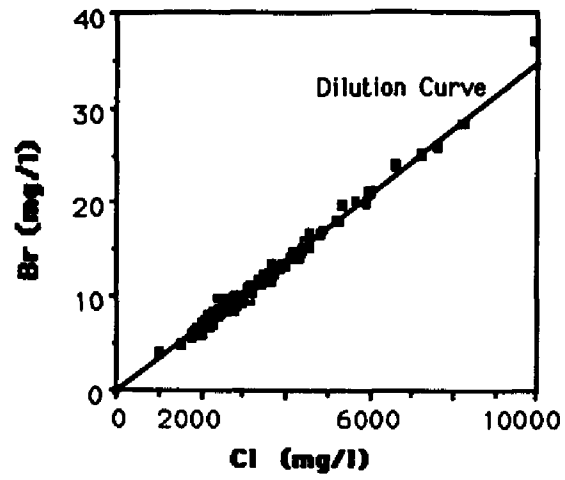
Mg in the ice (Fig.34d) is slightly enriched (1-2%) with respect to standard seawater and seawater collected from the sample sites indicating that an enrichment process is occurring. Bennington (1963) and Addison (1977) also found Mg enrichment in young sea ice and artificially grown sea ice. Nelson (1953) found that as brine temperature was lowered to -22.9°C the concentration of Mg in brine gradually increased as Na_2SO_4 crystallized from the brine. Between -22.9 and -36°C where NaCl forms, the increase in Mg concentration in the brine was much greater. Then as the freezing point was lowered below -36°C , the

Mg content of the brine decreased due to crystallization of Mg containing salts. Data from Assur (1960) shows that at -24°C the Mg:Cl ratio starts to increase until -50°C where $\text{MgCl}_2 \cdot 12\text{H}_2\text{O}$ begins to form and the ratio then decreases. Due to the increase in actual concentration and the increase in the Mg:Cl ratio, it appears that Mg may be precipitating with a salt other than Cl at higher temperatures.

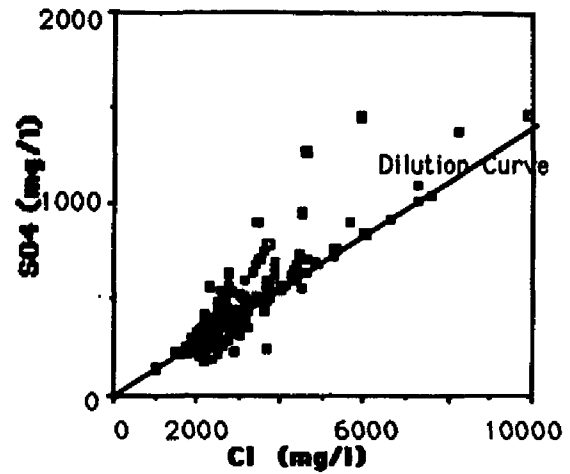
SO_4 (Fig. 34b) shows a considerable amount of scatter but does not appear to be enriched or depleted. Dilution curves for Na and K (Figs. 35-36) reveal that there was much more scatter in the 1986 samples than the 1987 samples. It is believed that this may be a result of differences in core handling techniques. The 1986 cores were collected and stored in core tubes for up to 3 days before processing. It seems possible that brine drainage may have occurred during storage. These samples were also rinsed with Milli-Q water which may also account for some of the scatter. Although the dilution curves for the 1987 samples are more linear, they show similar trends to the 1986 samples and overall there was not a significant difference between the two years. Na is fairly linear and does not show any trend toward enrichment or depletion. K, however shows a 1-2% depletion from seawater. Plots of K/Cl with depth from Bennington (1963) and Addison (1977) show depletion through most of the ice with respect to seawater. This is not surprising however, since the first K salt (KCl) does not form until -36.8°C , therefore, K should be more mobile than Cl and show a depletion with respect to seawater (Weeks and Ackley, 1982).

The nutrient curves (Fig. 37-38) all reveal enrichment with respect to seawater and show considerable scatter (89%- PO_4 , 70%- SiO_4 , 94%- NH_4 , 95%- NO_3 and 93%- NO_2) around the curve. The PO_4 curve (Fig. 37a) reveals that approximately 20% of the samples are depleted with respect to seawater, however, when all samples are considered the trend is toward enrichment. When actual concentrations are considered nutrients are higher in the surface water than in the ice with the exception of NH_4 which was usually higher in the bottom 10 cm of ice. This may be due to bacterial recycling (nutrient degradation and regeneration) (Horner and Schrader, 1982). Dilution curves for Weddell Sea ice samples (Clarke and Ackley, 1984) show different trends. PO_4 showed considerable scatter but approximated the dilution curve, whereas SiO_4 and NO_3 were depleted relative to the dilution curve which may be due to diatom growth and NO_2 was enriched due to nitrification of NH_4 by bacteria. However, nutrient enrichment, especially of inorganic nitrogen in ice from the Southern Beaufort Sea was observed by Alexander (1974) prior to the spring bloom. In this study, SiO_4 , NO_3 , NO_2 and NH_4 and possibly PO_4 were all enriched in the ice. Redfield ratios of N:P were calculated for the underlying water samples, first-year ice and multiyear ice in order to determine if the N:P ratio is consistent with that normally associated with oceanic organic matter (15:1). The N:P ratio for water collected at the ice/water interface is 4.6 which is significantly lower than the predicted 15. Maestrini et al. (1986) found an N:P ratio of 5.9 in water collected at the ice/water interface in Hudson Bay.

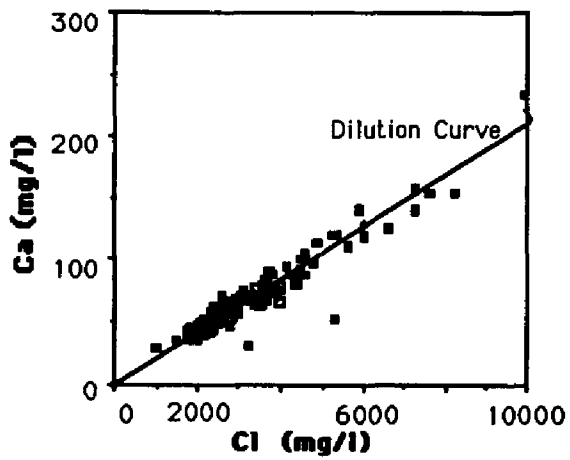
These low ratios may be the result of the substantially decreased biological activity in the water during the winter months. The mean N:P ratio for the first-year ice samples is 18.3. This value is much closer to the expected 15 than that found for the water. This indicates that nutrient enrichment in the ice is biologically active and the the N:P ratios, and therefore, concentrations are related to biological activity such as the degradation of relatively fresh organic matter or dying phytoplankton.



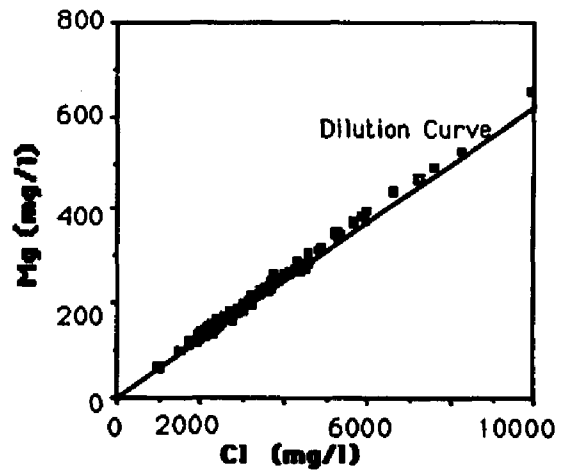
a



b

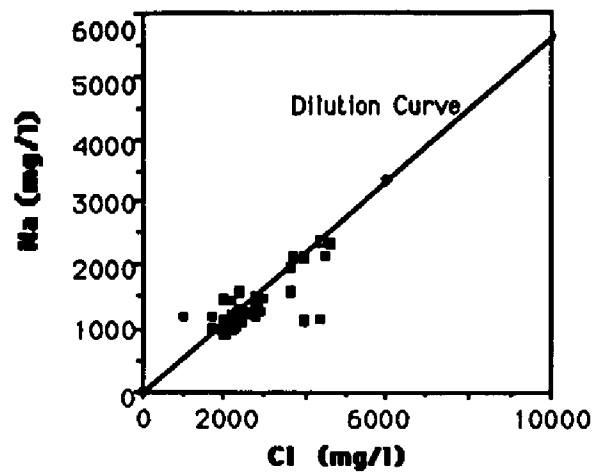


c

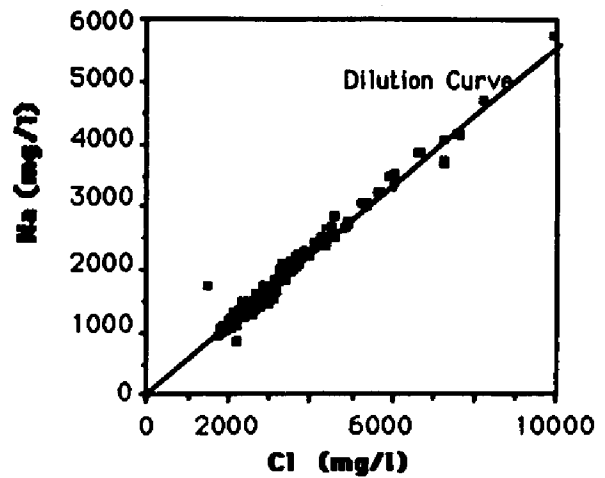


d

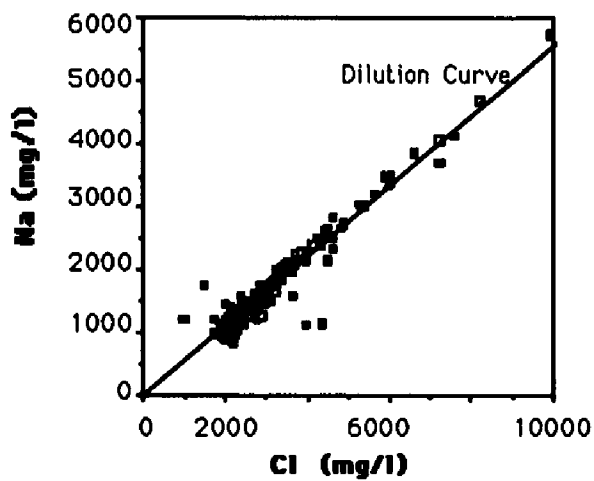
Fig. 34. Dilution curves for: a) Br, b) SO_4 , c) Ca and d) Mg for first-year ice.



a



b



c

Fig. 35. Dilution curves for: a) Na-1986 samples, b) Na-1987 samples and c) Na-all samples.

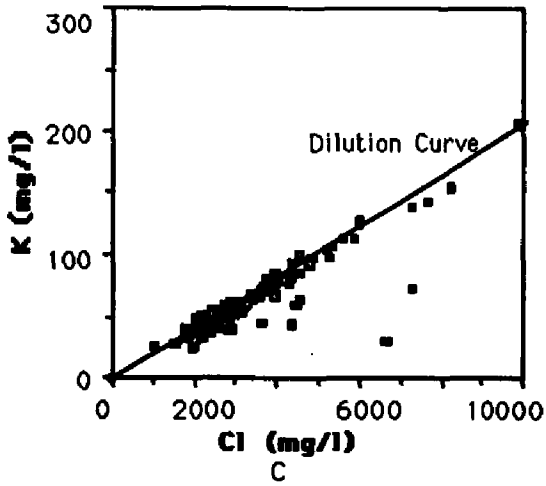
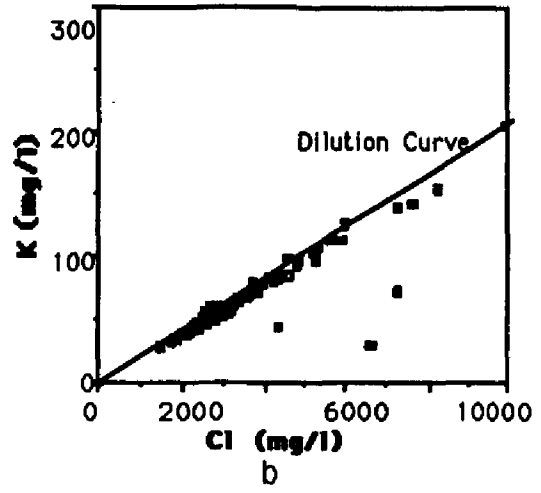
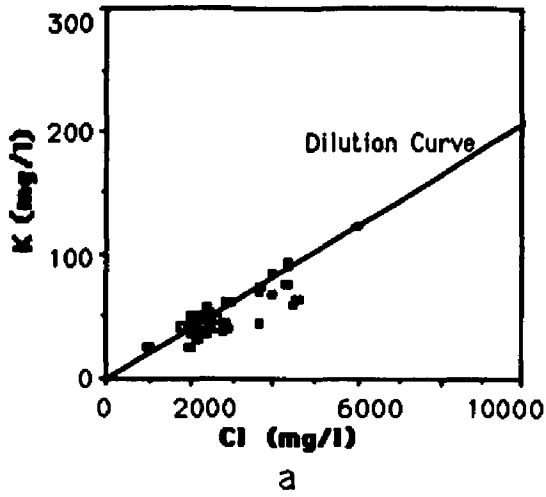
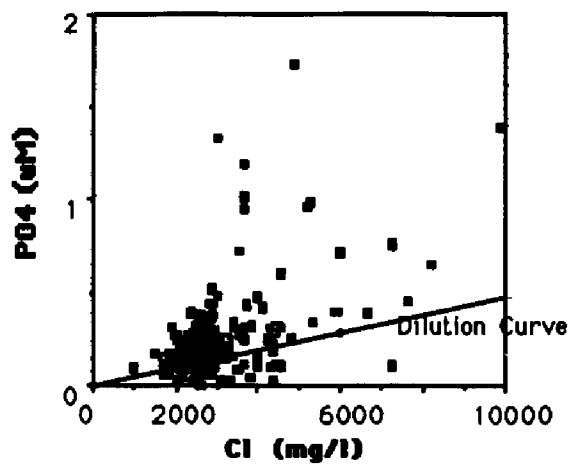
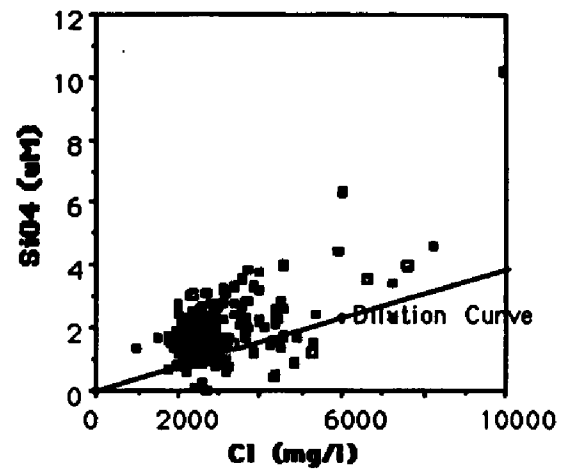


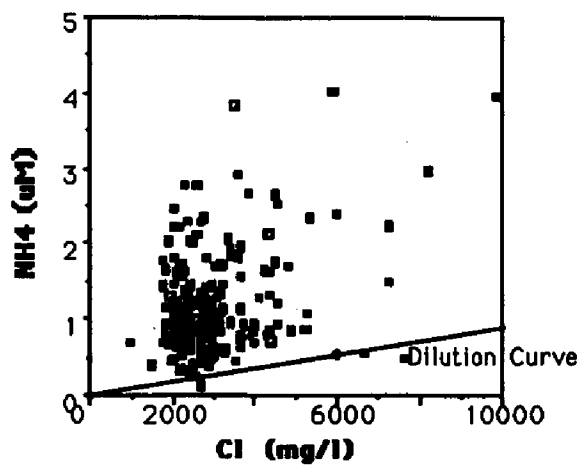
Fig. 36. Dilution curves for: a) K-1986 samples, b) K-1987 samples and c) K-all samples.



a

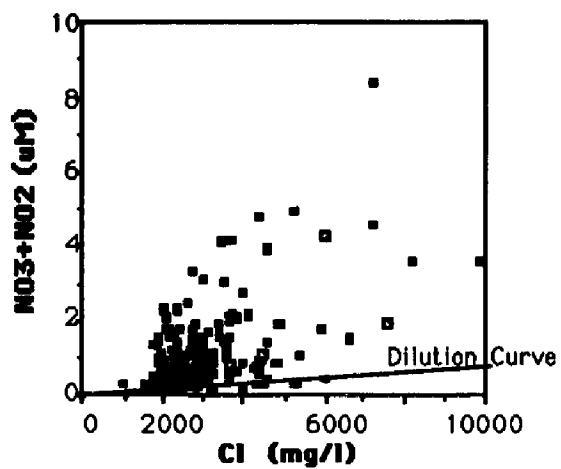


b

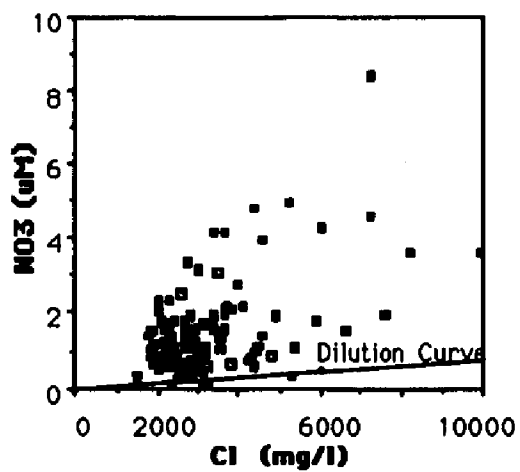


c

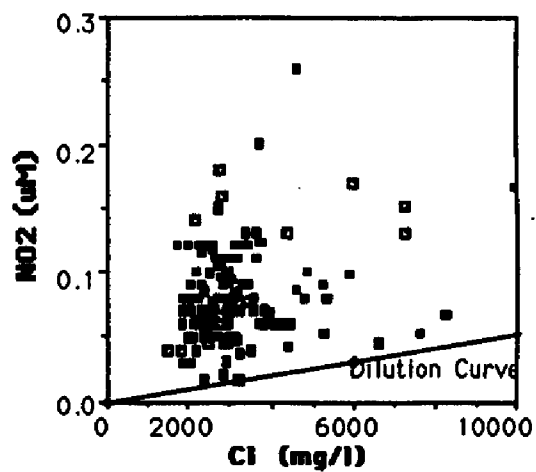
Fig. 37. Dilution curves for all samples for: a) PO₄, b) SiO₄ and c) NH₄.



a



b



c

Fig. 38. Dilution curves for: a) NO_3+NO_2 -1986 samples, b) NO_3 -1987 samples and c) NO_2 -1987 samples.

Cations/Anions

For each sample the sum of all cations and anions was obtained, the ratio between the two determined and an average of all samples calculated for each core. This was done in order to determine if significant differences exist between cores and to determine if, on average, cations or anions are enriched or depleted. For first-year ice the core average ratio ranged between 0.89-1.03. The average for all samples was 1.0 with a standard deviation of 0.04. The core with the lowest ratio (0.89) was SI86 which contained more granular ice than columnar ice. When this core was omitted from the calculation the average for all samples becomes 1.01 with a standard deviation of 0.017. This may indicate that cation:anion ratios may be affected by ice type, granular ice yielding a higher percentage of anions and congelation ice a slightly higher percentage of cations.

Linear Regressions

For each core collected, plots were produced for all chemical species analyzed versus Cl. In addition plots of Na to SO₄, experimental salinity to measured salinity, NO₃ to the other nutrients and NO₂ to the other nutrients were produced. Best-fit linear regressions were obtained for each core and the mean y-intercept, slope and R-value were calculated separately for all first-year samples, 1986 first-year samples and 1987 first-year samples. A summary table of the results is presented in Appendix C. These plots were produced to determine which chemical species

are linear with Cl (i.e. salinity) and which nutrients are linear with each other in order to assist in determining if factors other than salinity may be affecting ice chemistry.

Due to differences in sampling locations and sample handling between the 1986 and 1987 first-year ice the y-intercepts and slopes differ. However, some definitive trends exist. Br, Ca, K and Mg all have R-values above 0.9 indicating strong linearity and a strong dependence on salinity. SO₄ and Na have R-values between 0.76 and 0.98 indicating that they are still fairly linear with respect to Cl but exhibit more scatter, consistent with what was observed in the dilution curves. Plots of Cl to nutrients yield much weaker R-values (all <0.7) indicating that salinity effects are much less dominant and that other processes have affected nutrient concentrations. The average R-value for Na to SO₄ for the 1986 samples is 0.68 while that for the 1987 samples is 0.91. Because NaSO₄ is one of the first major salts to precipitate it appears that the low value obtained for the 1986 samples may be a result of sample processing as described above. Nutrients plotted against each other also show weak linear trends with R-values ranging from 0.43-0.64 which appears to indicate that the nutrients are not strongly affected by the same processes as the major elements.

Statistical Analysis

Statistical analyses including correlation coefficient matrices and factor analysis were performed on the various groups of chemical species of each core. Divisions between species were made for: all chemical species, major elements, nutrients, all species normalized to Cl, major elements normalized to Cl and nutrients normalized to Cl. Analyses were performed on the 3 major groups to determine what processes may be affecting chemical species variation in sea ice and determining which correlations are similar between cores. By separating the major elements and the nutrients it may be possible to determine if any of the major ions are behaving independently; by separating the nutrients it will be possible to determine if relationships exist between them, if they are controlled by similar processes or behave independently.

Tables 17-28 found within this section are summary tables. The summarized correlation coefficient matrices list those cores in which significant correlations at the 99% confidence intervals for the specified chemical species exist. For instance in Table 17, cores A, C, H, O and SI87 are listed for the correlation temperature-depth which means that for those cores there is significant correlation at the 99% confidence interval for temperature-depth.

The factor analysis tables have a similar format. Cores with high positive or negative loadings for a particular species

are listed under the appropriate factors. In Table 18, for depth, cores FY2, A, C, D and H all have high positive loadings and WD has a high negative loading in factor 1 in the individual factor analysis tables.

By compiling the data in this manner it is possible to compare correlations between cores and to evaluate the similarities and differences occurring between chemical species in the ice pack.

Statistical Analysis for all Chemical Species

Table 17 is the summary table for the correlation coefficient matrices for all chemical species. From the table it can be seen that in cores A and O there are significant correlations between temperature and depth and for most species. The reason for these correlations is unclear. The only similarity between these two cores is that they had the highest bulk salinities. It can also be seen from Table 17 that for the major elements almost all cores have significant correlations at the 99% confidence interval with the other major elements. Because these are the major elements in seawater this is not surprising and indicates that the ratios between ions remains fairly constant throughout the depth of the core and for the entire pack. However, there is much less consistency between nutrients in this regard. In 60% of the first-year cores there is a significant correlation at the 99% confidence interval between salinity and NO_3 . This indicates that NO_3 is strongly

salinity dependent. In 50% of the first-year cores, PO_4 correlates significantly at the 99% confidence interval with all major elements. In addition, three of these cores also had significant correlations between the major elements and NO_3 and also had significant correlations between NO_3 and PO_4 . Also, SiO_4 correlates significantly with all major elements in three cores and NO_2 correlates significantly with all the major elements and nutrients. Cores A and O with few exceptions have significant correlations between all chemical species. These two cores were collected in highly saline water and it appears that nutrients are highly correlated with salinity and that the effect from biological activity is a secondary process and appears to be less significant, perhaps due to the enhanced salinity. In addition, chlorophyll-a analyses were performed on 10 cm long sections in cores FY186 and SI87. When these are included in the statistics chlorophyll-a correlates with salinity at the 99% confidence interval for both cores. In addition, chlorophyll-a correlates significantly with all the major elements in core SI87. This further substantiates the belief that nutrients supplied by seasonal brine drainage may be responsible for development of internal biological populations as suggested by Ackley, et al. (1979) from samples collected from the Weddell Sea.

Factor analysis on this group of data (Table 18) substantiates the conclusions borne out from the correlation coefficient matrices. With few exceptions all major elements from all cores have high positive loadings in factor 1 indicating

that major element concentrations and salinity are strongly inter-related in the ice. The table also reveals that in a few cores some nutrients vary with the major elements. For example, cores C and O have high positive loadings in factor 1 for PO_4 and NO_3 and core A has a high positive loading on NH_4 indicating that their concentrations are also controlled by salinity and brine drainage. It can also be seen that the expected relationship between all elements in cores A and O (based on high positive loadings for all elements in factor 1) does not exist except for PO_4 for both A and O, NO_3 for core O and NH_4 for core A. Throughout the remainder of the table there appear to be no definitive trends with nutrients. This indicates that although the primary factor affecting nutrient concentrations is due to salinity, secondary processes are occurring but may not be consistent throughout the ice pack and may be location specific.

Table 17. Summary table for correlation coefficient matrices for first-year ice for all elements. Chlorophyll-a analyses were only performed on cores FY1 and SI87. All correlations listed are significant at the 99% confidence interval.

	Depth	Temp	Sal	Cl
Depth				
Temp	A, C, H, O SI87			
Sal	A, O, -SI86	A, O		
Cl	A, O, -SI86	A, O	A, C, D, H, SI86 SI87, O, WD, FY2	
Br	A, O, -SI86	A, O	FY2, SI86A, C, D H, O, SI87, WD	FY1, FY2, SI86, A C, D, H, O, SI87, WD
SO4	A, O	A, O	FY2, SI86, A, C D, H, O, SI87, WD	FY1, FY2, SI86, A C, D, H, O, SI87, WD
Na	A, O, -SI86	A, O	FY1, FY2, SI86, A C, D, H, O, SI87, WD	FY2, SI86, A, C, D H, O, SI87, WD
Ca	A, O, -SI86	A, O	FY2, SI86, A, C, D H, O, SI87, WD	FY1, FY2, SI86, A C, D, H, O, SI87, WD
K	A, SI87	A	FY2, SI86, A, C, D H, O, SI87, WD	FY1, FY2, SI86, A C, D, H, O, SI87, WD
Mg	A, O, -SI86	A, O	FY2, SI86, A, D H, O, SI87, WD	FY1, FY2, SI86, A C, D, H, O, SI87, WD
PO4	A, D, O, SI87	A, O	FY1, A, C H, O, SI87	A, C, H, O, SI87
SiO4	A, O, -WD FY1	A, O	FY2, A, O, WD	FY2, A, O, WD
NO3	A, O, -SI86, -WD	A, O	FY1, FY2, A, C H, O, WD	FY2, A, C, H, O, WD
NO2	A, O, -WD	A, O	A, H, O	
NH4	-WD	A	SI86, A, D, O	
Chl-a			FY1, SI87	SI87

Table 17. (cont.).

	Br	SO4	Na	Ca
Br				
SO4	FY1, FY2, SI86, A C, D, H, O, SI87, WD			
Na	FY2, SI86, A, C, D H, O, WD	FY2, SI86, A, C, D H, O, WD		
Ca	FY1, FY2, SI86, A C, D, H, O, SI87, WD	FY1, FY2, SI86, A C, D, H, O, SI87, WD	FY2, SI86, A, C, D H, O, SI87, WD	
K	FY1, FY2, SI86, A C, D, H, O, SI87, WD C, D, H, O, SI87, WD	FY1, FY2, SI86, A C, D, H, O, SI87, WD	FY2, SI86, A, C, D H, O, SI87, WD	FY1, FY2, SI86
Mg	FY1, FY2, SI86, A FY1, FY2, SI86, A C, D, H, O, SI87, WD	FY1, FY2, SI86, A H, O, SI87, WD	FY2, SI86, A, C, D C, D, H, O, SI87, WD C, D, H, O, SI87, WD	
PO4	A, C, H, O, SI87	A, C, H, O, SI87	FY1, A, C, H, O, SI87	A, C, H, O, SI87
SiO4	FY2, A, O, WD	FY2, A, O, WD	FY2, A, O, WD	FY2, A, O, WD
NO3	FY2, A, C, D, H, FY2, A, C, H, O, WD	FY2, A, C, D, O, WD	FY2, A, C, H, O, WD O, WD	
NO2	A, H, O.	A, C, H, O	A, H, O	A, H, O
NH4	A, D, H	SI86, A, D, O	SI86, A, H, O	SI86, A, D
Chl-a	SI87	SI87	FY1, SI87	SI87

	K	Mg	PO4	SiO4	NO3	NH4
K						
Mg	FY1, FY2, SI86, A C, D, H, O, SI87, WD					
PO4	A, C, H, O, SI87, WD	A, C, H, O, SI87				
SiO4	FY2, A, O	FY2, A, O, WD				
NO3	FY2, A, C, H, O, WD O, WD	FY2, A, C, H O, SI87	FY1, A, C, H	A, O, WD		
NO2	A, H, O	A, H, O	A, H, O	A, H, O, WD	A, H, O, WD	
NH4	SI86, A, D, O	SI86, A, D, O	FY2, A	FY2, A, H	A, C, O SI87, WD	
Chl-a	SI87	SI87	FY1, SI87		FY1	FY1

Table 18. Summary table for factor analysis results for first-year ice for all chemical species. Chlorophyll-a analyses were only performed on cores FY1 and SI87.

	Factor 1	Factor 2	Factor 3	Factor 4
Depth	-O A, C, D, H, -WD	FY2	FY2, SI87	FY2
Temp				
Sal	FY2, SI86 A, C, D, H, O, SI87, WD	FY1, C, D, H	SI87	
Cl	FY1, FY2, SI86 A, C, D, H, O, SI87, WD			
Br	FY1, FY2, SI86 A, C, D, H, O, SI87, WD			
SO4	FY1, FY2 A, O, WD			
Na	FY2, SI86 A, C, D, H, SI87, O	FY1		
Ca	FY1, FY2, SI86 A, C, D, H, O, WD			
K	FY1, FY2 A, C, D, H, SI87			
Mg	FY1, FY2, SI86 A, C, D, H, SI87, O, WD			
PO4	A, C, O	FY1, FY2, SI86, D	WD	
SiO4	A, O	SI86	FY1, -C	FY2
NO3	C, O	A	SI86, D	FY2, A
NO2	H, O		A	D
NH4	A	FY2, SI87, O	-FY2, C, D	
Chl-a	SI87	FY1		

Statistical Analysis for Major Elements

The summary table for correlation coefficient matrices for the major elements (Table 19) reveals that all correlations in all cores are significant at the 99% confidence interval. The exception to this is core FY1 where Na does not correlate significantly with any of the other major elements. The significant correlation between all major elements is expected because these are the conservative elements in seawater. This

indicates that the ratios of the elements are remaining fairly constant throughout the ice. Why Na in core FY1 does not correlate with the other elements is unclear.

Factor analysis for the major elements (Table 20) reveals that most cores have high positive loadings on all elements in factor 1. This is expected due to the salinity effect and substantiates the assumption that the incorporation of major ions at the ice/water interface is occurring and the ratios are consistent with seawater indicating that no significant fractionation of the major ions occurs in the ice. Factor 2 has fewer high loadings. The high loading on Na in factor 2 for FY1 is consistent with the correlation coefficient matrix indicating again (for reasons unknown) that Na is behaving differently than other elements in this core. Another interesting result is that 50% of the cores have high positive loadings on SO₄ in factor 2. This is the only indication of possible chemical species fractionation in these cores.

Table 19. Summary table for correlation coefficient matrices for first-year ice for major elements. All correlations listed are significant at the 99% confidence interval.

All species correlated significantly at the 99% confidence interval in all cores except for Na to any of the other species in core FY1

Table 20. Summary table for factor analysis results for first-year ice for major elements.

	Factor 1	Factor 2
Cl	FY1, FY2, SI86, A, C, D, H, O, SI87, WD	
Br	FY1, FY2, SI86, A, C, D, H, O, SI87, WD	
SO4	FY1, FY2, A, H, O, WD	SI86, C, D, H, SI87
Na	FY2, SI86, A, C, D, H, O, SI87, WD	FY1
Ca	FY1, FY2, SI86, A, C, D, H, O, SI87, WD	
K	FY1, FY2, A, C, D, H, SI87	FY2, O, WD
Mg	FY1, FY2, SI86, A, C, D, H, O, SI87, WD	

Statistical Analysis of Nutrients

The summary table for correlation coefficient matrices (Table 21) and for factor analysis (Table 22) for the nutrients reveals that there are fewer correlations and there is much less consistency between the nutrients than the major ions. To a certain extent, this is an expected result due to the many processes that can affect nutrient concentrations such as biological growth, brine drainage, bacterial regeneration, nitrification and denitrification. While it is possible to determine processes causing correlations that occur in individual cores, such as the correlation between NO_3 and NH_4 in cores FY1, A, D, O and SI87, (Table 21) resulting from winter nutrient buildup and local recycling of nutrients (Horner and Schrader, 1982), there are no consistent correlation trends between cores.

Chlorophyll-a concentrations were determined for 10 cm long sections in cores FY186 and SI87. Chlorophyll-a concentrations in core SI87 ranged from 0-73.3 mg/m^3 and from 0.13-21.84 mg/m^3 in core FY1 with concentrations increasing with depth. Surface water concentrations were 16.4 and 5.9 mg/m^3 for sites SI87 and FY1, respectively. When statistical analyses were performed on

these data it was found that significant correlations at the 99% confidence interval exist for NO₃ and chlorophyll-a to PO₄ and for chlorophyll-a and NO₃. Factor analysis shows high positive loadings for PO₄, NO₃, NH₄ and chlorophyll-a in factor 1. This suggests that the existence of a chlorophyll-a population is dependent on the availability of nutrients in the ice but perhaps it was too early in the spring bloom for biological utilization to strongly deplete nutrient concentrations which would result in the expected negative correlations between nutrients and chlorophyll-a.

Table 21. Summary table of correlation coefficient matrices in first-year ice for nutrients. Chlorophyll-a analyses were only performed on cores FY1 and SI87. All correlations listed are significant at the 99% confidence interval.

	PO4	SiO4	NO3	NO2	NH4
PO4					
SiO4	A				
NO3	FY1, A, H, SI87	FY2, A, O, WD			
NO2	A, C, H, O	A, O, WD	A, C, H, O, WD		
NH4	FY1, FY2, A	A, H	FY1, A, D, O, SI87	A, C, SI87, WD	
Chl-a	FY1, SI87		FY1		FY1

Table 22. Summary table for factor analysis results for first-year ice for nutrients.

	Factor 1	Factor 2
PO4	FY1, SI86, A, H, SI87	FY2, D, O, WD
SiO4	FY2, SI86, A, O, WD	FY1, C, H, SI87
NO3	FY1, FY2, C, D, H, O, WD	SI86, A
NO2	O	-D, SI87
NH4	FY1, A	FY2, H, SI87, WD
Chl-a	FY1, SI87	FY1

Statistical Analysis for All Chemical Species Normalized to Cl

In order to determine if there are secondary processes affecting chemical concentrations other than salinity, all species were normalized to Cl. A summary table for the correlation coefficient matrices (Table 23) reveals that there are fewer correlations than before normalization. There is no definitive trend to the correlations and there are few similarities between cores, indicating that secondary processes are involved that may be due to factors which are site specific such as the thermal history of the ice and biological processes.

Table 23. Summary table for correlation coefficient matrices for first-year ice for all chemical species normalized to Cl. All correlations listed are significant at the 99% confidence interval.

	Br	SO4	Na	Ca	K	Mg	PO4	SiO4	NO3	NO2
Br										
SO4										
Na	FY1, H	C, H, WD								
Ca	FY1		FY1							
K	FY1			FY1, SI87						
Mg	O		FY2, SI87		A					
PO4	A			WD	WD	A				
SiO4	-SI86			FY1, -FY2			SI86			
NO3		D	FY1	FY1				FY2, C		
NO2								H, WD	C	
NH4		D	FY1	-D, WD			WD	WD	FY1, D	
	SI87, WD									

Table 24. Summary table for factor analysis results for first-year ice for all chemical species normalized to Cl.

	Factor 1	Factor 2	Factor 3	Factor 4	Factor 5
Br			SI86,D	A,C,SI87,WD	-FY2
SO4	H	FY1, -FY2,A,WD			
Na	FY1,FY2,C,H	SI86,SI87,WD	A,O		
Ca	A		FY2,H	SI86,SI87	
K	O	FY1	D,WD	FY2,H	
Mg		D,SI87	-FY1	WD	
PO4	SI86,SI87	C		FY1, -FY2, A,D,O	
SiO4	FY1, -FY2	-C,D,O			
NO3	FY1, -FY2, C,D,SI87	H,O,SI86	-WD		
NO2	A	D	C,SI87		
NH4	FY1,D,O,WD	FY2, -A	C,SI87		H

Statistical Analysis for Major Elements Normalized to Cl

As with all species normalized to Cl there is little consistency between the correlation coefficient matrices (Table 25) and the factor analysis results (Table 26). However, correlations do exist indicating that there are secondary processes affecting the chemistry but the cause is unclear and may actually vary between cores.

Table 25. Summary table of correlation coefficient matrices for first-year ice for major elements normalized to Cl. All correlations listed are significant at the 99% confidence interval.

	Br	SO4	Na	Ca	K	Mg
Br						
SO4						
Na	FY1,H	C,H,WD				
Ca	FY1		FY1			
K	FY1			FY1,SI87		
Mg	O		FY2,SI87		A	

Table 26. Summary table for factor analysis results for first-year ice for major elements normalized to Cl.

	Factor 1	Factor2	Factor 3
Br	A,C,O	SI86,SI87,WD	-FY2
SO4	FY1,SI86 -D,WD	A,C,O	FY2
Na	FY2,SI86 H,SI87,WD	A,C,D	
Ca	FY1,D	FY2,H,SI87	SI86
K	FY1,A	-FY2,D	H,WD
Mg	FY2,A,O SI87	-FY1	

Statistical Analysis for Nutrients Normalized to Cl

Based on the few correlations in the summary table (Table 27) it is difficult to identify specific processes affecting nutrient concentration in the ice. However, some processes that may be affecting nutrient concentration include, for instance, sediment incorporation in core SI86 where a significant correlation exists between PO_4 and SiO_4 due to dissolution and desorption from the sediment. Many of the remaining correlations were observed in core WD. This core was collected close to a shore-based desalination plant and it is possible that the close proximity of this core to the plant could be affecting nutrient concentrations in the ice. If the desalination plant is creating an impact on nutrient concentration in the area then it could play a major role in the annual local nutrient cycle and spring bloom.

Statistics were also performed on cores FY186 and SI87 with chlorophyll-a normalized to Cl. The only additional significant

correlation at the 99% confidence interval was between chlorophyll-a and PO₄ in core FY186. In factor analysis chlorophyll-a and PO₄ had high positive loadings in factor 2 also for core FY186. This suggests that at least for this core, when the salinity effect has been removed chlorophyll-a and PO₄ are strongly dependent.

Table 27. Summary table for correlation coefficient matrices for first-year ice for nutrients normalized to Cl.

	PO4	SiO4	NO3	NO2	NH4
PO4					
SiO4	SI86				
NO3					
NO2		H, O, WD			
NH4	WD	WD	FY1, D	H, SI87, WD	

Table 28. Summary table for factor analysis results for first-year ice for nutrients normalized to Cl.

	Factor 1	Factor 2	Factor 3
PO4	FY2, SI86, C	FY1, A, H, O, SI87	D
SiO4	FY1, A, -C, H, O		
NO3	FY1, D, H, O	FY2, SI86, C, WD	
NO2	A, H, SI87	C, D, O	
NH4	FY1, A, D, SI87, WD		

MULTIYEAR ICE

Core Profiles

A detailed description of each multiyear core is given below. Summary tables of statistical analyses are provided (Tables 29-40) at the end of this section.

CORE F1SA86

This core was taken from a weathered ridge approximately 9 m thick from which the upper 5 m were collected. The floe was approximately 60 m in diameter and ice thickness varied from 154 cm to 990 cm in the thickest ridge. The core consisted of approximately 50% columnar ice and approximately 50% granular ice. The granular ice may be from new growth occurring on the bottom of the ridge at the beginning of a winter season or may have resulted from void infilling and refreezing between blocks. The structural profile (Fig. 39) shows sections of alternating layers of granular and columnar ice between 20 and 450 cm. This is overlain by 10 cm of pond or fresh water ice and 10 cm of snow ice. A vertical thin section between 30-40 cm shows a sharp transition from coarse to finer grained columnar ice (Fig. 39). The section between 80-90 cm consists of platy ice and at 290 cm shows columnar ice with randomly aligned c-axes.

Salinity (Fig. 39) and major element-depth profiles (Fig. 40) all show the same trends, while nutrient profiles are generally scattered with varying trends. High salinity and major

element concentration peaks occurring at approximately 100, 240 and 360 cm may be indicative of annual growth layers. When major element concentration peaks are compared to structure, all major peaks correlate with finer-grained ice whether they be of granular or columnar crystal texture.

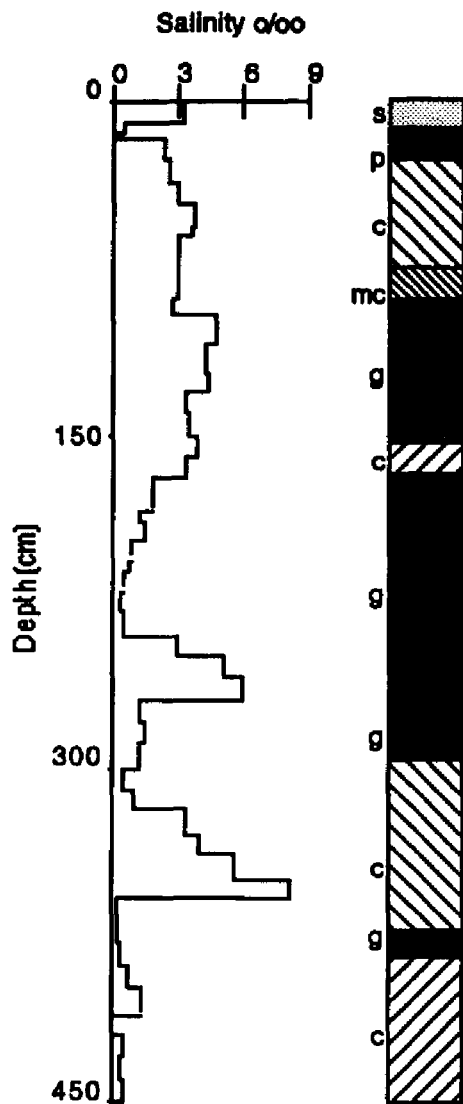


Fig. 39. Structure-salinity profiles from core F1SA86. In the structure diagram the symbols s, p, c, mc, c and g designate snow-ice, pond ice, congelation ice, medium-grained congelation and granular ice respectively.

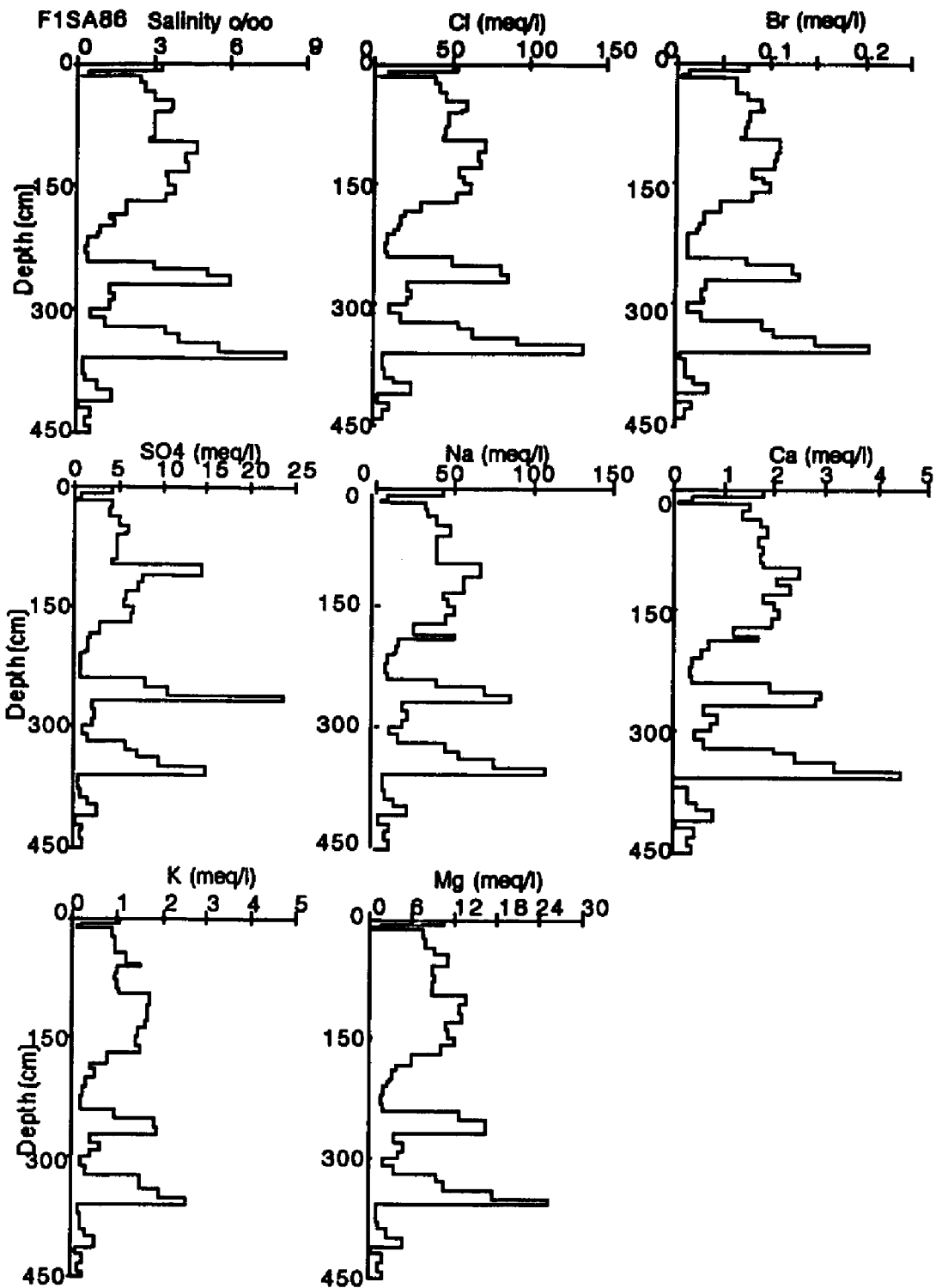


Fig. 40. Chemistry profiles for core F1SA86.

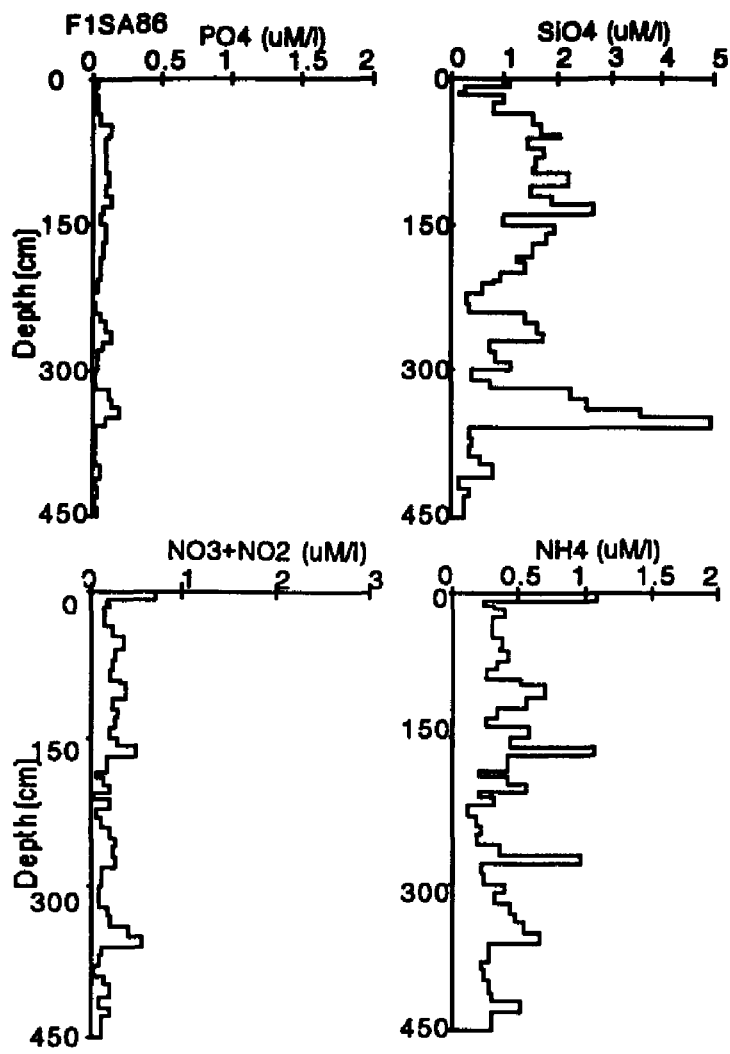


Fig. 40. (cont.).

CORE F1SB86

Core F1SB86 was collected from the same floe as the previous core, however, this core was collected in a melt pond. This core was 204 cm long and consisted of 6 cm of snow ice followed by 6 cm of pond ice underlain by 184 cm of columnar ice.

Photomicrographs of horizontal thin sections show the varied structure of this core (Fig. 41). The section at 50 cm shows retextured medium-grained congelation ice proving that this is multiyear ice. Between 50-175 cm crystals increase in size and their c-axes become more aligned with depth.

Salinity (Fig. 41) and depth profiles for all species analyzed (Fig. 42) show a C-profile more typical of first-year sea ice. This may be an indication that this may have been remnant ice with one years growth. Nutrient concentrations show considerable scatter with no apparent trends. There does not appear to be a correlation between stratigraphic changes (ice type) and chemical concentration patterns.

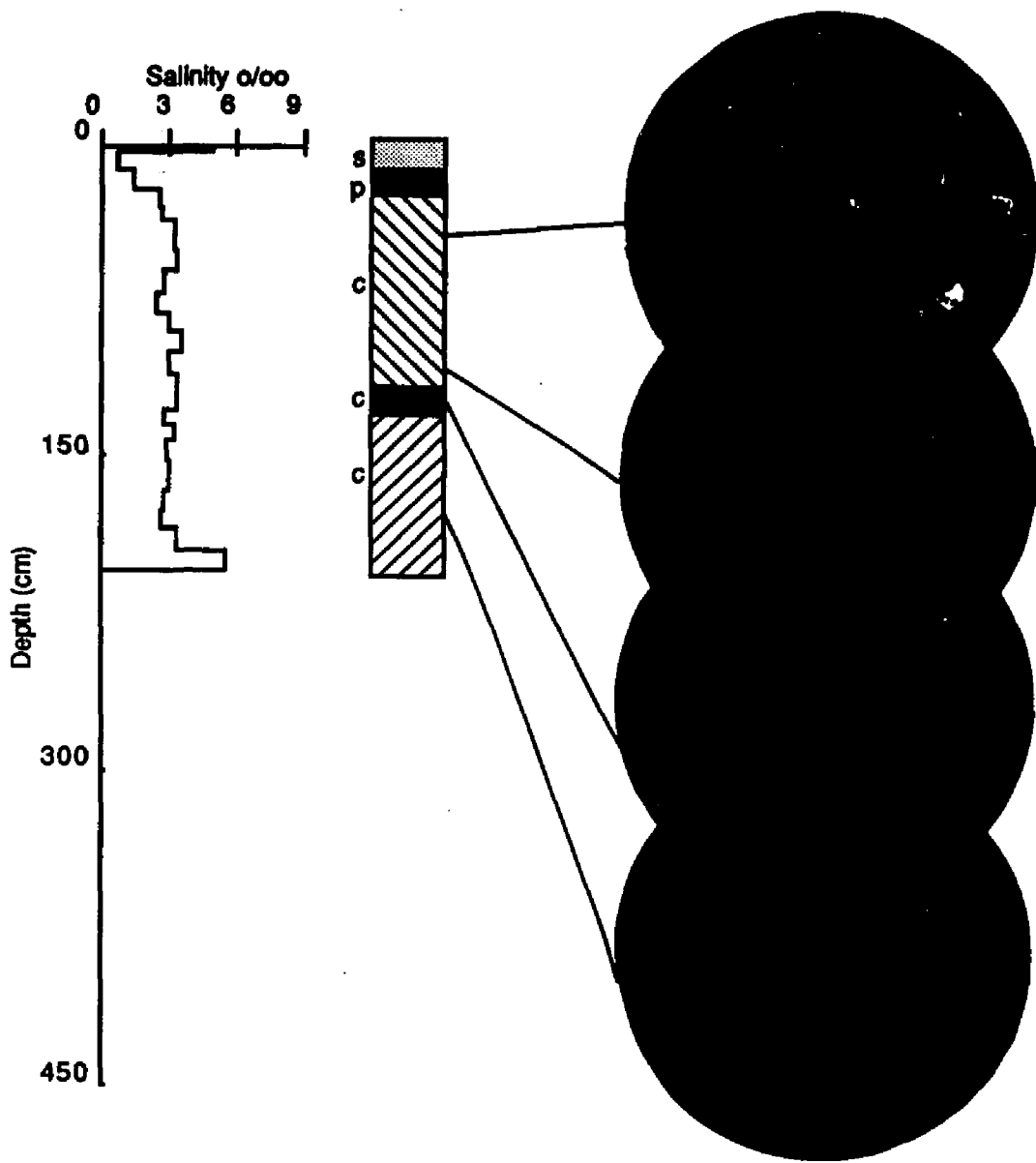


Fig. 41. Salinity-structure profiles for core F1SB86. In the structure diagram. All symbols are as described previously.

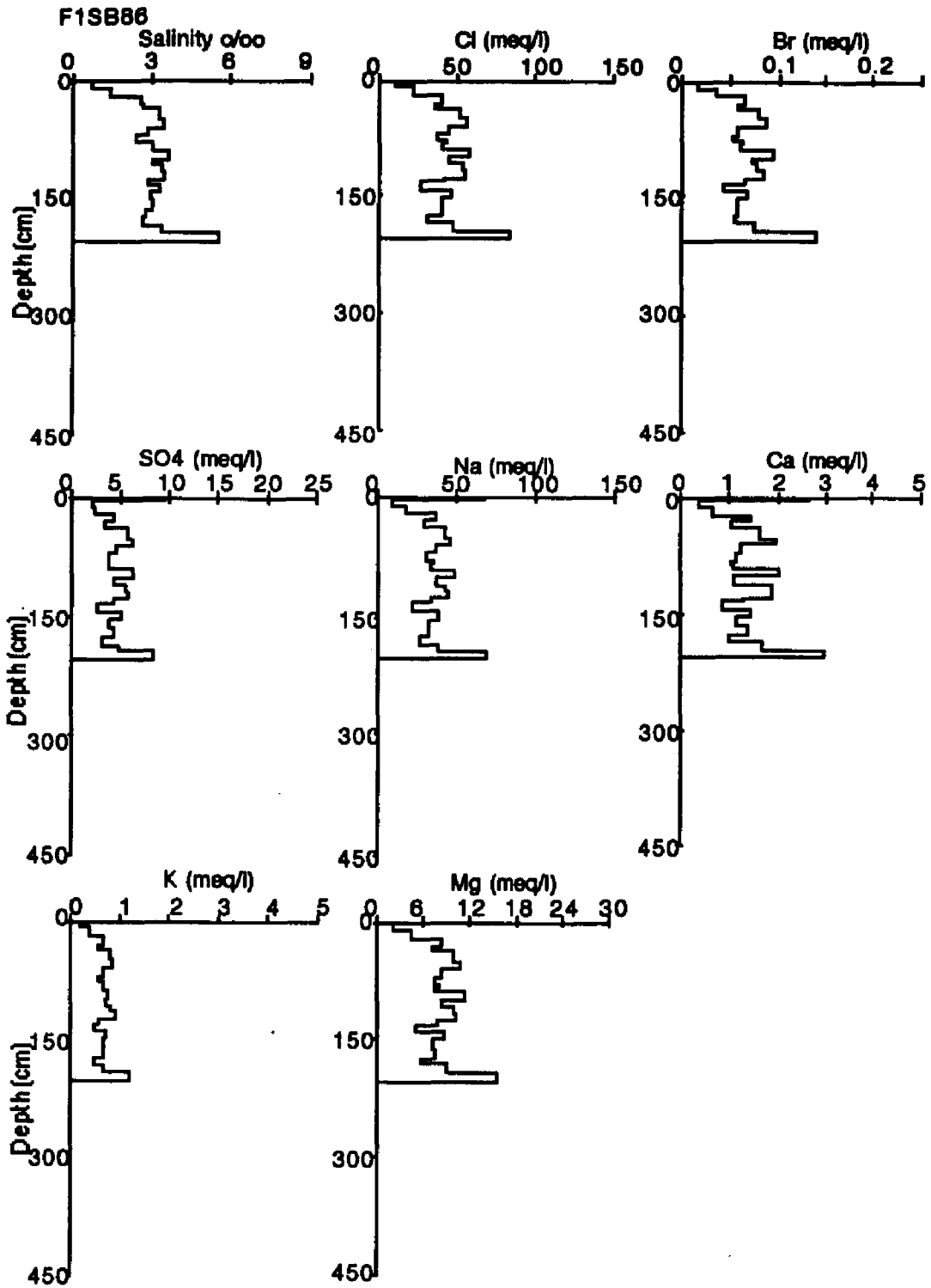


Fig. 42. Chemistry profiles for core F1SB86.

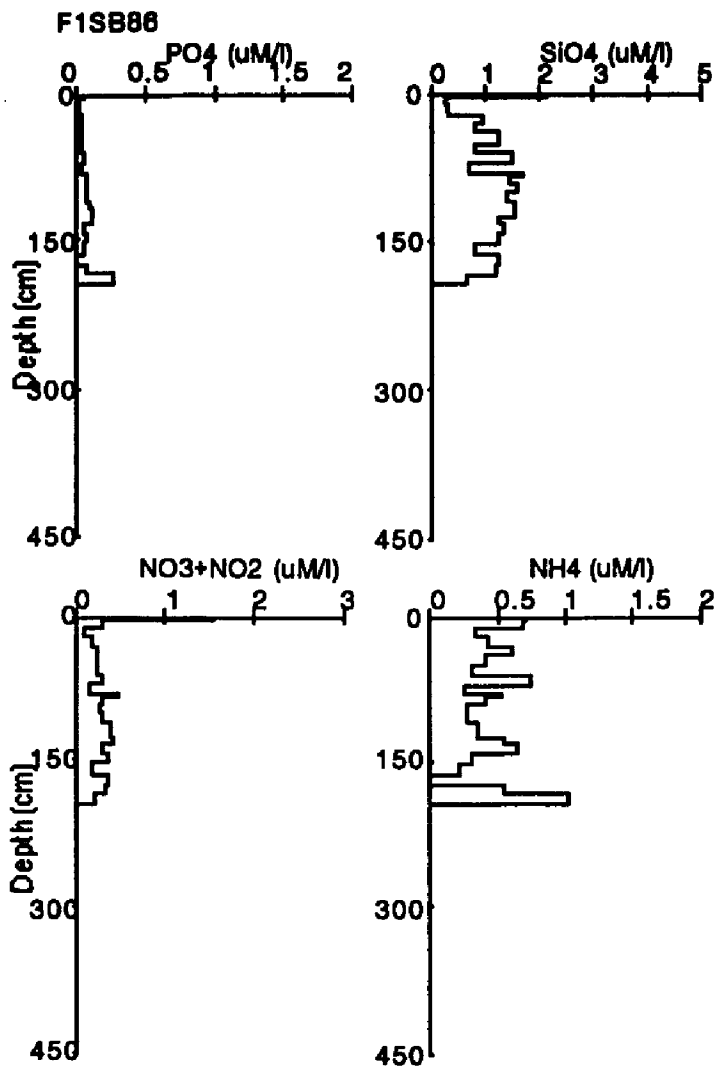


Fig. 42. (cont.).

Core F1SC86

Core F1SC86 was collected from the same floe as the two previous cores and was also collected from a melt pond. The core was 208 cm long, consisting of 198 cm of columnar ice overlain by 10 cm of snow ice. A photomicrograph of a vertical thin section taken between 0-12 cm shows the transition between snow ice and columnar ice. A photomicrograph of a horizontal thin section taken at 30 cm shows unoriented medium-grained columnar ice (Fig. 43). The section taken at 60 cm shows columnar ice with aligned c-axes and the section taken from 90 cm shows that the ice in this region has been retextured. At 170 cm the ice is oriented congelation and at the bottom of the core (200 cm) crystal c-axes have become very strongly aligned. As with core F1SB86 this is also remnant ice with one years growth.

Depth profiles for salinity (Fig. 43) and the major elements (Fig. 44) all track each other with the exception of K. NO_3+NO_2 and NH_4 also track each other. SiO_4 concentrations are the highest in the center of the core between 70-130 cm. As with core F1SB86 the salinity profile is similar to that of first-year ice, therefore, this core may have also been a melt pond that melted through and then refroze the following year. Salinity and major element concentrations are high in the snow ice whereas the lowest values are found in the pond ice.

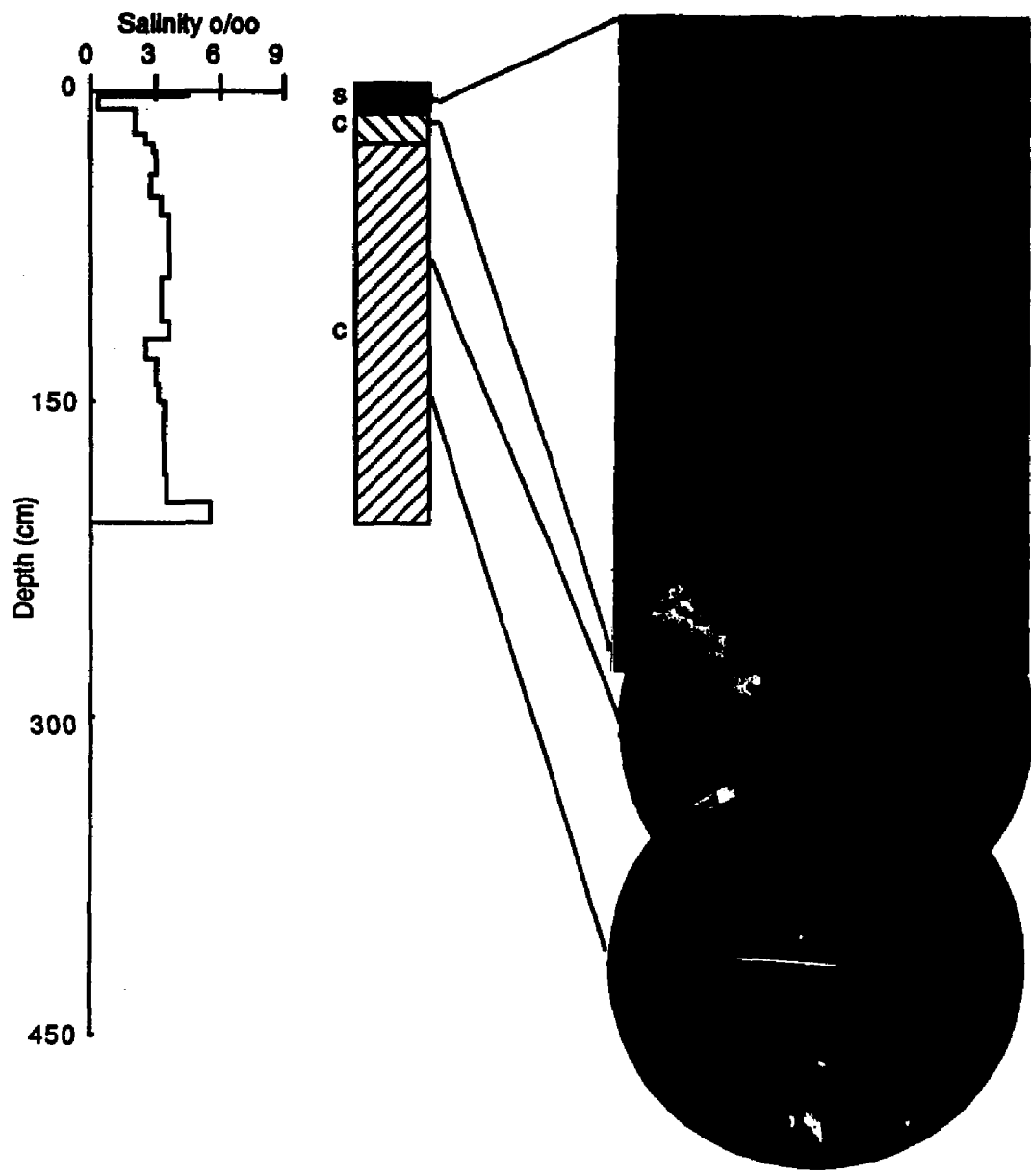


Fig. 43. Salinity-structure profiles for core F1SC86. Symbols in the structure profile are as described previously.

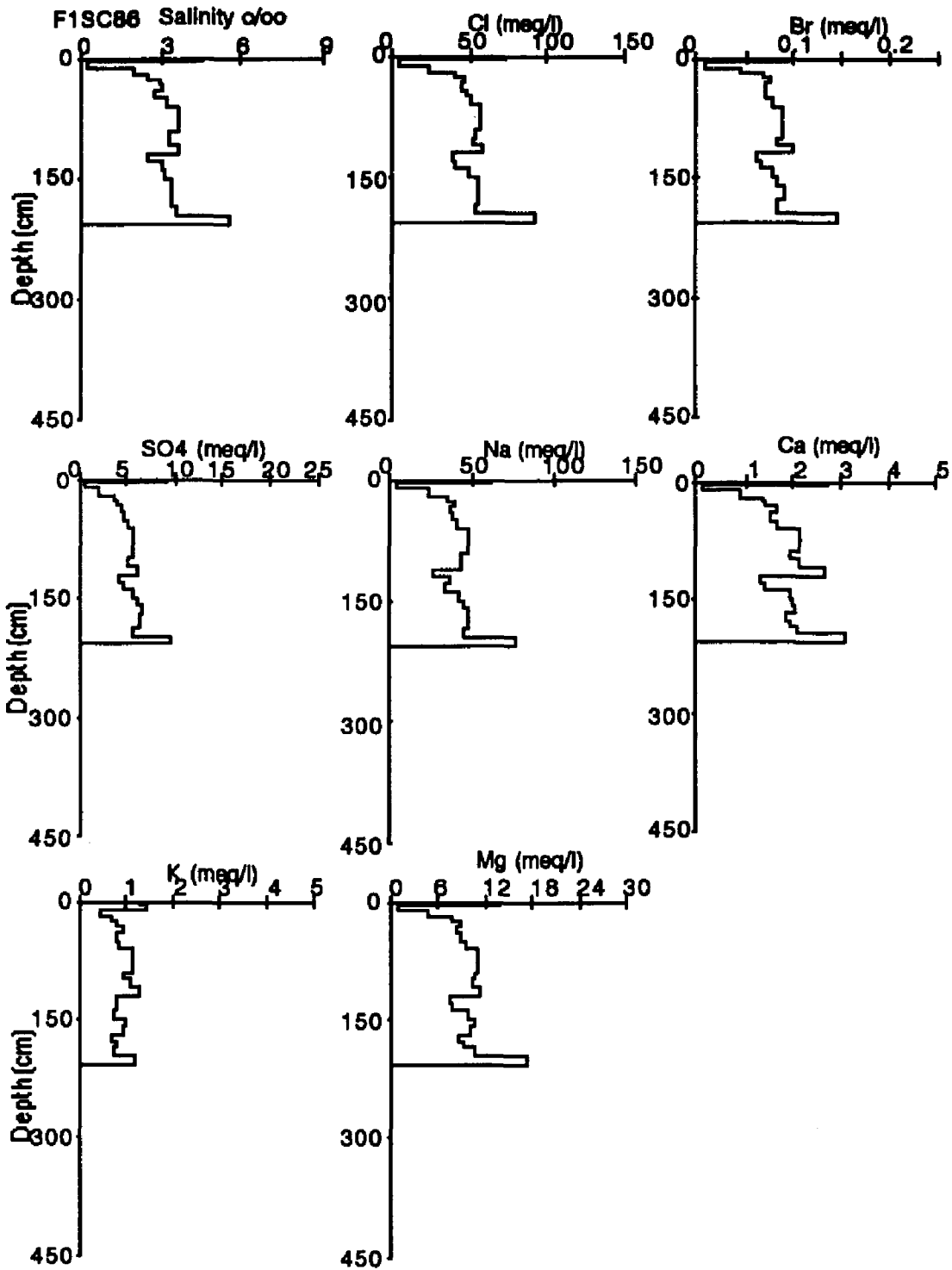


Fig. 44. Chemistry profiles for core F1SC86.

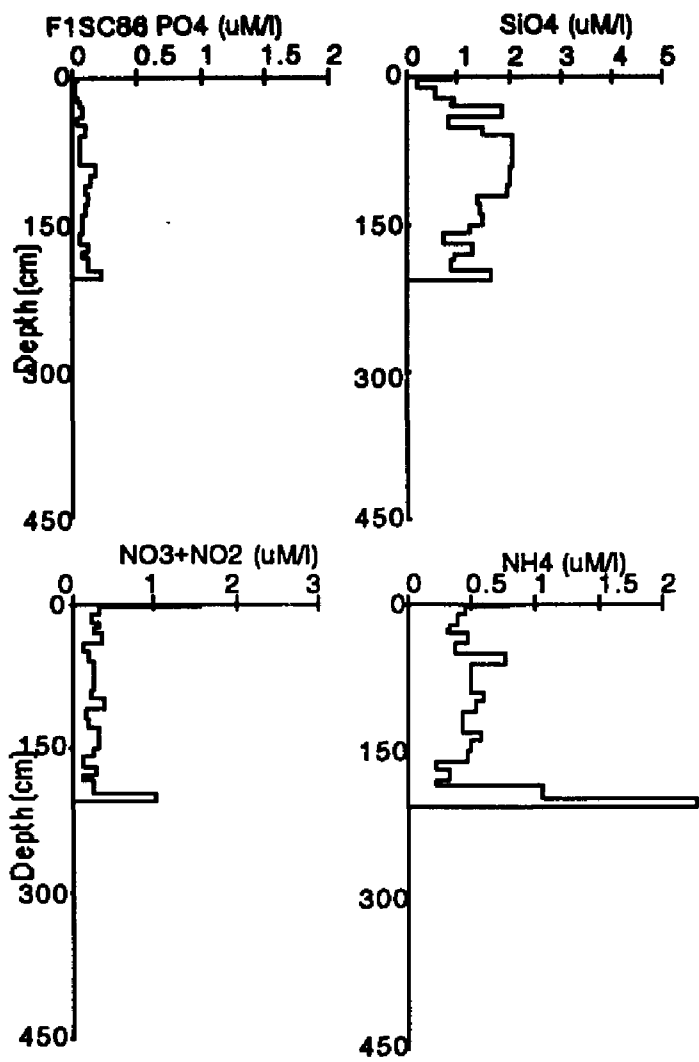


Fig. 44. (cont.).

CORE F1SD86

This core was collected from the same floe as the previous three cores and was collected in a melt pond. Core F1SD86 was 225 cm long. The top 45 cm was composed of clear pond ice followed by a 6 cm transition zone leading to opaque congelation ice (Fig. 45). A horizontal thin section at 20 cm shows the large crystals typical of pond ice. A section taken at 55 cm shows retextured columnar ice. A section at 175 cm shows medium-grained unoriented ice while one taken at 207 cm shows oriented large-grained columnar ice with medium sized grains intermixed. A vertical section between 207-219 cm shows typical columnar ice structure. This relatively simple structure can be related to the current winters' ice growth overlain by remnant old ice.

Salinity (Fig. 45) and major element (Fig. 46) depth profiles all track each other. Each shows extremely low concentrations in the pond ice. The highest concentrations occur in the ice between 140 cm and the bottom which probably represents the current winter's growth. Nutrient concentrations are scattered and show no apparent trend with depth or structure.

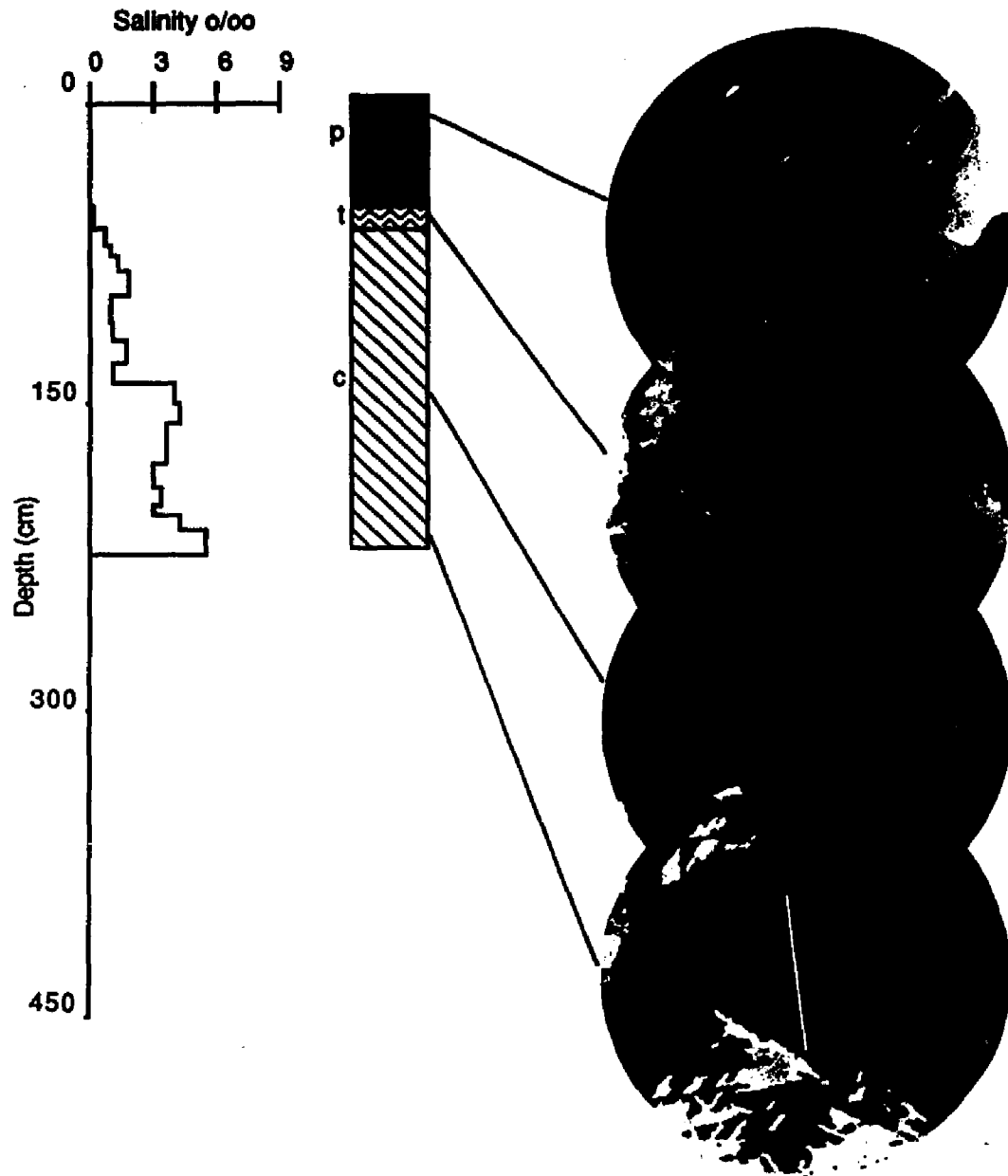


Fig. 45. Salinity-structure profiles for core F1SD86. Symbols in the structure profile are as described previously.

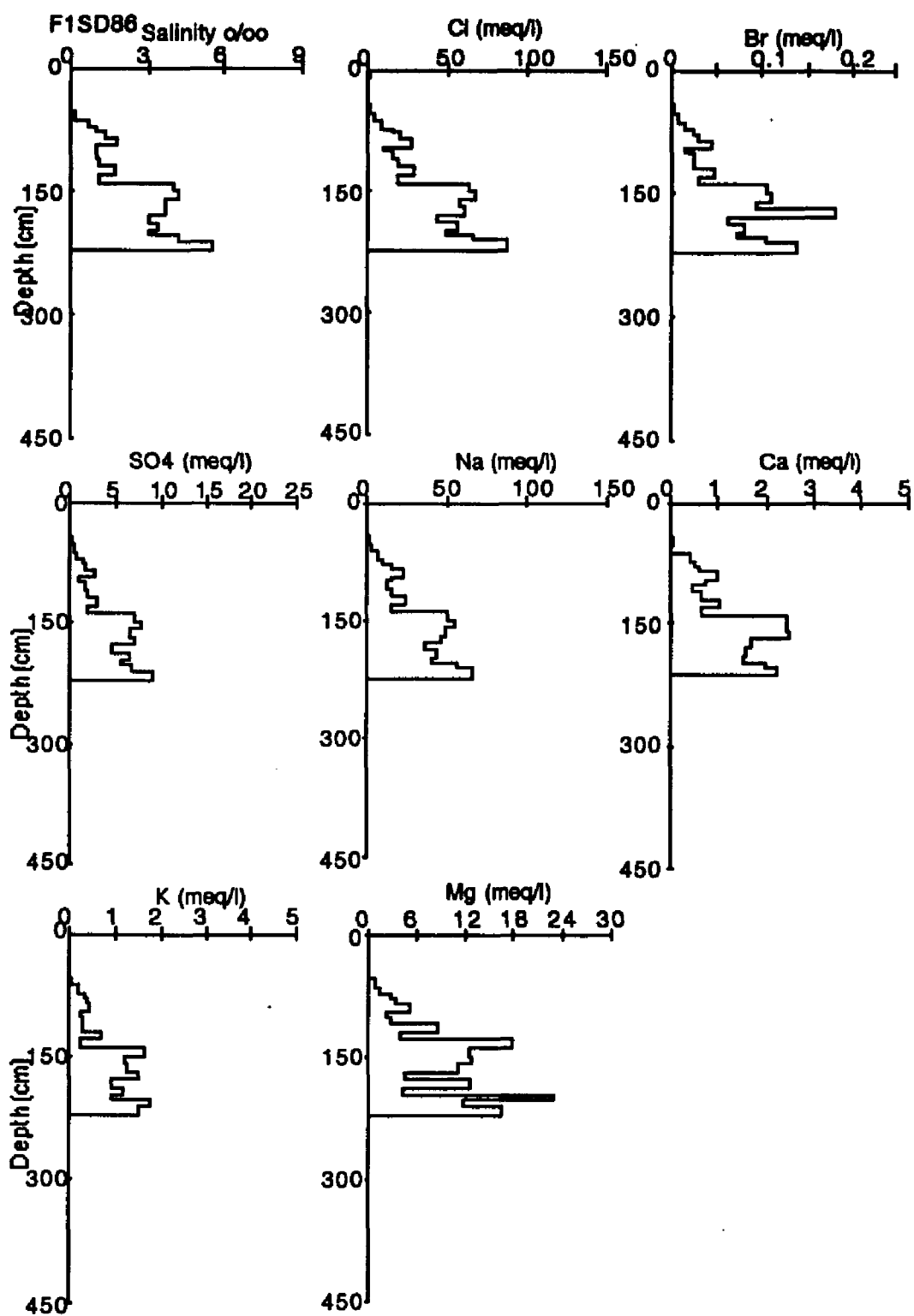


Fig. 46. Chemistry profiles for core F1SD86.

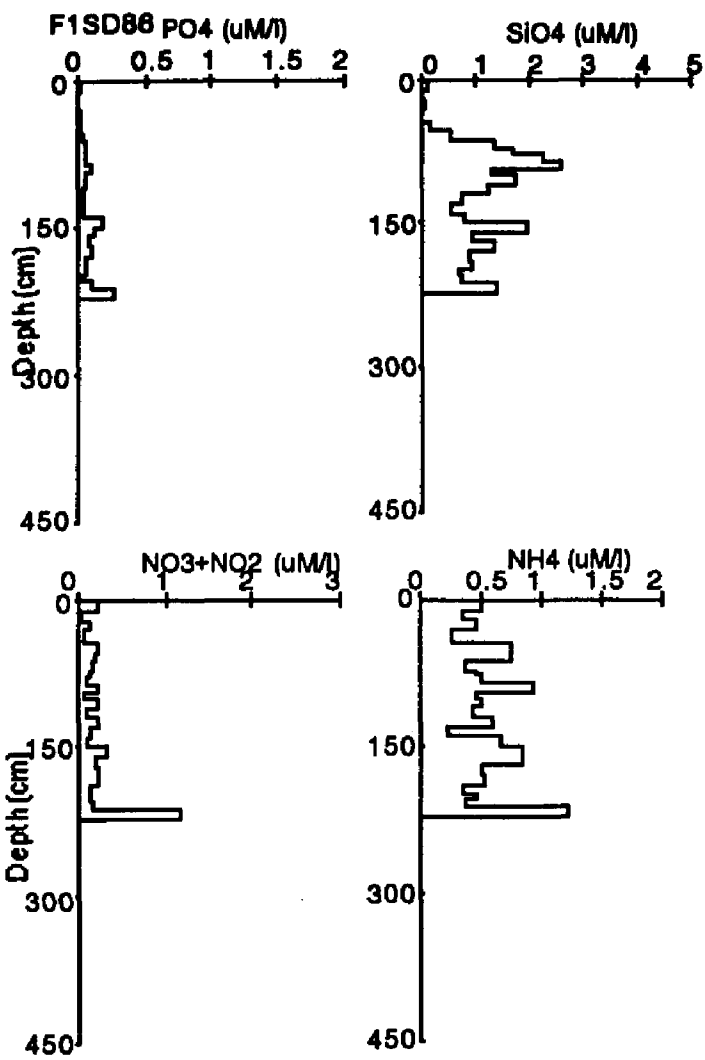


Fig. 46. (cont.).

CORE F2SA86

The floe from which this core was collected was located approximately 1 km northeast of F186 and was between 100-500 m in diameter. This thickness of this floe ranged from 160 to 640 cm. Core F2SA86 was 238 cm long and was composed of 7 cm of snow ice underlain by a 3 cm clear transition zone leading to columnar ice which included a zone of fine-grained columnar ice between 51 and 73 cm. Photomicrographs of horizontal thin sections show that at 25 cm the ice is composed of medium-grained columnar ice that appears to have been retextured (Fig. 47). The sections from 80 and 130 cm are retextured fine to medium-grained columnar ice. At 180 cm the ice is oriented columnar ice. At 210 cm the ice is composed of oriented columnar ice with granular ice mixed in. The section from 232 cm shows aligned crystals of columnar ice.

Salinity (Fig. 47) and major element depth profiles (Fig. 48) all track each other. The nutrients scatter with no real trend (Fig. 48). The exception to this is NH_4 which has several high peaks (0.8 to 1.4 μM) within the core. The 3 peaks in the interior of the core correlate with areas where the ice has been retextured or is finer-grained.

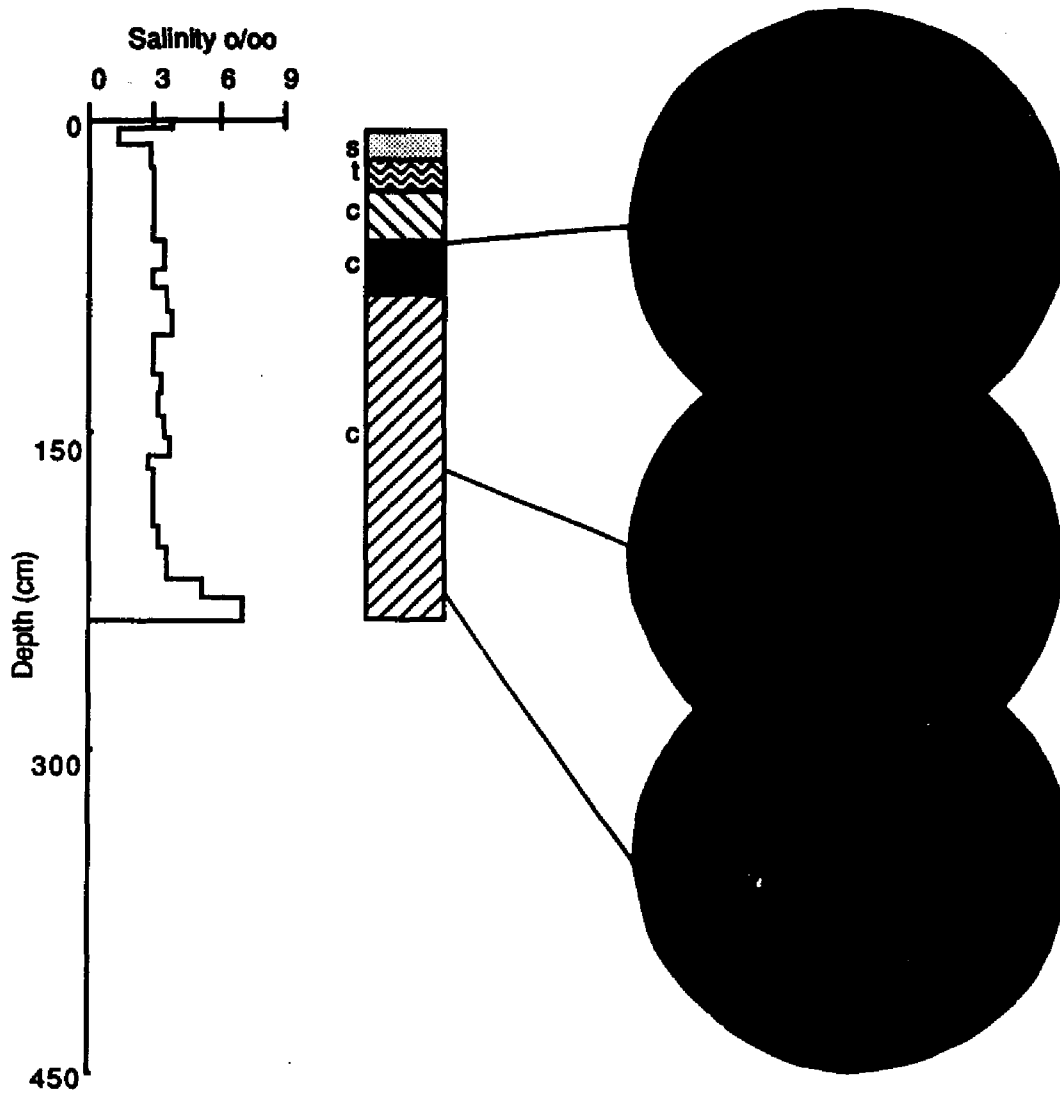


Fig. 47. Salinity-structure profiles for core F2SA86. Symbols in the structure profile are as described previously.

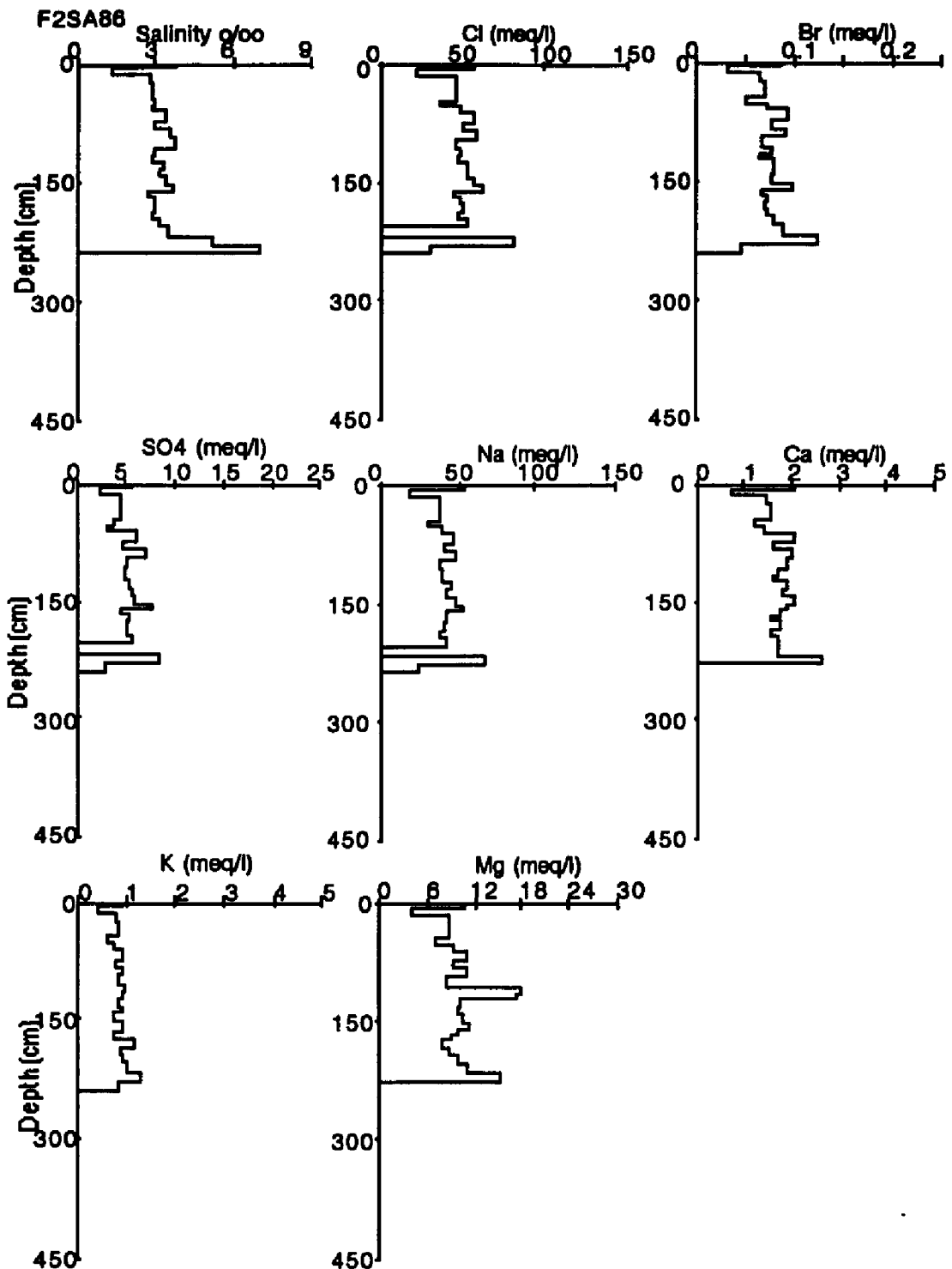


Fig. 48. Chemistry profiles for core F2SA86.

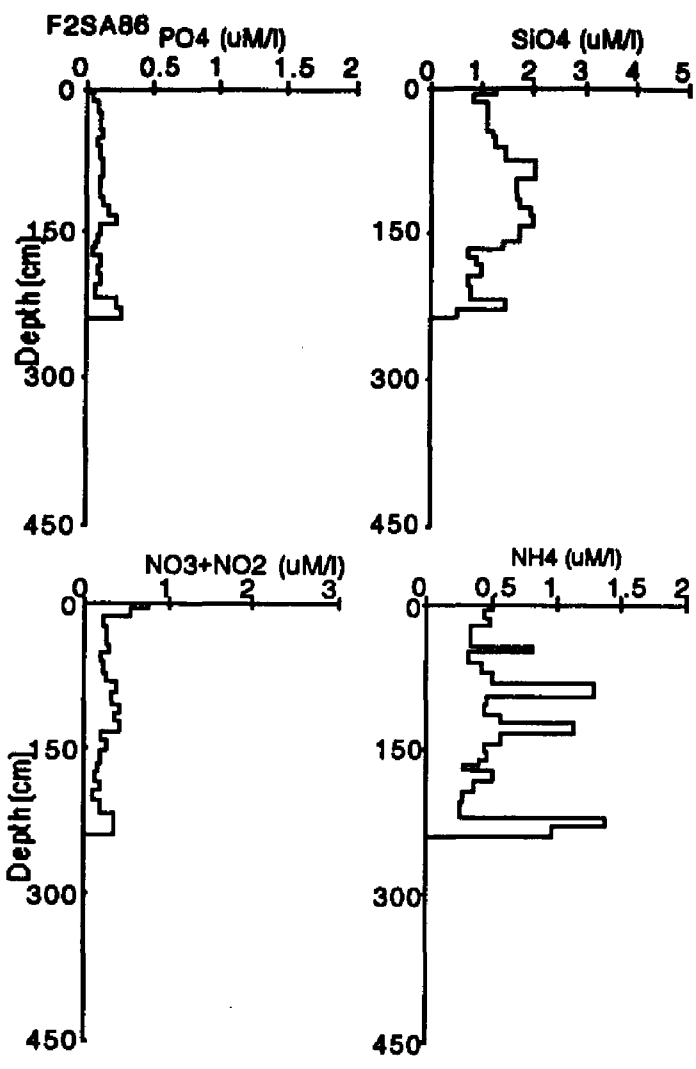


Fig. 48. (cont.).

CORE F3SA86

F3SA86 was a 302 cm long core located in a multiyear floe approximately 10 miles northeast of F186 and F286. The floe was between 100-500 m in diameter with thicknesses varying between 174 and 669 cm. In this core the top 10 cm was composed of bubbly pond ice. Below this the entire core was composed of columnar ice of various textures. Between 100 and 132 cm a change in orientation was observed. Finer-grained ice was observed between 206 and 214 cm. Photomicrographs of some of the thin sections taken throughout the core show the various textures observed (Fig. 49).

Salinity (Fig. 49) and major element (Fig. 50) depth profiles all track each other. The diminished salinity in the top layers is typical of a melt pond. The peaks in the interior of the core combined with textural changes may be indicative of annual growth layers. The peak between 206 and 213 cm corresponds to a layer of fine-grained ice. NO_3+NO_2 and SiO_4 also have higher peaks in this area. The NH_4 depth profile shows several high peaks within the core that do not appear to correspond with salinity peaks or structural changes.

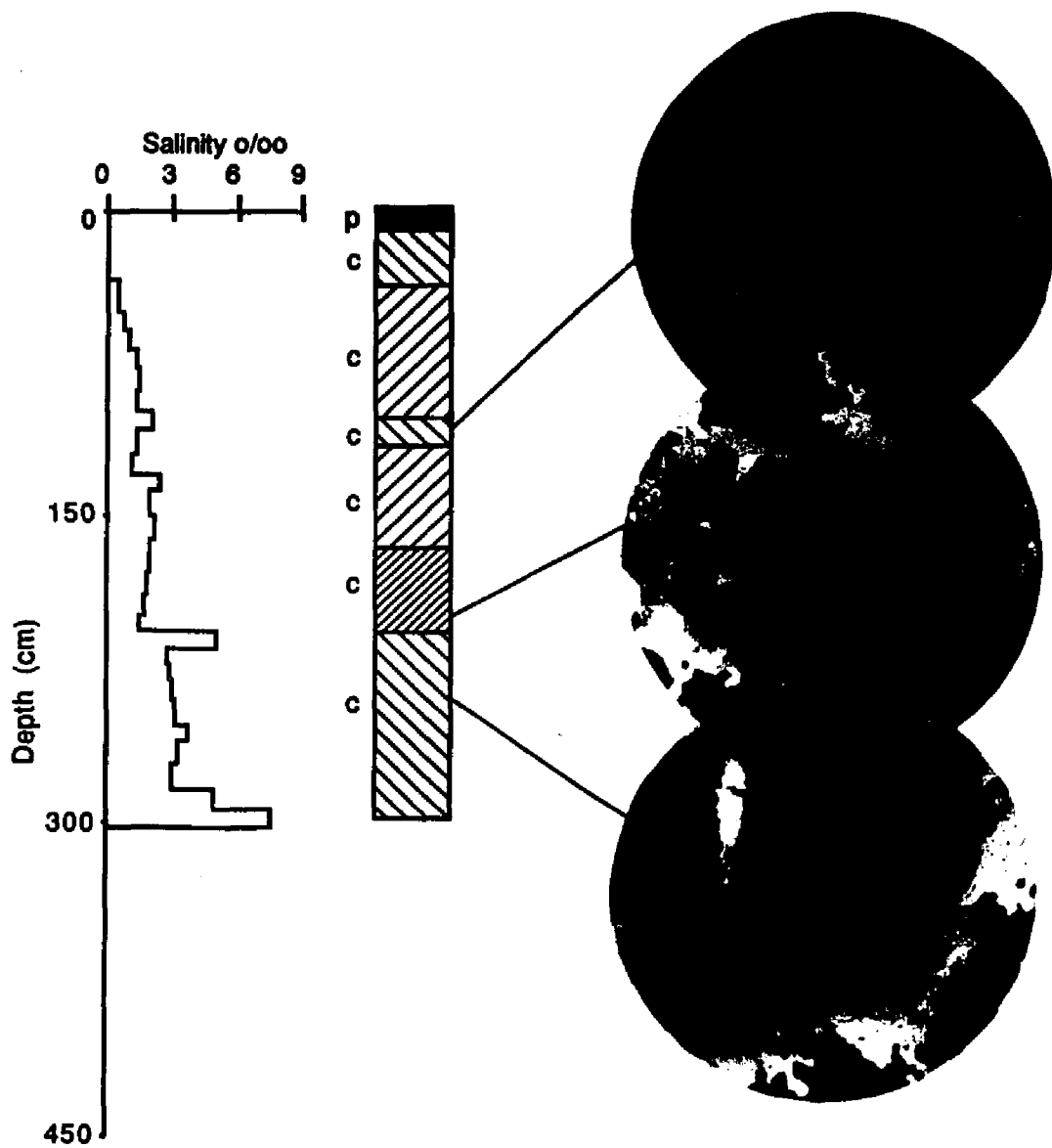


Fig. 49. Salinity-structure profiles of core F3SA86. All symbols in the structure diagram are as described previously.

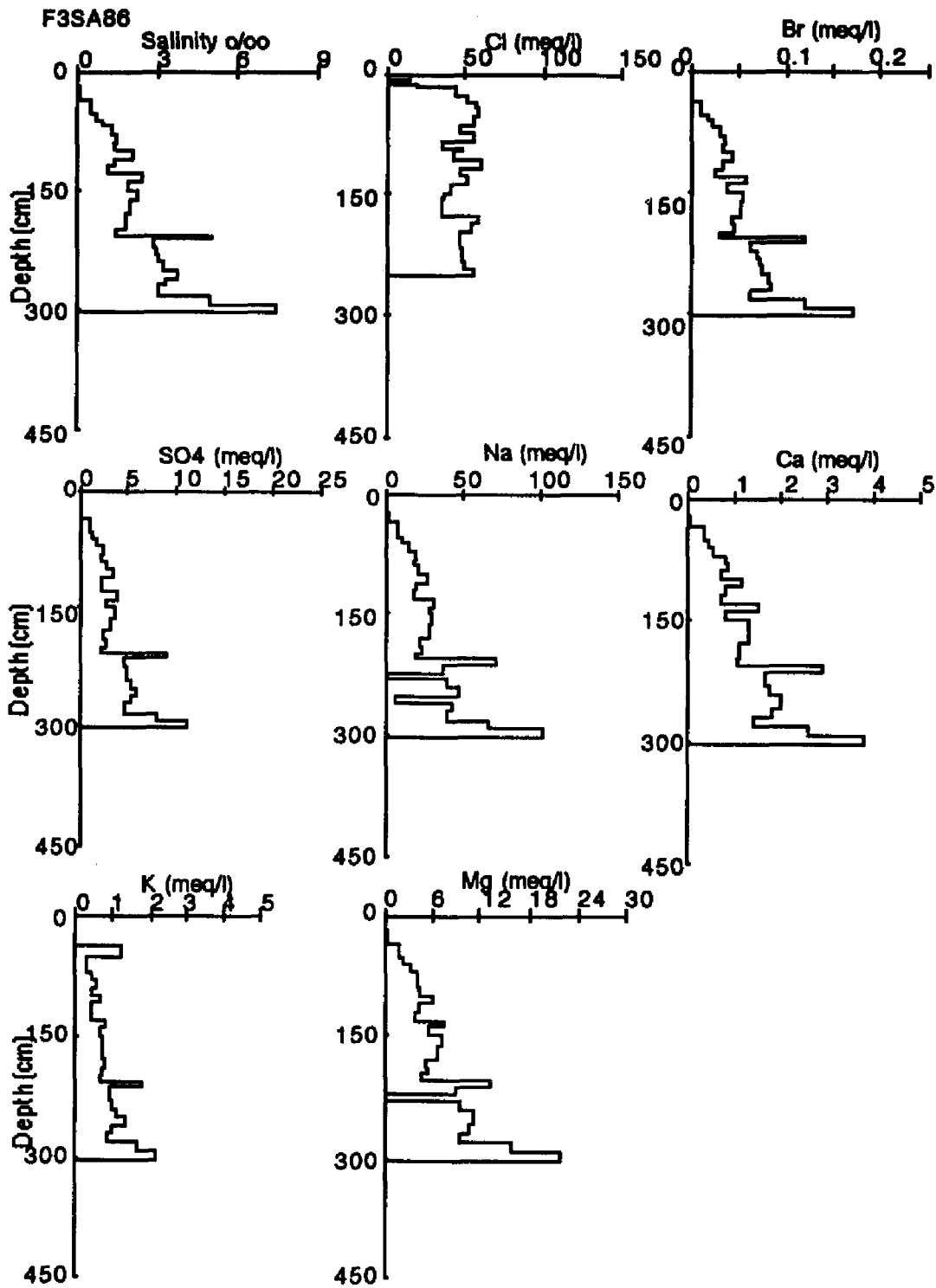


Fig. 50. Chemistry profiles for core F3SA86.

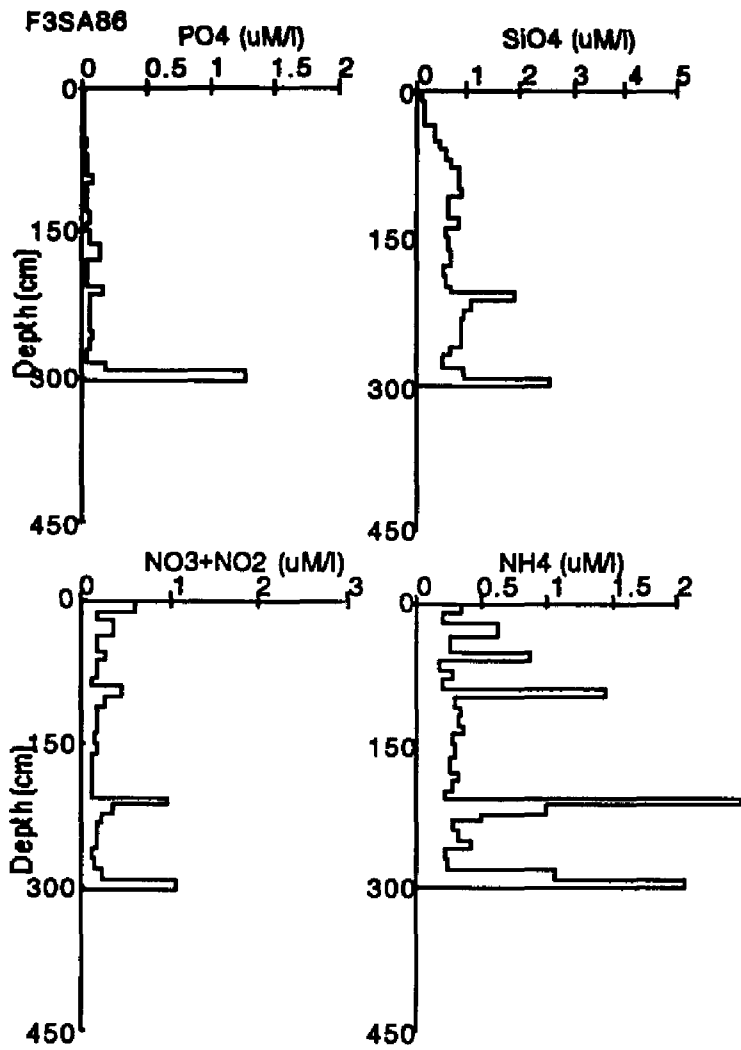


Fig. 50. (cont.).

CORE F4SA86

This 270 cm long core was taken between a hummock and a depression from a multiyear floe that was located approximately 1 mile north of F186 and F286. The floe was between 100-500 m in diameter and ranged from 231 to 1081 cm in thickness. The top 8 cm of the core consisted of bubbly snow ice which was followed by a clearer 5 cm layer below which was a 3 cm melt layer. The remaining 254 cm was composed of columnar ice. A vertical thin section taken between 10 and 20 cm shows the transition between columnar ice and pond ice (Fig. 51). Photomicrographs show the various textures observed in this core. A vertical section between 244 and 256 cm shows an inclined transition that is probably due to the rafting of two blocks or ridging.

Depth plots for salinity (Fig. 51) and all the major elements (Fig. 52) track each other but do not appear to show any correlation with structure. Nutrients vary and show no trends with salinity and as with the major elements show no correlation with structure. NH_4 has several high concentration peaks in this core most of which correspond to fine to medium-grained columnar ice.

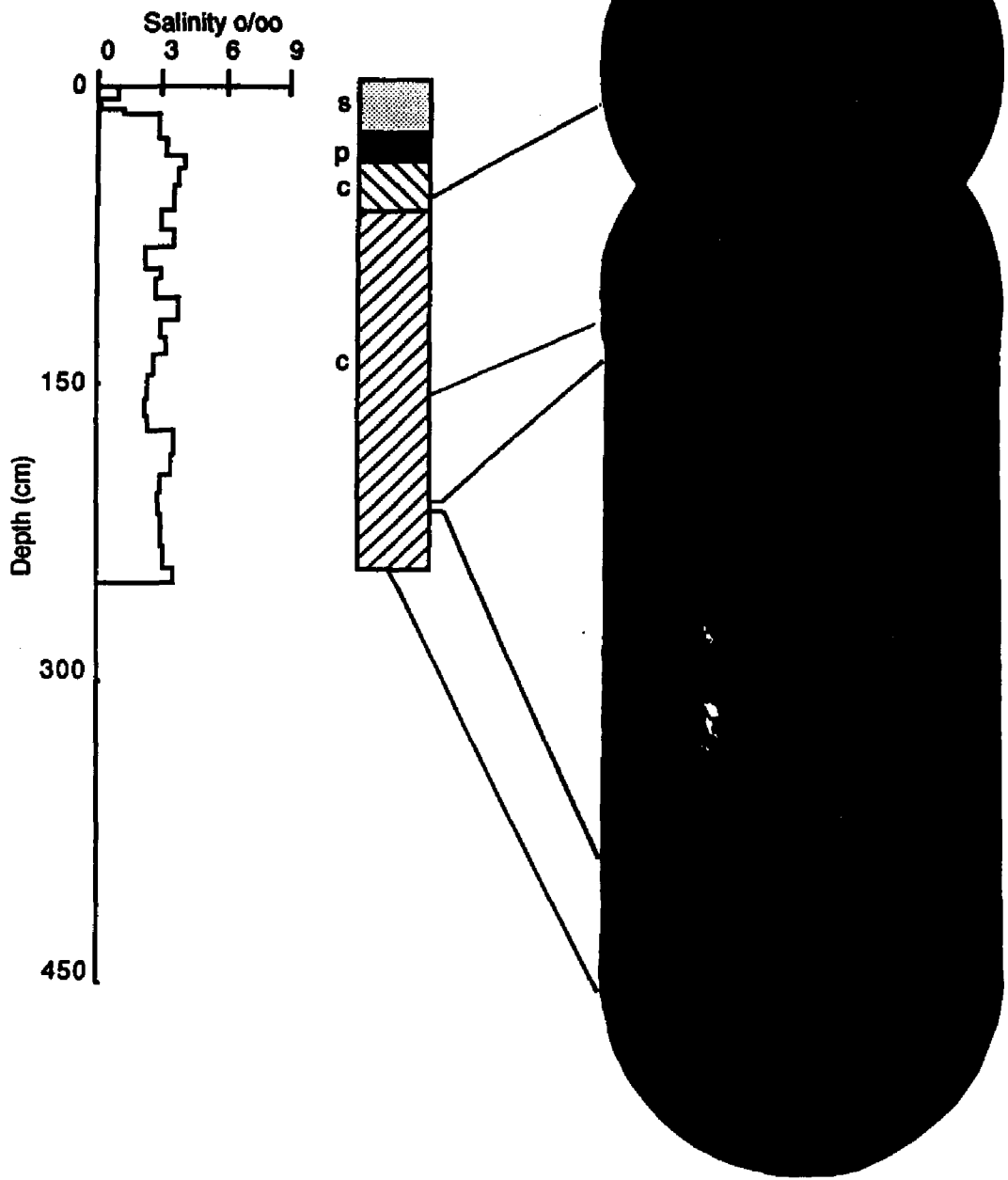


Fig. 51. Salinity-structure profiles for core F4SA86. Symbols in the structure profile are as described previously.

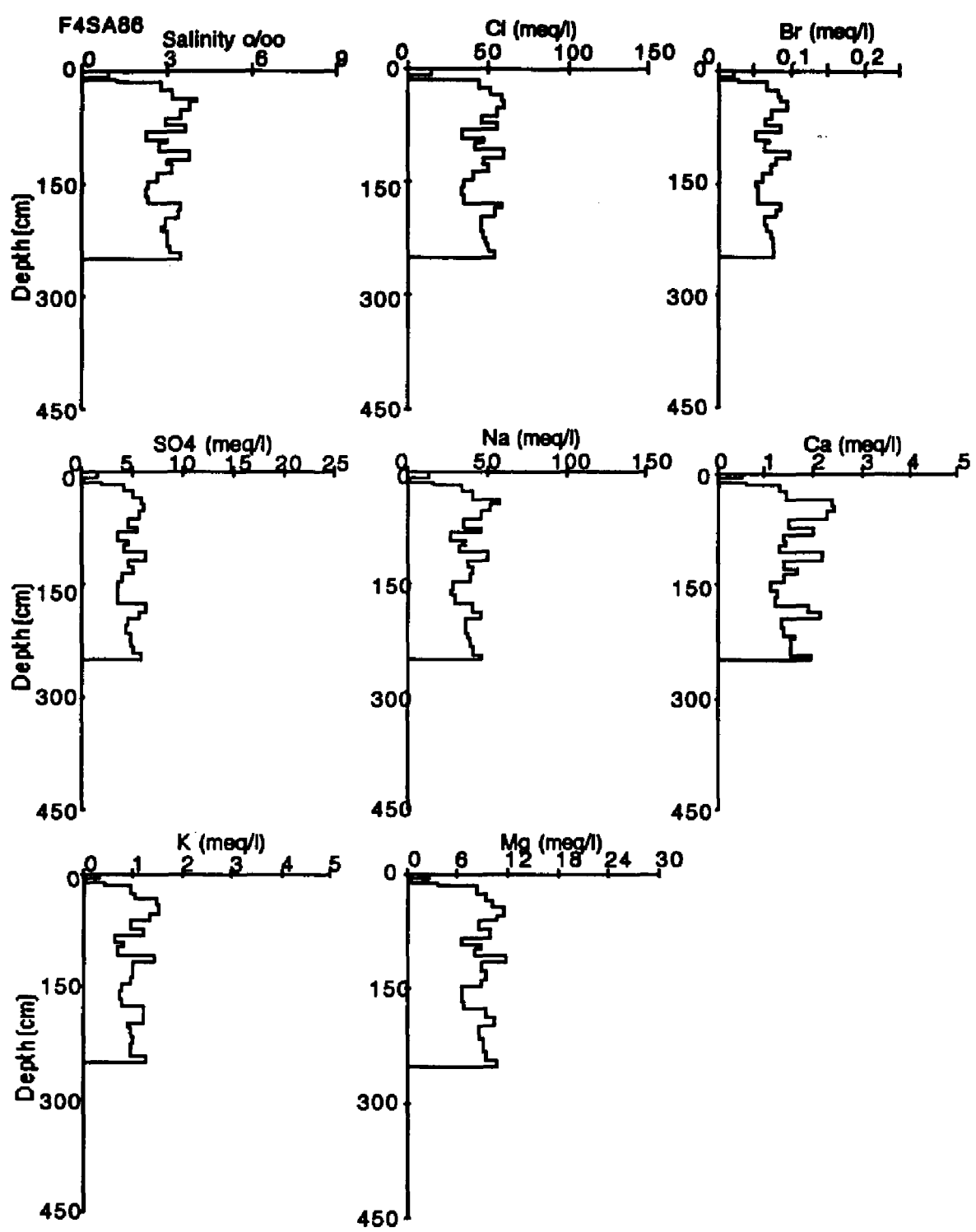


Fig. 52. Chemistry profiles for core F4SA86.

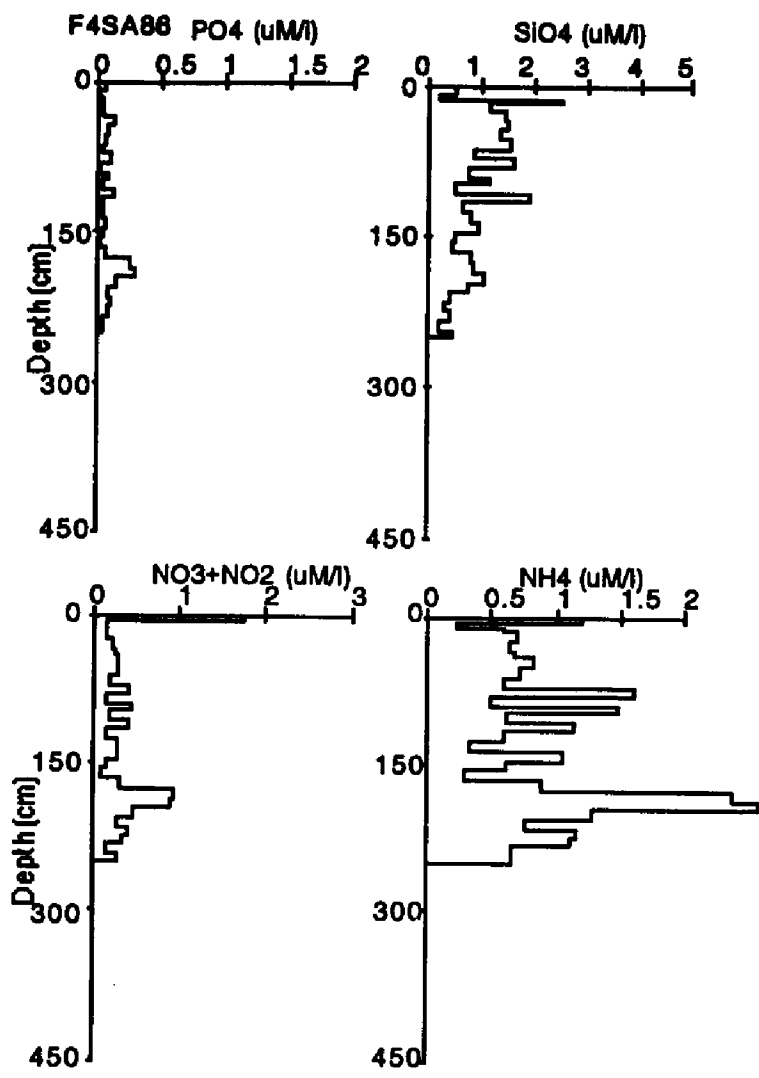


Fig. 52. (cont.).

CORE F1SA87

This 382 cm long core was taken in a melt pond from a multiyear floe that was located approximately 7 miles north of Cottle Island (Fig. 9). The floe was approximately 600 m in diameter and ice thickness ranged from 168 to 1123 cm. The top 8 cm of the core consisted of bubbly pond ice followed by 22 cm of clear pond ice, a 10 cm transition zone and 292 cm of columnar ice. Photomicrographs of thin sections taken throughout the core show the variable textures (Fig. 53). Most of this core is composed of medium-grained columnar ice that was finer grained than most congelation ice observed in other cores.

Depth profiles of salinity (Fig. 53) and the major elements (Fig. 54) track each other. The nutrients do not appear to show any correlation with salinity, with each other or with structure.

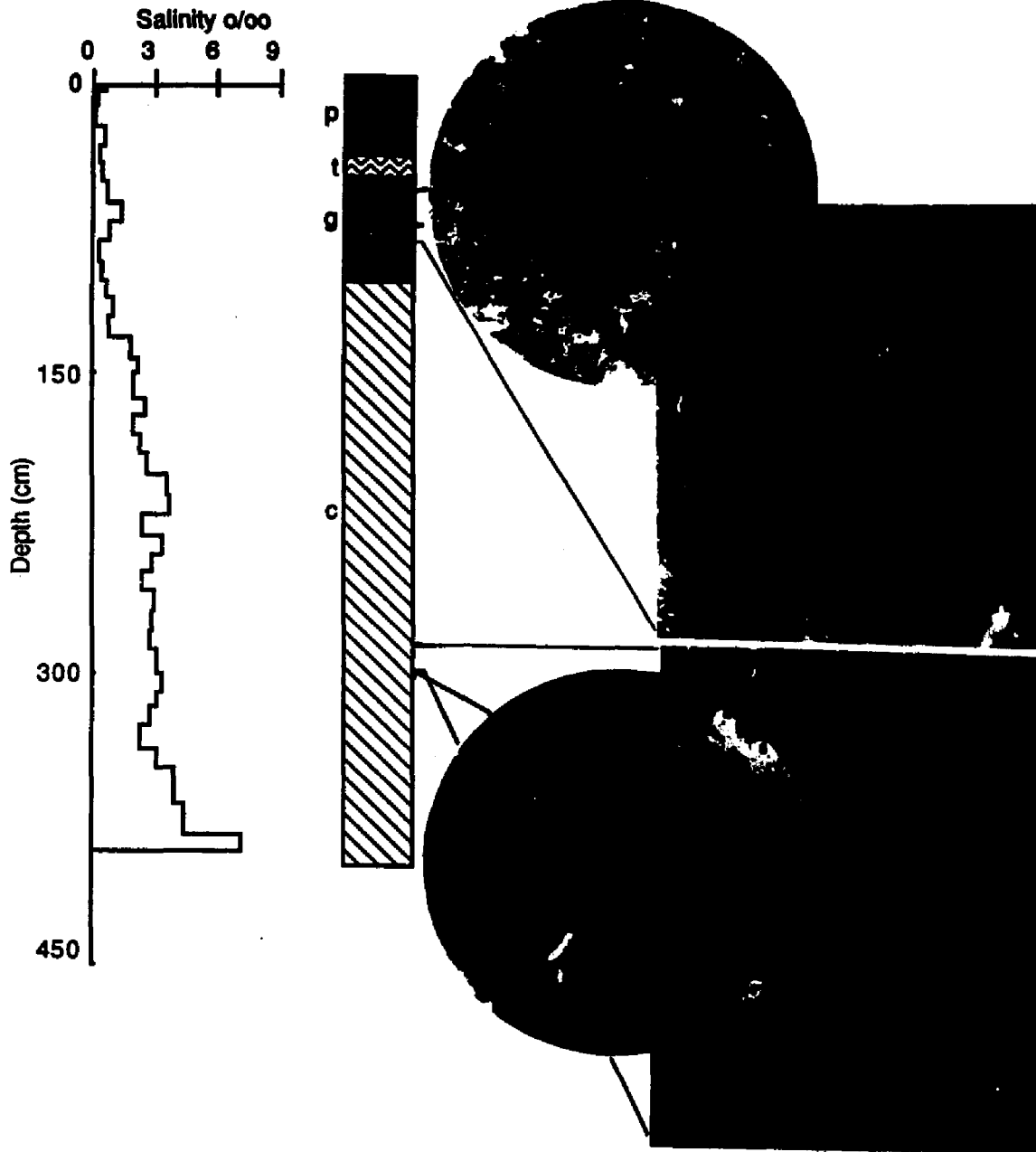


Fig. 53. Salinity-structure profile of core F1SA87. Symbols in the structure profile are as described previously.

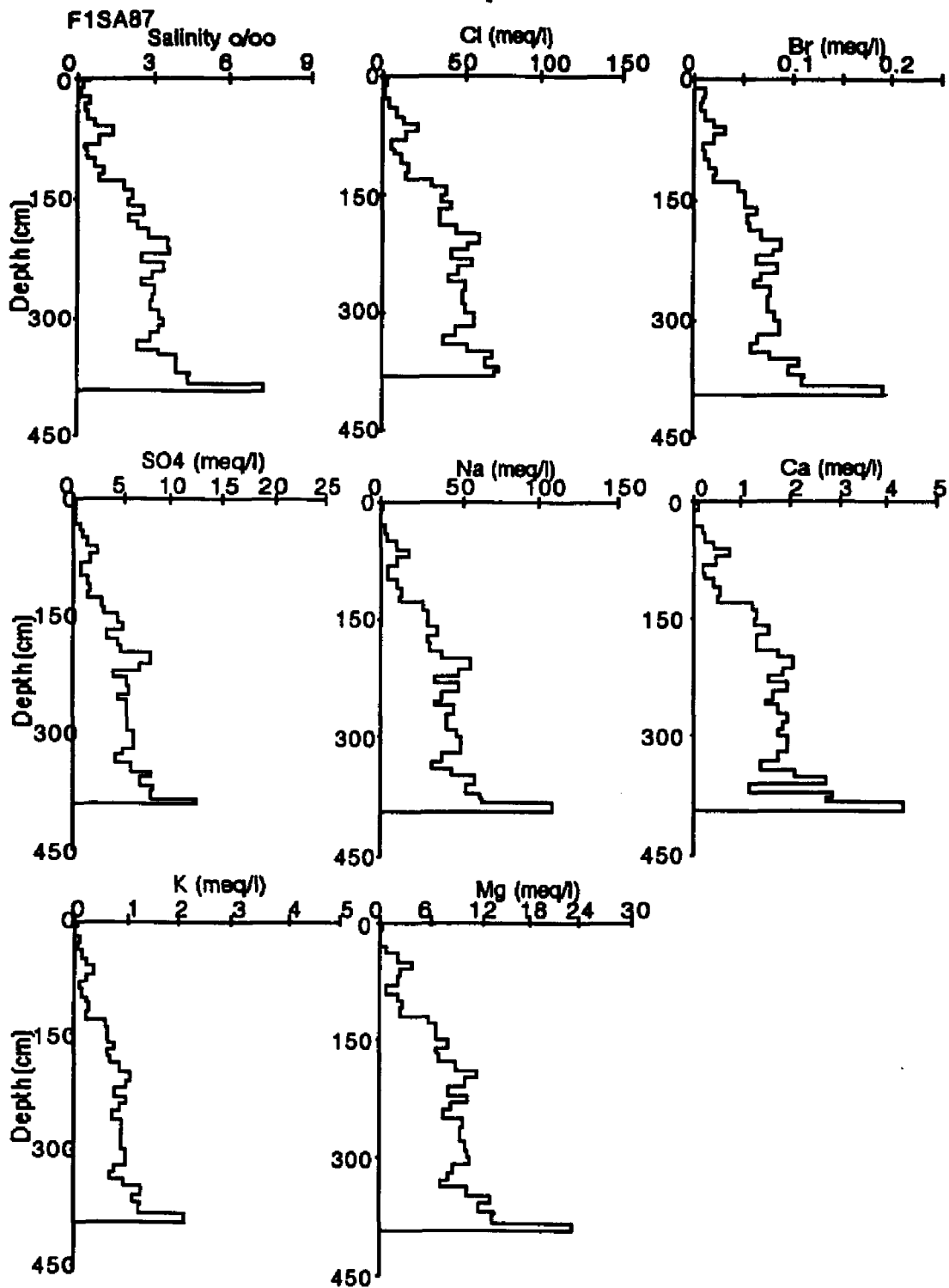


Fig. 54. Chemistry profiles for core F1SA87.

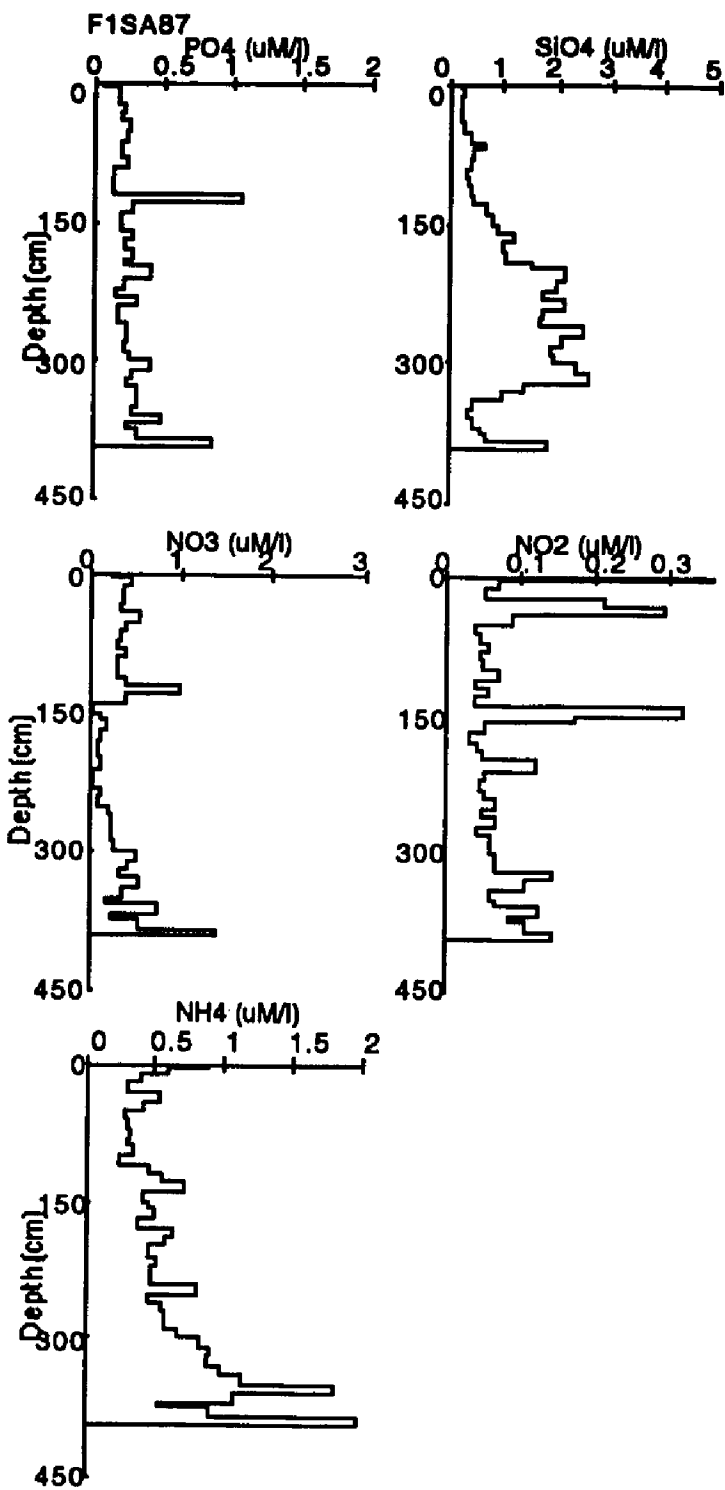


Fig. 54. (cont.).

CORE F1SB87

This core was collected from the same floe as the above core. Core F1SB87 was 396 cm long. The top 40 cm was composed of porous, bubbly friable ice underlain by 356 cm of coarse-grained columnar ice exhibiting a variety of crystal textures. Two sections between 90-100 and 200-220 cm exhibit tilted structure that may indicate the existence of inclined blocks implicating that ridging had occurred. Breaks in the structure profile below 150 cm indicate alternating layers of opaque and clear columnar ice.

Salinity (Fig. 55) and major element depth profiles (Fig. 56) all track each other. Peaks occurring within the core may be indicative of annual growth cycles. Nutrient profiles (Fig. 56) all show considerable scatter with no definitive trends.

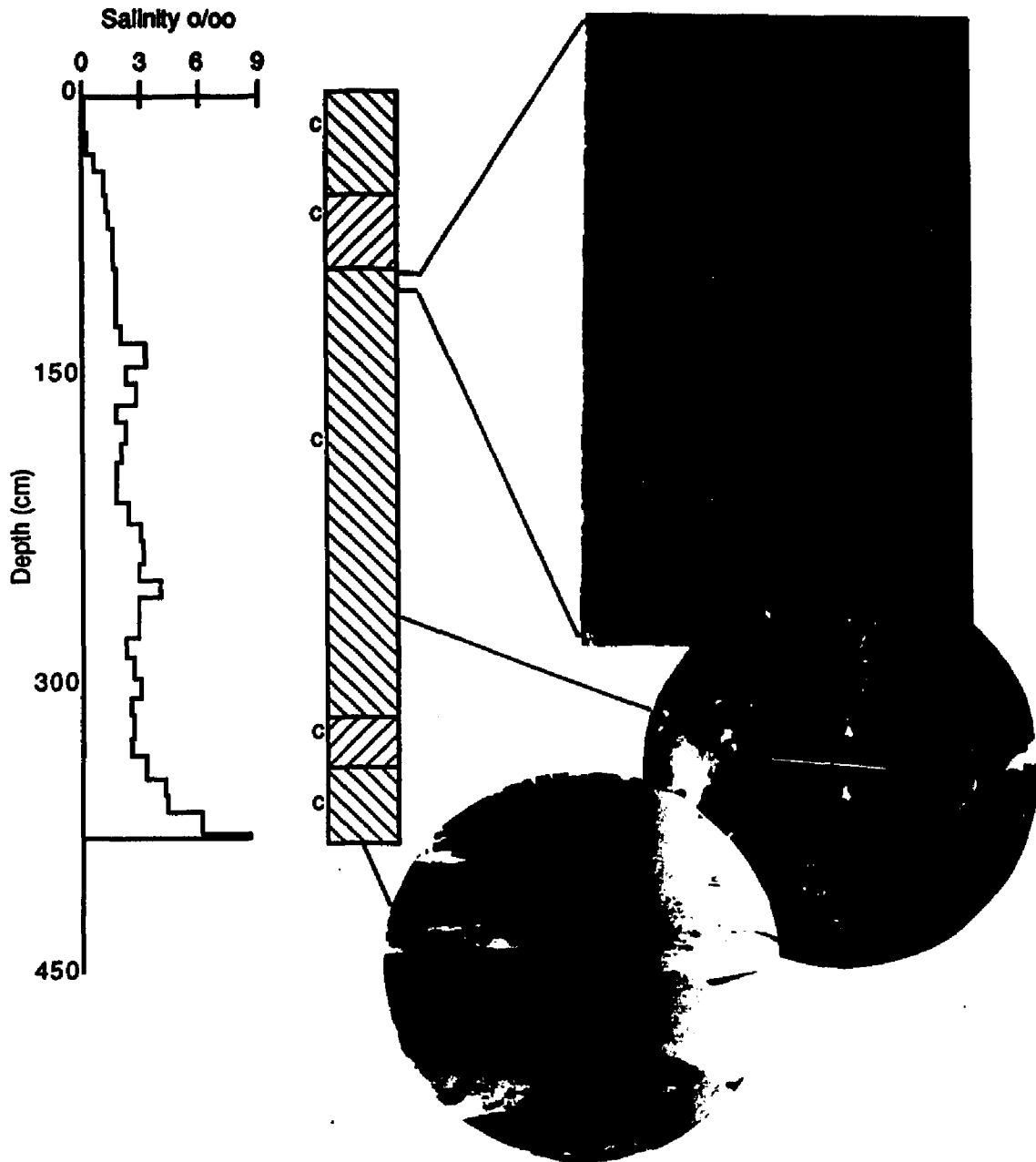


Fig. 55. Salinity-structure profile of core F1SB87. Symbols in the structure profile are as described previously.

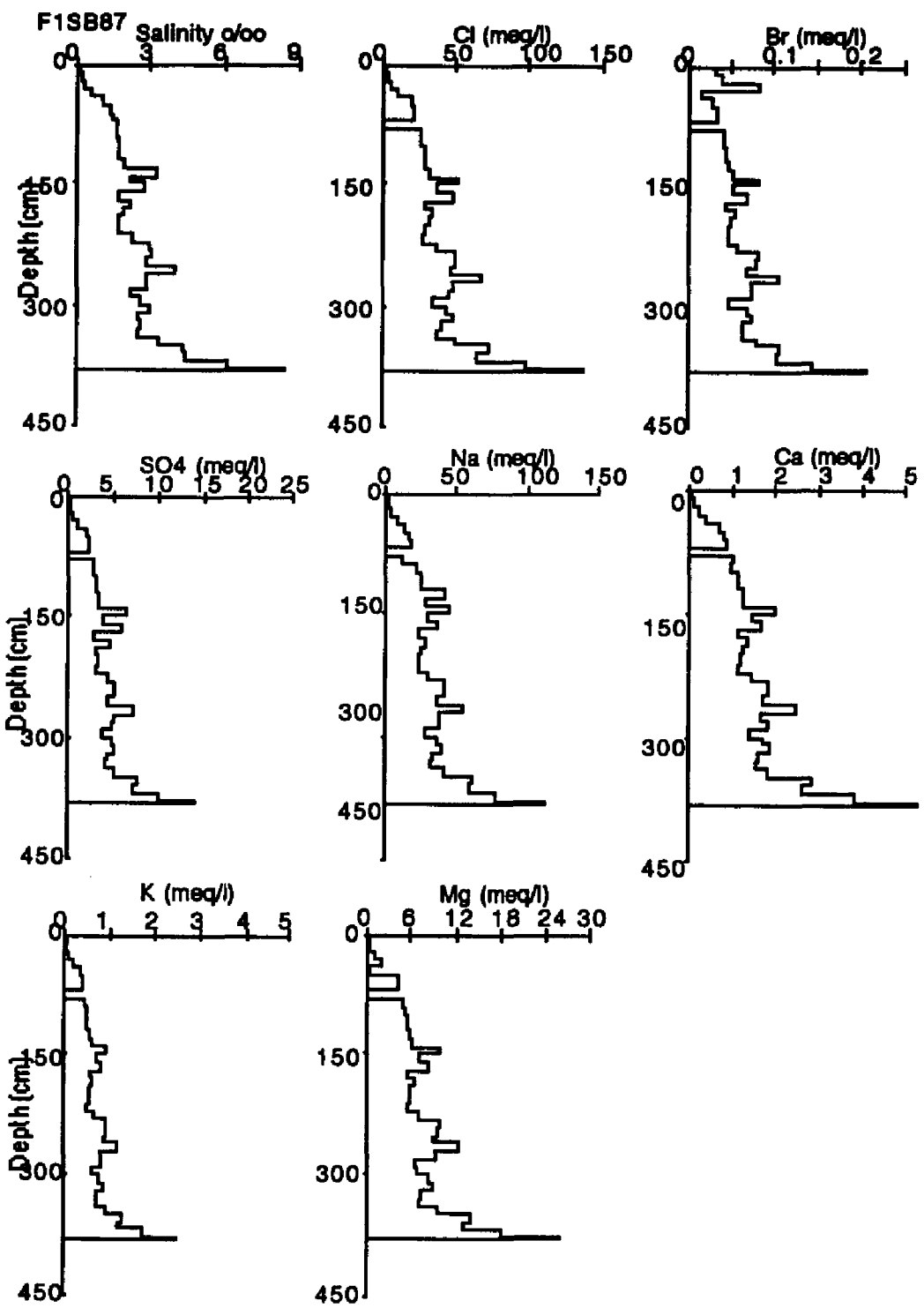


Fig. 56. Chemistry profiles for core F1SB87.

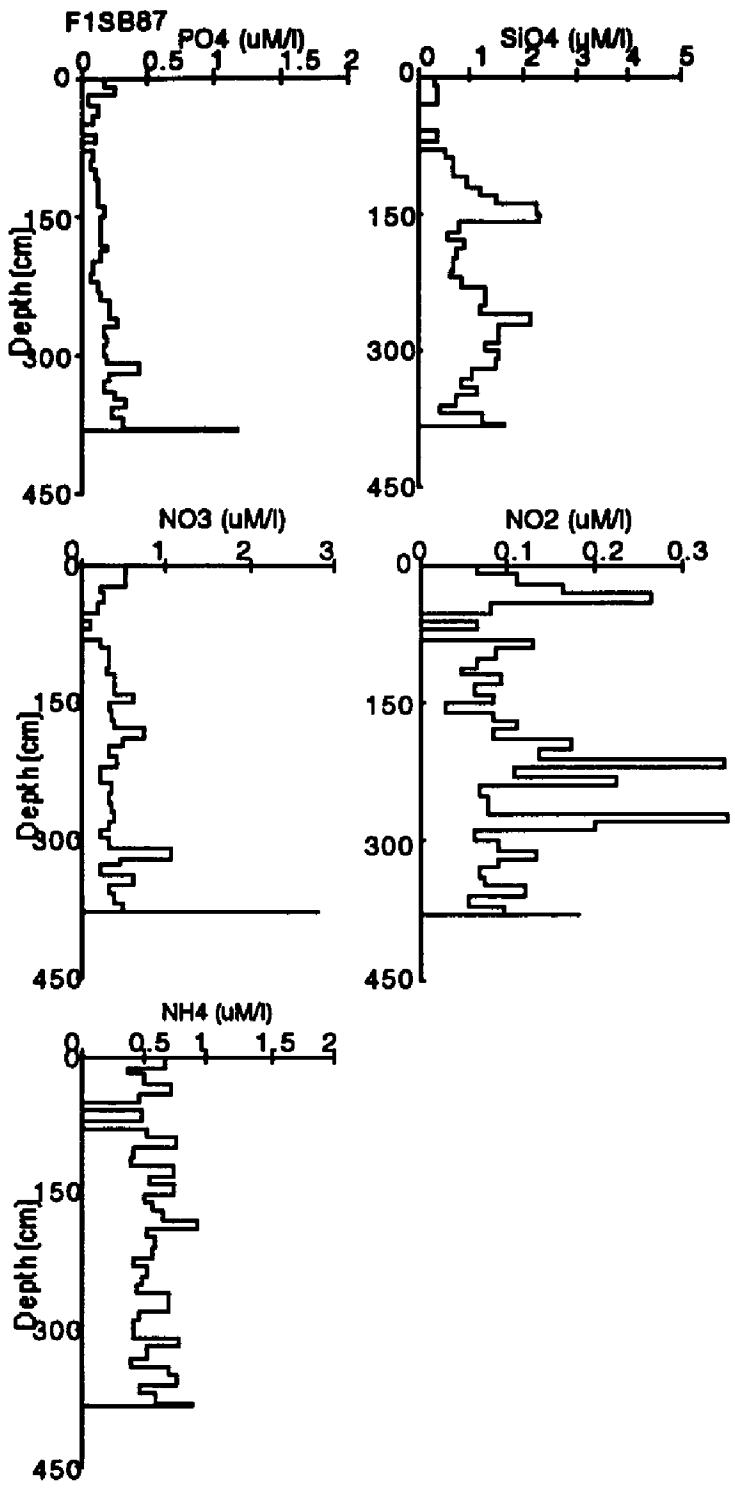


Fig. 56. (cont.).

CORE F2SA87

Core F2SA87 was 218 cm long and was taken from a multiyear floe adjacent to F187 that was approximately 400 m in diameter. The top 20 cm was composed of bubbly ice followed by a 10 cm thick transitional zone underlain by 172 cm of columnar ice. Photomicrographs of thin sections show that there are two areas of retextured ice in this core at 50 and 80 cm (Fig. 57). Below 170 cm the columnar ice shows oriented c-axes.

This core has the highest bulk salinity of the multiyear cores. In addition, an increase occurs at approximately 100 cm. This may indicate that this core is two years old with the second year's growth beginning at 100 cm. Depth profiles for salinity (Fig. 57) and major elements (Fig. 58) all track each other. The salinity profile shows a peak at 10 cm that does not occur in any of the other profiles including nutrients. It is believed that this may have been an erroneous salinity reading. Nutrient profiles all vary when compared to the major species and the other nutrients. A peak occurs for NO_3 and NH_4 at 125 cm which corresponds to a section of retextured medium-grained columnar ice.

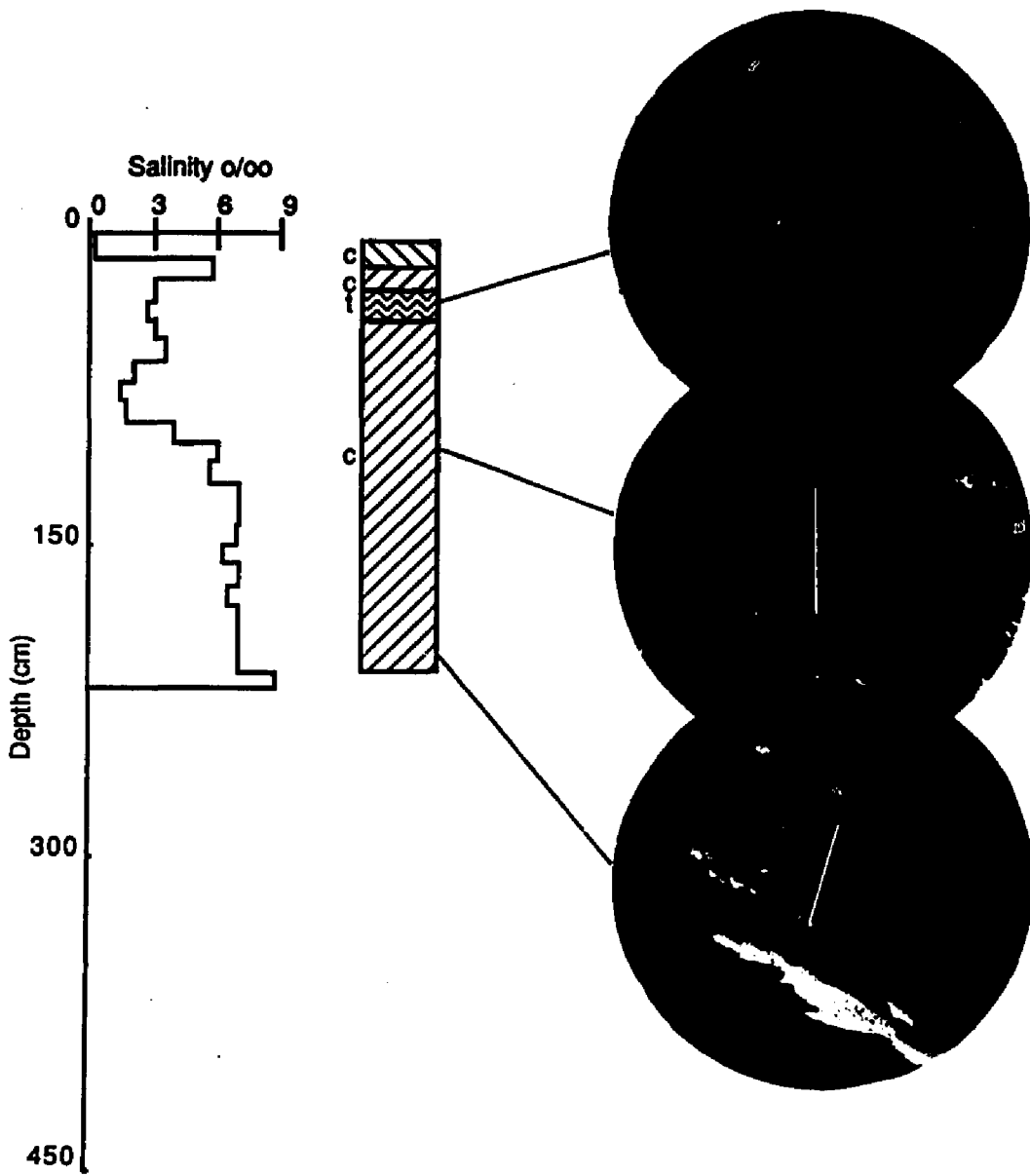


Fig. 57. Salinity-structure profiles for core F2SA87. Symbols in the structure profile are as described previously.

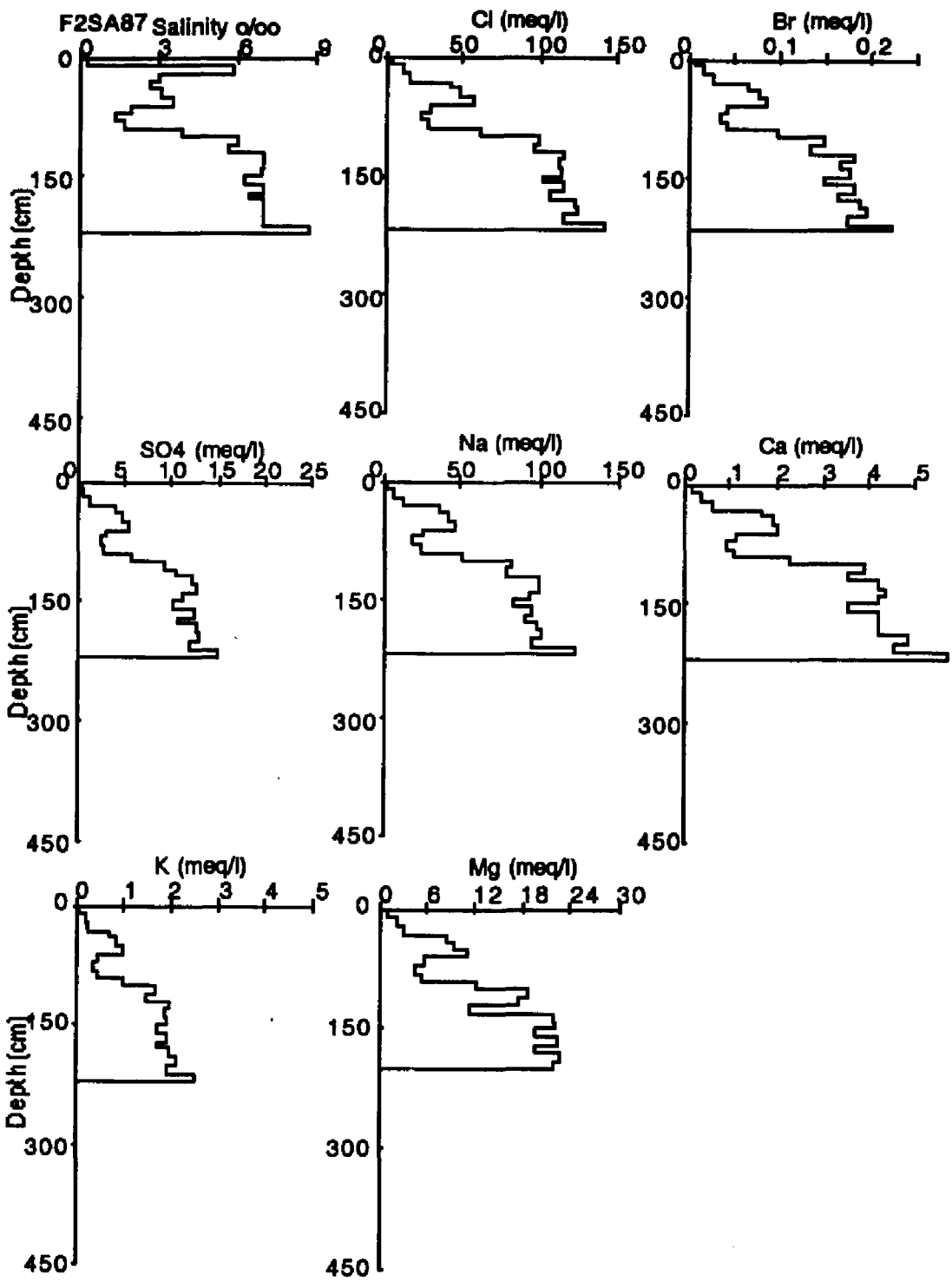


Fig. 58. Chemistry profiles for core F2SA87.

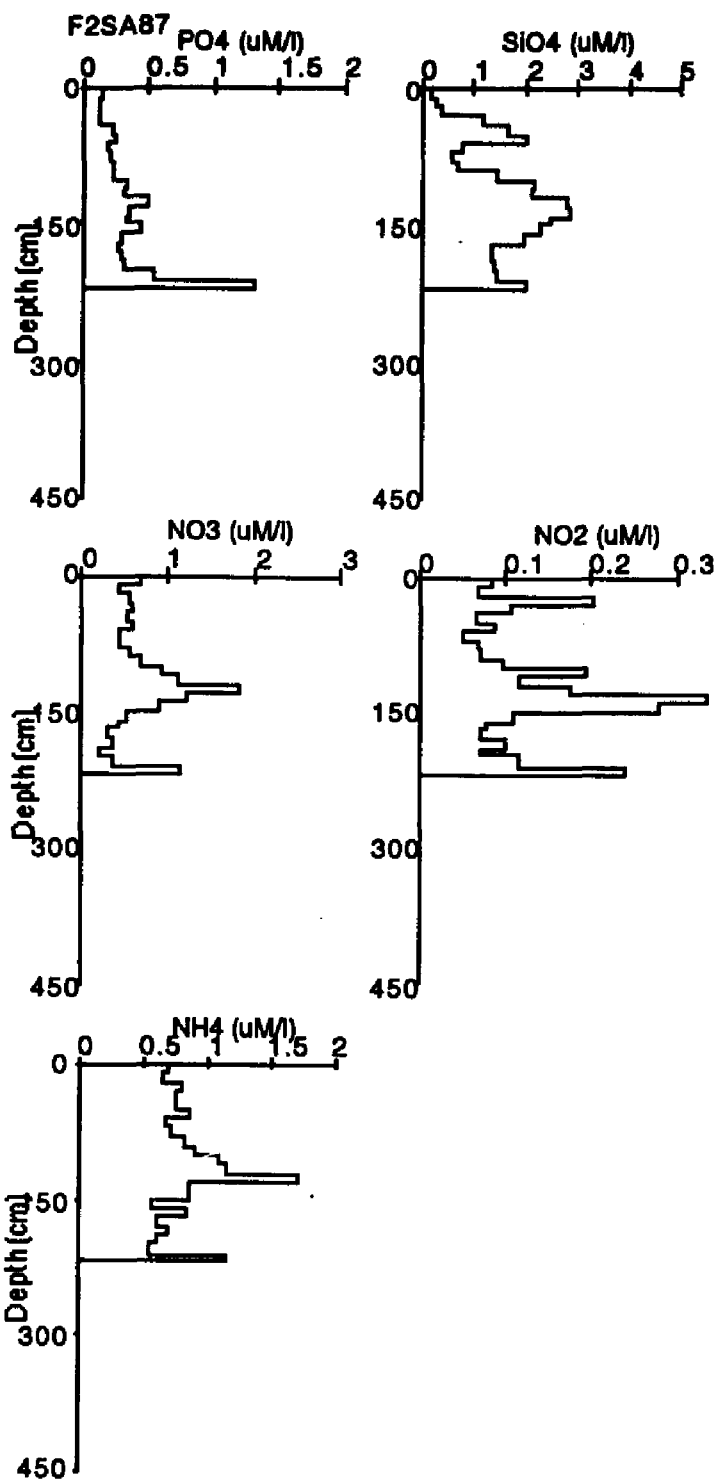


Fig. 58. (cont.).

Bulk Salinity

The average bulk salinity for all multiyear samples collected is 2.84 while that obtained by Tucker and Gow (1987) in Fram Strait during MIZEX-84 is 2.1. As with the first-year ice the higher average salinity from the Prudhoe Bay area may be attributable to differences in the time of year samples were collected. Cores from the Prudhoe Bay area were collected earlier in the spring than those collected during MIZEX-84, therefore, the lower salinities obtained from MIZEX-84 may be a result of increased brine drainage associated with increasing temperatures in the ice. A plot of average bulk salinity versus thickness was produced (Fig. 59) and a best-fit linear regression obtained:

$$S_i = 4.92 - 0.685h$$

The low R-value of 0.44 is not significant at the 90% confidence interval and indicates a poor correlation between samples. When the two highest values and the lowest value are eliminated the regression changes, however, eliminating 33% of the samples is not statistically valid. Compared to Gow and Tucker (1987), Gow et al. (1987) and Tucker and Gow (1987) this regression yields higher salinities of 0.75 o/oo for 3 m of ice which correlates well with actual values. When compared to values obtained by Cox and Weeks (1974) for cold ice the difference for 3 m thick ice is only 0.24 o/oo indicating that the ice from the Prudhoe Bay area was indeed cold ice (-14.5° C surface ice temperature) and spring brine drainage had not yet started.

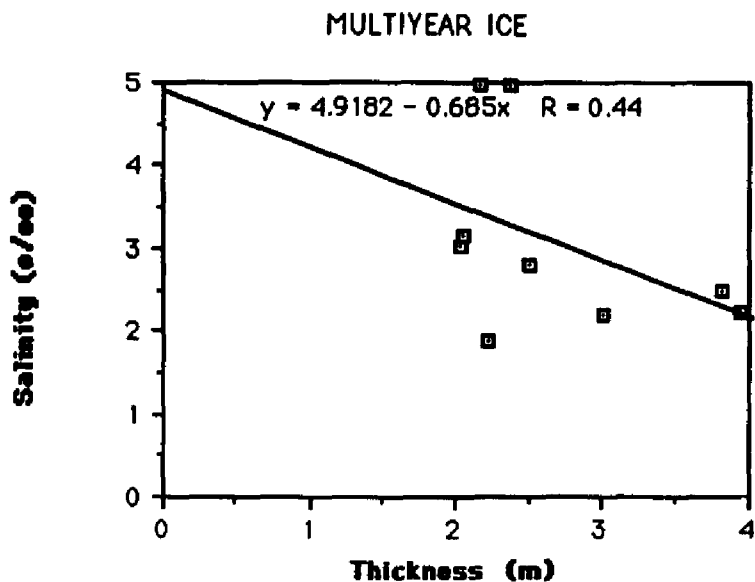


Fig.59 Bulk salinity versus thickness for multiyear ice.

Dilution Curves

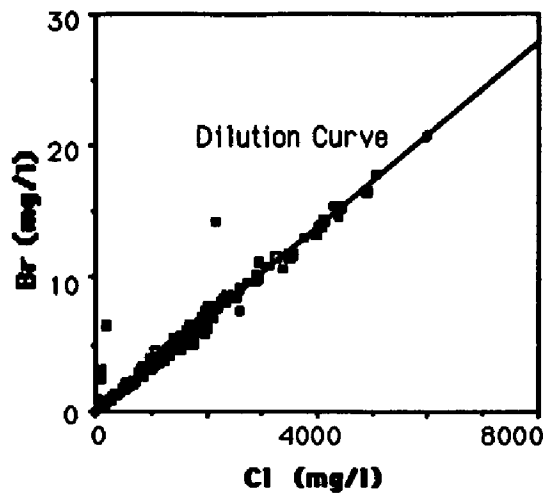
Dilution curves were produced for all major ions and nutrients to determine which chemical species are enriched or depleted relative to seawater (Figs. 60-65). Br, SO₄, Na, and Mg showed similar trends for both years and are summarized in Fig. 60. Mg showed the most variation around the dilution curve between the two years as can be seen in Figs. 61. It is believed that this is due to variations in sample handling and storage as described previously. As with the first-year ice Mg shows a slight enrichment (1-2%) relative to seawater and K shows a slight depletion. It is therefore believed that the explanations provided for first-year ice are further substantiated indicating that Mg is precipitating with a salt other than Cl at higher

temperatures and that K is more mobile than Cl and is preferentially depleted.

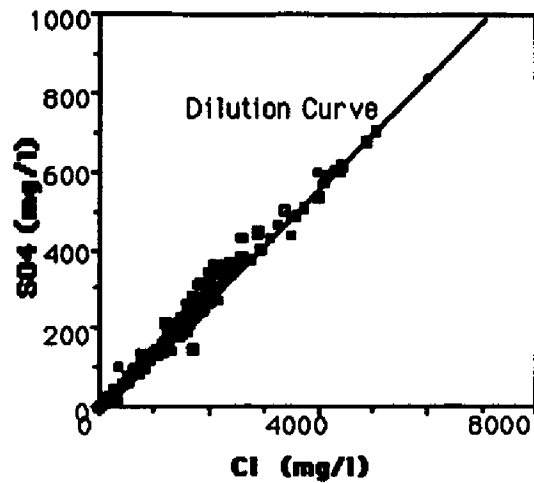
Nutrient dilution curves show varied results but all show considerable scatter around the curve (92%-PO₄, 96%-SiO₄, 96%-NO₃, 94%-NO₂ and 92%-NH₄). PO₄ shows scatter around the curve in 1986 but is enriched in the 1987 samples (Fig. 63). NO₃ is enriched in both the 1986 and 1987 samples (Fig. 64). NO₂ concentrations were obtained only for the 1987 samples which are all enriched (Fig. 64c). NH₄ is enriched in all samples for both years (Fig. 65). These results correlate well with that found for first-year ice. When actual concentrations of first-year and multiyear ice are compared NO₃ and NO₂ concentrations show appreciable variations. However, PO₄, SiO₄ and NH₄ concentrations are within the same range. NO₃ concentrations are as much as 4 μM lower in multiyear ice whereas NO₂ concentrations are up to 0.15 μM higher. The decrease in NO₃ and increase in NO₂ concentrations in the multiyear ice may be an indication that nitrogen reduction occurs in the ice during the summer.

As with the first-year ice, N:P ratios were calculated for the multiyear ice to determine if they are consistent with the Redfield ratio of 15:1 which is the ratio for oceanic organic matter. For multiyear ice the N:P ratio is 7.5 which is lower than the 18.3 found for first-year ice, however, it is higher than that of the underlying surface water (4.6). Because the multiyear ice may have originated in different parts of the Arctic it is difficult to compare values found in the Beaufort Sea with that of the sampled ice. However, since Maestrini et

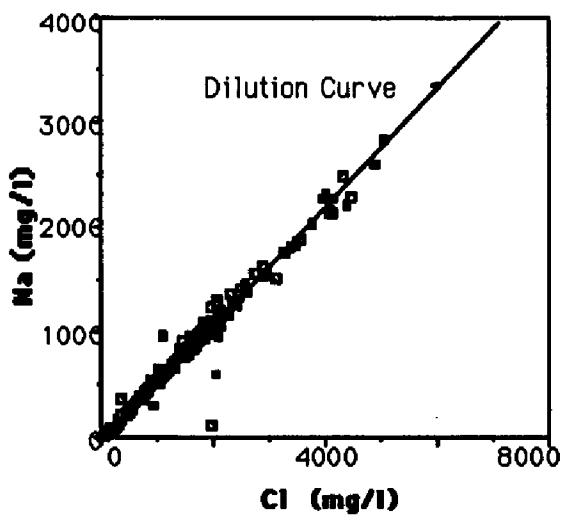
al. (1986) also found a decreased ratio in the water in Hudson Bay, this may be a consistent trend throughout the Arctic waters in winter. If this is the case, the increased ratio for multiyear ice indicates that biological activity has and/or is occurring in the ice but that other processes may be affecting the nutrient ratios and concentrations.



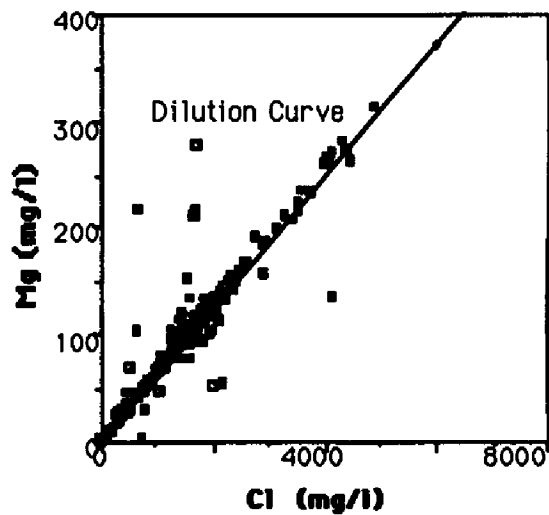
a



b



c



d

Fig. 60. Dilution curves for multiyear ice for: a) Br-all samples combined, b) SO_4 -all samples combined, c) Na-all samples combined and d) Mg-all samples combined.

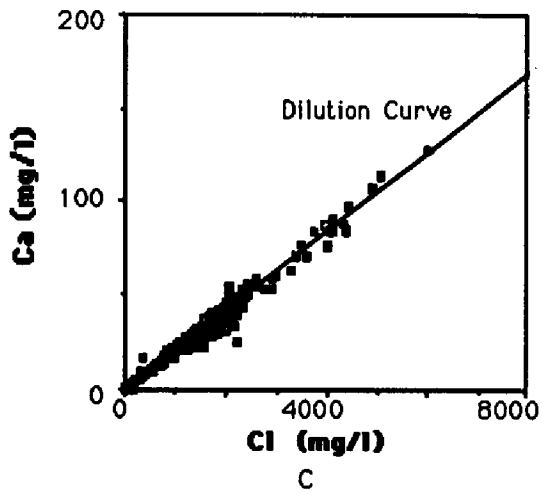
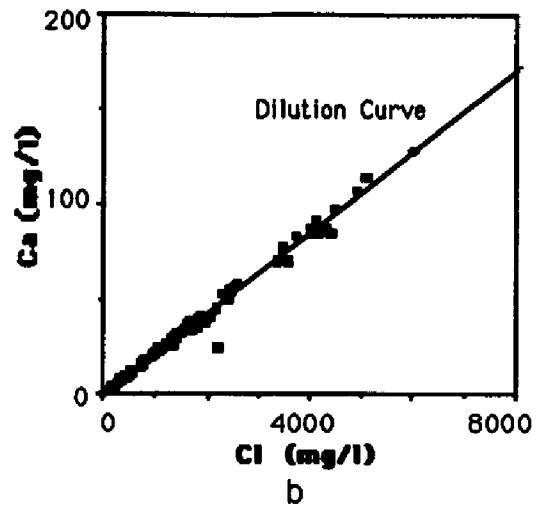
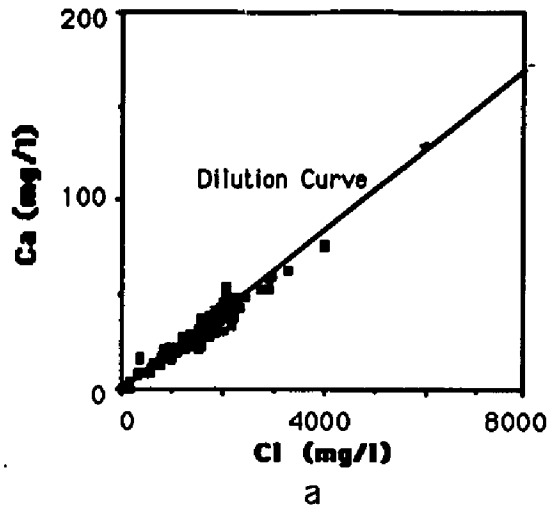


Fig. 61. Dilution curves for multiyear ice for: a) Ca-1986 samples, b) Ca-1987 samples and c) Ca-all samples combined.

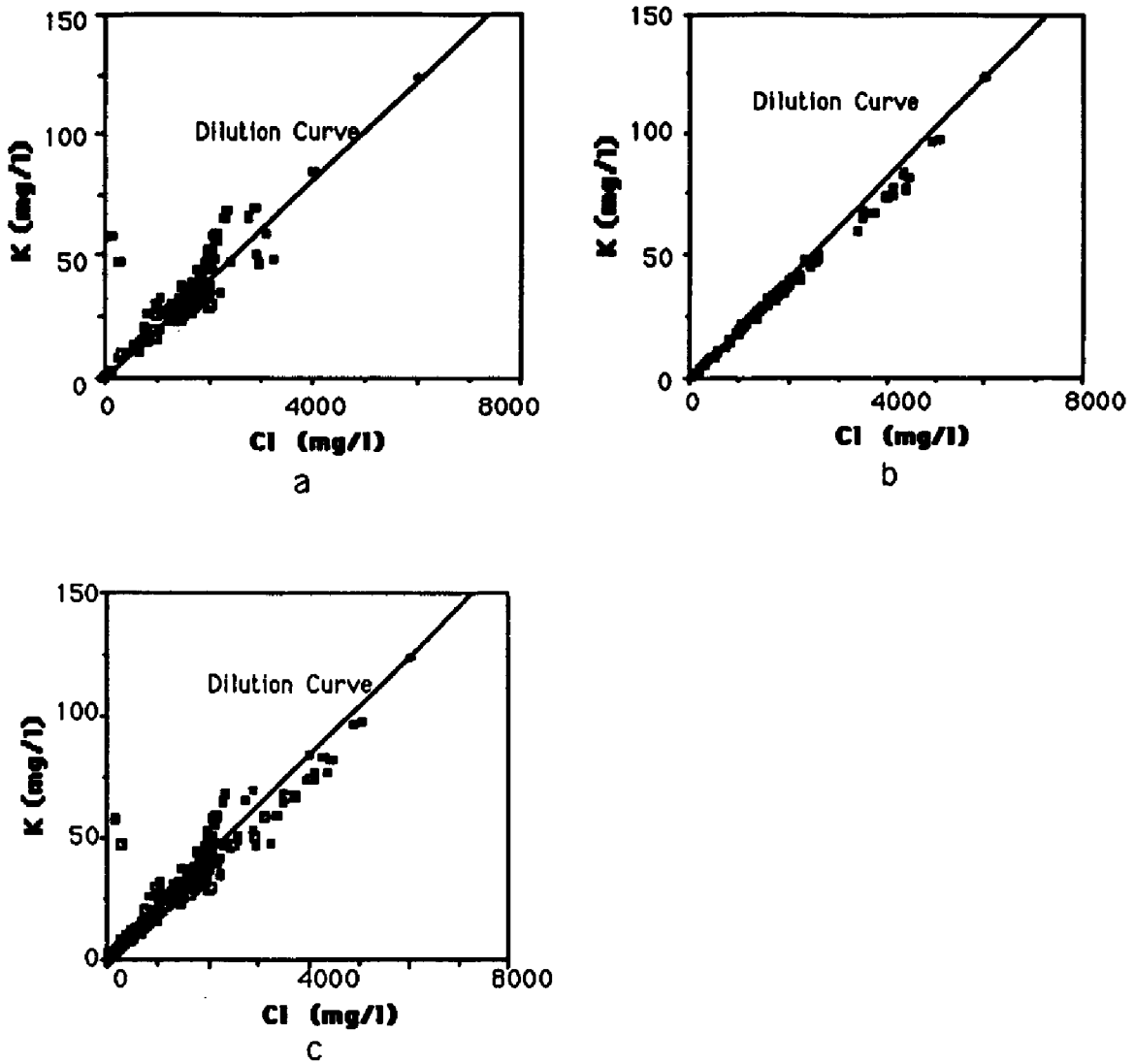
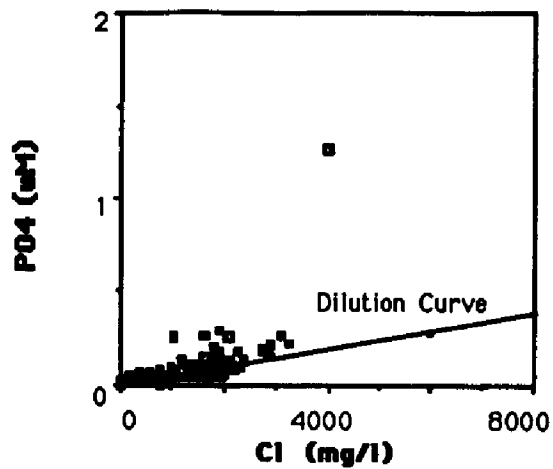
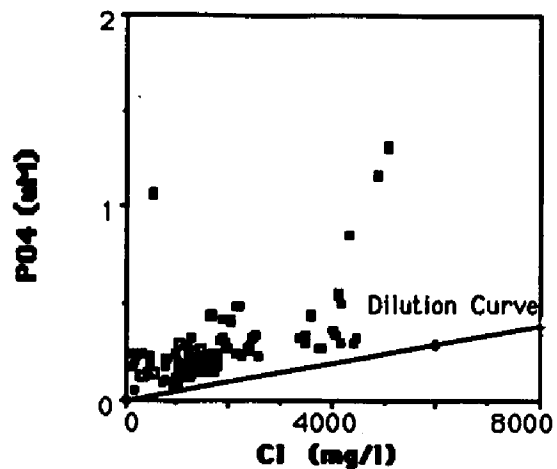


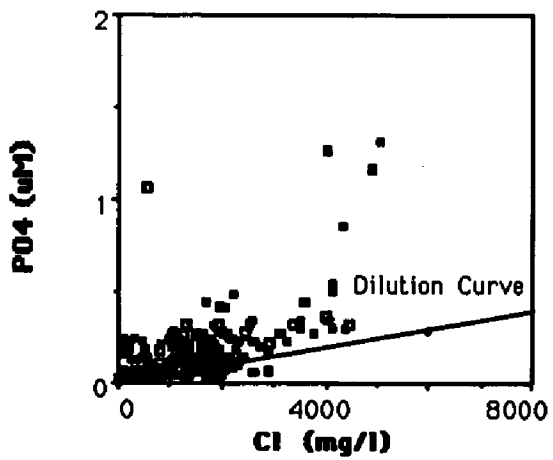
Fig. 62. Dilution curves for multiyear ice for: a) K-1986 samples, b) K-1987 samples and c) K-all samples combined.



a

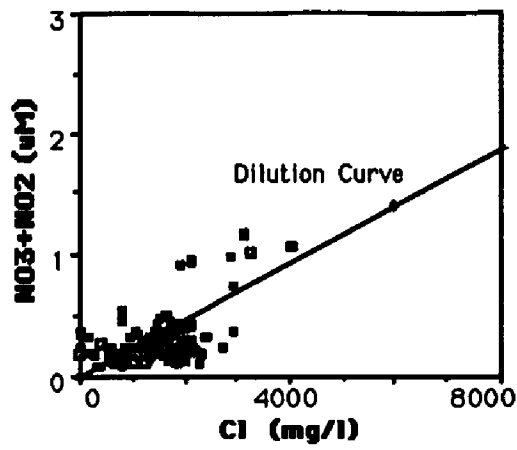


b

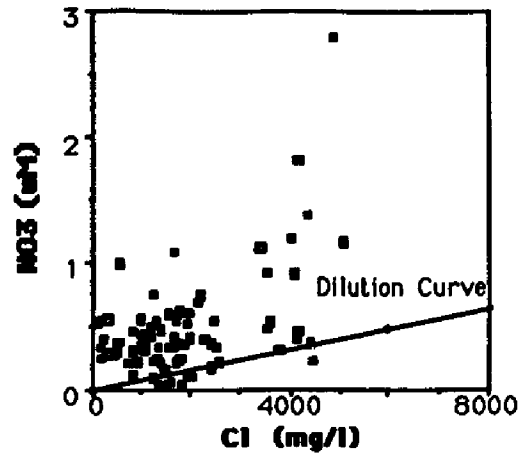


c

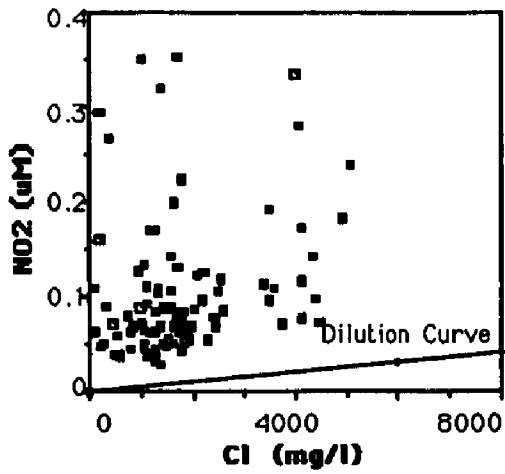
Fig. 63. Dilution curves for multiyear ice for: a) PO_4 -1986 samples, b) PO_4 -1987 samples and c) PO_4 -all samples combined.



a

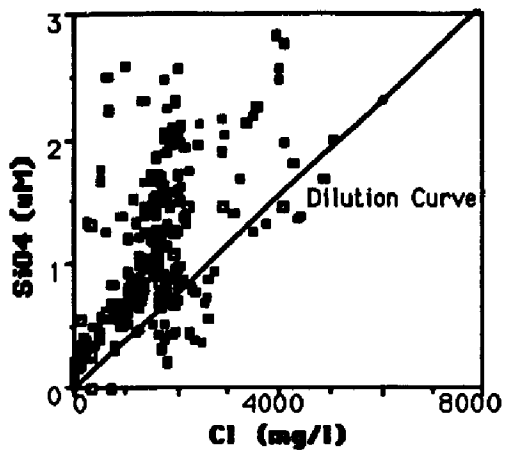


b

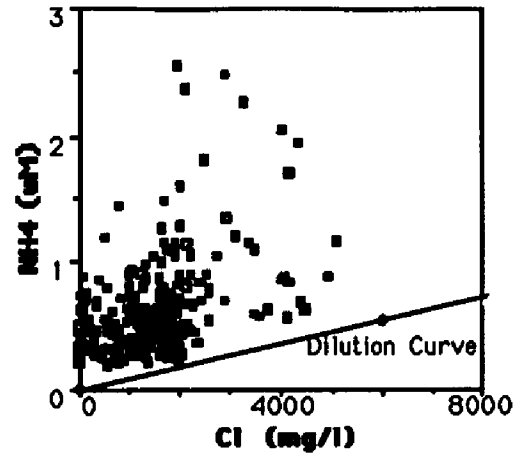


c

Fig. 64. Dilution curves for multiyear ice for: a) NO_3+NO_2 -1986 samples, b) NO_3 -1987 samples and c) NO_2 -all samples combined.



a



b

Fig. 65. Dilution curves for multiyear ice for: a) SiO_4 -all samples combined and b) NH_4 -all samples combined.

Linear Regression

For each core best-fit linear regressions were obtained for each chemical species analyzed versus Cl. In addition, regressions were obtained for Na to SO_4 , experimental salinity to measured salinity, NO_3 to the other nutrients and NO_2 to the other nutrients. In addition to the regressions the mean y-intercept, slope and R-value were calculated for all multiyear samples, 1986 multiyear samples and 1987 multiyear samples. A summary table of the results is presented in Appendix C. The purpose of this analysis was to determine which chemical species vary linearly with Cl and which nutrients are linear with each other in order to determine if factors other than salinity are affecting ice chemistry.

The results for the multiyear ice data are very similar to those found for first-year ice data. Br, SO_4 , Ca and Mg all have R-values greater than 0.9 indicating strong linearity with and a strong dependence on salinity. K and Na have R-values above 0.85 still indicating strong linearity which is probably weakened by fractionation occurring within the ice. All nutrients versus Cl have R-values less than 0.7 indicating that salinity effects are much less dominant and that other processes have affected nutrient concentrations. Regressions for all nutrients versus each other also show weak linear trends, with R-values less than 0.7, indicating that there is little correlation between nutrients and that they may all be affected by separate processes or affected differentially by the same process.

Cations/Anions

The sum of all analyzed cations and anions was obtained for each multiyear ice sample and the ratio between the two calculated. In addition, an average ratio was calculated for each core and an average for all cores determined. For multiyear ice the core average ranged between 0.97-1.04. The average for all cores is 0.99. The average values for all cores are within 98% of that obtained for first-year ice indicating that all the major cations and anions were analyzed and that there are no consistent errors in analytical methods.

Average cation to anion ratios were also calculated for pond ice and granular ice (snow ice and frazil ice combined). The average ratio for the three types of ice is 0.98 which is slightly lower than that obtained for congelation ice but significantly higher than that obtained for first-year frazil ice (0.89). Why the ratio for first-year frazil ice should be so much lower is not clear. The only first-year core with significant amounts of frazil was SI86 which was located close to shore and near an artificial island which may have had an impact on the ice chemistry as the water froze.

Statistical Analysis

Statistical analyses were performed on the multiyear ice data in the same manner as the first-year ice data. Correlation coefficient matrices and factor analysis tables were produced on

various groups of chemical species. Divisions between species were made for: all chemical species, major elements, nutrients, all species normalized to Cl, major elements normalized to Cl and nutrients normalized to Cl. Analyses were performed on the three major groups to determine what processes may be affecting chemical species variation in sea ice and determining similar correlations between cores. By separating the major elements and nutrients and performing statistics on the individual groups it may be possible to determine how the major elements interact. By treating the nutrients separately it may be possible to determine if inter-relationships exist and if these inter-relationships are controlled by similar process such as nitrification, reduction or oxidation.

Tables found within this section are summary tables which follow the same format as those for first-year ice.

Statistical Analysis for all Chemical Species

Table 29 is the summary table for the correlation coefficient matrices for all chemical species. From the table it can be seen that for most cores there are significant correlations at the 99% confidence interval between the major elements and between the major elements and PO_4 , SiO_4 and NO_3 . For cores F1SC86, F3SA86 and F1SA87, NH_4 correlates with most other species at the 99% confidence interval. This may indicate the presence of a significant bacterial population in the ice.

Factor analysis on these data (Table 30) indicates that most cores have high positive loadings in factor 1 on the major elements indicating the strong dependence on salinity. High positive loadings for the nutrients are found in factors 2 and 3. However, no definitive trends were detected indicating that there may be various processes affecting nutrient concentration in multiyear ice.

Table 29. Summary table of correlation coefficient matrices for multiyear ice based on all chemical species.

	Depth	Temp	Sal	Cl	Br
Temp	1A7, 2A7				
Sal	1D6, 3A6, 1A7 1B7, 2A7	1A7, 2A7			
Cl	1D6, 2A6, 3A6 1A7, 1B7	1A7, 2A7	1A6, 1B6, 1C6, 1D6 1A7, 1B7, 2A7		
Br	1C6, 1D6, 3A6 1A7, 1B7, 2A7	1A7, 2A7	1A6, 1B6, 1C6, 1D6, 2A6 3A6, 4A6, 1A7, 1B7, 2A7	1A6, 1B6, 1C6, 1D6 2A6, 3A6, 4A6 1A7, 1B7, 2A7	
SO4	1C6, 1D6, 3A6 1A7, 1B7, 2A7	1A7, 2A7	1A6, 1B6, 1C6, 1D6, 2A6 3A6, 4A6, 1A7, 1B7, 2A7	1A6, 1B6, 1C6, 1D6 2A6, 3A6, 4A6 1A7, 1B7, 2A7	1A6, 1B6, 1C6, 1D6 2A6, 3A6, 4A6 1A7, 1B7, 2A7
Na	1D6, 3A6 1A7, 1B7, 2A7	1A7, 2A7	1A6, 1B6, 1C6, 1D6, 2A6 3A6, 4A6, 1A7, 1B7, 2A7	1A6, 1B6, 1C6, 1D6 2A6, 3A6, 4A6 1A7, 1B7, 2A7	1A6, 1B6, 1C6, 1D6 2A6, 3A6, 4A6 1A7, 1B7, 2A7
Ca	1D6, 3A6 1A7, 1B7, 2A7	1A7, 2A7	1A6, 1B6, 1C6, 1D6, 2A6 3A6, 4A6, 1A7, 1B7, 2A7	1A6, 1B6, 1C6, 1D6 2A6, 3A6, 4A6 1A7, 1B7, 2A7	1A6, 1B6, 1C6, 1D6 2A6, 3A6, 4A6 1A7, 1B7, 2A7
K	1D6, 2A6, 3A6 1A7, 1B7, 2A7	1A7, 2A7	1A6, 1B6, 1C6, 1D6, 2A6 2A6, 3A6, 4A6 1A7, 1B7, 2A7	1A6, 1B6, 1C6, 1D6 2A6, 3A6, 4A6 1A7, 1B7, 2A7	1A6, 1B6, 1C6, 1D6 2A6, 3A6, 4A6 1A7, 1B7, 2A7
Mg	1D6, 3A6	1A7, 2A7	1A6, 1B6, 1C6, 1D6, 2A6	1A6, 1B6, 1C6, 1D6 2A6, 3A6, 4A6 1A7, 1B7, 2A7	1A6, 1B6, 1C6 2A6, 3A6, 4A6 1A7, 1B7, 2A7
PO4	1B6, 1C6, 2A6 1B7, 2A7	2A7	1A6, 1C6, 1D6, 2A6, 3A6 1B7, 2A7	1A6, 1C6, 1D6, 2A6 3A6, 1B7, 2A7	1A6, 1C6, 1D6, 2A6 3A6, 1B7, 2A7
SiO4	1A7, 1B7, 2A7	2A7	1A6, 1B6, 3A6 1A7, 1B7, 2A7	1A6, 1B6, 3A6 1A7, 1B7, 2A7	1A6, 1B6, 1C6, 3A6 1A7, 1B7, 2A7
NO3	-1A6		1A6, 1B6, 3A6 1B7	1A6, 1B6, 3A6 1B7	1A6, 1B6, 3A6 1B7
NO2					
NH4	1A7	1A7 1A7	1C6, 2A6, 3A6 1A7	1C6, 3A6 1A7	1C6, 3A6

Table 29. (cont.)

	SO4	Na	Ca	K	Mg
SO4					
Na	1A6, 1B6, 1C6, 1D6 2A6, 3A6, 4A6 1A7, 1B7, 2A7				
Ca	1A6, 1B6, 1C6, 1D6 2A6, 3A6, 4A6 1A7, 1B7, 2A7	1A6, 1B6, 1C6, 1D6 2A6, 3A6, 4A6 1A7, 1B7, 2A7			
K	1A6, 1B6, 1C6, 1D6 2A6, 3A6, 4A6 1A7, 1B7, 2A7	1A6, 1B6, 1C6, 1D6 2A6, 3A6, 4A6 1A7, 1B7, 2A7	1A6, 1B6, 1C6, 1D6 2A6, 3A6, 4A6 1A7, 1B7, 2A7		
Mg	1A6, 1B6, 1C6 2A6, 3A6, 4A6 1A7, 1B7, 2A7	1A6, 1B6, 1C6 2A6, 3A6, 4A6 1A7, 1B7, 2A7	1A6, 1B6, 1C6, 1D6 2A6, 3A6, 4A6 1A7, 1B7, 2A7	1A6, 1B6, 1C6, 1D6 2A6, 3A6, 4A6 1A7, 1B7, 2A7	
PO4	1A6, 1C6, 1D6 1A6, 1C6, 3A6 1A7, 1B7, 2A7	1A6, 1C6, 1D6 3A6, 4A6 1B7, 2A7	1A6, 1C6, 1D6 3A6, 1B7, 2A7	1A6, 1D6, 3A6 2A6, 3A6, 4A6 1A7, 2A7	1B7, 2A7
SI04	1A6, 1B6, 3A6 1A6, 1B6, 3A6 1A7, 1B7, 2A7	1A6, 1B6, 3A6 1A7, 1B7, 2A7 1A7, 1B7, 2A7	1A6, 1B6, 1C6 1A7, 1B7, 2A7	1A6, 1B6, 3A6 3A6, 1A7, 1B7, 2A7	
NO3	1A6, 1B6, 1C6, 3A6 1A6, 1B6, 1C6	1A6, 1B6, 1C6, 3A6 1B7	1A6, 1B6, 3A6 1B7	1A6, 1B6 1A7	1B7 2A7
NO2					
NH4	1C6, 3A6 1A7	1C6, 3A6 1A7	1C6, 3A6 1A7	1A7	1C6, 3A6 1A7

	PO4	SI04	NO3	NO2	NH4
PO4					
SI04	1A6, 1C6, 2A6, 3A6 2A7				
NO3	1A6, 3A6, 4A6 1A7, 1B7, 2A7	1A6, 1B6, 3A6 2A7			
NO2		2A7	2A7		
NH4	1C6, 2A6, 3A6, 4A6 1A7, 1B7, 2A7	3A6, 2A7	1A6, 1C6, 1D6, 3A6 4A6, 1A7, 1B7, 2A7		

Table 30. Summary table of factor analysis for multiyear ice for all samples.

	Factor 1	Factor 2	Factor 3
Depth	1A7, 2A7	1B6, -1C6, 2A6	-1A6, 4A6
Temp	1A7, 2A7	2A6	
Sal	1A6, 1B6, 1C6, 1D6, 3A6 4A6, 2A7		
Cl	1A6, 1B6, 1C6, 1D6, 2A6, 3A6 3A6, 4A6, 2A7		
Br	1A6, 1B6, 1C6, 1D6, 2A6, 3A6 3A6, 4A6, 2A7		
SO4	1B6, 1C6, 1D6, 3A6 3A6, 4A6, 1B7, 2A7		
Na	1A6, 1B6, 1C6, 1D6, 2A6, 3A6 3A6, 4A6, 1B7, 2A7		
Ca	1A6, 1B6, 1C6, 1D6, 2A6, 3A6 3A6, 4A6, 1B7, 2A7		
K	1A6, 1B6, 1D6, 2A6, 3A6 3A6, 4A6, 1B7, 2A7		C
Mg	1A6, 1B6, 1C6, 1D6, 2A6, 3A6 3A6, 4A6, 1B7, 2A7		
PO4		1B6, 1A7, 1B7	2A6
SiO4	1A6, 3A6, 1A7		1C6, 1D6, 2A6, -4A6
NO3		1C6, 1D6, -2A6, 3A6 1A7, 1B7, 2A7	
NO2			1A7, 1B7
NH4	1A7	1A6, 1D6, 3A6, 4A6 1B7, 2A7	1B6, 2A6

Statistical Analysis for Major Elements

The summary table for correlation coefficient matrices for the major elements (Table 31) reveals that all correlations in 70% of the cores are significant at the 99% confidence interval. Chemical species for which all cores do not have significant correlations at the 99% confidence interval include K and Mg which indicates that some process other than the salinity effect may be influencing these species. Dilution curves indicate that Mg was enriched and K depleted in relation to seawater most likely due to precipitation and drainage, respectively.

Therefore, it can be seen that statistical analyses may be useful in determining where variations occur between species.

Factor analysis on this group of data (Table 32) reveals that between 60-90% of the cores have high positive loadings on all species in factor 1. Mg has the highest number of cores (40%) with high positive loadings in factor 2 substantiating that it is affected by some process and as stated earlier is probably precipitating with another species. resulting in statistical differences between Mg and the other major elements.

Table 31. Summary table for correlation coefficient matrices for multiyear ice for major elements. In cores 1A6, 1B6, 3A6, 4A6, 1A7, 1B7 and 2A7 all correlations are significant at the 99% confidence and are not listed here. Cores in which all correlations are not significant are included in the table (1C6,1D6,2A6).

	Cl	Br	SO ₄	Na	Ca	K	Mg
Cl							
Br	1C6,1D6 2A6						
SO ₄	1C6,1D6 2A6	1C6,1D6 2A6					
Na	1C6,1D6 2A6	1C6,1D6 2A6	1C6,1D6 2A6				
Ca	1C6,1D6 2A6	1C6,1D6 2A6	1C6,1D6 2A6	C, D, 2A6			
K	1D6, 2A6	1D6, 2A6	1D6, 2A6	1D6, 2A6	1D6, 2A6		
Mg	1C6, 2A6	1C6, 2A6	1C6	1C6	1C6, 1D6 2A6	2A6	

Table 32. Summary table of factor analysis for multiyear ice for major elements.

	Factor 1	Factor 2
Cl	1A6, 1B6, 1C6, 1D6, 2A6 3A6, 4A6, 1A7, 1B7, 2A7	
Br	1A6, 1B6, 1C6, 1D6, 2A6 3A6, 4A6, 1A7, 1B7, 2A7	-4A6, 1B7
SO4	1A6, 1B6, 1C6, 1D6, 2A6 3A6, 4A6, 1A7, 1B7, 2A7	1A6
Na	1A6, 1B6, 1C6, 1D6, 2A6 3A6, 4A6, 1A7, 1B7, 2A7	-3A6
Ca	1A6, 1B6, 1C6, 1D6, 2A6 3A6, 4A6, 1A7, 1B7, 2A7	1B6, 4A6
K	1A6, 1B6, 1D6, 3A6, 4A6, 1A7, 1B7, 2A7	1C6, 3A6
Mg	1A6, 1B6, 1C6 3A6, 4A6, 1A7, 1B7, 2A7	1D6, 2A6, 1A7, 2A7

Statistical Analysis for Nutrients

The summary table for correlation coefficient matrices (Table 33) and for factor analysis (Table 34) for nutrients reveals that there are fewer correlations and much less consistency between the nutrients than for the major ions. This behavior parallels that seen in the first-year ice data.

The most important finding in this multiyear data set is that 80% of the cores had significant correlations at the 99% confidence interval for NO_3 and NH_4 . This may be an indication that bacterial reduction of NO_3 to NH_4 is occurring, a situation also substantiated by factor analysis. Significant correlations exist in 60-70% of the cores for NO_3 and NH_4 to PO_4 . This suggests winter nutrient buildup (Horner and Schrader, 1982) similar to that indicated in the first-year ice data.

Table 33. Summary table for correlation coefficient matrices for multiyear ice for nutrients.

	PO4	SiO4	NO3	NO2	NH4
PO4					
SiO4	1A6, 1C6, 3A6				
NO3	1A6, 1D6, 3A6, 4A6 1A7, 1B7, 2A7	1A6, 1B6, 3A6 2A7			
NO2		2A7	2A7		
NH4	1C6, 1D6, 3A6, 4A6 1A7, 1B7	3A6, 2A7	1A6, 1C6, 1D6, 3A6 4A6, 1A7, 1B7, 2A7		

Table 34. Summary table of factor analysis for multiyear ice for nutrients.

	Factor 1	Factor 2
PO4	1A6, 1C6, 1D6, 2A6	1B6, 3A6 4A6, 1A7, 1B7
SiO4	1A6, 1B6, 1C6, 3A6	1D6, 4A6, 1A7
NO3	1B6, 1D6, 3A6	1A6, 1C6, 2A6 1A7, 1B7, 2A7
NO2		-1A7, 1B7
NH4	1D6, 2A6, 3A6, 4A6	1A6, 1B6, 1C6 2A7

Statistical Analysis for All Chemical Species Normalized to Cl

In order to determine if there are any secondary processes affecting chemical concentrations all species were normalized to Cl in order to remove the salinity effect. A summary table for the correlation coefficient matrices (Table 35) reveals fewer correlations at the 99% confidence interval than before normalization. There is no definitive trend to the correlations and few similarities between cores indicating that secondary processes are involved. These situations may involve factors such as the thermal history of the ice and may be site specific, thereby, making it difficult to identify them.

Table 35. Summary table for correlation coefficient matrices for multiyear ice for all elements normalized to Cl.

	Br	SO4	Na	Ca	K	Mg
Br						
SO4	1B6					
Na		1B6, 2A7				
Ca		1B6, 3A6 4A6, 2A7	1A6, -1C6 1D6, 4A6 2A7			
K	1A7, 2A7	1B6, -2A7	4A6	4A6		
Mg			1B6, -1A7	3A6		
PO4	3A6, 1A7 1B7	-3A6, -1B7 -2A7		-3A6	1A6, 1C6 1A7, 2A7	-1A6, -3A6
SiO4	3A6, 1A7 -2A7	-3A6, -1B7	-3A6, 1A6	1A6, 1A7 2A7	-3A6	1B7
NO3	3A6, 1A7	1B6, -3A6 -1B7, -2A7	1B6	-3A6 1A7, 2A7	1A6, 1B6	-3A6, 1B7 1C6
NO2	1A7, 1B7	-1B7, -2A7			1A7, 2A7	
NH4	3A6, 1A7 1B7	1B6, -3A6 -1B7, -2A7	1B6	-3A6	1A6, 1B6, 1C6 1A7, 2A7	-3A6

	PO4	SiO4	NO3	NO2	NH4
PO4					
SiO4	1A6, 1C6, 1D6, 3A6 1A7, 1B7, 2A7				
NO3	1A6, 1C6, 1D6, 3A6 4A6, 1A7, 1B7, 2A7	3A6, 1A7, 1B7 2A7			
NO2	1A7, 1B7, 2A7	1A7, 1B7, 2A7	1A7, 1B7, 2A7		
NH4	1A6, 1C6, 1D6, 3A6 4A6, 1A7, 1B7, 2A7	1A6, 3A6, 1A7 1B7, 2A7	1A6, 1B6, 1C6 1D6, 3A6, 4A6 1A7, 1B7, 2A7	1A7, 1B7, 2A7	

Table 36. Summary table of factor analysis for multiyear ice for all elements normalized to Cl.

	Factor 1	Factor 2	Factor 3	Factor 4	Factor 5
Br	1A6, 1C6, 2A7	1A6, 2A6			
SO4			-1C6, 1A7	1A6, 2A6	
Na		1A6, -1C6, -2A6 1A7, 1B7, 2A7	3A6		2A6
Ca		1A6, 1C6, 1D6 1B7, 2A7	1A7		
K	1C6	3A6, 4A6	1D6, 2A6		
Mg		1B6, -1A7 1B7, 2A7	1C6, -1D6, 4A6		
PO4	1A6, 1D6, 3A6 1A7, 1B7, 2A7	-2A6	1B6		
SiO4	2A6, 3A6 1A7, 1B7, 2A7	-1B6	1C6	4A6	
NO3	1A6, 1B6, 1C6, 1D6, 2A6, 3A6, 1A7, 1B7, 2A7				
NO2	1B7, 2A7				
NH4	1A6, 1B6, 1C6 1D6, 3A6, 4A6 1A7, 1B7, 2A7				

Statistical Analysis for Major Elements Normalized to Cl

As with the first-year ice data there are fewer correlations after normalization. Also, little consistency exists between the correlation coefficient matrices (Table 37) and the factor analysis results (Table 38). However, correlations do exist suggesting that secondary processes act on the ice chemistry but it is not possible to identify them at this time. Possibilities may include fractionation, differential drainage with melt water and biological utilization.

Table 37. Summary table of correlation coefficient matrices for multiyear ice for major elements normalized to Cl.

	Br	SO4	Na	Ca	K	Mg
Br						
SO4	-1B7, -2A7					
Na		1B6, 2A7				
Ca		1B6, 3A6 4A6, 2A7	1A6, -1C6 4A6, 2A7			
K	1A7, 2A7	1B6, -2A7	4A6	4A6, 1B7		
Mg			1B6, -1A7	3A6	1B7	

Table 38. Summary table for factor analysis for multiyear ice for major elements normalized to Cl.

	Factor 1	Factor 2	Factor 3
Br	1B6, 1A7	1A6, -1B7	2A6
SO4	1B6, -2A7	1C6, -4A6, 1B7	1A6, 2A6, 1A7
Na	1A6, -1C6, 2A6, 4A6	3A6, 1A7, 2A7	
Ca	1A6, 1B6, 1C6, 1D6 2A6, 3A6, 4A6	2A7	1A7
K	4A6, 1A7, 1B7, 2A7	1A6, 1D6, 2A6, 3A6	1C6
Mg	3A6, 1B7	-1A6, 1B6, -1D6 2A6	4A6, -1A7

Statistical Analysis for Nutrients Normalized to Cl

Of all of the sets of statistics performed these are probably the most interesting and surprising. The summary table of the correlation coefficient matrices (Table 39) shows a significant number of correlations (30-90%) between PO_4 and SiO_4 , NO_3 and NH_4 . Even more interesting is the factor analysis table (Table 40) in which it can be seen that 70-100% of the cores have high positive loadings in factor 1 on PO_4 , NO_3 and NH_4 . This suggests that in multiyear ice nutrients are not salinity

dependent and that biological activity may strongly control nutrient concentrations. In factor 2, 70% of the cores have high positive loadings on SiO₄ indicating that SiO₄ is dependent on some other process.

Table 39. Summary table for correlation coefficient matrices for multiyear ice for nutrients normalized to Cl.

	PO4	SiO4	NO3	NO2	NH4
PO4					
SiO4	1A6, 1C6, 1D6, 3A6, 4A6, 1A7, 1B7, 2A7				
NO3	1A6, 1D6, 3A6, 4A6, 1A7, 1B7	1D6, 4A6, 1A7, 1B7, 2A7			
NO2	1A7, 1B7, 2A7	1B7, 2A7	1A7, 1B7, 2A7		
NH4	1A6, 1C6, 1D6, 2A6, 3A6, 4A6, 1A7, 1B7, 2A7	1A6, 1D6, 4A6, 1A7, 1B7, 2A7	1A6, 1B6, 1C6, 1D6, 4A6, 1A7, 1B7, 2A7	1A7, 1B7, 2A7	

Table 40. Summary table of factor analysis for multiyear ice for nutrients normalized to Cl.

	Factor 1	Factor 2
PO4	1D6, 2A6, 3A6, 4A6, 1A7, 1B7, 2A7	-1A7
SiO4	1D6, 1A7, 1B7, 2A7	1A6, 1B6, 1C6, 2A6, 3A6, 4A6, 2A7
NO3	1A6, 1B6, 1C6, 1D6, 3A6, 4A6, 1A7, 1B7, 2A7	1D6, 2A6
NO2	1A7, 1B7, 2A7	1A7, 1B7
NH4	1A6, 1B6, 1C6, 1D6, 2A6, 3A6, 4A6, 1A7, 1B7, 2A7	1A7

Comparison of First-year and Multiyear Ice

In order to determine if similarities exist between first-year and multiyear ice statistics were performed on all first-year ice samples combined and all multiyear ice samples combined and the results are summarized in the following tables. In first-year ice

high concentrations of most chemical species exist in the top and bottom 10 cm. It was unknown as to how this was affecting the statistics, therefore, these samples were removed from the first-year data set and additional statistics were performed on the top samples, bottom samples and remaining interior samples. These results are also summarized in this section.

Statistical Analysis for all Chemical Species

Table 41 is the summary table for the correlation coefficient matrices for all chemical species for the groups of samples listed above. From the table it can be seen that significant correlations at the 99% confidence interval exist between all species for multiyear ice and most species for first-year ice. In addition, most groups have significant correlations between all the major species. The main differences are with the first-year top, bottom and interior samples for nutrients. However, in general it can be seen that when large numbers of first-year and multiyear ice are grouped together the chemistry is statistically very similar. This table also indicates that the top and bottom samples do not have a significant effect on overall statistics.

Factor analysis (Table 42) reveals that all groups of samples have high positive loadings for the major elements in factor 1. In factor 2 differences between first-year and multiyear ice can be seen where depth and temperature have high positive loadings for first-year ice and nutrients have high positive loadings for multiyear ice. This further substantiates previous statistical

analyses where it was suggested that nutrients in multiyear ice are independent of salinity (major ion chemistry) and affected by some other process(es).

Table 41. Summary for correlation coefficient matrices for first-year and multiyear ice for all chemical species. All correlations listed are significant at the 99% confidence interval. M, F, I, T and B designate multiyear, first-year, interior first-year, top first-year and bottom first-year ice respectively.

	D	Temp	Sal	Cl	Br
D					
Temp	F, M, I				
Sal	M	M			
Cl	M	M	M, F, I, T, B		
Br	M	M	M, F, I, T, B	M, F, I, T, B	
SO4	M	M	M, F, I, T, B	M, F, I, T, B	M, F, I, T, B
Na	M	M	M, F, I, T, B	M, F, I, T, B	M, F, I, T, B
Ca	M	M	M, F, I, T, B	M, F, I, T, B	M, F, I, T, B
K	M	M	M, F, I, T, B	M, F, I, T, B	M, F, I, T, B
Mg	M	M	M, F, I, T, B	M, F, I, T, B	M, F, I, T, B
PO4	M	M, F, I	M, F, T	M, F, T	M, F, T
SiO4	M	M	M, F, T, B	M, F, T, B	M, F, T, B
NO3+NO2	M	M	M, F	M, F	M, F
NH4	M	M, F, T, -I	M, F, B	M, F, I, B	M, F, I, B

	SO4	Na	Ca	K	Mg
Na	M, F, I, T, B				
Ca	M, F, I, T, B	M, F, I, T, B			
K	M, F, I, T, B	M, F, I, T, B	M, F, I, T, B		
Mg	M, F, I, T, B				
PO4	M, F, T	M, F, T	M, F, T	M, F, T	M, F
SiO4	M, F, T, B	M, F, T, B			
NO3+NO2	M, F	M, F	M, F	M, F	M, F
NH4	M, F, B	M, F, I, B	M, F, B	M, F, I, B	M, F, I, B

Table 41. (cont).

	PO4	SiO4	NO3+NO2	NH4
SiO4	M, T			
NO3+NO2	M, F, I	M, F, I		
NH4	M	M, F, B	M, F	

Table 42. Summary of factor analysis for first-year and multiyear ice for all chemical species. M, F, I, T and B designate multiyear, first-year, interior first-year, top first-year and bottom first-year ice respectively.

	Factor 1	Factor 2	Factor 3
D		F, I, -T, B	M
Temp		F, I, -T	
Sal	M, F, I, T, B		
Cl	M, F, I, T, B		
Br	M, F, I, T, B		
SO ₄	M, F, I, B		
Na	M, F, I, T, B		
Ca	M, F, I, T, B		
K	M, F, I, B		
Mg	M, F, I, T, B		
PO ₄		M, -B	
SiO ₄			I
NO ₃ +NO ₂		M	I
NH ₄		M, T	

Statistical Analysis for Major Elements

Correlation coefficient matrices for all groups of samples showed significant correlations at the 99% confidence interval for all major elements to each other. This indicates that major element chemistry is not significantly different between first-year and multiyear ice. Factor analysis (Table 44) further substantiates this. It can be seen that most groups have high positive loadings in factor 1 for all elements. The main exception to this is SO₄ where high positive loadings exist for multiyear, first-year and first-year interior ice indicating that fractionation of SO₄ is occurring in most samples.

Table 43. Summary for correlation coefficient matrices for first-year and multiyear ice for major elements. All correlations listed are significant at the 99% confidence interval. M, F, I, T and B designate multiyear, first-year, interior first-year, top first-year and bottom first-year ice respectively.

All major elements correlate significantly with each other for all groups of samples.

Table 44. Summary of factor analysis for first-year and multiyear ice for major elements. M, F, I, T and B designate multiyear, first-year, interior first-year, top first-year and bottom first-year ice respectively.

	Factor 1	Factor 2	Factor 3
Cl	M, F, I, T, B, I		
Br	M, F, I, T, B, I		
SO ₄	M, F, B	M, F, I	
Na	M, F, T, B	I	
Ca	M, F, I, T, B	B	
K	M, F, I, B	T	
Mg	M, F, I, T, B		

Statistical Analysis for Nutrients

Tables 45 and 46 reveal that essentially no significant difference exists between multiyear, first-year and first-year interior ice for nutrients again suggesting that no major chemical differences exist between first-year and multiyear ice.

Table 45. Summary for correlation coefficient matrices for first-year and multiyear ice for nutrients. All correlations listed are significant at the 99% confidence interval. M, F, I, T and B designate multiyear, first-year, interior first-year, top first-year and bottom first-year ice respectively.

	PO ₄	SiO ₄	NO ₃ +NO ₂	NH ₄
PO ₄				
SiO ₄	M, F, T			
NO ₃ +NO ₂	M, F, I	M, F, I		
NH ₄	M	M, F, I, B	M, F, I	

Table 46. Summary of factor analysis for first-year and multiyear ice for nutrients. M, F, I, T and B designate multiyear, first-year, interior first-year, top first-year and bottom first-year ice respectively.

	Factor 1	Factor 2	Factor 3
PO4	T	F,I,B	
SiO4	T,B	M	
NO3+NO2	M,F,I	T	
NH4	M,F,I,B		

Statistical Analysis for All Chemical Species Normalized to Cl

As with individual cores, statistics on all species normalized to Cl show few similarities between groups of samples indicating that secondary processes do affect ice chemistry but are not consistent throughout. Variations between first-year and multiyear ice as seen in Tables 47 and 48 may be valuable in providing information as to what further information is necessary in order to determine these secondary processes.

Table 47. Summary for correlation coefficient matrices for first-year and multiyear ice for all chemical species normalized to Cl. All correlations listed are significant at the 99% confidence interval. M, F, I, T and B designate multiyear, first-year, interior first-year, top first-year and bottom first-year ice respectively.

	Br	SO4	Na	Ca	K	Mg
Br						
SO4						
Na	F,I	F,T				
Ca	F,I		M,F,I			
K	I		F,I			
Mg	F,I					
PO4	M				M	
SiO4	M					
NO3+NO2		F		-M,I		-I
NH4		T		-M		

Table 47. (cont.).

	PO4	SiO4	NO3+NO2	NH4
Br				
SO4				
Na				
Ca				
K				
Mg				
PO4				
SiO4	M			
NO3+NO2	M, I	M, F, I		
NH4	M	M	M, F, I	

Table 48. Summary of factor analysis for first-year and multiyear ice for all chemical species normalized to Cl. M, F, I, T and B designate multiyear, first-year, interior first-year, top first-year and bottom first-year ice respectively.

	Factor 1	Factor 2	Factor 3	Factor 4
Br		F, T, I	M	
SO4			I	M, F
Na		M		
Ca		M, F		T
K		F		M
Mg		T	M	
PO4			F, I, T	
SiO4	M, F			M
NO3+NO2	M, F, I, T			
NH4	M, F, I			

Statistical Analysis for Major Species Normalized to Cl

As with all species normalized to Cl there is little consistency between the correlation coefficient matrices (Table 49) and the factor analysis results (Table 50). Correlations do exist, essentially for first-year ice, indicating that there are secondary processes affecting the chemistry but the cause is unclear.

Because more correlations exist for first-year ice this may be an indication that first-year ice chemistry is more dynamic and affected more readily by other processes.

Table 49. Summary for correlation coefficient matrices for first-year and multiyear ice for major species normalized to Cl. All correlations listed are significant at the 99% confidence interval. M, F, I, T and B designate multiyear, first-year, interior first-year, top first-year and bottom first-year ice respectively.

	Br	SO4	Na	Ca	K	Mg
Br						
SO4						
Na	F, I	F, T				
Ca	I		M, F, I			
K	I		F, I			
Mg	F, I					

Table 50. Summary of factor analysis for first-year and multiyear ice for the major species normalized to Cl. M, F, I, T and B designate multiyear, first-year, interior first-year, top first-year and bottom first-year ice respectively.

	Factor 1	Factor 2	Factor 3
Br	F, I	M, T	
SO4	T, B	F	M
Na	M, I, T, B	F	
Ca	M, I	B	T
K	I	M, B	
Mg	F	I	

Statistical Analysis for Nutrients Normalized to Cl

Although more correlations exist for multiyear ice (Table 51) there is considerable consistency between multiyear, first-year and first-year interior ice. This indicates that nutrient concentrations in general are affected by process(es) other than salinity and may be due to an interior biological population.

Table 51. Summary for correlation coefficient matrices for first-year and multiyear ice for nutrients normalized to Cl. All correlations listed are significant at the 99% confidence interval. M, F, I, T and B designate multiyear, first-year, interior first-year, top first-year and bottom first-year ice, respectively.

	PO4	SiO4	NO3+NO2	NH4
PO4				
SiO4	M			
NO3+NO2	M, I	M, F, I		
NH4	M	M, F, I	M, F, I	

Table 52. Summary of factor analysis for first-year and multiyear ice for nutrients normalized to Cl. M, F, I, T and B designate multiyear, first-year, interior first-year, top first-year and bottom first-year ice respectively.

	Factor 1	Factor 2
PO4		M, F, I, T
SiO4	M, B	T
NO3+NO2	M, F, T	B
NH4	M, F, I, B	

V. SUMMARY

At least 90% of the ice collected was composed of columnar (congelation) ice. Salinity depth profiles compared to textural changes revealed that a chemical gradation exists where decreasing grain size results in increasing salinity, and therefore, increasing major ion chemistry. This indicates that finer grained (faster growing) ice entraps more impurities between crystal platelets.

In order to determine if ice type affects ice chemistry, statistical analyses were performed on a first-year core that consisted of 50% granular ice and 50% columnar ice. Statistics were performed on the data for each ice type and for all samples combined. These results indicate that major ions vary consistently with salinity and ratios remain fairly constant with those in seawater and are not affected by ice type. In this instance, processes affecting nutrient concentrations are independent of salinity. In addition, PO_4 and the nitrogen species appear to be affected by ice type. Therefore, it is clear that samples to be used for chemical analyses should always be subsectioned on the basis of ice type rather than using a predetermined depth interval.

The only chemical analysis routinely performed in the past is average bulk salinity. When compared to past data, particularly that for ice collected in Fram Strait during MIZEK-84 (Gow and Tucker, 1987; Gow et al., 1987 and Tucker et al., 1987) the average bulk salinity for both first-year and multiyear ice in the Southern Beaufort Sea is higher (up to 12‰ for first-year ice and 26‰ for

multiyear ice). These higher salinities are due to the time of year samples were collected. Cores in the Southern Beaufort Sea were collected earlier in the season while the ice was still cold and brine drainage had not yet begun resulting in higher bulk salinities.

In order to determine if enrichment or depletion of the major chemical species and/or nutrients had occurred with respect to seawater, dilution curves were produced. These results show that in both first-year and multiyear ice enrichment of Mg and depletion of K exists. For Mg enrichment to occur a salt other than Cl must be precipitating with Mg at temperatures higher than -36° C (Assur, 1958). This suggests that a revision in the phase diagram may be necessary. Although actual K depletion has not been previously reported plots of K/Cl with depth from Bennington (1963) and Addison (1977) show depletion through most of the ice with respect to seawater. As the first K salt (KCl) does not form until -36.8° C, K should be more mobile than Cl and show a depletion (Weeks and Ackley, 1982). Results from this study substantiate this tenet.

Dilution curves for the major ions show decreased scatter around the curve between 1986 and 1987 data. This is probably a result of delayed core processing of the 1986 samples and indicates that for major ion chemistry samples should be sectioned as soon as possible after sampling.

Nutrient dilution curves for first-year and multiyear ice all show enrichment with respect to seawater and show considerable scatter around the curve. Alexander (1974) also working in the Southern Beaufort Sea found that nitrogen nutrient levels in water

drained from sea ice during spring ice bloom were considerably higher than seawater levels. Nutrient levels in the upper water column typically increase over the winter due to low levels of biological activity and are then readily depleted in the spring. N:P ratios are 4.6, 18.3 and 7.5 for water collected at the ice/water interface, first-year ice and multiyear ice, respectively. The low N:P ratio for the underlying surface waters, also found by Maestrini et al. (1986) in Hudson Bay, indicate that the winter surface water is biologically inactive. The 18.3 ratio for first-year ice indicates that the N:P ratio is very similar to that of the Redfield ratio (15:1) for oceanic organic material indicating that biological activity is occurring in the ice and is controlling the nutrient ratios. This was also found by Alexander (1974) in the Southern Beaufort Sea where inorganic nitrogen was enriched with respect to P and is probably due to the high nitrogen concentration of the river waters entering the coastal areas. The lower ratio of 7.5 for multiyear ice indicates that some biological activity has and/or is occurring but is not as consistent as first-year ice indicating that other processes are occurring that are controlling the nutrient ratios and concentrations.

Linear regressions were obtained for all major ions to Cl, nutrients to Cl and nutrients to NO_3 and nutrients to NO_2 in order to determine if linear relationships exist. All regressions were significant at the 99% confidence interval. The regressions showed that Br, Ca, K and Mg are all strongly linear with salinity ($R > 0.9$), while Na and SO_4 are slightly less ($R > 0.78$). Weaker R-values were obtained for nutrients to Cl indicating that salinity

effects are much less dominant and that other processes such as biological activity have affected nutrient concentrations. Nutrients plotted against each other also show weak linear trends which indicate that the various nutrients are affected by some of the same general processes, however, overall each nutrient behaves differently and is being affected by different processes.

Cation to anion ratios were determined in order to ascertain if all of the major species had been accounted for in the analyses and as a test of accuracy of the analyses. Ratios of 1.01 and 0.99 for first-year and multiyear ice respectively, were obtained and indicate that all major species are accounted for.

Statistical analysis on the major ions indicates that the ratios in sea ice remain fairly constant compared to that of seawater and major fractionation is not occurring in either first-year or multiyear ice. This indicates that brine drainage from sea ice will not affect major ion ocean chemistry over long periods of time. In addition, no apparent trends exist between major ions and nutrients indicating that nutrient concentrations are independent of salinity effects and that processes affecting nutrient concentrations may not be consistent throughout the ice pack and may be location specific. In first-year ice fewer correlations exist between the nutrients than the major ions and there is much less consistency between cores. This is a result of processes that can affect nutrient concentrations such as biological activity, brine drainage, bacterial regeneration, nitrification and denitrification. In multiyear ice statistical analysis on nutrients showed that 60-70% of the cores had significant

correlations at the 99% confidence interval for NO_3 and NH_4 . In addition significant correlations exist in 80% of the cores for NO_3 and NH_4 to PO_4 . This indicates biological activity as was also observed in first-year ice.

When all species are normalized to Cl and statistical analyses performed, little consistency exists and no trends are identifiable. The existence of significant correlations indicates that secondary processes affect ice chemistry but are not definable at this time. The exception to this is for nutrients in multiyear ice where factor analysis for nutrients normalized to Cl show that 70-100% of the cores have high positive loadings in factor 1 on PO_4 , NO_3 and NH_4 . This suggests that in multiyear ice nutrients are not salinity dependent and biological activity may strongly control nutrient concentrations.

Although dilution curves for multiyear ice showed similar trends to first-year ice when actual nutrient concentrations were compared the only variation seen was that between NO_3 and NO_2 where NO_3 was as much as $4\mu\text{M}/\text{l}$ lower in multiyear ice and NO_2 concentrations were up to $0.15\ \mu\text{M}/\text{l}$ higher in multiyear ice. The decrease in NO_3 and increase in NO_2 concentrations in multiyear ice may be an indication that nitrogen reduction occurs in the ice during the summer.

VI. CONCLUSIONS

The chemical and structural properties of Arctic sea ice in the southern Beaufort Sea were studied to obtain detailed chemical profiles for first-year and multiyear sea ice. The following conclusions were made:

- Through dilution curves, linear regressions and statistical analyses it was shown that major ion chemistry is strictly associated with salinity. In many cores, including first-year and multiyear ice, it also became apparent that nutrient concentrations are also correlated to the major ions and, are therefore, strongly controlled by salinity. When this occurs it may be an indication that a bacterial or other biological population does not exist in the ice.
- Comparisons of chemical concentrations to structure profiles reveal chemical gradations in which concentration decreases with increasing crystal size.
- Statistical analysis based on ice type further substantiated a correlation between chemistry and ice type. Indicating that when sectioning cores for salinity and chemical profiles careful consideration must be given to ice type.
- Minimal fractionation of Ca, Na and/or SO₄ was detected in several cores. However, no definitive trends were observed.

The reasons for this have not been determined but may be related to the thermal history of the ice.

- Mg is enriched in ice samples suggesting that it may be precipitating with a salt other than Cl at temperatures higher than that shown on the phase diagram (-43° C) suggesting that a possible revision in the phase diagram is in order.
- K is depleted in the ice indicating that it drains preferentially due to the low temperature (-36.8° C) at which KCl forms allowing K to be more mobile than Cl.
- Cation to anion ratios are the same for first-year and multiyear ice showing that despite brine drainage and desalination of ice as it ages there are no significant changes in major element chemistry.
- Normalization of all chemical species to Cl to remove bulk salinity effects revealed that while secondary processes may affect ice chemistry they do not have an impact on the overall chemistry.
- Nutrients in first-year ice show a slight N enrichment with respect to P, but the overall ratio of 18.3 is close to the Redfield ratio of 15, indicating that the nutrients in first-year ice are controlled by biological activity. The N enrichment is consistent with that found by Alexander (1974)

and is probably due to the high N concentrations of the river water entering into the Southern Beaufort Sea.

- Nutrients in multiyear ice appear to be controlled by a combination of biological activity and other processes that tend to reduce the N:P ratio.
- Comparison of statistical analyses of multiyear, first-year, top first-year, bottom first-year and interior first-year ice samples indicate that overall there is little variation between first-year and multiyear ice. Secondary processes are indicated by the results but cannot be defined.
- Ratios of the major elements remain fairly consistent with seawater indicating that sea ice does not have a significant effect on major ion oceanic chemistry over long periods of time.

VII. FUTURE WORK

Results of the current studies indicate that:

1) The most important work that can be done in the future would be time-series experiments where both first-year and multiyear ice can be sampled on a regular basis throughout their freezing season. These experiments will provide valuable information concerning chemical changes with time for the determination of processes affecting fractionation. An important aspect of this work would be to freeze thermistors into the ice and monitor ice temperatures. This would also allow for procurement of more accurate ice temperatures which would assist in verifying the phase diagram.

2) Experiments should be performed in conjunction with biologists studying bacterial populations in order to identify processes affecting nutrient concentration levels.

3) Scanning electron micrographs of brine pockets may reveal the element(s) combining with Mg.

4) Collection of pure brine samples in cold ice must be attempted. Brine samples would provide true chemical data rather than depending on thawed whole ice samples which result in appreciable dilution.

5) The age of multiyear ice is difficult to determine. It is possible that the use of various radionuclides found in seawater may provide a means of dating older ice.

6) Salinity concentrations in the bottom ice layers may be much higher than reported due to brine drainage that occurs as the sample is collected and fragile nature of the skeletal layer

at the bottom of the ice. True concentrations of the brine during initial salt entrapment may be determined by divers collecting brine with syringes or other means from the interior of the bottom skeleton layer.

REFERENCES CITED

- Aagaard, K. (1984) The Beaufort Undercurrent. In *The Alaskan Beaufort Sea-Ecosystems and Environments*, (P.W. Barnes, D.M. Schell and E. Reimnitz, Eds.), pp. 47-72.
- Addison, J.R. (1977) Impurity concentrations in sea ice. *Journal of Glaciology*, 18(78):117-127.
- Anderson and Jones (1985) Measurements of total alkalinity, calcium and sulfate in natural sea ice. *Journal of Geophysical Research*, 90(C5):9194-9198.
- Andreas, E.L. and S.F. Ackley (1982) On the differences in ablation seasons of Arctic and Antarctic sea ice. *Journal of Atmospheric Science*, 39:440-447.
- Antonov, V.S. (1958) The role of continental runoff in the current regime of the Arctic Ocean. *Problemy Severa*, 1:52-64.
- Assur, A. (1960) Composition of sea ice and its tensile strength. SIPRE Research Report, 44, 49 p.
- Barnes, P.W., D.M. Schell and E. Reimnitz (1984) Preface. In *The Alaskan Beaufort Sea-Ecosystems and Environments*, (P.W. Barnes, D.M. Schell and E. Reimnitz, Eds.), Academic Press, London, pp. xv-xvi.
- Bennington, K.O. (1963) Some chemical composition studies on Arctic sea ice. In *Ice and Snow* (W.D. Kingery, Ed.), MIT Press, Cambridge, MA, pp. 248-257.
- Broecker, W.S and T.-H. Peng (1982) *Tracers in the Sea*. Eldigio Press, NY.
- Clarke, D.B. and S.F. Ackley (1984) Sea ice structure and biological activity in the Antarctic marginal ice zone. *Journal of Geophysical Research*, 89(C2):2087-2095.
- Cox, G.F.N. and W.F. Weeks (1975) Brine drainage and initial salt entrapment in sodium chloride ice. CRREL Research Report 345, 85 p.
- Cox, G.F.N. and W.F. Weeks. (1974) Salinity variations in ice. *Journal of Glaciology*, 13:109-120.
- Craig, P.C., W.B. Griffiths, S.R. Johnson and D.M. Schell (1984) Trophic dynamics in an Arctic lagoon. In *The Alaskan Beaufort Sea-Ecosystems and Environment* (P.W. Barnes, D.M. Schell and E. Reimnitz, Eds.), Academic Press, London, pp.347-380.
- Cragin, J.H., A.J. Gow and A. Kovacs (1986) Chemical fractionation of brine in the McMurdo Ice Shelf, Antarctica. *Journal of Glaciology*, 32(112):307-313.
- Feldman, D., J. Gagnon, R. Hofmann and J. Simpson (1986) Statview 512+, version 1.01. Abacus Concepts, Inc. Published by Brain Power, Inc.
- Glibert, P.L. and T.C. Loder (1977) Automated analysis of nutrients in seawater: A manual of techniques. Woods Hole Oceanographic Institution Technical Report 77-47.
- Gow, A.J. (1987) Crystal structure and salinity of sea ice in Hebron Fiord and vicinity, Labrador. CRREL Report 87-4, 18 p.
- Gow, A.J., S.F. Ackley, K.R. Buck and K.M. Golden (1987) Physical and structural characteristics of Weddell Sea pack ice. CRREL Report 87-14, 70 p.
- Gow, A.J. and D. Langston (1977) Growth history of lake ice in relation to its stratigraphic, crystalline and mechanical structure. CRREL Report 77-1, 24 pp.

- Gow, A.J. and W.B. Tucker (1987) Physical properties of sea ice discharged from Fram Strait. *Science*, 236:436-439.
- Gow, A.J., W.B. Tucker and W.F. Weeks (1987) Physical properties of summer sea ice in the Fram Strait, June-July 1984. CRREL Report 87-16, 81 pp.
- Horner, R. and G.C. Schrader (1982) Relative contributions of ice algae, phytoplankton, and benthic microalgae to primary production in nearshore regions of the Beaufort Sea. *Arctic*, 35:485-503.
- Hufford, G.L. (1974) Dissolved oxygen and nutrients along the north Alaskan shelf. In *Coast and Shelf of the Beaufort Sea*. (J.C. Reed and J.E. Sater, Eds.), Arctic Institute of North America, Arlington, pp. 567-588.
- Kaltenback, A. (1976) Major cations in interstitial waters of Long Island Sound. unpublished Masters thesis, University of Connecticut, pp. 16-18.
- Kim, J. (1975) Factor Analysis. In *SPSS-Statistics Package for the Social Sciences*, 2nd ed. (N.H. Nie, C.H. Hull, J.G. Jenkins, K. Steinbrenner and D. Bent, Eds.), McGraw-Hill, NY, pp. 468-514.
- Kovacs, A. and M. Mellor (1974) Sea ice morphology and ice as geological agent in the Sothern Beaufort Sea. In *The Coast and Shelf of the Beaufort Sea* (J.C. Reed and J.E. Sater, Eds.), AINA, Arlington, pp. 113-124.
- Kuznetsov, L.L. (1980) Chlorophylls and primary production associated with ice of Amur Bay, Sea of Japan. *Soviet Journal of Marine Biology*, 6:297-299.
- Lake, R.A. and E.L. Lewis (1970) Salt rejection by sea ice during growth. *Journal of Geophysical Research*, 75(3):583-597.
- Langhorne, P.J. (1983) Laboratory experiments on crystal orientation in NaCl ice. *Annals of Glaciology*, 4:163-169.
- Langhorne, P.J. and W.B. Robinson (1986) Alignment of crystals in sea ice due to fluid motion. *Cold Regions Science and Technology*, 12(2):197-214.
- Lewis and Thompson (1950) The effect of freezing on the sulfate/chlorinity ratio of sea water. *Journal of Marine Research*, 9:211-217.
- MacDonald, R.W., C.S. Wong and P.E. Erickson (1987) The distribution of nutrients in the Southeastern Beaufort Sea: Implications for water circulation and primary production. *Journal of Geophysical Research*, 92(C3):2939-2952.
- Maestrini, S.Y., M. Rochet, L. Legendre and S. Demers. (1986) Nutrient limitation of the bottom-ice microalgal biomass (southeastern Hudson Bay, Canadian Arctic) *Limnological Oceanography*, 31(5):969-982.
- Martin, S. (1979) A field study of brine drainage and oil entrapment in sea ice. *Journal of Glaciology*, 22(88):473-502.
- Maykut, G.A. (1985) An introduction to ice in the polar oceans. APL-UW 8510, University of Washington, Seattle, 107 p.
- Maykut, G.A. and N. Untersteiner (1971) Some results from a time dependent thermodynamic model of sea ice. *Journal of Geophysical Research*, 76(6):1150-1570.
- McPhee, M.G. (1980) Physical oceanography of the seasonal sea ice zone. *Cold Regions Science and Technology*, 2:93-118.
- Meese, D. A. (1985) The physical, structural and chemical characteristics of Estuarine ice in Great Bay, New Hampshire. Unpublished Master's thesis, University of New Hampshire. 113 p.
- Moore, R.M., M.G. Lowings and F.C. Tan (1983) Geochemical profiles in the Central Arctic Ocean: Their relation to freezing

and shallow circulation. *Journal of Geophysical Research*, 88(C4):2667-2674.

Norusis, M.J. (1985) *SPSS-x Advanced Statistics Guide*. McGraw-Hill, NY. pp. 125-157.

Overgaard, S., P. Wadhams and M. Lepparanta (1983) Ice properties in the Greenland and Barents Sea during summer. *Journal of Glaciology*, 29(101):142-164.

Perkin Elmer Corporation (1976) Analytical methods for atomic absorption spectrophotometry. Norwalk, Connecticut.

Reeburgh, W.S. and M. Springer-Young (1983) New measurements of sulfate and chlorinity in natural sea ice. *Journal of Geophysical Research*, 88:2959-2966.

Subba Rao D.V. Subba and T. Platt (1984) Primary production of Arctic waters. *Polar Biology*, 3:191-201.

Smith, R., E.M. Bezuidenhout and A.M van Heerden (1983) The use of interference suppressants in the direct flame atomic absorption determination of metals in water. *Water Research*, 17(11):1483-1489.

Strickland, J.D. and T.R. Parsons (1972) A practical handbook of seawater analysis. *Bulletin of Fisheries Resources Board of Canada*, No. 167, 310 pp.

Tucker, W.B., A.J. Gow and J.A. Richter (1984) On small-scale horizontal variations of salinity in first-year sea ice. *Journal of Geophysical Research*, 89(C4):6505-6514.

Tucker, W.B., A.J. Gow and W.F. Weeks (1987) Physical properties of summer sea ice in the Fram Strait. *Journal of Geophysical Research*, 92(C7):6787-6803.

Tucker, W.B., W.F. Weeks, A. Kovacs and A.J. Gow (1980) Nearshore ice motion at Prudhoe Bay, Alaska. In *Sea Ice Processes and Models* (R. S. Pritchard Ed.), University of Washington Press, Seattle, pp. 261-272.

Tucker, W.B., W.F. Weeks and M. Frank (1979) Sea ice ridging over the Alaskan continental shelf. *Journal of Geophysical Research*, 84:4885-4897.

Untersteiner, N. (1968) Natural desalination and equilibrium salinity profile of perennial sea ice. *Journal of Geophysical Research*, 73:1251-1257.

Weeks, W.F. and S.F. Ackley (1982) The growth, structure and properties of sea ice. CRREL Monograph 82-1, 130 pp.

Weeks, W.F. and A.J. Gow (1980) Crystal alignments in the fast ice of arctic Alaska. *Journal of Geophysical Research*, 84(C10):1137-1146.

Weeks, W.F. and A.J. Gow (1978) Preferred crystal orientations along the margins of the Arctic Ocean. *Journal of Geophysical Research*, 84:5105-5121.

Whitledge, T.E., S.C. Malloy, C.J. Patton and C.D. Ulirick (1981) Automated nutrient analyses in seawater. Brookhaven National Laboratory Report #51398, Upton, NY.

Wilson, A.T. and A.J. Heine (1964) The chemistry of shelf brines. *Journal of Glaciology*, 5(38):265-266.

WMO (1956) Abridged Ice Nomenclature, Executive Committee Report, vol. 8, pp. 107-116.

APPENDIX A

**Concentration of Chemical Species in Sea Ice as Reported in the
Literature**

Reference		Salinity	Cl (g/l)	SO4 (g/l)
Lewis and Thompson (1950)	Ice		6.82 o/oo	2.347
Laboratory	Water		16.8 o/oo	2.942
Bennington, K.O. (1963)			3-8 o/oo	0.3-3o/oo
Arctic				
Wilson and Heine (1964)			2.3-3.3	.221-.316
Ross Ice Shelf				
Lake and Lewis (1970)		.52-4.76		
Cambridge Bay, NWT				
Kuznetsov (1980)	Ice			
Amur Bay, Sea of Japan	Water			
Moore et al. (1983)	Surface Water			
88 40'N 139 50'W to				
89 9'N 97 7'W				
Anderson and Jones				
CESAR 86 N 110 W	First-year	.087-11.33		1.042- 8.393
Fram Strait	First-year	2.54-7.66		
	Multiyear	.113-3.75		
Addison (1977)	Lab (-30)		3.8-12 o/oo	9-.3
	Lab (-15)		.2-1.1	.01-.12
	Fort Churchill	1-4	.1-.8	
Anderson and Jones (1985)				
Barrow, Alaska--First-year		1.95-4.05	.297-.575 o/oo	
T-3--Multiyear			.09-6.98	.012- 1.28
Clarke and Ackley (1984)				
Weddell Sea				
Meese (1985)	Ice	1-14	.02-10	.006-2.98
Great Bay, NH				
Cragin et al. (1986)		.4-30	1.2-10	.002- 3.8
McMurdo Ice Shelf				

	Na o/oo	Ca o/oo	Delta Ca	K o/oo	Mg o/oo
Lewis and Thompson					
Bennington, K.O.	1-5	.03-.15		.03-.15	.15-.3
Wilson and Heine				.05-.06	
Lake and Lewis					
Kuznetsov					
Moore et al.					
Anderson and Jones					
CESAR 86 N 110 W		30-3253 um/l	-77-11		
Fram Strait			-7-(-9) -5-(-8)		
	2.5-7	.3-.1		.25-.08	.3-.8
Addison	0.004-.6	.001-.025		.001-.03	.001-.07
	.5-2	.01-.03		.02-.05	.08-.2
Anderson and Jones					
First-year					
T-3-Multiyear					
Clarke and Ackley					
Meese					
Cragin et al.	.08-11	.155-.36		.1-.37	.13-1.29

	PO4 (um/l)	SiO4 (um/l)	NO3 (um/l)	NO2 (um/l)	NH4 (um/l)	Chl-a (ug/l)	Phaeo (ug/l)
Lewis and Thompson							
Bennington, K.O.							
Wilson and Heine							
Lake and Lewis							
Kuznetsov						1.5-13.99	11.-70
						.57-7.33	41-63
Moore et al.	.8-1.25	7.5-13					
Anderson and Jones							
CESAR 86 N 110 W							
Fram Strait							
Addison							
Anderson and Jones							
First-year							
T-3-Multiyear							
Clarke and Ackley	0-1.75	1-16	0-6	0-1.4		.09-3.8 mg/m3	
Meese	0-1.93	0-14.33	0-.37		.3-2.9	0-1.8	
Cragin et al.							

	Na/Cl	SO4/Na	K/Cl	Ca/Cl	Mg/Cl	Mg/K	SO4/Cl
Lewis and Thompson							0.1412
Laboratory							0.1397
Bennington, K.O.							
Arctic							
Wilson and Heine							0.0962
Ross Ice Shelf							
Lake and Lewis							
Cambridge Bay, NWT							
Kuznetsov (1980)							
Amur Bay							
Moore et al.							
Anderson and Jones							
CESAR 86 N 110 W							
Fram Strait							
	.5-1.25	.15-1.4	.035-.018	.055-.019	.06-.1	3-(5)	
Addison	.04-.07	0-.45	0-.025	0-.02	0-.16	0-8	
	.05-.07	.01-.05	.01-.018	.008-.012	.06-.08	3.3-4.1	
Anderson and Jones							
First-year							
T-3-Multiyear							
Clarke and Ackley							
Weddell Sea							
Cragin et al.		.02-.68					

	del Na/Cl	del Ca/Cl	del K/Cl	del Mg/Cl	del SO4/Cl
Lewis and Thompson					
Bennington, K.O.	-0.05- 0.03	-.001- (-.0015)	-.0015 -.005	-.01- .01	-.05- .232
Wilson and Heine					
Lake and Lewis					
Kuznetsov					
Moore et al.					
Anderson and Jones					
CESAR 86 N 110 W					
Fram Strait					
Addison					
Anderson and Jones					
First-year					
T-3--Multiyear					
Clarke and Ackley					
Cragin et al.					

APPENDIX B

Ice and Water Data

Core FY186

Depth (cm)	Salinity (o/oo)	Cl (meq/l)	Br (meq/l)	SO ₄ (meq/l)	Na (meq/l)
10	4.0	122.39	0.19	13.75	49.89
20	4.0	111.56	0.17	11.38	49.37
30	4.8	79.13	0.12	7.49	60.86
40	5.4	67.14	0.1	6.79	68.9
50	5.0	55.95	0.08	5.81	63.03
60	4.0	62.35	0.1	6.51	43.11
70	4.5	60.88	0.1	6.43	50.55
80	4.7	55.19	0.08	5.5	40.24
90	4.6	55.98	0.09	5.94	39.28
100	4.2	48.84	0.07	5.12	52.81
110	4.3	64.58	0.1	6.77	48.55
120	4.2	27.71	0.05	3.02	52.64
130	4.4	64.94	0.1	6.81	55.38
140	3.8	61.67	0.09	6.29	46.94
150	5.5	60.12	0.1	6.24	62.12
160	7.3	103.97	0.17	10.56	93.18
FY1 water		359.44	0.54	38.25	365.14
Seawater	35	545.75	0.84	56.46	468.97

Core FY186 (cont.).

Depth (cm)	Ca (meq/l)	K (meq/l)	Mg (meq/l)	PO ₄ (uM)	SiO ₄ (uM)
10	4.28	1.97	23.6	0.1	1.57
20	3.32	1.75	21.35	0.1	2.19
30	2.64	1.13	14.98	0.07	2.74
40	2.45	0.95	13.15	0.1	3.07
50	2.03	0.66	11.04	0.12	2.48
60	2.27	1.26	12.23	0.07	1.49
70	2.16	1.31	11.88	0.11	1.75
80	2.02	1.13	10.83	0.07	1.61
90	2.41	1.28	11.18	0.08	1.48
100	2.11	1.02	9.71	0.12	1.62
110	2.62	1.31	12.69	0.1	1.55
120	1.45	0.66	5.1	0.09	1.3
130	2.5	1.27	12.72	0.11	0.96
140	2.45	1.13	12.13	0.06	0.67
150	2.6	1.3	11.6	0.19	1.34
160	3.79	1.89	19.84	1.19	2.03
FY1 water	16.37	7.08	86.87	0.72	6.42
Seawater	20.56	10.2	105.62		

Core FY186 (cont.).

Depth (cm)	NO ₃ +NO ₂ (uM)	NH ₄ (uM)	Chl-a (mg/m ³)
10	0.33	0.8	0.131
20	0.21	0.84	0.207
30	0.27	0.51	0.163
40	0.23	0.66	0.163
50	0.54	1.47	0.213
60	0.33	0.53	0.523
70	0.47	1.22	0.184
80	0.43	0.7	0.25
90	0.45	1	0.098
100	0.54	1.45	0.183
110	0.42	0.93	0.121
120	0.32	0.7	0.247
130	0.22	0.8	0.283
140	0.24	0.64	0.296
150	0.4	1.12	0.609
160	0.84	1.96	21.84
FY1 water	1.77	1.07	5.938
Seawater			

Core FY2

Depth (cm)	Salinity (o/oo)	Cl (meq/l)	Br (meq/l)	SO ₄ (meq/l)	Na (meq/l)
3	7.75	123.26	0.19	13.92	103.79
10	7.0	111.95	0.17	11.89	93.18
20	5.0	78.82	0.12	7.73	66.38
30	4.2	67.29	0.11	6.87	56.9
38	3.5	55.3	0.08	5.75	48.46
48	3.8	62.55	0.09	6.59	53.46
53	3.8	61.36	0.09	6.45	52.85
60	3.5	55.92	0.09	5.9	48.89
70	3.5	56.03	0.08	5.92	48.33
80	3.1	49.49	0.08	5.2	43.44
90	4.0	65.11	0.09	6.86	55.68
100	3.9	61.31	0.09	6.5	53.16
113	4.1	65.28	0.1	6.8	56.16
122	3.8	61.98	0.1	6.55	53.59
132	4.2	66.89	0.1	6.93	57.07
142	6.4	102.31	0.15	10.32	85.7
FY2 water	35	244.8	0.38	43.95	365.14
Seawater	35	545.75	0.84	56.46	468.97

Core FY286 (cont.).

Depth (cm)	Ca (meq/l)	K (meq/l)	Mg (meq/l)	PO ₄ (uM)	SiO ₄ (uM)
3	4.28	2.38	23.31	0.18	2.11
10	3.74	2.17	21.06	0.15	3.17
20	2.64	1.56	15.12	0.13	2.32
30	2.24	1.34	12.93	0.09	1.17
38	1.89	1.06	10.9	0.09	0.82
48	2.19	1.18	12.3	0.09	1.47
53	2.14	1.2	11.88	0.07	1.17
60	1.89	1.18	10.97	0.06	0.76
70	1.84	1.16	10.83	0.07	1.15
80	1.73	1.04	9.78	0.06	0.63
90	2.24	1.22	12.58	0.09	1.45
100	1.99	1.3	11.95	0.04	0.55
113	2.14	1.23	12.58	0.05	0.83
122	2.14	1.	12.09	0.06	0.75
132	2.19	1.44	12.79	0.11	0.91
142	3.36	1.79	19.14	1.01	2.29
FY2 water	8.93	5.32	46.64	0.97	9.27
Seawater	20.56	10.2	105.62		

Core FY2 (cont.).

Depth (cm)	NO ₂ +NO ₃ (uM)	NH ₄ (uM)
3	0.72	0.87
10	0.88	0.7
20	0.8	1.04
30	0.4	0.61
38	0.29	0.69
48	0.31	0.62
53	0.35	0.78
60	0.2	0.49
70	0.34	0.79
80	0.28	0.68
90	0.41	0.66
100	0.33	0.33
113	0.34	0.66
122	0.23	0.35
132	0.35	0.71
142	0.58	1.56
FY2 water	0.13	2.11
Seawater		

Core SI86

Depth (cm)	Salinity (o/oo)	Cl (meq/l)	Br (meq/l)	SO ₄ (meq/l)	Na (meq/l)
10	8	128.76	0.21	14.78	101.88
20	7.5	125.94	0.19	11.7	94.09
30	6.0	102.28	0.14	5.02	68.82
40	4.9	81.39	0.13	4.91	55.33
50	4.7	78.11	0.12	6.02	51.9
60	4.6	73.29	0.11	9.26	55.33
70	4.0	60.8	0.09	8.74	46.55
80	3.6	58.32	0.09	6.1	39.32
90	4.5	73.01	0.11	7.29	54.07
100	3.5	56.23	0.08	6.52	40.89
110	3.7	60.04	0.09	6.23	43.98
120	4.2	68.39	0.12	7.06	48.68
130	4.4	66.04	0.11	6.95	48.68
140	4.0	64.83	0.11	6.75	45.81
150	3.7	59.28	0.1	6.18	42.24
160	3.7	60.71	0.09	6.33	50.68
170	3.8	62.6	0.09	6.48	49.68
180	3.4	53.97	0.08	5.6	42.2
190	3.4	53.89	0.08	5.6	42.2
200	5.2	82.94	0.13	8.43	64.77
SI86 water	32	359.44	0.54	38.25	
Seawater	35	545.75	0.84	56.46	468.97

Core SI86 (cont.).

Depth (cm)	Ca (meq/l)	K (meq/l)	Mg (meq/l)	PO ₄ (uM)	SiO ₄ (uM)
10	4.39	1.63	25.43	0.11	2.59
20	4.54	1.55	22.64	0.12	1.31
30	3.99	1.17	19.34	0.12	2.1
40	3.44	1.03	15.62	0.09	1.59
50	2.29	1.0	14.91	0.09	1.55
60	2.74	1.06	13.99	0.1	1.29
70	2.24	0.99	11.74	0.17	1.63
80	2.13	1.07	11.32	0.22	2.2
90	2.59	1.23	13.92	0.38	2.65
100	2.26	0.93	10.97	0.27	2.73
110	2.24	0.96	11.6	0.24	1.9
120	2.83	1.05	13.5	0.09	0.96
130	2.64	1.13	12.35	0.13	1.94
140	2.34	0.99	12.79	0.12	0.96
150	2.29	0.85	11.6	0.09	1.25
160	2.44	0.84	11.88	0.12	2.01
170	2.49	0.93	12.3	0.12	2.33
180	2.04	0.66	10.13	0.14	1.92
190	1.89	0.65	10.69	0.1	1.67
200	2.88	1.56	15.76	0.1	2.52
SI86 water	12.72	4.35	67.62		
Seawater	20.56	10.2	105.62		

Core SI86 (cont.).

Depth (cm)	NO ₃ +NO ₂ (μM)	NH ₄ (μM)
10	0.48	1.21
20	0.28	2.66
30	0.5	1.14
40	0.3	0.59
50	0.33	0.78
60	0.24	0.83
70	0.42	1.01
80	0.52	1.62
90	0.27	0.99
100	0.47	1.06
110	0.45	0.97
120	0.29	0.71
130	0.57	0.77
140	0.39	0.81
150	0.52	0.63
160	0.89	0.86
170	1.13	0.8
180	1.06	0.86
190	0.89	0.66
200	1.36	1.22
SI86 water		
Seawater		

Core A87

Depth (cm)	Salinity (o/oo)	Cl (meq/l)	Br (meq/l)	SO ₄ (meq/l)	Na (meq/l)
4	10.2	158.63	0.25	18.87	139.9
10	5.7	88.13	0.14	12.56	
20	2.6	42.02	0.06	4.68	76.74
30	3.7	61.19	0.09	4.66	36.74
40	3.8	62.89	0.1	5.24	48.95
50	4.2	71.06	0.11	5.57	55.4
60	4.6	78.4	0.11	7.26	62.11
70	4.2	66.83	0.1	6.2	58.86
80	5.0	88.27	0.13	8.3	66.96
90	5.7	85.45	0.13	10.94	72.12
100	4.8	76.99	0.12	8.57	68.58
110	6.3	95.6	0.15	10.8	87.2
120	6.5	104.06	0.16	11.65	91.89
130	6.9	112.24	0.17	11.86	97.26
140	7.0	104.9	0.16	12.38	96.97
150	8.4	129.44	0.19	13.35	109.52
160	10.5	169.2	0.27	17.51	152.62
170	18.0	279.46	0.46	30.47	249.84
A87 water	56	978.54	1.51	101.09	852.51
Seawater	35	545.75	0.84	56.41	468.97

Core A87 (cont.).

Depth (cm)	Ca (meq/l)	K (meq/l)	Mg (meq/l)	PO ₄ (uM)	SiO ₄ (uM)
4	5.54	2.89	30.65		
10	3.52	1.46	16.9	0.196	3.219
20	1.75	.73	8.16	0.169	1.665
30	2.2	1.02	11.16	0.192	1.887
40	2.18	1.14	12.03	0.199	2.176
50	3.03	1.46	13.38	0.181	2.553
60	2.86	1.25	13.57	0.177	2.575
70	2.36	1.15	12.7	0.193	2.486
80	3.35	1.43	16.21	0.215	2.819
90	3.52	1.54	16.08	0.171	2.753
100	3.19	1.45	15.22	0.305	2.531
110	3.15	1.72	18.64	0.337	2.775
120	3.68	1.86	19.97	0.308	2.842
130	4.03	1.98	21.48	0.476	3.752
140	4.49	2.05	21.55	0.431	3.885
150	4.38	2.17	23.71	0.311	3.974
160	5.94	3.24	32.55	0.719	6.327
170	11.73	5.25	53.63	1.387	10.2
A87 water	19.31	18.31	164.44		
Seawater	20.56	10.2	105.62		

Core A87 (cont.).

Depth (cm)	NO ₃ (uM)	NO ₂ (uM)	NH ₄ (uM)
4			
10	0.417	0.082	0.586
20	0.296	0.04	0.398
30	0.541	0.059	0.674
40	0.771	0.063	0.903
50	0.72	0.099	1.01
60	0.707	0.097	1.071
70	0.704	0.085	1.001
80	0.993	0.089	0.91
90	0.943	0.093	0.963
100	1.505	0.104	0.955
110	1.929	0.077	0.969
120	2.091	0.06	0.658
130	2.758	0.069	0.924
140	2.159	0.123	0.944
150	1.432	0.086	0.951
160	4.272	0.17	2.386
170	3.6	0.166	3.95
A87 water			
Seawater			

Core C87

Depth (cm)	Temp (°C)	Salinity (o/oo)	Cl (meq/l)	Br (meq/l)	SO ₄ (meq/l)
1.5	-11.2	9.0	129.16	0.19	26.44
4.5	-11.2	4.4	64.16	0.1	11.76
6.5	-11.2	4.8	75.29	0.12	6.66
10	-11.2	4.6	72.47	0.11	5.33
20	-11.3	5.0	77.13	0.12	6.35
30	-11.2	5.4	82.06	0.13	9.45
40	-10.9	5.5	87.7	0.12	10.7
50	-10.6	5.5	82.63	0.13	11.14
60	-10.1	5.3	76.99	0.12	12.08
70	-9.7	4.8	71.06	0.11	10.04
80	-9.4	4.5	69.37	0.11	6.64
90	-8.8	5.1	82.34	0.13	8.22
100	-8	5.0	75.58	0.12	10.51
110	-7.5	4.6	69.65	0.11	9.31
120	-6.7	5.1	79.81	0.12	8.89
130	-6	5.3	82.63	0.13	9.08
140	-5	4.6	72.47	0.11	7.85
150	-4.4	4.2	67.54	0.11	7.35
160	-3.6	4.8	75.58	0.12	8.39
169	-1.7	9.5	147.49	0.23	15.32
C87 water		31.2	470.94	0.71	48.51
Seawater		35	545.75	0.84	56.46

Core C87 (cont.).

Depth (cm)	Na (meq/l)	Ca (meq/l)	K (meq/l)	Mg (meq/l)	PO ₄ (uM)
1.5	123.76	5.19	2.54	24.69	0.604
4.5	59.6	2.92	1.16	12.66	0.244
6.5	60.12	3.35	1.41	14.34	0.262
10	56.38	2.86	1.23	13.85	0.236
20	63.42	3.03	1.43	14.79	0.233
30	67.51	3.19	1.49	15.59	0.22
40	69.03	3.35	1.43	16.25	0.252
50	75.86	3.35	1.45	15.36	0.28
60	67.38	3.03	1.54	15.02	0.235
70	61.12	2.86	1.35	13.8	0.232
80	57.2	2.7	1.33	12.83	0.209
90	67.64	3.35	1.37	15.74	0.227
100	65.29	2.86	1.29	14.39	0.139
110	60.25	2.7	1.25	13.38	0.203
120	66.64	3.03	1.45	15.17	0.442
130	75.52	3.35	1.54	15.61	0.284
140	59.42	2.7	1.35	13.65	0.317
150	56.81	2.67	1.24	13.19	0.277
160	62.47	3.03	1.54	14.42	0.228
169	133.63	6.04	2.65	28.52	0.964
C87 water	402.51	18.66	8.28	85.71	
Seawater	468.97	20.56	10.2	105.62	

Core C87 (cont.).

Depth (cm)	SiO ₄ (uM)	NO ₃ (uM)	NO ₂ (uM)	NH ₄ (uM)
1.5	1.73	3.94	0.26	2.539
4.5	0.999	1.26	0.116	1.378
6.5	1.01	1.15	0.111	1.352
10	0.836	1.08	0.118	2.104
20	0.915	0.534	0.067	0.823
30	1.064	0.494	0.049	0.777
40	1.373	0.419	0.048	0.848
50	1.636	0.543	0.065	1.079
60	1.578	0.52	0.066	0.924
70	1.542	0.554	0.065	0.911
80	1.599	0.551	0.064	0.848
90	1.862	0.732	0.061	0.659
100	3.114	1.818	0.148	0.118
110	1.469	0.269	0.046	0.391
120	1.364	1.153	0.045	1.42
130	0.73	0.57	0.046	0.895
140	0.189	0.697	0.078	1.226
150	0.061	0.532	0.058	1.449
160	0	0.301	0.051	0.781
169	1.186	4.944	0.091	0.869
C87 water				
Seawater				

Core D87

Depth (cm)	Temp (°C)	Salinity (o/oo)	Cl (meq/l)	Br (meq/l)	SO ₄ (meq/l)
0	-11.1	6.4	98.42	0.15	14.74
2.5	-11.1	6.4	98.42	0.15	14.74
5	-11.1	5.6	87.7	0.14	12.47
6.5	-11.1	6.5	94.75	0.15	13.47
8	-11.1	5.5	85.73	0.13	10.6
10	-11.1	5.6	90.52	0.14	10.08
14.5	-11.1	4.4	67.96	0.11	6.35
16.5	-11.0	6.5	107.44	0.16	13.22
18	-11.0	5.5	87.98	0.13	9.62
23	-10.8	5.9	87.7	0.13	9.2
30	-10.7	4.9	79.95	0.12	7.87
40	-10.1	4.6	75.29	0.11	7.47
50	-9.8	5.4	86.86	0.13	7.33
60	-9.4	5.0	76.42	0.12	7.87
70	-9.2	5.2	81.5	0.12	8.89
80	-8.9	4.8	73.04	0.11	11.35
90	-8.5	4.2	63.17	0.1	8.35
100	-8.0	4.1	64.58	0.1	7.45
110	-7.5	3.7	61.19	0.09	6.6
120	-6.3	3.4	52.45	0.08	5.95
130	-5.6	3.4	54.99	0.08	5.77
140	-4.8	3.3	52.45	0.08	5.54
150	-3.9	4.3	65.71	0.1	7.04
160	-2.9	4.5	74.45	0.11	7.83
170	-2.3	4.4	64.58	0.1	6.81
177	-1.8	9.5	150.31	0.25	15.91
D87 water		28.5	420.18	0.64	43.72
Seawater		35	545.75	0.84	56.46

Core D87 (cont.).

Depth (cm)	Na (meq/l)	Ca (meq/l)	K (meq/l)	Mg (meq/l)	PO ₄ (μM)
0	92.61	3.5	1.74	18.46	0.085
2.5	92.61	3.5	1.74	18.46	0.085
5	75.82	3.35	1.52	16.2	0.028
6.5	89.52	3.42	1.72	17.97	0.021
8	75.86	3.42	1.51	16.05	0.021
10	74.82	3.35	1.56	16.78	0.025
14.5	57.64	3.14	1.22	13.43	0.028
16.5	100.92	4.36	1.82	20.13	0.041
18	73.43	3.35	1.49	16.4	0.023
23	79.	3.45	1.49	16.88	0.023
30	64.95	3.1	1.35	14.6	0.069
40	61.47	3.19	1.35	14.08	0.081
50	73.34	3.74	1.53	16.42	0.184
60	66.38	2.86	1.33	14.84	0.121
70	69.03	3.19	1.41	15.62	0.191
80	65.29	2.93	1.35	14.03	0.066
90	58.03	2.45	1.08	11.98	0.048
100	58.99	2.36	1.1	12.18	0.069
110	51.77	2.42	1.09	11.57	0.044
120	46.81	1.83	.93	9.94	0.178
130	48.02	2.01	.97	10.41	0.169
140	45.94	2.08	.89	10.04	0.179
150	54.81	2.76	1.11	12.54	0.268
160	60.86	2.86	1.33	13.92	0.269
170	57.03	2.52	1.18	12.09	0.238
177	131.94	6.04	2.73	28.36	0.34
D87 water	363.66	19.22	7.66	79.97	
Seawater	468.97	20.56	10.2	105.62	

Core D87 (cont.).

Depth (cm)	SiO ₄ (uM)	NO ₃ (uM)	NO ₂ (uM)	NH ₄ (uM)
0	2.05	3.07	0.04	3.83
2.5	2.05	3.07	0.04	3.83
5	1.626	1.72	0.11	1.72
6.5	1.47	1.72	0.13	2.07
8	1.25	1.06	0.08	1.28
10	1.22	0.91	0.07	1.14
14.5	0.91	0.62	0.07	0.77
16.5	1.2	0.66	0.07	0.81
18	0.87	0.62	0.07	0.92
23	0.89	0.87	0.12	1.34
30	1.01	0.75	0.09	1.07
40	1.38	0.73	0.06	0.89
50	2.25	1.05	0.05	1.07
60	1.8	0.63	0.06	1.3
70	2.52	0.64	0.07	1.25
80	1.99	0.5	0.07	1.18
90	2.99	0.96	0.12	1.64
100	1.77	1.03	0.07	1.0
110	1.75	1.21	0.08	1.06
120	1.58	1.02	0.07	1.16
130	1.57	0.74	0.05	0.47
140	1.55	0.87	0.08	0.82
150	1.79	1.2	0.06	1.14
160	1.74	1.21	0.07	1.21
170	1.3	0.78	0.06	0.99
177	2.4	1.08	0.08	2.34
D87 water				
Seawater				

Core H87

Depth (cm)	Temp (°C)	Salinity (o/oo)	Cl (meq/l)	Br (meq/l)	SO ₄ (meq/l)
0	-12.8	10.7	166.46	0.25	30.08
7.5	-12.8	10.7	166.46	0.25	30.08
10	-12.8	6	100.96	0.15	15.64
20	-12.8	3.3	53.58	0.08	6.1
30	-12.5	3.3	57.25	0.09	4.25
40	-12.0	4.2	66.55	0.1	4.04
50	-11.3	3.6	61.9	0.09	3.89
60	-10.8	4.0	69.8	0.1	4.68
70	-10.2	4.9	84.04	0.12	6.45
80	-9.7	5.3	90.52	0.13	7.27
90	-9.2	6.0	100.67	0.15	9.31
100	-8.6	5.8	95.6	0.14	14.34
110	-8.1	5.0	82.63	0.12	8.77
120	-7.4	7.0	109.13	0.16	14.49
130	-6.5	8.5	126.2	0.2	19.86
140	-5.9	7.3	118.44	0.18	13.03
150	-5.3	8.0	135.22	0.21	14.53
160	-4.5	7.5	122.95	0.18	12.7
170	-3.6	7.5	122.39	0.18	12.68
180	-2.8	12.3	203.89	0.32	21.03
Seawater		35	545.75	0.84	56.46

Core H87 (cont.).

Depth (cm)	Na (meq/l)	Ca (meq/l)	K (meq/l)	Mg (meq/l)	PO ₄ (uM)
0	151.38	7.02	2.9	31.75	0.4
7.5	151.38	7.02	2.9	31.75	0.4
10	92.7	3.15	1.72	18.33	0.303
20	48.24	1.83	0.93	10.19	0.312
30	46.89	2.07	0.97	10.65	0.17
40	54.64	2.33	1.09	12.06	0.156
50	50.59	2.3	1.08	11.54	0.151
60	57.38	2.45	1.23	13.08	0.176
70	63.47	3.19	1.5	15.37	0.183
80	72.12	3.35	1.5	16.3	0.204
90	87.44	3.33	1.74	19.12	0.268
100	81.26	3.85	1.63	18.02	0.307
110	68.3	3.19	1.39	15.34	0.194
120	98.96	3.68	1.86	20.75	0.318
130	115.75	5.07	2.19	23.24	0.316
140	108.88	4.36	2.05	22.45	0.251
150	116.8	4.84	2.36	25.5	0.247
160	104.88	4.03	2.12	22.19	0.23
170	107.66	4.2	2.12	22.21	0.311
180	176.48	6.99	3.57	38.14	0.759
Seawater	468.97	20.56	10.2	105.62	

Core H87 (cont.).

Depth (cm)	SiO ₄ (uM)	NO ₃ (uM)	NO ₂ (uM)	NH ₄ (uM)
0	4.44	1.82	0.098	4.02
7.5	4.44	1.82	0.098	4.02
10	2.66	1.06	0.07	2.91
20	1.37	0.64	0.03	2.03
30	1.51	0.44	0.03	1.8
40	1.91	0.86	0.05	2.27
50	1.75	0.54	0.04	1.74
60	2.23	0.83	0.05	2.01
70	2.67	1.01	0.05	1.69
80	3.09	1.15	0.07	1.72
90	3.56	1.34	0.08	1.81
100	3.33	1.6	0.09	1.92
110	2.73	1.58	0.06	1.44
120	3.33	2.09	0.06	2.67
130	2.85	1.12	0.06	1.75
140	1.42	0.76	0.06	1.65
150	0.84	0.87	0.08	1.7
160	0.5	0.58	0.06	1.64
170	0.41	0.81	0.06	2.14
180	2.38	4.6	0.13	2.23
Seawater				

Core 087

Depth (cm)	Temp (°C)	Salinity (o/oo)	Cl (meq/l)	Br (meq/l)	SO ₄ (meq/l)
0	-7.5	14.2	231.8	0.35	28.5
4	-7.5	14.2	231.8	0.35	28.5
10	-7.4	13.0	214.32	0.32	21.84
14	-7.3	11.3	186.97	0.3	19.16
24	-6.8	7.6	124.36	0.19	15.27
34	-5.9	5.4	91.65	0.14	9.86
44	-5.2	5.0	81.5	0.12	9.26
54	-4.3	4.8	80.37	0.11	9.05
64	-3.6	4.2	67.12	0.11	7.7
74	-2.6	5.5	91.65	0.13	9.9
84	-1.7	5.4	88.83	0.14	9.32
89		9.3	148.61	0.22	15.87
O87 water		29.5	513.86	0.8	53.12
Seawater		35	545.75	0.84	56.41

Core 087 (cont.).

Depth (cm)	Na (meq/l)	Ca (meq/l)	K (meq/l)	Mg (meq/l)	PO ₄ (μ M)
0	204.19	7.68	3.96	43.31	0.651
4	204.19	7.68	3.96	43.31	0.651
10	180.7	7.68	3.66	40.47	0.456
14	167.69	6.29	.78	36.05	0.39
24	113.23	4.38	2.14	23.45	0.296
34	85.74	3.52	1.61	17.54	0.249
44	73.21	3.19	1.37	15.22	0.293
54	72.38	3.03	1.37	14.81	0.218
64	64.03	2.45	1.17	13.24	0.191
74	81.26	1.57	1.57	17.49	0.203
84	79.56	3.52	1.48	16.98	0.153
89	132.76	2.63	2.51	28.22	0.986
O87 water	432.3	18.16	8.87	92.05	
Seawater	468.97	20.56	10.2	105.62	

Core O87 (cont.).

Depth (cm)	SiO ₄ (μM)	NO ₃ (μM)	NO ₂ (μM)	NH ₄ (μM)
0	4.61	3.614	0.068	2.972
4	4.61	3.614	0.068	2.972
10	3.964	1.984	0.053	0.489
14	3.558	1.55	0.046	0.568
24	2.28	0.948	0.043	0.703
34	1.656	0.573	0.038	0.621
44	1.271	0.445	0.031	1.06
54	1.018	0.237	0.021	1.093
64	0.808	0.125	0.018	0.667
74	0.75	0.093	0.017	0.571
84	0.54	0.12	0.018	0.637
89	1.486	0.317	0.053	1.061
O87 water				
Seawater				

Core SI87

Depth (cm)	Temp (°C)	Salinity (o/oo)	Cl (meq/l)	Br (meq/l)	SO ₄ (meq/l)
10	-10.3	7.75	102.08	0.16	12.3
20	-10.1	5.4	82.63	0.12	7.04
30	-9.9	5.1	76.14	0.12	7.41
40	-9.4	5.2	80.93	0.12	8.18
50	-8.9	5.3	82.91	0.12	9.04
60	-8.4	5.2	76.14	0.11	7.39
70	-7.6	5.2	78.82	0.12	8.12
80	-7.1	5.5	80.65	0.12	9.33
90	-6.4	5.3	78.54	0.12	11.31
100	-6.1	5.3	75.58	0.11	9.89
110	-5.6	4.6	67.12	0.1	8.49
120	-4.8	4.7	71.06	0.11	7.81
130	-5.0	5.4	84.32	0.12	8.52
140	-4.4	5.2	81.22	0.12	8.33
150	-3.5	5.5	85.31	0.13	8.87
160	-3.2	6.5	99.26	0.15	10.45
170	-2.6	6.1	102.08	0.15	10.53
180	-1.8	9.0	137.62	0.21	14.37
SI87 water		30	513.24	0.79	52.26
Seawater		35	545.75	0.84	56.46

Core SI87 (cont.).

Depth (cm)	Na (meq/l)	Ca (meq/l)	K (meq/l)	Mg (meq/l)	PO ₄ (uM)
10	91.31	4.01	1.79	19.13	0.25
20	69.95	3.03	1.35	15.22	0.16
30	65.6	2.86	1.3	14.57	0.18
40	67.21	3.03	1.35	14.94	0.21
50	76.52	3.19	1.41	15.74	0.29
60	65.6	2.86	1.28	14.27	0.34
70	67.77	2.95	1.34	14.75	0.34
80	75.43	3.03	1.39	15.37	0.38
90	67.64	3.1	1.41	14.87	0.27
100	69.95	2.86	1.37	14.6	0.37
110	61.86	2.7	1.26	12.86	0.39
120	65.34	2.7	1.35	13.75	0.32
130	75.43	3.19	1.5	15.57	1.33
140	70.21	3.19	1.5	15.22	0.518
150	73.78	3.35	1.57	16.14	0.486
160	86.74	4.01	1.74	18.5	0.73
170	88.48	4.18	1.83	19.08	0.95
180	118.62	5.71	2.51	26.11	1.73
SI87 water	414.82	19.96	8.98	94.76	
Seawater	468.97	20.56	10.2	105.62	

Core SI87 (cont.).

Depth (cm)	SiO ₄ (μ M)	NO ₃ (μ M)	NO ₂ (μ M)	NH ₄ (μ M)	Chl-a (mg/m ³)
10	1.87	1.61	0.11	0.71	-0.1
20	1.62	1.2	0.1	0.56	-0.6
30	1.68	1.1	0.11	0.66	0.2
40	1.88	1.03	0.11	0.54	-1.1
50	1.97	1.17	0.11	0.49	-0.2
60	1.94	1.51	0.11	0.55	0.3
70	2.11	1.31	0.11	0.51	-0.2
80	2.18	1.38	0.11	0.57	0.1
90	2.2	1.91	0.16	1.8	-0.2
100	2.03	1.42	0.08	0.43	-0.3
110	1.64	1.1	0.07	0.32	-0.3
120	1.61	0.66	0.06	0.26	0.7
130	1.51	3.12	0.1	0.88	-0.4
140	1.02	1.1	0.08	0.37	0.3
150	1.04	1.1	0.08	0.54	2.1
160	2.13	1.48	0.08	0.46	57.5
170	1.69	1.99	0.13	0.8	1.3
180	1.69	1.94	0.1	0.85	73.3
SI87 water					16.4
Seawater					

Core WD87

Depth (cm)	Salinity (o/oo)	Cl (meq/l)	Br (meq/l)	SO ₄ (meq/l)	Na (meq/l)
2	14.7	204.31	0.31	22.9	161.6
4.5	7.75	123.52	0.19	14.32	106.62
5.5	7.5	104.06	0.16	16.36	95.13
8	6.7	96.44	0.15	18.76	90.96
9	5.25	77.41	0.12	13.22	70.47
11	3.6	56.12	0.09	6.83	48.42
12.5	4.4	67.96	0.1	5.64	57.25
16.0	3.2	49.35	0.07	4.48	41.33
17.5	4.7	75.86	0.11	8.81	63.99
20	3.8	60.07	0.09	6.52	51.03
21	4.2	64.58	0.1	6.89	56.9
23.5	3.9	57.53	0.09	6.2	50.16
25	4.6	73.04	0.12	7.87	58.9
35	3.3	51.32	0.08	4.85	42.93
45	3.4	54.14	0.08	4.87	44.85
55	4.2	65.14	0.11	6.16	56.16
65	4.2	65.71	0.1	6.39	53.07
75	4.2	61.76	0.1	7.62	55.55
85	4.3	63.45	0.1	7.45	57.2
95	3.9	58.09	0.09	7.04	53.11
105	3.4	52.45	0.08	6.1	46.85
115	3.7	57.81	0.09	6.87	52.42
125	4.6	63.45	0.1	7.72	56.81
135	3.8	59.22	0.09	7.25	55.03
145	4.1	60.91	0.1	7.41	56.64
155	5.7	89.96	0.14	9.2	78.08
165	7.4	116.18	0.18	12.01	104.97
WD87 Water	30.2	525.93	0.78	52.15	426.78
Seawater	35	545.75	0.84	56.46	468.97

Core WD87 (cont.).

Depth (cm)	Ca (meq/l)	K (meq/l)	Mg (meq/l)	PO ₄ (uM)	SiO ₄ (uM)
2	7.83	1.85	38.37	0.11	3.39
4.5	4.26	1.12	22.58	0.03	2.56
5.5	3.52	1.9	19.08		
8	3.52	1.72	18.37	0.16	2.39
9	2.95	1.4	15.01	0.17	2.19
11	2.08	0.96	10.21	0.17	1.72
12.5	2.67	1.19	12.68	0.16	2.07
16	2.0	0.84	9.24	0.15	1.72
17.5	3.35	1.37	14.34	0.19	2.35
20	2.25	1.03	11.17	0.21	1.97
21	2.75	1.15	12.38	0.19	2.1
23.5	2.5	1.0	10.75	0.25	1.93
25	3.52	1.35	14.02	0	2.2
35	2.33	0.92	9.69	0.13	1.58
45	2.08	0.96	10.03	0.09	1.66
55	2.42	1.15	12.53	0.12	2.09
65	2.25	1.08	11.34	0.11	1.91
75	2.33	1.09	11.4	0.12	1.99
85	2.42	1.08	11.58	0.12	2.02
95	2.17	1.04	10.86	0.14	1.92
105	2.0	0.94	9.73	0.1	1.52
115	2.17	0.96	10.58	0.03	1.45
125	2.54	1.19	12.56	0.09	1.47
135	2.17	0.99	10.87	0.09	1.2
145	2.25	1.1	11.32	0.09	0.92
155	3.35	1.58	17.21	0.18	0.92
165	4.67	2.16	21.66	0.42	2.0
WD87 Water	19.96	9.38	95.59		
Seawater	20.56	10.2	105.62		

Core WD87 (cont.).

Depth (cm)	NO ₃ (μ M)	NO ₂ (μ M)	NH ₄ (μ M)
2	8.38	0.15	1.48
4.5	4.81	0.13	1.31
5.5	4.2	0.2	
8	4.15	0.12	1.85
9	3.34	0.18	2.34
11	2.32	0.12	2.22
12.5	1.8	0.12	2.02
16	1.39	0.12	1.78
17.5	1.74	0.15	2.28
20	1.61	0.14	2.22
21	2.31	0.12	2.78
23.5	2.07	0.08	2.47
25	2.5	0.12	2.79
35	1.46	0.04	1.65
45	1.17	0.08	1.29
55	1.38	0.09	1.3
65	1.41	0.09	1.24
75	1.73	0.1	1.56
85	1.61	0.08	1.23
95	1.78	0.07	1.19
105	1.56	0.06	0.94
115	2.08	0.09	1.21
125	1.16	0.06	0.77
135	0.82	0.05	0.68
145	0.94	0.06	0.99
155	0.99	0.12	1.47
165	2.18	0.06	1.27
WD87 Water			
Seawater			

MULTIYEAR ICE
Core F1SA86

Depth (cm)	Salinity (o/oo)	Cl (meq/l)	Br (meq/l)	SO ₄ (meq/l)	Na (meq/l)
0	3.3	53.1	0.08	4.27	42.67
7.5	3.3	53.1	0.08	4.27	42.67
14	0.5	7.9	0.01	0.82	6.53
15	0.2	2.93	0.01	0.32	2.3
25	2.4	38.75	0.06	4.18	31.62
35	2.6	41.99	0.06	4.08	33.45
45	3.0	46.95	0.08	5.0	38.45
58	3.7	59.61	0.09	5.93	47.72
61	3.6	57.27	0.09	5.87	46.85
71	3.0	47.26	0.08	4.66	38.15
81	3.0	48.56	0.08	4.75	38.85
91	3.0	46.95	0.07	4.62	38.44
95	2.8	45.04	0.07	4.33	39.19
110	4.7	71.26	0.11	14.26	65.73
120	4.2	66.61	0.11	7.52	55.2
130	4.3	67.57	0.11	7.0	55.11
140	3.4	55.22	0.08	5.66	42.93
150	3.5	58.26	0.09	5.58	45.2
160	3.8	62.6	0.1	6.52	49.42
170	3.4	53.55	0.08	6.2	43.89
183.5	1.9	30.06	0.05	2.83	24.8
190	1.3	20.08	0.03	2.0	49.33
200	1.5	17.15	0.03	1.75	14.7
207	0.9	14.97	0.02	1.54	12.31
210.5	0.8	13.48	0.02	1.38	11.44
220	0.5	8.97	0.01	0.94	7.44
230	0.4	7.36	0.01	0.77	6.13
240	0.5	8.8	0.01	0.91	7.18
250	3.0	50.31	0.08	7.81	38.19
260	5.1	81.89	0.12	10.47	68.64
270	6.0	85.31	0.13	23.59	83.78
280	1.3	21.63	0.03	2.08	17.39
290	1.5	23.97	0.03	2.41	19.62
300	1.3	21.07	0.03	2.14	17.05
310	0.6	9.33	0.01	0.96	7.79
320	1.1	17.31	0.03	1.75	14.05
330	3.4	55.47	0.09	5.68	43.89
340	4.0	64.27	0.11	6.93	52.33
350	5.6	93.4	0.15	9.35	74.17
360	8.2	134.85	0.21	14.91	108.01
370	0.3	5.19	0.01	0.58	4.61
380	0.3	5.3	0.01	0.6	4.83
390	0.4	6.74	0.01	0.77	5.92
400	0.8	13.45	0.02	1.52	11.31
410	1.4	23.83	0.03	2.56	20.27
420	0.1	1.89		0.2	1.58
430	0.6	9.98	0.02	1.13	8.44
440	0.4	6.12	0.01	0.72	5.44
450	0.6	10.58	0.02	1.11	8.79

Core F1SA86 (cont.).

Depth (cm)	Ca (meq/l)	K (meq/l)	Mg (meq/l)	PO ₄ (uM)	SiO ₄ (uM)
0	1.75	1.03	10.65	0.04	1.09
7.5	1.75	1.03	10.65	0.04	1.09
14	0.37	0.23	1.57	0.02	0.22
15	0.1	0.09		0.01	0.13
25	1.49	0.9	7.66	0.05	0.99
35	1.34	0.91	8.02	0.04	0.82
45	1.69	0.91	9.17	0.07	1.57
58	1.86	1.2	11.29	0.13	1.71
61	1.83	1.49	11.01	0.12	2.08
71	1.67	1.	9.06	0.09	1.47
81	1.78	0.94	9.21	0.1	1.75
91	1.7	1.01	9.03	0.09	1.6
95	1.75	1.05	9.03	0.1	1.58
110	2.47	1.7	13.62	0.12	2.23
120	2.06	1.68	12.62	0.09	1.51
130	2.3	1.64	13.19	0.13	1.93
140	1.74	1.61	10.86	0.08	2.7
150	1.99	1.46	11.29	0.06	1.02
160	2.08	1.39	12.15	0.11	1.97
170	1.95	1.48	10.29	0.09	1.81
183.5	1.16	0.77	5.9	0.08	1.55
190	1.68	0.43	3.76	0.06	1.27
200	0.69	0.53	3.19	0.06	1.39
207	0.55	0.33	2.89	0.06	0.97
210.5	0.54	0.32	2.59	0.04	0.81
220	0.36	0.26	1.73	0.04	0.59
230	0.32	0.23	1.38	0.01	0.3
240	0.37	0.23	1.67	0.02	0.32
250	1.9	0.95	12.71	0.07	1.41
260	2.9	1.83	16.18	0.11	1.66
270	2.78	1.84	16.14	0.14	1.76
280	0.6	0.41	3.31	0.08	0.74
290	0.85	0.61	4.65	0.05	0.83
300	0.73	0.44	4.13	0.05	1.13
310	0.4	0.23	1.82	0.02	0.4
320	0.59	0.34	3.34	0.03	0.74
330	2.0	1.49	9.65	0.12	2.25
340	2.41	1.52	10.64	0.14	2.57
350	3.17	1.93	17.26	0.2	3.58
360	4.48	2.55	25.16	0.11	4.94
370		0.18	0.92	0.03	0.35
380	0.26	0.2	0.91	0.03	0.4
390	0.27	0.22	1.22	0.03	0.36
400	0.46	0.33	2.53	0.03	0.57
410	0.75	0.5	4.66	0.07	0.81
420	0.06	0.09	0.33	0.02	0.14
430	0.39	0.27	1.9	0.04	0.32
440	0.28	0.18	1.09	0.03	0.23
450	0.37	0.27	1.97	0.04	0.26

Core F1SA86 (cont.).

Depth (cm)	NO ₃ +NO ₂ (μM)	NH ₄ (μM)
0	0.7	1.08
7.5	0.7	1.08
14	0.19	0.24
15	0.2	0.33
25	0.16	0.4
35	0.16	0.31
45	0.23	0.3
58	0.36	0.39
61	0.36	0.38
71	0.28	0.42
81	0.24	0.35
91	0.22	0.27
95	0.32	0.53
110	0.39	0.7
120	0.24	0.56
130	0.3	0.34
140	0.27	0.27
150	0.2	0.58
160	0.3	0.45
170	0.49	1.07
183.5	0.18	0.43
190	0.08	0.21
200	0.15	0.42
207	0.21	0.57
210.5	0.05	0.21
220	0.21	0.33
230	0.08	0.14
240	0.12	0.19
250	0.22	0.23
260	0.26	0.19
270	0.25	0.37
280	0.27	0.97
290	0.11	0.23
300	0.12	0.24
310	0.1	0.41
320	0.09	0.33
330	0.17	0.45
340	0.21	0.48
350	0.4	0.54
360	0.57	0.67
370	0.13	0.28
380	0.09	0.29
390	0.04	0.22
400	0.14	0.26
410	0.2	0.29
420	0.1	0.3
430	0.21	0.52
440	0.13	0.32
450	0.12	0.32

Core F1SB86

Depth (cm)	Salinity (o/oo)	Cl (meq/l)	Br (meq/l)	SO ₄ (meq/l)	Na (meq/l)
3	5.0	80.91	0.13	9.41	66.64
10	0.7	9.98	0.02	2.15	9.42
20	1.4	22.17	0.03	2.4	17.92
30	2.5	39.71	0.06	4.29	36.15
39	2.6	35.33	0.06	3.38	29.89
50	3.2	50.82	0.08	5.77	42.07
60	3.4	55.75	0.09	6.28	45.81
70	2.8	43.88	0.06	4.44	36.07
80	2.4	37.2	0.05	3.81	31.02
82	3.0	42.5	0.06	3.96	34.81
90	3.0	39.76	0.06	3.81	33.23
100	3.6	57.22	0.09	6.29	48.29
110	3.0	44.33	0.07	4.37	36.99
118	3.3	52.37	0.08	5.48	42.32
128	3.4	54.23	0.09	5.73	43.45
133	2.8	40.75	0.06	4.38	33.7
143	3.2	25.86	0.04	2.75	21.54
153	2.9	45.29	0.07	4.96	37.84
163	3.0	38.92	0.06	3.78	32.46
173	2.7	39.56	0.06	4.27	32.77
184	2.6	30.63	0.05	3.12	26.84
194	3.3	46.25	0.07	4.89	38.04
204	5.5	83.19	0.14	8.35	68.02
F1SB water		364.15	0.56	41.31	294.93
Seawater	35	545.75	0.84	56.41	468.97

Core F1SB86 (cont.).

Depth (cm)	Ca (meq/l)	K (meq/l)	Mg (meq/l)	PO ₄ (uM)	SiO ₄ (uM)
3	2.64	1.35	15.33	0.06	2.16
10	0.4	0.21	1.97	0.01	0.27
20	0.67	0.38	4.31	0.01	0.32
30	1.42	0.66	8.34	0.04	0.96
39	1.04	0.6	7.07	0.04	0.83
50	1.61	0.79	9.74	0.04	1.28
60	1.95	0.88	10.65	0.04	0.82
70	1.23	0.69	8.42	0.06	1.52
80	1.16	0.61	7.35	0.04	0.71
82	1.07	0.66	8.02	0.06	1.72
90	1.11	0.67	7.49	0.08	1.45
100	2.03	0.78	11.23	0.07	1.62
110	1.11	0.71	8.42	0.07	1.43
118	1.86	0.84	9.88	0.09	1.57
128	1.88	0.89	10.13	0.12	1.57
133	1.3	0.6	7.81	0.11	1.26
143	0.88	0.5	4.96	0.06	1.38
153	1.46	0.73	8.59	0.07	1.28
163	1.16	0.66	7.24	0.05	0.8
173	1.38	0.69	7.51		1.26
184	1.02	0.51	5.76	0.08	1.22
194	1.69	0.68	8.87	0.27	0.68
204	2.99	1.2	15.55		2.03
F1SB water	11.93	2.58	68.77		
Seawater	20.56	10.2	105.62		

Core F1SB86 (cont.).

Depth (cm)	NO ₃ +NO ₂ (μM)	NH ₄ (μM)
3	1.52	0.7
10	0.32	0.68
20	0.09	0.32
30	0.19	0.42
39	0.24	0.6
50	0.24	0.41
60	0.24	0.3
70	0.32	0.75
80	0.14	0.25
82	0.47	0.52
90	0.3	0.41
100	0.28	0.27
110	0.3	0.27
118	0.4	0.35
128	0.39	0.35
133	0.42	0.54
143	0.31	0.64
153	0.35	0.3
163	0.2	0.21
173	0.35	
184	0.34	0.55
194	0.22	1.02
204	0.73	
F1SB water		
Seawater		

Core F1SC86

Depth (cm)	Salinity (o/oo)	Cl (meq/l)	Br (meq/l)	SO ₄ (meq/l)	Na (meq/l)
3.5	4.5	72.67	0.09	8.96	60.6
10	0.3	4.43	0.01	0.55	3.88
20	2.0	23.87	0.04	2.07	23.9
27	2.5	39.71	0.07	3.71	34.87
30	2.9	46.02	0.07	4.0	38.14
40	3.0	44.47	0.07	4.41	36.47
50	2.8	46.78	0.07	4.56	36.91
60	3.2	50.22	0.08	5.05	40.54
90	3.6	57.3	0.09	5.67	46.59
100	3.3	53.92	0.09	5.57	43.11
110	3.3	51.47	0.08	5.24	43.13
120	3.6	57.42	0.1	6.2	25.99
130	2.5	38.49	0.06	4.14	36.14
140	3.0	40.5	0.06	4.54	32.99
150	3.1	49.18	0.08	5.55	41.63
160	3.4	54.26	0.08	6.22	44.15
170	3.4	55.61	0.09	6.53	47.28
180	3.4	55.19	0.09	6.39	46.94
185	3.4	55.24	0.08	6.46	46.76
197	3.5	53.38	0.08	5.57	44.37
207	5.5	92.13	0.14	9.69	76.21
F1SC water		308.71	0.48	45.87	261.35
Seawater	35	545.75	0.84	56.46	468.97

Core F1SC86 (cont.).

Depth (cm)	Ca (meq/l)	K (meq/l)	Mg (meq/l)	PO ₄ (uM)	SiO ₄ (uM)
3.5	2.72	1.3	13.96	0.05	0.88
10	0.17	1.47	0.85	0.02	0.18
20	0.85	0.46	4.79	0.03	0.59
27	1.35	0.73	7.67	0.05	0.95
30	1.42	0.83	8.74	0.06	0.9
40	1.63	0.95	8.31	0.08	1.86
50	1.49	0.84	8.83	0.05	0.84
60	1.64	0.87	9.5	0.11	1.53
90	2.11	1.15	11.04	0.07	2.09
100	1.92	0.97	10.67	0.18	2.04
110	2.11	1.14	10.16	0.15	2.0
120	2.65	1.31	11.25	0.11	1.97
130	1.32	0.79	7.42	0.12	1.39
140	1.42	0.84	7.6	0.11	1.43
150	1.91	0.78	9.64	0.09	1.49
160	2.0	1.0	10.69	0.08	1.23
170	2.05	0.97	9.99	0.06	0.7
180	1.83	0.74	8.67	0.12	1.28
185	1.91	0.82	9.22	0.08	0.95
197	2.06	0.78	10.55	0.12	0.89
207	3.11	1.23	17.47	0.23	1.68
F1SC water	10.93	5.83	59.39		
Seawater	20.56	10.2	105.62		

Core F1SC (cont.).

Depth (cm)	NO ₃ +NO ₂ (uM)	NH ₄ (uM)
3.5	1.54	0.79
10	0.33	0.47
20	0.23	0.39
27	0.33	0.34
30	0.26	0.31
40	0.36	0.49
50	0.13	0.38
60	0.2	0.77
90	0.28	0.51
100	0.25	0.6
110	0.39	0.54
120	0.19	0.44
130	0.22	0.45
140	0.35	0.58
150	0.34	0.5
160	0.27	0.48
170	0.15	0.24
180	0.29	0.34
185	0.15	0.24
197	0.28	1.06
207	1.01	2.27
F1SC water		
Seawater		

Core F1SD86

Depth (cm)	Salinity (o/oo)	Cl (meq/l)	Br (meq/l)	SO ₄ (meq/l)	Na (meq/l)
10	0	0.39			
20	0	0.07			
30	0	0.27		0.01	
44	0	0.19		0.01	
52	0	0.96		0.12	1.1
62	0.2	3.86	0.01	0.53	3.23
72	0.7	8.6	0.01	0.85	7.19
78	1.0	15.66	0.02	1.55	10.74
85	1.3	19.74	0.03	1.86	16.36
95	1.8	28.02	0.04	2.78	23.35
100	1.0	10.14	0.01	0.99	15.66
110	0.95	15.91	0.02	1.6	13.27
120	1.1	18.45	0.02	1.89	15.29
130	1.7	29.24	0.05	3.04	24.3
140	1.1	18.99	0.03	1.98	15.81
150	4.0	63.62	0.1	7.15	50.42
160	4.2	67.57	0.11	7.76	54.59
170	3.6	57.07	0.09	6.45	47.76
180	3.6	60.46	0.18	7.08	45.63
190	3.0	43.54	0.06	4.56	35.89
200	3.4	56.51	0.08	6.58	42.89
203	3.0	48.48	0.07	5.58	39.66
212	4.2	65.42	0.1	6.86	55.29
223	5.5	87.53	0.14	8.96	65.77
F1SD water					
Seawater					

Core F1SD86 (cont.).

Depth (cm)	Ca (meq/l)	K (meq/l)	Mg (meq/l)	PO ₄ (uM)	SiO ₄ (uM)
10	0.01	0.01	0.07	0.02	0.09
20			0.01	0.01	0.04
30	0.01	0.01	0.05	0.01	0.06
44			0.21	0.02	0.04
52	0.04	0.02	0.22	0.03	0.14
62	0.02	0.07	0.98	0.05	0.55
72	0.42	0.21	1.64	0.06	1.33
78	0.52	0.35	2.91	0.06	1.67
85	0.61	0.39	3.59	0.06	2.24
95	0.98	0.42	5.31	0.1	2.59
100	0.78	0.26	2.44	0.07	1.31
110	0.46	0.3	3.02	0.07	1.76
120	0.68	0.31	8.74	0.05	1.25
130	1.07	0.71	4.05	0.04	0.75
140	0.68	0.27	17.97	0.05	0.57
150	2.42	1.67	12.47	0.18	0.8
160	2.42	1.22	12.76	0.13	1.94
170	2.46	1.25	11.04	0.09	0.98
180	1.66	1.52	4.58	0.11	1.33
190	1.61	0.89	12.6	0.07	0.9
200	1.54	1.15	4.47	0.06	0.97
203	1.97	0.91	23.02	0.02	0.7
212	2.19	1.75	11.81	0.1	0.77
223		1.5	16.55	0.27	1.41
F1SD water					
Seawater					

Core F1SD86 (cont.).

Depth (cm)	NO ₃ +NO ₂ (μM)	NH ₄ (μM)
10	0.23	0.5
20	0.04	0.35
30	0.13	0.46
44	0.08	0.26
52	0.24	0.74
62	0.19	0.75
72	0.17	0.37
78	0.13	0.45
85	0.12	0.5
95	0.22	0.92
100	0.07	0.46
110	0.22	0.5
120	0.1	0.44
130	0.23	0.6
140	0.15	0.22
150	0.1	0.66
160	0.32	0.84
170	0.2	0.84
180	0.22	0.51
190	0.22	0.52
200	0.13	0.35
203	0.13	0.46
212	0.17	0.36
223	1.16	1.21
F1SD water		
Seawater		

Core F2SA86

Depth (cm)	Temp (°C)	Salinity (o/oo)	Cl (meq/l)	Br (meq/l)	SO ₄ (meq/l)
7	-10.8	3.8	56.03	0.09	5.59
14	-10.9	1.3	22.16	0.03	2.3
23	-10.8	2.8	44.64	0.07	4.4
43	-10.6	2.9	45.68	0.07	4.51
51	-10.4	3.0	35.08	0.05	3.65
61	-10.1	2.9	48.17	0.07	3.01
73	-9.6	3.4	56.03	0.09	5.96
83	-9.5	3.0	48.73	0.08	4.72
93	-9.0	3.6	56.82	0.09	7.12
104	-8.6	3.8	44.56	0.07	5.13
114	-8.0	3.0	47.49	0.08	4.81
123	-7.5	2.9	46.53	0.07	4.75
133	-7.0	3.3	52.25	0.08	5.34
143	-6.6	3.2	51.83	0.08	5.54
153	-6.0	3.4	56.63	0.08	5.71
160	-5.5	3.7	62.63	0.1	7.61
166	-5.0	2.7	44.44	0.07	4.4
173		3.0	48.36	0.07	5.4
183	-4.7	3.0	49.35	0.07	5.21
193	-4.2	2.9	45.91	0.07	5.03
203	-3.8	3.2	51.8	0.08	5.53
217.5	-3.3	3.5		0.09	
227.5	-2.6	5.2	82.29	0.12	8.39
238	-1.9	7.0	29.67	0.05	2.77
F2SA water			134.2	.24	45.49
Seawater		35	545.75	.84	56.46

Core F2SA86 (cont.).

Depth (cm)	Na (meq/l)	Ca (meq/l)	K (meq/l)	Mg (meq/l)	PO4 (uM)
7	53.64	2.08	0.94	10.73	0.05
14	18.45	0.75	0.4	4.13	0.03
23	36.41	1.46	0.78	8.63	0.08
43	36.89	1.56	0.81	8.74	0.11
51	29.63	1.2	0.61	6.94	0.12
61	38.69	1.44	0.75	9.24	0.08
73	46.2	2.08	0.92	10.95	0.11
83	39.59	1.63	0.78	9.24	0.12
93	46.85	1.99	0.92	10.81	0.13
104	37.61	1.89	0.81	8.26	0.11
114	38.22	1.73	0.96	17.91	0.11
123	38.05	1.63	0.91	17.55	0.12
133	44.11	1.9	0.82	9.96	0.16
143	40.69	1.81	0.9	9.9	0.21
153	47.42	2.04	0.74	10.26	0.11
160	51.77	1.92	0.9	11.08	0.08
166	41.47	1.78	0.91	9.64	0.07
173	41.05	1.56	0.74	8.77	0.05
183	40.44	1.74	1.14	7.8	0.1
193	36.84	1.58	0.86	8.73	0.08
203	41.89	1.72	0.91	9.67	0.09
217.5		1.7	1.04	10.78	0.07
227.5	67.47	2.63	1.3	15.54	0.22
238	23.94		0.84		0.26
F2SA water	137.68	6.44	3.48	24.68	
Seawater	468.97	20.56	10.2	105.62	

Core F2SA86 (cont.).

Depth (cm)	SiO ₄ (uM)	NO ₃ +NO ₂ (uM)	NH ₄ (uM)	Chl-a (mg/m ³)
7	1.26	0.77	0.49	0.83
14	0.83	0.53	0.44	0.44
23	1.12	0.21	0.49	0.43
43	1.09	0.24	0.34	0.44
51	1.22	0.27	0.82	0.9
61	1.25	0.19	0.32	1.
73	1.48	0.22	0.43	1.06
83	2.01	0.26	0.52	0.56
93	2.04	0.39	1.29	0.68
104	1.66	0.31	0.48	0.86
114	1.65	0.4	0.46	0.75
123	1.7	0.36	0.58	0.68
133	1.95	0.41	1.12	0.7
143	1.99	0.19	0.57	0.75
153	1.71	0.26	0.45	0.84
160	1.75	0.2	0.47	
166	1.43	0.18	0.41	
173	0.75	0.17	0.28	
183	0.92	0.12	0.51	
193	0.99	0.2	0.36	0.79
203	0.73	0.1	0.29	
217.5	0.81	0.2	0.27	1.0
227.5	1.46	0.36	1.36	1.0
238	0.52	0.36	0.96	4.32
F2SA water				0.17
Seawater				

Core F3SA86

Depth (cm)	Salinity (o/oo)	Cl (meq/l)	Br (meq/l)	SO ₄ (meq/l)	Na (meq/l)
10	0	0.1		0.01	0.09
20	0	0.13		0.01	0.13
37	0.05	1.21		0.11	1.07
53	0.5	8.43	0.01	1.02	7.16
60	0.7	11.39	0.02	1.32	10.95
70	0.95	15.59	0.02	1.72	14.1
80	1.3	21.71	0.03	2.41	19.2
90	1.5	21.22	0.04	2.37	17.17
100	1.4	22.22	0.03	2.77	19.91
110	2.1	31.98	0.04	3.37	25.84
120	1.4	22.03	0.03	2.33	19.43
130	1.1	18.82	0.03	2.17	16.77
140	2.4	37.59	0.06	3.93	30.44
150	1.9	27.87	0.04	2.68	28.13
162	2.2	36.07	0.05	3.71	29.89
180	2.0	33.87	0.05	3.22	27.91
190	1.8	27.45	0.04	2.55	21.79
200	1.75	28.4	0.04	2.75	22.71
206	1.5	23.81	0.03	2.39	19.25
213	5.1	81.16	0.12	9.24	71.43
223	2.8	45.99	0.06	4.68	36.5
230	2.9	46.28	0.07	4.83	
240	3.0	48.53	0.07	4.92	39.16
250	3.2	52.45	0.07	5.3	46.34
260	3.8	55.78	0.08	5.85	5.02
270	3.3	54.0	0.08	5.45	43.12
282	3.0	49.41	0.06	4.68	39.67
292	5.0	76.96	0.12	7.86	67.82
302	7.5	113.0	0.17	11.14	101.09
F3SA water	29	270.18	0.42	31.33	228.64
Seawater	35	545.75	0.84	56.46	468.97

Core F3SA86 (cont.).

Depth (cm)	Ca (meq/l)	K (meq/l)	Mg (meq/l)	PO ₄ (uM)	SiO ₄ (uM)
10			0.01	0.02	0.09
20			0.02	0.01	0.16
37	0.04	0.02	0.21	0.02	0.15
53	0.32	1.22	1.57	0.02	0.39
60	0.44	0.27	2.19	0.05	0.49
70	0.55	0.32	2.97	0.02	0.58
80	0.78	0.44	4.09	0.04	0.69
90	0.85	0.53	3.97	0.05	0.83
100	0.7	0.42	4.16	0.08	0.83
110	1.13	0.68	6.04	0.04	0.87
120	0.79	0.45	4.16	0.03	0.65
130	0.69	0.39	3.55	0.04	0.61
140	1.46	0.77	7.21	0.06	0.81
150	0.78	0.66	5.33	0.05	0.58
162	1.27	0.72	6.94	0.06	0.64
180	1.27	0.7	6.51	0.14	0.69
190	1.09	0.77	5.11	0.05	0.54
200	1.09	0.74	5.4	0.05	0.6
206	1.02	0.67	4.51	0.05	0.69
213	2.91	1.79	13.11	0.16	1.89
223	1.66	0.95	8.81	0.07	1.07
230	1.61	0.93		0.07	0.96
240	1.7	0.98	9.24	0.06	0.88
250	1.97	1.09	11.17	0.07	0.88
260	1.99	1.34	10.96	0.08	0.87
270	1.8	0.99	10.3	0.07	0.66
282	1.39	0.88	9.17	0.05	0.51
292	2.62	1.69	15.79	0.19	0.94
302	3.8	2.15	21.6	1.26	2.56
F3SA water	9.35	5.79	52.05		
Seawater	20.56	10.2	105.62		

Core F3SA86 (cont.).

Depth (cm)	NO ₃ +NO ₂ (uM)	NH ₄ (uM)
10	0.59	0.34
20	0.18	0.21
37	0.35	0.63
53	0.17	0.26
60	0.26	0.87
70	0.16	0.19
80	0.16	0.28
90	0.12	0.21
100	0.45	1.44
110	0.25	0.31
120	0.17	0.34
130	0.18	0.32
140	0.17	0.37
150	0.14	0.29
162	0.16	0.31
180	0.11	0.26
190	0.11	0.33
200	0.11	0.28
206	0.12	0.22
213	0.97	2.48
223	0.34	0.99
230	0.23	0.5
240	0.16	0.29
250	0.16	0.33
260	0.17	0.44
270	0.12	0.22
282	0.13	0.24
292	0.24	1.05
302	1.06	2.05
F3SA water		
Seawater		

Core F4SA86

Depth (cm)	Salinity (o/oo)	Cl (meq/l)	Br (meq/l)	SO ₄ (meq/l)	Na (meq/l)
9	0.9	14.3	0.02	1.45	13.01
14	0.05	1.18		0.13	1.02
17	1.2	19.16	0.03	2.0	15.98
27	2.8	44.44	0.07	4.13	34.41
37	3.2	51.49	0.08	4.99	40.93
43	4.0	58.52	0.09	5.87	57.5
53	3.8	59.98	0.1	5.99	52.38
63	3.5	55.86	0.07	5.6	46.74
73	2.9	45.99	0.06	4.5	35.78
83	3.6	55.5	0.09	5.46	46.85
93	2.2	34.23	0.05	3.46	27.35
97	3.0	47.4	0.07	4.58	37.61
107	2.7	42.61	0.07	3.94	33.48
117	3.8	60.29	0.1	6.23	51.16
127	3.0	47.18	0.08	4.46	38.47
137	3.2	50.45	0.07	4.99	40.58
147	2.6	41.43	0.06	3.92	39.16
157	2.3	35.96	0.05	3.37	29.16
167	2.2	34.21	0.06	3.49	27.97
177	2.3	35.7	0.05	3.36	29.53
187	3.5	59.11	0.09	6.23	41.54
197	3.4	54.12	0.08	5.5	46.55
207	2.9	46.25	0.06	4.44	36.32
217	2.8	45.85	0.07	4.42	36.14
224	3.0	47.69	0.07	4.8	38.38
234	3.0	48.45	0.08	4.72	39.38
244	3.1	50.14	0.08	4.88	40.72
250	3.5	54.74	0.08	5.79	46.85
F4SA water					
Seawater	35	545.75	0.84	56.46	468.97

Core F4SA86 (cont.).

Depth (cm)	Ca (meq/l)	K (meq/l)	Mg (meq/l)	PO ₄ (uM)	SiO ₄ (uM)
9	0.5	0.32	2.73	0.07	0.5
14	0.04	0.02		0.02	0.21
17	0.62	0.4	3.65	0.04	2.5
27	1.3	.95	8.34	0.05	1.14
37	1.46	1.04	9.5	0.06	1.45
43	2.38	1.47	10.22	0.13	1.5
53	2.44	1.51	11.6	0.09	1.37
63	2.28	1.36	10.63	0.08	1.58
73	1.49	0.94	8.74	0.05	0.86
83	2.01	1.23	9.9	0.12	1.6
93	1.38	0.64	6.5	0.04	0.77
97	1.44	0.81	8.83	0.1	1.17
107	1.3	0.7	8.05	0.06	0.51
117	2.16	1.43	11.72	0.14	1.93
127	1.42	1.0	8.85	0.05	0.64
137	1.66	1.0	9.35	0.05	0.8
147	1.39	0.97	8.99	0.07	0.97
157	1.11	0.78	6.69	0.05	0.48
167	1.25	0.72	6.43	0.04	0.45
177	1.2	0.78	6.86	0.07	0.8
187	1.88	1.23	9.37	0.26	0.88
197	2.13	1.2	10.54	0.3	1.08
207	1.37	0.92	8.74	0.15	0.74
217	1.42	0.95	8.7	0.09	0.43
224	1.61	1.0	9.12	0.12	0.31
234	1.51	0.97	9.24	0.1	0.39
244	1.56	0.94	9.46	0.05	0.21
250	1.96	1.28	10.69	0.06	0.45
F4SA water					
Seawater	20.56	10.2	105.62		

Core F4SA86 (cont.).

Depth (cm)	NO ₃ +NO ₂ (uM)	NH ₄ (uM)
9	1.74	1.19
14	0.16	0.23
17	0.19	0.61
27	0.18	0.71
37	0.24	0.64
43	0.25	0.68
53	0.3	0.82
63	0.29	0.72
73	0.2	0.61
83	0.43	1.61
93	0.18	0.5
97	0.45	1.49
107	0.22	0.63
117	0.41	1.14
127	0.16	0.61
137	0.29	0.34
147	0.31	1.05
157	0.18	0.63
167	0.11	0.3
177	0.33	0.88
187	0.94	2.37
197	0.91	2.56
207	0.49	1.27
217	0.28	0.77
224	0.41	1.16
234	0.37	1.11
244	0.19	0.66
250	0.28	0.66
F4SA water		
Seawater		

Core F1SA87

Depth (cm)	Temp (°C)	Salinity (o/oo)	Cl (meq/l)	Br (meq/l)	SO4 (meq/l)
0	-14.5	0.5	1.27		0.08
4	-14.5	0.5	1.27		0.08
10	-14.5	0.2	2.67		0.23
20	-14.5	0.1	0.83	0.01	0.07
30	-14.5	0.5	0.74	0.01	0.09
40	-13.7	0.3	4.88	0.01	0.6
50	-13.3	0.4	7.87	0.01	0.83
60	-13.7	0.7	12.75	0.02	1.28
70	-13.3	1.4	21.77	0.03	2.21
80	-13.3	0.8	13.71	0.02	1.63
90	-13.4	0.3	5.81	0.01	0.59
100	-13.3	0.4	7.5	0.01	0.72
110	-13.2	0.7	11.9	0.02	1.21
120	-13.0	1.0	15.4	0.02	1.55
130	-13.1	0.8	14.86	0.02	1.43
140	-12.8	1.8	30.17	0.05	2.73
150	-12.8	2.15	38.07	0.05	2.94
160	-12.6	2.0	35.67	0.05	4.21
170	-12.6	2.6	42.02	0.06	4.77
180	-12.0	2.0	34.97	0.05	3.12
190	-11.7	2.3	34.97	0.06	4.25
200	-11.0	2.7	44.84	0.07	4.46
210	-10.7	3.6	58.52	0.09	7.6
220	-10.3	3.7	51.89	0.08	6.5
230	-10.3	2.5	41.03	0.07	3.73
240	-9.5	3.4	54.14	0.08	5.1
250	-8.9	2.9	45.12	0.07	5.37
260	-8.6	2.45	39.48	0.06	4.18
270	-8.1	3.0	49.49	0.08	5.14
280	-7.8	2.9	49.07	0.08	5.16
290	-7.3	2.8	48.22	0.08	5.21
300	-7.0	3.2	50.76	0.08	5.25
310	-6.5	3.4	55.27	0.09	5.75
320	-6.0	3.2	55.55	0.09	5.75
330	-4.7	2.8	43.99	0.07	4.66
340	-4.7	2.3	37.22	0.06	3.93
350	-4.3	3.2	52.17	0.08	5.64
360	-3.9	4.0	68.53	0.11	7.6
370	-3.4	4.0	62.6	0.1	6.45
374	-2.9	4.5	73.04	0.11	7.91
384	-2.3	4.4	70.22	0.11	7.56
394	-1.8	7.2	121.54	0.19	12.66
F1SA water		35	569.64	0.78	52.47
Seawater		35	545.75	0.84	56.46

Core F1SB87 (cont.).

Depth (cm)	Na (meq/l)	Ca (meq/l)	K (meq/l)	Mg (meq/l)	PO ₄ (uM)
0	0.98	0.05		0.24	0.059
4	0.98	0.05		0.24	0.059
10	2.15	0.11	0.05	0.51	0.167
20	0.72	0.03	0.02	0.16	0.16
30	0.69	0.03	0.1	0.19	0.202
40	3.81	0.2	0.08	1.03	0.186
50	4.14	0.28	0.14	2.3	0.242
60	10.43	0.46	0.21	3.85	0.225
70	17.7	0.79	0.37	2.49	0.176
80	10.06	0.5	0.23	2.4	0.181
90	4.35	0.19	0.1	1.04	0.227
100	3.97	0.25	0.13	2.25	0.125
110	9.83	0.46	0.21	2.84	0.135
120	12.65	0.57	0.27	2.63	0.136
130	11.77	0.54	0.25	5.73	1.065
140	25.9	1.25	0.56	6.6	0.286
150	29.06	1.31	0.62	6.5	0.186
160	29.26	1.3	0.62	7.99	0.19
170	34.72	1.59	0.74	6.5	0.262
180	28.6	1.33	0.62	6.78	0.212
190	29.93	1.35	0.64	8.7	0.26
200	37.29	1.75	0.8	11.22	0.21
210	54.89	2.05	1.05	9.77	0.409
220	47.56	1.83	0.94	7.86	0.205
230	33.35	1.59	0.74	10.04	0.141
240	47.14	1.92	0.96	8.36	0.316
250	37.12	1.67	0.81	7.51	0.165
260	33.11	1.51	0.7	9.5	0.17
270	44.55	1.75	0.85	9.37	0.223
280	39.85	1.92	0.86	9.33	0.214
290	40.92	1.84	0.85	9.75	0.207
300	45.96	1.75	0.88	10.19	0.243
310	48.88	1.92	0.94	10.4	0.416
320	48.52	1.92	0.97	8.53	0.282
330	37.12	1.75	0.76	8.07	0.215
340	30.98	1.43	0.66	7.1	0.318
350	43.21	2.08	0.89	10.1	0.311
360	57.69	2.75	1.23	13.2	0.273
370	51.51	1.21	1.07	11.61	0.482
374	60.32	2.86	1.26	13.78	0.227
384	61.87	2.75	1.21	13.4	0.316
394	108.63	4.38	2.14	23.22	0.854
F1SA water	428.39	19.98	9.16	96.13	
Seawater	468.97	20.56	10.2	105.62	

Core F1SA87 (cont.).

Depth (cm)	SiO ₄ (uM)	NO ₃ (uM)	NO ₂ (uM)	NH ₄ (uM)
0	0.187	0.214	0.358	0.89
4	0.187	0.214	0.358	0.89
10	0.24	0.457	0.072	0.6
20	0.208	0.352	0.052	0.406
30	0.208	0.343	0.21	0.298
40	0.208	0.324	0.204	0.543
50	0.25	0.55	0.09	0.418
60	0.395	0.369	0.04	0.27
70	0.624	0.301	0.046	0.31
80	0.458	0.29	0.058	0.328
90	0.416	0.386	0.048	0.311
100	0.312	0.279	0.05	0.34
110	0.354	0.28	0.072	0.238
120	0.395	0.378	0.038	0.449
130	0.437	0.992	0.058	0.557
140	0.686	0.38	0.038	0.717
150	0.79	0.036	0.32	0.421
160	0.892	0.099	0.17	0.469
170	1.202	0.165	0.055	0.503
180	0.991	0.098	0.033	0.379
190	1.051	0.082	0.043	0.633
200	1.506	0.069	0.05	0.573
210	2.107	0.097	0.122	0.455
220	1.959	0.035	0.052	0.523
230	1.707	0.034	0.048	0.473
240	2.1	0.105	0.055	0.472
250	1.723	0.064	0.069	0.799
260	1.658	0.203	0.051	0.45
270	2.467	0.222	0.068	0.552
280	2.049	0.22	0.044	0.566
290	1.88	0.217	0.062	0.58
300	1.898	0.256	0.059	0.667
310	2.291	0.515	0.069	0.828
320	2.559	0.404	0.069	0.91
330	1.392	0.325	0.142	0.875
340	0.994	0.544	0.108	0.987
350	0.43	0.354	0.06	1.138
360	0.366	0.172	0.068	1.808
370	0.444	0.736	0.125	1.066
374	0.571	0.212	0.085	0.538
384	0.691	0.538	0.107	0.903
394	1.8112	1.383	0.142	1.951
F1SA water				
Seawater				

Core F1SB87

Depth (cm)	Salinity (o/oo)	Cl (meq/l)	Br (meq/l)	SO ₄ (meq/l)	Na (meq/l)
10	0.1	2.05	0.03	0.15	1.66
20	0.18	2.44	0.04	0.22	2.03
30	0.3	5.22	0.08	0.5	4.06
40	0.6	9.87	0.02	0.97	8.17
50	1.1	20.76	0.03	1.86	15.31
60	1.3	21.32	0.03	2.14	17.42
70	1.4	22.11	0.03	2.23	19.03
80	1.6				
90	1.65	26.23	0.04	2.64	13.3
100	1.75	26.85	0.04	2.75	22.28
110	1.8	28.76	0.04	2.91	25.41
120	1.8	29.89	0.04	2.96	25.16
130	2.0	30.17	0.05	3.1	41.46
140	3.2	32.43	0.05	3.21	28.38
150	2.2	50.48	0.08	6.41	44.88
160	2.8	37.79	0.05	3.73	30.93
170	1.8	48.36	0.07	5.89	37.4
180	2.2	30.17	0.04	2.73	24.69
190	2.0	34.26	0.06	4.46	29.62
200	1.8	32.43	0.05	2.83	26.19
210	1.8	29.89	0.05	3.16	24.91
220	2.3	28.2	0.05	2.91	24.25
230	3.0	36.94	0.06	4.35	30.98
240	3.1	50.2	0.08	5.0	41.05
250	2.9	50.2	0.08	4.96	41.21
260	4.0	46.81	0.07	4.33	37.7
270	2.9	68.24	0.11	7.31	54.45
280	2.9	47.38	0.07	4.93	38.86
290	2.2	45.4	0.07	4.79	38.34
300	2.6	34.4	0.05	3.58	28.84
310	3.0	43.99	0.07	4.58	36.46
320	2.5	47.66	0.07	4.98	39.68
330	2.6	39.76	0.06	4.1	33.54
340	2.5	37.79	0.06	3.96	31.83
350	3.3	50.2	0.08	5.23	41.16
360	4.2	72.19	0.11	7.81	63.45
370	4.3	65.14	0.11	7.14	58.92
380	6.1	98.42	0.15	10.08	79.09
382	8.5	137.48	0.21	14.07	112.91
F1SB water					
Seawater	35	545.75	0.84	56.46	468.97

Core F1SB87 (cont.).

Depth (cm)	Ca (meq/l)	K (meq/l)	Mg (meq/l)	PO ₄ (uM)	SiO ₄ (uM)
10	0.08	0.04	0.38	0.17	0.293
20	0.09	0.04	0.45	0.245	0.354
30	0.19	0.08	0.96	0.048	0.338
40	0.38	0.17	1.83	0.127	0
50	0.71	0.32	0.47	0.093	0
60	0.79	0.39	4.03		
70	0.84	0.38	4.13	0.102	0.341
80					
90	1.0	0.45	4.87	0.081	0.505
100	0.96	0.47	5.14	0.076	0.669
110	1.12	0.51	5.4	0.114	0.696
120	1.12	0.51	5.56	0.128	0.93
130	1.21	0.52	5.76	0.121	1.198
140	1.19	0.58	6.21	0.121	1.517
150	2.02	0.92	9.67	0.169	2.249
160	1.43	0.68	7.17	0.142	2.31
170	1.69	0.81	8.15	0.147	0.797
180	1.12	0.54	5.5	0.137	0.6
190	1.29	0.61	6.39	0.185	0.893
200	1.23	0.56	5.85	0.146	0.719
210	1.16	0.54	5.73	0.078	0.676
220	1.11	0.52	5.63	0.073	0.651
230	1.43	0.66	7.07	0.12	0.849
240	1.83	0.87	9.71	0.144	1.29
250	1.83	0.89	9.56	0.217	1.302
260	1.75	0.83	8.95	0.214	1.221
270	2.5	1.18	12.34	0.262	2.127
280	1.66	0.81	9.04	0.17	1.544
290	1.84	0.81	6.53	0.196	1.556
300	1.35	0.62	6.6	0.171	1.327
310	1.75	0.76	8.2	0.188	1.562
320	1.92	0.85	8.98	0.434	1.538
330	1.59	0.7	7.5	0.206	1.048
340	1.51	0.67	7.2	0.164	0.837
350	1.83	0.9	9.57	0.24	1.147
360	2.85	1.28	13.92	0.331	0.732
370	2.62	1.21	12.83	0.23	0.391
380	3.85	1.74	17.96	0.301	1.259
382	5.34	2.47	25.85	1.167	1.68
F1SA water					
Seawater	20.56	10.2	105.62		

Core F1SA87 (cont.).

Depth (cm)	NO ₃ (uM)	NO ₂ (uM)	NH ₄ (uM)
10	0.517	0.064	0.661
20	0.529	0.108	0.36
30	0.245	0.161	0.507
40	0.274	0.266	0.707
50	0.201	0.081	0.464
60			
70	0.118	0.064	0.469
80			
90	0.216	0.128	0.525
100	0.338	0.088	0.764
110	0.34	0.066	0.42
120	0.314	0.046	0.38
130	0.403	0.092	0.742
140	0.411	0.062	0.545
150	0.603	0.084	0.745
160	0.322	0.029	0.496
170	0.376	0.084	0.565
180	0.406	0.11	0.641
190	0.751	0.084	0.919
200	0.485	0.17	0.511
210	0.337	0.134	0.581
220	0.436	0.35	0.562
230	0.235	0.106	0.407
240	0.22	0.225	0.529
250	0.379	0.067	0.473
260	0.341	0.078	0.433
270	0.368	0.078	0.7
280	0.407	0.353	0.681
290	0.325	0.199	0.465
300	0.225	0.063	0.409
310	0.33	0.089	0.416
320	1.074	0.131	0.787
330	0.461	0.089	0.529
340	0.247	0.068	0.38
350	0.631	0.076	0.683
360	0.327	0.118	0.763
370	0.391	0.055	0.447
380	0.48	0.097	0.589
382	2.804	0.182	0.887
F1SA water			
Seawater			

Core F2SA87

Depth (cm)	Temp (°C)	Salinity (o/oo)	Cl (meg/l)	Br (meg/l)	SO ₄ (meg/l)
10	-12.6	0.2	3.24	0.01	0.18
20	-12.0	5.8	9.88	0.02	0.38
30	-11.5	3.0	15.82	0.03	1.31
40	-11.3	2.7	43.29	0.07	4.14
50	-10.8	3.1	48.5	0.08	4.89
60	-10.4	3.5	56.96	0.09	5.58
70	-10.1	2.0	29.47	0.04	3.04
80	-9.8	1.4	23.01	0.04	2.56
90	-9.4	1.7	27.52	0.04	2.96
100	-9.3	3.9	61.34	0.1	5.64
110	-9.0	6.0	98.14	0.15	9.14
120	-6.4	5.6	95.32	0.13	10.43
130	-6.2	7.0	116.47	0.18	12.12
140	-5.6	7.0	112.24	0.17	12.47
150	-5.2	6.9	113.93	0.18	11.2
160	-4.6	6.25	100.96	0.15	10.2
170	-4.0	7.0	116.47	0.18	12.24
180	-3.4	6.5	105.75	0.16	10.66
190	-2.7	7.0	123.8	0.19	12.47
200	-2.0	7.0	125.21	0.19	12.78
210		7.0	115.9	0.17	11.91
218		8.7	142.69	0.22	14.64
F2SA water		32	524.52	0.83	54.96
Seawater		35	545.75	0.84	56.46

Core F2SA87 (cont.).

Depth (cm)	Na (meq/l)	Ca (meq/l)	K (meq/l)	Mg (meq/l)	PO ₄ (uM)
10	2.5	0.12	0.06	0.63	0.148
20	6.88	0.34	0.18	1.87	0.122
30	13.2	0.57	0.28	2.99	0.121
40	36.46	1.67	0.75	8.31	0.14
50	42.81	1.92	0.85	9.43	0.238
60	47.01	2.01	1.03	11.03	0.265
70	26.15	1.12	0.5	5.52	0.19
80	20.27	0.9	0.39	4.39	0.206
90	24.63	1.08	0.47	5.32	0.24
100	51.28	2.27	1.03	12.07	0.242
110	81.25	3.85	1.67	18.5	0.335
120	78.46	3.52	1.52	17.25	0.32
130	98.8	4.2	1.97	11.25	0.505
140	98.83	4.36	1.89	21.64	0.356
150	92.76	4.2	1.91	21.99	0.336
160	82.4	3.5	1.72	19.4	0.437
170	93.33	4.2	1.91	22.3	0.295
180	89.18	4.18	1.72	19.32	0.268
190	96.16	4.2	1.97	22.63	0.292
200	99.84	4.84	2.1	21.8	0.315
210	94.57	4.57	1.94		0.543
218	122.71	5.68	2.51		1.316
F2SA water	18.0	18.57	32.42		
Seawater	468.97	20.56	10.2	105.62	

Core F2SA87 (cont.).

Depth (cm)	SiO ₄ (uM)	NO ₃ (uM)	NO ₂ (uM)	NH ₄ (uM)
10	0.165	0.695	0.085	0.701
20	0.246	0.437	0.068	0.649
30	0.39	0.575	0.203	0.803
40	1.178	0.585	0.107	0.769
50	1.634	0.541	0.066	0.763
60	1.99	0.604	0.087	0.876
70	0.799	0.429	0.05	0.671
80	0.568	0.451	0.069	0.716
90	0.691	0.553	0.072	0.83
100	1.46	0.696	0.097	0.91
110	2.19	0.917	0.192	1.103
120	2.14	1.119	0.114	1.16
130	2.764	1.819	0.173	1.712
140	2.82	1.193	0.334	0.869
150	2.49	0.908	0.281	0.874
160	2.26	0.532	0.108	0.583
170	1.97	0.456	0.077	0.845
180	1.32	0.313	0.072	0.628
190	1.36	0.369	0.099	0.696
200	1.38	0.225	0.073	0.622
210	1.46	0.392	0.116	0.559
218	1.99	1.154	0.239	1.163
F2SA water				
Seawater				

APPENDIX C

Linear Regression Data

All First-year Samples

		y-intercept	Slope	R-value
Cl-Br	Mean	-0.003	0.002	0.992
	Range	0.016	0.0002	0.02
	Std. Dev	0.005	0.00008	0.006
Cl-SO4	Mean	-0.968	0.112	0.882
	Range	7.305	0.155	0.28
	Std. Dev	2.115	0.044	0.104
Cl-Ca	Mean	-0.001	0.034	0.971
	Range	1.233	0.042	0.08
	Std. Dev	0.331	0.012	0.022
Cl-K	Mean	0.525	0.084	0.915
	Range	4.165	0.696	0.26
	Std. Dev	1.262	0.218	0.095
Cl-Na	Mean	3.909	0.794	0.917
	Range	55.466	0.841	0.7
	Std. Dev	14.998	0.234	0.217
Cl-Mg	Mean	0.512	0.396	0.999
	Range	4.142	2.091	0.01
	Std. Dev	1.204	0.659	0.003
Cl-PO4	Mean	-0.34	0.004	0.549
	Range	3.482	0.009	0.89
	Std. Dev	1.11	0.003	0.343
Cl-NO3	Mean	0.004	0.018	0.648
	Range	1.86	0.057	0.68
	Std. Dev	0.566	0.018	0.272
Cl-NO2	Mean			
	Range			
	Std. Dev			
Cl-NH4	Mean	-0.234	0.014	0.606
	Range	2.611	0.014	0.66
	Std. Dev	0.811	0.006	0.209
Cl-SiO4	Mean	0.385	0.017	0.6
	Range	2.785	0.037	0.97
	Std. Dev	1.201	0.015	0.429
Na-SO4	Mean	-0.67	0.135	0.841
	Range	9.5	0.141	0.74
	Std. Dev	2.44	0.039	0.218
Exp-Meas	Mean	0.307	0.949	0.937
	Range	2.033	0.53	0.61
	Std. Dev	0.564	0.154	0.192
NO3-PO4	Mean	0.033	0.301	0.573
	Range	0.615	1.33	0.81
	Std. Dev	0.206	0.409	0.304
NO3-NO2	Mean	0.058	0.016	0.6
	Range	0.056	0.034	0.7
	Std. Dev	0.02	0.011	0.244
NO3-NH4	Mean	0.653	0.739	0.567
	Range	1.73	2.36	0.79
	Std. Dev	0.628	0.676	0.296
NO3-SiO4	Mean	1.26	0.714	0.503
	Range	1.99	4.07	0.86
	Std. Dev	0.559	1.109	0.338

All First-year Samples (cont.).

		y-intercept	Slope	R-value
NO ₂ -PO ₄	Mean	0.125	2.93	0.44
	Range	0.839	12.057	0.76
	Std. Dev	0.262	4.44	0.339
NO ₂ -NH ₄	Mean	0.343	11.61	0.625
	Range	2.4	36.18	0.78
	Std. Dev	0.843	11.08	0.255
NO ₂ -SiO ₄	Mean	0.558	23.332	0.521
	Range	2.75	76.127	0.82
	Std. Dev	1.012	27.95	0.281

1986 First-year Samples

		y-intercept	Slope	R-value
Cl-Br	Mean	0.0004	0.002	0.987
	Range	0.0004	0.0001	0.01
	Std. Dev	0.0002	0.00005	0.006
Cl-SO4	Mean	0.332	0.068	0.897
	Range	1.995	0.094	0.28
	Std. Dev	1.099	0.048	0.162
Cl-Ca	Mean	0.315	0.022	0.973
	Range	0.676	0.03	0.04
	Std. Dev	0.34	0.016	0.023
Cl-K	Mean	1.567	0.242	0.893
	Range	3.733	0.694	0.14
	Std. Dev	2.151	0.4	0.071
Cl-Na	Mean	15.38	0.573	0.76
	Range	44.47	0.647	0.7
	Std. Dev	24.59	0.358	0.398
Cl-Mg	Mean	0.567	0.185	0.997
	Range	0.462	0.008	0.01
	Std. Dev	0.232	0.004	0.006
Cl-PO4	Mean	-0.019	0.002	0.365
	Range	0.446	0.006	0.27
	Std. Dev	0.315	0.004	0.191
Cl-NO3	Mean	0.345	0.002	0.55
	Range	0.998	0.012	0.6
	Std. Dev	0.706	0.008	0.424
Cl-NO2	Mean			
	Range			
	Std. Dev			
Cl-NH4	Mean	0.16	0.01	0.56
	Range	0.145	0.006	0.08
	Std. Dev	0.103	0.004	0.057
Cl-SiO4	Mean			
	Range			
	Std. Dev			
Na-SO4	Mean	1.551	0.1	0.683
	Range	5.266	0.087	0.74
	Std. Dev	2.662	0.045	0.386
Exp-Meas	Mean	0.696	0.837	0.797
	Range	1.68	458	0.61
	Std. Dev	0.951	0.257	0.352
NO3-PO4	Mean	-0.056	0.534	0.433
	Range	0.505	1.328	0.55
	Std. Dev	0.256	0.678	0.289
NO3-NO2	Mean			
	Range			
	Std. Dev			
NO3-NH4	Mean	0.541	0.915	0.513
	Range	1.004	2.363	0.77
	Std. Dev	0.515	1.192	0.385
NO3-SiO4	Mean	1.084	1.139	0.483
	Range	1.985	4.067	0.81
	Std. Dev	1.046	2.071	0.411

1986 First-year Samples (cont.).

NO2-PO4	Mean			
	Range			
	Std. Dev			
NO2-NH4	Mean			
	Range			
	Std. Dev			
NO2-SiO4	Mean			
	Range			
	Std. Dev			

1987 First-year Samples

		y-intercept	Slope	R-value
Cl-Br	Mean	-0.004	0.002	0.994
	Range	0.016	0.0002	0.01
	Std. Dev	0.006	0.00009	0.005
Cl-SO4	Mean	-1.526	0.131	0.876
	Range	6.77	0.076	0.24
	Std. Dev	2.258	0.027	0.086
Cl-Ca	Mean	-0.137	0.039	0.97
	Range	0.703	0.013	0.07
	Std. Dev	0.232	0.004	0.023
Cl-K	Mean	0.078	0.016	0.924
	Range	0.756	0.011	0.26
	Std. Dev	0.265	0.004	0.107
Cl-Na	Mean	-1.005	0.888	0.984
	Range	17.122	0.197	0.03
	Std. Dev	6.474	0.067	0.01
Cl-Mg	Mean	0.488	0.487	1
	Range	4.142	2.086	0
	Std. Dev	1.468	0.787	0
Cl-PO4	Mean	-0.431	0.004	0.61
	Range	3.482	0.008	0.89
	Std. Dev	1.258	0.003	0.373
Cl-NO3	Mean	0.023	0.676	0.676
	Range	0.045	0.64	0.64
	Std. Dev	0.018	0.253	0.253
Cl-NO2	Mean	0.04	0.00038	0.63
	Range	0.079	0.0003	0.76
	Std. Dev	0.034	0.00016	0.325
Cl-NH4	Mean	-0.365	0.015	0.622
	Range	2.611	0.014	0.66
	Std. Dev	0.914	0.006	0.243
Cl-SiO4	Mean	0.611	0.015	0.552
	Range	2.785	0.037	0.97
	Std. Dev	1.192	0.015	0.462
Na-SO4	Mean	-1.622	0.15	0.909
	Range	5.412	0.072	0.18
	Std. Dev	1.745	0.027	0.065
Exp-Meas	Mean	0.14	0.996	0.997
	Range	0.773	0.198	0.01
	Std. Dev	0.26	0.068	0.005
NO3-PO4	Mean	0.078	0.185	0.643
	Range	0.544	0.537	0.81
	Std. Dev	0.186	0.185	0.311
NO3-NO2	Mean	0.058	0.016	0.6
	Range	0.056	0.034	0.7
	Std. Dev	0.02	0.011	0.244
NO3-NH4	Mean	0.71	0.65	0.593
	Range	1.728	0.884	0.69
	Std. Dev	0.717	0.369	0.279
NO3-SiO4	Mean	1.337	0.533	0.511
	Range	0.762	1.352	0.86
	Std. Dev	0.286	0.535	0.338

1987 First-year Samples (cont.).

		y-intercept	Slope	R-value
NO2-PO4	Mean	0.125	2.93	0.44
	Range	0.839	12.057	0.76
	Std. Dev	0.262	4.438	0.339
NO2-NH4	Mean	0.377	12.952	0.587
	Range	2.398	36.175	0.73
	Std. Dev	0.905	11.244	0.25
NO2-SiO4	Mean	0.558	23.332	0.521
	Range	2.745	76.127	0.82
	Std. Dev	1.012	27.946	0.281

All Multiyear Samples

		y-intercept	Slope	R-value
Cl-Br	Mean	0.001	0.002	0.97
	Range	0.018	0.001	0.09
	Std. Dev	0.005	0.00014	0.031
Cl-SO4	Mean	-0.176	0.109	0.968
	Range	0.604	0.029	0.14
	Std. Dev	0.218	0.009	0.047
Cl-Ca	Mean	0.012	0.035	0.971
	Range	0.323	0.008	0.07
	Std. Dev	0.096	0.002	0.022
Cl-K	Mean	3.182	0.028	0.873
	Range	31.367	0.108	0.79
	Std. Dev	9.873	0.032	0.245
Cl-Na	Mean	0.53	0.817	0.977
	Range	3.569	0.117	0.07
	Std. Dev	1.105	0.034	0.027
Cl-Mg	Mean	0.546	0.351	0.91
	Range	2.341	1.734	0.44
	Std. Dev	0.741	0.543	0.152
Cl-PO4	Mean	0.02	0.004	0.572
	Range	0.263	0.017	0.6
	Std. Dev	0.068	0.005	0.214
Cl-NO3	Mean	0.056	0.006	0.488
	Range	0.478	0.011	0.6
	Std. Dev	0.178	0.004	0.221
Cl-NO2	Mean			
	Range			
	Std. Dev			
Cl-NH4	Mean	0.159	0.011	0.521
	Range	0.615	0.011	0.33
	Std. Dev	0.21	0.004	0.136
Cl-SiO4	Mean	0.416	0.017	0.6
	Range	0.57	0.02	0.66
	Std. Dev	0.2	0.007	0.255
Na-SO4	Mean	-0.077	0.129	0.952
	Range	1.325	0.055	0.11
	Std. Dev	0.351	0.015	0.043
Exp-Meas	Mean	-0.075	1.015	0.97
	Range	0.508	0.124	0.1
	Std. Dev	0.164	0.043	0.036
NO3-PO4	Mean	0.075	0.34	0.568
	Range	0.375	0.757	0.91
	Std. Dev	0.103	0.265	0.263
NO3-NO2	Mean			
	Range			
	Std. Dev			
NO3-NH4	Mean	0.321	0.91	0.626
	Range	0.6	1.896	0.62
	Std. Dev	0.182	0.532	0.224
NO3-SiO4	Mean	0.811	0.93	0.377
	Range	0.825	3.928	0.66
	Std. Dev	0.286	1.147	0.26

All Multiyear Samples (cont.).

		y-intercept	Slope	R-value
NO2-PO4	Mean			
	Range			
	Std. Dev			
NO2-NH4	Mean			
	Range			
	Std. Dev			
NO2-SiO4	Mean			
	Range			
	Std. Dev			

1986 Multiyear Samples

		y-intercept	Slope	R-value
Cl-Br	Mean	-0.001	0.002	0.969
	Range	0.013	0.0004	0.09
	Std. Dev	0.004	0.0001	0.031
Cl-SO4	Mean	-0.205	0.111	0.957
	Range	0.604	0.029	0.14
	Std. Dev	0.252	0.01	0.053
Cl-Ca	Mean	0.019	0.034	0.963
	Range	0.323	0.006	0.06
	Std. Dev	0.116	0.002	0.021
Cl-K	Mean	4.544	0.033	0.819
	Range	31.367	0.106	0.77
	Std. Dev	11.79	0.039	0.28
Cl-Na	Mean	0.742	0.806	0.969
	Range	2.832	0.071	0.07
	Std. Dev	1.104	0.028	0.028
Cl-Mg	Mean	0.649	0.181	0.884
	Range	2.107	0.029	0.44
	Std. Dev	0.846	0.011	0.179
Cl-PO4	Mean	0.003	0.004	0.553
	Range	0.178	0.017	0.6
	Std. Dev	0.056	0.006	0.239
Cl-NO3	Mean	0.056	0.006	0.488
	Range	0.478	0.011	0.6
	Std. Dev	0.178	0.004	0.221
Cl-NO2	Mean			
	Range			
	Std. Dev			
Cl-NH4	Mean	0.156	0.011	0.474
	Range	0.615	0.011	0.3
	Std. Dev	0.231	0.005	0.134
Cl-SiO4	Mean	0.41	0.017	0.574
	Range	0.57	0.02	0.66
	Std. Dev	0.216	0.007	0.264
Na-SO4	Mean	-0.077	0.131	0.936
	Range	1.325	0.055	0.1
	Std. Dev	0.409	0.018	0.041
Exp-Meas	Mean	-0.05	1.005	0.982
	Range	0.295	0.114	0.07
	Std. Dev	0.121	0.039	0.027
NO3-PO4	Mean	0.071	0.309	0.497
	Range	0.375	0.757	0.72
	Std. Dev	0.125	0.319	0.257
NO3-NO2	Mean			
	Range			
	Std. Dev			
NO3-NH4	Mean	0.292	0.985	0.607
	Range	0.6	1.896	0.6
	Std. Dev	0.199	0.589	0.222
NO3-SiO4	Mean	0.781	1.185	0.39
	Range	0.825	3.578	0.66
	Std. Dev	0.311	1.25	0.29

1986 Multiyear Samples (cont.).

		y-intercept	Slope	R-value
NO2-PO4	Mean			
	Range			
	Std. Dev			
NO2-NH4	Mean			
	Range			
	Std. Dev			
NO2-SiO4	Mean			
	Range			
	Std. Dev			

1987 Multiyear Samples

		y-intercept	Slope	R-value
Cl-Br	Mean	0.005	0.001	0.973
	Range	0.011	0.0002	0.07
	Std. Dev	0.006	0.0001	0.038
Cl-SO4	Mean	-0.111	0.106	0.993
	Range	0.218	0.003	0.01
	Std. Dev	0.12	0.002	0.006
Cl-Ca	Mean	-0.004	0.037	0.99
	Range	0.049	0.003	0.02
	Std. Dev	0.025	0.001	0.01
Cl-K	Mean	0.004	0.017	1
	Range	0.027	0.001	0
	Std. Dev	0.013	0.001	0
Cl-Na	Mean	0.034	0.842	0.997
	Range	2.083	0.064	0.01
	Std. Dev	1.144	0.036	0.006
Cl-Mg	Mean	0.304	0.749	0.97
	Range	0.855	1.724	0.04
	Std. Dev	0.444	0.992	0.02
Cl-PO4	Mean	0.059	0.004	0.617
	Range	0.181	0.003	0.34
	Std. Dev	0.091	0.001	0.17
Cl-NO3	Mean			
	Range			
	Std. Dev			
Cl-NO2	Mean			
	Range			
	Std. Dev			
Cl-NH4	Mean	0.166	0.01	0.64
	Range	0.317	0.002	0.02
	Std. Dev	0.224	0.002	0.014
Cl-SiO4	Mean			
	Range			
	Std. Dev			
Na-SO4	Mean	-0.077	0.125	0.99
	Range	0.433	0.006	0.02
	Std. Dev	0.225	0.003	0.01
Exp-Meas	Mean	-0.125	1.034	0.947
	Range	0.508	0.102	0.09
	Std. Dev	0.255	0.053	0.045
NO3-PO4	Mean	0.081	0.404	0.71
	Range	0.118	0.25	0.51
	Std. Dev	0.06	0.125	0.259
NO3-NO2	Mean			
	Range			
	Std. Dev			
NO3-NH4	Mean	0.424	0.645	0.69
	Range	0.027	0.022	0.44
	Std. Dev	0.019	0.016	0.311
NO3-SiO4	Mean	0.87	0.42	0.35
	Range	0.55	1.758	0.47
	Std. Dev	0.277	0.88	0.243

1987 Multiyear Samples (cont.).

		y-intercept	Slope	R-value
NO2-PO4	Mean	0.209	0.401	0.213
	Range	0.133	1.66	0.35
	Std. Dev	0.072	0.856	0.183
NO2-NH4	Mean	0.589	0.828	0.267
	Range	0.145	0.952	0.26
	Std. Dev	0.073	0.496	0.136
NO2-SiO4	Mean	1.042	0.893	0.313
	Range	0.513	8.465	0.49
	Std. Dev	0.258	4.428	0.246